Investigating the Relationship Between Structure, Ice Recrystallization Inhibition Activity and Cryopreservation Ability of Various Galactopyranose Derivatives

Jacqueline Tokarew

Thesis submitted to the
Faculty of Graduate & Postdoctoral Studies
University of Ottawa
in partial fulfillment of the requirements for the
M.Sc. degree in the
Ottawa-Carleton Chemistry Institute

Candidate	Supervisor
Jacqueline Tokarew	Professor Robert N. Ben

Abstract

The goal of our research is to generate cryopreservation agents derived from antifreeze glycoproteins. One postulated mechanism of cell cryo-injury is ice recrystallization. It is known that simple saccharides and cryopreservation agents (DMSO) display ice recrystallization inhibition (IRI). This study assessed the cytotoxicity and cryopreservation ability of these sugars in relation to their IRI. It was determined that compounds with greater IRI have increased cytotoxicity yet confer cryoprotection. To further investigate how structure is affecting IRI activity, several galactopyranoside derivatives were synthesized. A series of deoxy and α-*C*-allyl-deoxy galactopyranoses were prepared. Testing determined that removal of any hydroxyl group removes IRI. 3-deoxy-β-thiophenyl galactose was also synthesized and had surprisingly better IRI than β-thiophenylgalactose. Also, 6-azido galactose had similar IRI to 6-deoxy galactose. Lastly, a series of β- thioalkylgalactosides was synthesized and testing gave contradicting results which suggest that predicting IRI based on hydrophilicity is more complicated than initially hypothesized.

Acknowledgements

I would like to first thank my supervisor Dr. Robert Ben for his guidance and assistance during the course of my undergraduate and graduate studies. He was always willing to discuss research and provide suggestions where improvement was required. He also taught me the invaluable lesson of independent problem solving, and more importantly, thinking of the "bigger picture" when presenting my research to the research group and at several conferences which I had the opportunity of attending. Thank you for proof-reading this thesis and always "being on our side." Also, I would like to thank the University of Ottawa and Natural Sciences and Engineering Research Council for the generous scholarships I have received throughout my studies.

I would also like to thank my fellow co-workers and undergraduate students who have helped with the completion of my thesis. Thank you to Adam Ray and Jason Kwok, for being excellent students who were willing to learn and willing to work. I would like to thank you for preparing important materials for my projects. Also, special thanks to Dr. Mathieu Leclere, Luke Wu, Louise Guolla, Dr. Dave Allan and Dr. C. Scott Findlay for their help with the planning and execution of the biology experiments.

I would also like to thank all past and present members of the Ben Lab for their guidance and friendship. Liz von Moos, thank you for all your guidance in the cell lab and sharing your passion for cycling with me. Thanks to Ruoying Gong, Sandra Ferreira, Wendy Campbell and Anna Balcerak for bringing life into the lab. Dr. Jennifer Chaytor, thanks for the guidance in my undergraduate years, the fun trip to France and your friendship. Thanks to John Trant for the encouragement, fun abstract discussions and helpful tips. Taline Boghossian, my older sister, thanks for all the fun and quirky chats. Dr. Pawel Czechura, Taz Cheema, Chantelle Capicciotti, and Dr. Michael Souweha, thanks for supplementing my free time with much needed extracurricular activities. Dr. Roger Tam, thank you for your time and patience in helping me edit this thesis and for providing me with much needed balance and encouragement.

Finally, thanks to my friends and family for their love and support. Lili and Flo, thanks for helping me wind down from a long week at the lab with non-chemistry related chats and outings. Dan, you always believed in me and never let me ever give up on anything I tried. Mom, thank you for the support and the necessary push to help me complete this degree. Dad, you always taught me valuable life lessons through fun little rhymes: "If you snooze, you lose!", "If you play now, you gotta pay for it later!" Thanks Mom and Dad for equipping me with the most important tools I will ever use in my life: perseverance and patience.

"*Nothing in the world can take the place of persistence. Talent will not; nothing is more common than unsuccessful men with talent. Genius will not; unrewarded genius is almost a proverb. Education will not; the world is full of educated derelicts. Persistence and determination alone are omnipotent. The slogan, 'press on' has solved, and always will solve, the problems of the human race*." - Calvin Coolidge

Table of Contents

List of Figures

List of Tables

List of Graphs

List of Schemes

List of Abbreviations

α	alpha
β	beta
γ	gamma
δ	delta
7-AAD	7-Aminoactinomycin D
^{1}H	proton
^{13}C	carbon
2D	two-dimensional
3D	three-dimensional
Ac	acetyl
Ac_2O	acetic anhydride
AFGP(s)	antifreeze glycoprotein (s)
AFGP8	antifreeze glycoprotein, fraction-8
AFP(s)	antifreeze protein(s)
AFP I	antifreeze protein type I
AIBN	1,1-azobisisobutyronitrile
Ala	alanine
ANOVA	analysis of variance
Atm	atmospheres
$BF_3 \bullet OEt_2$	boron trifluoride diethyl etherate
Bn	benzyl
BnBr	benzylbromide
br	broad
Bu_3SnH	tributyltin hydride
Bz	benzoyl
BzCl	benzoylchloride
Cat.	Catalytic
$CDCl_3$	deuterated chloroform
CD_3OD	deuterated methanol
CGG	cysteine-glycine-glycine
CH_3CN	acetonitrile
cm^{-1}	wavenumber
CPA	cryoprotective agent
CSA	camphor sulfonic acid
$CuSO_4$	copper sulfate
d	doublet
D_2O	deuterium oxide
dd	doublet of doublets
DCM	dichloromethane
DIS	dynamic ice shaping
DMAP	dimethylaminopyridine
DMF	dimethyl formamide
DMSO	dimethyl sulfoxide

dt	doublet of triplets
ESI	electrospray ionization
Et	ethyl
Et_2O	diethyl ether
EtOAc	ethyl acetate
EtOH	ethanol
FBS	fetal bovine serum
Gal	galactose
Glc	glucose
Gly	glycine
HEK 293	human kidney cell line
HBr	hydrobromic acid
HCl	hydrochloric acid
HPLC	high performance liquid chromatography
IIF	intracellular ice formation
iPrOH	isopropanol
IR	Infrared
IR resin	Amberlite ion exchange resin
IRI	ice-recrystallization inhibition
kcal	kilocalorie
kPa	kiloPascals
Lac	lactose
KGG	lysine-glycine-glycine
kDa	kiloDaltons
m	multiplet
M	molar
M^+	parent molecular ion
Man	mannose
Me	methyl
$MeC(OEt)_3$	triethyl orthoformate
MEM	Minimum essential medium
MeOH	methanol
MGS	mean grain size
$MgSO_4$	magnesium sulfate
MHz	mega Hertz
mM	millimolar
MS	mass spectrometry
MS	molecular sieves
MTT	methylthiasolydiphenyl-tetrazolium bromide
NaCl	sodium chloride
NHAc	*N*-acetyl
NaH	sodium hydride
Na_2SO_4	Sodium sulfate
$NaHCO_3$	sodium bicarbonate
NaN_3	sodium azide

$NaNO_2$	sodium nitrite
NaOH	sodium hydroxide
NaOMe	sodium methoxide
NBS	*N*-bromosuccinimide
NH_4I	*tert*-butyl ammonium iodide
NIS	N-iodosuccinimide
NMR	Nuclear Magnetic Resonance
OGG	ornithine-glycine-glycine
OMe	*O*-methoxy
OTf	trifluoromethane sulfonate
PBS	phosphate buffered saline
Pd/C	palladium on carbon
Ph	phenyl
$PhCH(OMe)_2$	benzaldehyde dimethyl acetal
Piv	pivaloyl
PivCl	pivaloyl chloride
ppm	parts per million
Pr	Propyl
pTsOH	para-toluene sulfonic acid
q	quartet
QLL	quasi-liquid layer
Rf	Retention factor
s	singlet
SAA	serine-alanine-alanine
Ser	serine
SGG	serine-glycine-glycine
$SiMe_3$	trimethyl silyl
SPh	thiophenyl
t	triplet
T	temperature
Tal	talose
TBAF	*tert*-butylammonium fluoride
TBDMSCl	*tert*-butyldimethylsilyl chloride
TBS	*tert*-butyldimethylsilyl
tBuOK	potassium *tert*-butoxide
TCDI	*N*,*N*'-thiocarbonyldiimidazole
TEA	triethylamine
TFA	trifluoroacetic acid
Tf_2O	triflic anhydride
TH	thermal hysteresis
THF	tetrahydrofuran
Thr	threonine
WRL-68	human embryonic liver cell line

Chapter 1: Introduction to Cryopreservation, Biological Antifreezes and Carbohydrate Hydration

1.1 Introduction

The loss in cell viability post cryopreservation is an issue which needs addressing due to increasing demands from regenerative and transplant medicine.[1] It was originally postulated that the formation of intracellular and extracellular ice *in vivo* may account for mechanical (rupturing plasma membrane) [2,3] and biochemical (induce enzymatic loss of function and degradation) damage to cells.[4] However, the morphology of ice crystals has more detrimental effects on cell survival than ice crystal presence alone. Long spicule-like crystals confer cell membrane damage, while smaller sized crystals reduce pressure on the membrane.[5,6] Since the 1950s, many cell penetrating and non-penetrating cryoprotectants and cryoadjuvants have been used to increase cell viability post freeze-thaw by arresting or reducing ice formation.[7] Unfortunately, the exact mode of actions of these cryoprotectants and cryoadjuvants are still unknown. Interestingly, the discovery of biological antifreezes in cold inhabiting organisms has provided insight into the mode of action of cell preservation in these sub-zero temperatures.[8] In order to further understand the mechanism of cryopreservation and improve freezing protocols, further research conducted on biological antifreezes and analogous compounds is required. This section will provide a brief overview of the current knowledge regarding cell damage during cryopreservation, cryoprotective agents and biological antifreeze modes of action, and structure activity relationship studies on biological antifreezes.

1.2 Cryopreservation of cells

1.2.1 Mechanisms of Cell Injury in Sub-Zero Environments

The life of a cell can be prolonged by storage in liquid nitrogen (-196°C).[7] The temperature drop results in reduced cellular function by slowing the rate of biochemical reactions.[7] The cold-mediated preservation of cells is known as cryopreservation and this process has many applications in research, health care,[1,9] agriculture and the food industry.[10,11]

In health care, the ability to store embryonic and adult stem cells, reproductive cells, tissues and whole organs is becoming more important due to pressing demands from regenerative and transplant medicine.[1] Therefore, the efficient cold storage of cells, tissues and organs is required. However, freezing is lethal to almost all living organisms (humans, plants, insects and fish) with the exception of certain organisms which have adapted to sub-zero climates. [8,12] Thus, a significant amount of cell death occurs upon freezing and this is reflected by the fact that all attempts to freeze large whole organs and tissues, while maintaining their function and viability upon post-thawing, have been unsuccessful.[13] Despite much research into improving cryopreservation protocols, there are no current freezing protocols that are able to provide 100% cell viability post cryopreservation for such large organs.[7] In the hope of improving freezing protocols, many hypotheses and studies have attempted to explain eukaryotic cell freeze damage. A brief summary of these will be described.

Reduced temperatures can affect protein conformation and activity by altering their hydrophilic and hydrophobic interactions, and affecting cellular metabolism.[14] However, it was determined that the main target of cell injury in cryopreservation is the cellular membrane.[15] The central issue associated with cell freezing is the formation of both extracellular and intracellular

ice crystals.[2-7] Extracellular ice crystals can damage cell membranes in three ways: by increasing intracellular solute concentrations,[4] altering osmotic pressure across the cell membrane[16] and by mechanical stress (or shearing)[2] with increasing crystal size (Figure 1.1).

The solute concentration within a cell is much higher than surrounding medium so that the colligative freezing point of the intracellular cytoplasm is around -5°C.[7] Therefore, upon supercooling (cooling below 0 °C), ice nucleation will occur more readily in the more diluted extracellular environment to form extracellular ice crystals while the cytoplasm remains unfrozen.[7] As the ice crystals outside the cell grow, they cause mechanical stress on the membrane to deform the cell membrane (Figure 1.1A).[2] The residual unfrozen extracellular environment is more concentrated in ionic solutes.[4] This results in an increase in osmotic pressure across the cell membrane and causes the rapid efflux of water molecules from the cytoplasm to the extracellular environment which causes osmotic shrinkage of the cell. (Figure 1.1A)[16] Although dehydration will reduce the osmotic pressure across the cell membrane, it will also consequently increase intracellular solute concentrations. This further reduces the freezing point of the intracellular environment and consequently the solubility of solutes within the cell. Below the eutectic point of the system (at which liquid water solidifies), most solutes will precipitate out of the cytoplasm, which alters pH and affects cellular function (Figure 1.1A).[4,7]

Moreover, the rate of water efflux generated from increased extracellular solute concentrations greatly affects the change in osmotic pressure across the cell membrane and leads to several detrimental effects.[7] Firstly, distorted and compromised cell membranes may occur if the osmotic pressure across the cell membrane is much larger than the efflux of water molecules during freezing.[17] Secondly, formation of small intracellular ice crystals can occur if the efflux of water is significantly slower relative to the rate of cooling (either because of low water

permeability or large intracellular volume to cell membrane surface ratio) (Figure 1.1A).[17] Mazur and Toner both independently postulated that intracellular ice formation (IIF) is the major cause of cellular injury since the freezing of the cytoplasm is believed to alter cellular function.[18,19]

1.2.2 Ice Recrystallization as a Major Source of Cell Injury during Cryopreservation

However, there has been much debate over the direct influence of IIF on cellular cryoinjury.[19,20] In 1959, Salt discovered that fat cells in goldenrod gall fly larvae (*Eurosta solidaginis*) undergo significant IIF yet still retain cell viability post-thaw. Salt also noted that the ice crystals formed were small in size, and has led to the assumption that both intracellular and extracellular ice recrystallization, rather than IIF, cause significant membrane damage.[21] It is reported that at -100°C, ice recrystallization can occur, and the rate of recrystallization is proportional to temperature and inversely proportional to ice crystal size.[22] Thus, the largest cell damage occurs during the thawing process during which higher temperatures and smaller ice crystals are present (Figure 1.1B). Upon warming, the enthalpically favoured recrystallization of ice will occur outside and inside the cell causing mechanical stress on the membrane.[7] Therefore, the less thermodynamically stable and smaller ice crystals will merge into larger ones which then apply stress on the cytoplasmic and plasma membranes. The result is a ruptured membrane which undoubtedly induces cell death.[7] Figure 1.1 offers a schematic summary of the different postulated mechanisms of cell injury during the freezing and thawing processes of cryopreservation. [2-4,7,12-19]

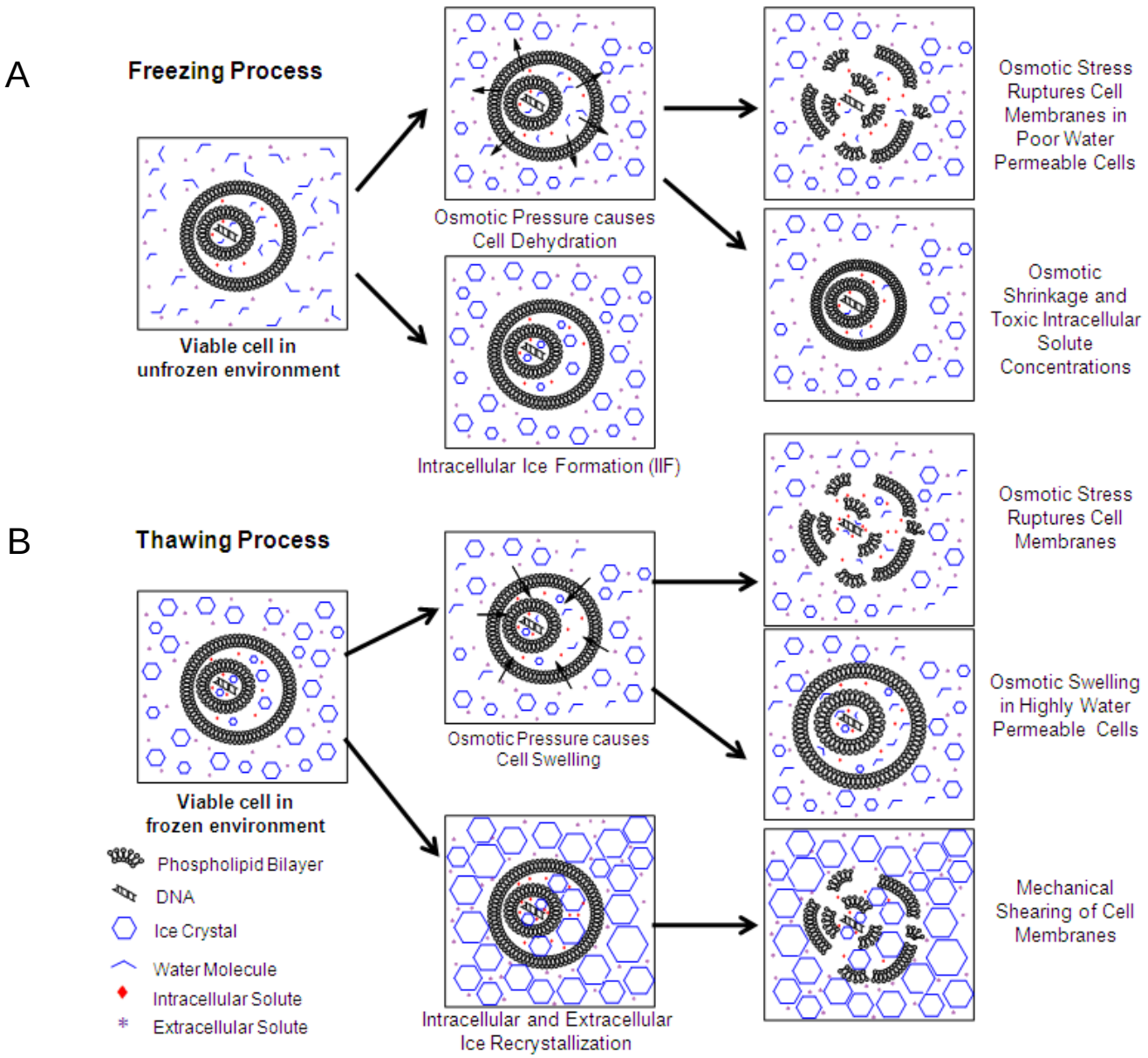

Figure 1.1 Schematic representations of the various postulated mechanisms of freeze-thaw injury during (**A**) the freezing process and (**B**) the thawing process.[2-4,7,12-19]

1.2.3 Current Cryopreservation Protocols

Given the variety of postulated cell cryoinjury mechanisms associated with cryopreservation (long exposure to high intracellular solute concentrations, large osmotic pressure changes and ice recrystallization), more than one cryopreservation protocol was

developed to address some or all of these mechanisms of cell injury.[23] Currently, there are three ways to preserve cells which include: vitrification,[24] slow-freeze cryopreservation[23] and fast freeze cryopreservation.[23]

Fast cooling with a viscous solvent (or vitrification) aims to completely eliminate formation of ice crystals.[24] As the viscous sample cools, it cannot nucleate due to high concentrations of cryoprotectants and therefore supercools. As the sample is further cooled, it solidifies as a solid hard glass rather than form ice crystals.[24] This completely eliminates the formation of ice during cell preservation and results in high cell viability post freeze-thaw. This method is currently used to preserve stem cells and reproductive cells.[24] Unfortunately, large amounts of cryoprotective agents (CPA) are required and render this process impractical for tissue and organ preservation. [7,24]

Slow freezing reduces the rate of IIF and osmotic stress by allowing osmotic equilibration between higher extracellular and lower intracellular solute concentration.[7,23] Since there is no IIF, there are no seed crystals within the cell that can recrystallize and harm the cell upon warming. Therefore, warming the cells too quickly will cause the cells to burst since the intracellular solute concentrations are higher than extracellular solute concentrations at the time of thawing. [7,23] Therefore, a slow freeze must accompany a slow thaw. Unfortunately, given that different cell types have different water permeabilities, it is difficult to obtain a slow enough cooling rate in some low water permeable cell types to allow sufficient dehydration to inhibit IIF and therefore ice recrystallization will always occur and cause cell death.[7]

As a slow thawing rate must accompany a slow cooling rate, a fast freeze procedure must also be followed by fast thawing.[7,23] This is rationalized by the fact that fast freezing produces

small intracellular ice crystals and if the sample is warmed too slowly, the ice crystals begin to recrystallize, which is lethal to the cell.[7,23] The success of this freezing procedure relies on cell type and the fact that large osmotic pressure changes do not affect the membrane integrity of the chosen cell type.[7,23]

Interestingly, certain cells such as red blood cells and microorganisms, can be frozen in a salt solution, given that the cooling rate and thawing rate are optimized.[7] In other words, the cooling rate is slow enough to inhibit IIF and large osmotic pressure changes, but fast enough to inhibit exposure to high intracellular solute concentrations. Also, the thawing rate is fast enough to limit exposure to high intracellular solute concentrations but slow enough to inhibit large osmotic pressure changes and most importantly, ice recrystallization. For most mammalian cells, the optimum rate cannot be obtained without the aid of a cryoprotective agent (CPA).[7]

1.2.4 Cryopreservation Agents

CPAs that are currently used can either be penetrating (glycerol or dimethyl sulfoxide) or non-penetrating (salts, sugars and polymers) to the cell. Polge, Smith and Parkes in 1949 were the first to use glycerol to enhance the cell viability of spermatozoa.[25] Only a few years later, the more cell permeable dimethyl sulfoxide (DMSO) was discovered to be equally as effective, if not more effective for certain cell types.[26] Lovelock and Meryman further proposed that CPAs which have a low molecular weight and are cell permeable will provide the best protection against cellular cryoinjury.[7,26,27] It was initially believed that these CPAs were solvating the residual solutes present outside and inside the cell which reduces osmotic efflux (cell dehydration) and decreases intracellular solute concentrations respectively.[7,26,27] However, their ability to inhibit ice recrystallization has not been fully documented. Furthermore, addition of

neutral CPAs increases the solute concentration both inside and outside the cell which further reduces ice formation and cell damage. Several hypotheses explaining the mechanism of action of DMSO have emerged. Firstly, it is proposed that DMSO replaces water within the cell to inhibit cell membrane rupture.[28,29] Secondly, it dilutes residual ionic solutes on the extracellular surface and reduces cell dehydration.[7,26,27] Thirdly, it is proposed that DMSO interacts with the phospholipid bilayer to stabilize and protect it from damage.[28,29] Finally, it is proposed that DMSO may allow formation of aqua pores within the cell membrane to relieve osmotic stress.[28,29] Although Lovelock and Meryman postulated that in order for a CPA to be effective it must enter the cell, the documented use of non-penetrating CPAs suggests otherwise.[30]

The discovery that many large macromolecules such as peptides (from peptone) and polymers (polyvinylpyrrolidone and polyethylene glycol, Figure 1.2) can protect cells from damage, as well as DMSO and glycerol alone, provides proof against the necessity of effective CPAs to be cell permeable and have low molecular weight.[30]

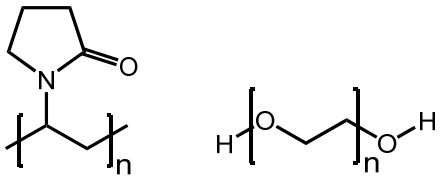

Figure 1.2 Repeating polymeric units in (**A**) polyvinylpyrrolidone and (**B**) polyethylene glycol[31,32]

It was proposed that the non-colligative freezing point depression achieved using polyvinylpyrrolidone is resulting from hydrogen bonding of water to the macromolecule.[33] It is also thought that water molecules bound to the polymer will reduce the amount of free water available for ice formation.[33] Unfortunately, the ice recrystallization ability of these cryoprotective polymers has also not been assessed.

Other common low molecular weight and non-penetrating CPAs are carbohydrates (mainly D-sucrose and D-trehalose).[34] D-Sucrose at 0.350 M can successfully protect red blood cells, chloroplasts and marrow stem cells from cryoinjury despite causing osmotic stress since it is unable to penetrate these cells at physiological temperatures.[15] More importantly, it has recently been noted that certain carbohydrates can inhibit ice growth during cryopreservation due to their unique hydration properties.[35,36] It therefore may be possible that hydration of carbohydrates within a frozen sample is preventing lethal ice recrystallization which enhances cell viability post cryopreservation.

It is also common to find cryoprotective "cocktails" which use a variety of penetrating and non-penetrating CPAs to preserve cells and this renders determining their individual mechanisms of action difficult.[37] One important fact overlooked is the considerable cytotoxicity of DMSO which produces harmful effects in patients receiving cell transplants preserved in DMSO.[38] Although it is proposed that high concentrations of carbohydrates (sucrose) cause osmotic shock,[15,16] full assessment of the cytotoxicity of these non-penetrating cryoprotectants has not been documented at physiological temperatures. Therefore, alternative non-toxic CPAs must be used. Currently, in the Ben Lab, new potential CPAs are being derived from a naturally occurring biological antifreeze polymer.[5,8]

1.3 Biological Antifreezes

1.3.1 Native Origins and Structures of Biological Antifreezes

Biological antifreezes are a class of peptide and glycopeptide polymers which have the ability to prevent uncontrolled ice growth *in vivo* and are found in a wide variety of amphibians, plants and fish. [39,40] These compounds were first discovered in Antarctic dwelling fish Antarctic Notothenioid *(Pagothenia borchgrevinki)* and Atlantic Cod *(Gadus morhua)* (Figure 1.3), which are able to survive in temperatures reaching -1.9 °C, which is 1.2 degrees lower than the freezing point of their isolated blood serum and internal fluids.[41] It is known that higher concentrations of sea salt can depress the equilibrium melting/freezing point of water to -1.9 °C by colligative effects.[42] However, the plasma of these fish contain only about one-third of the solute molarity of the surrounding sea water.[43]

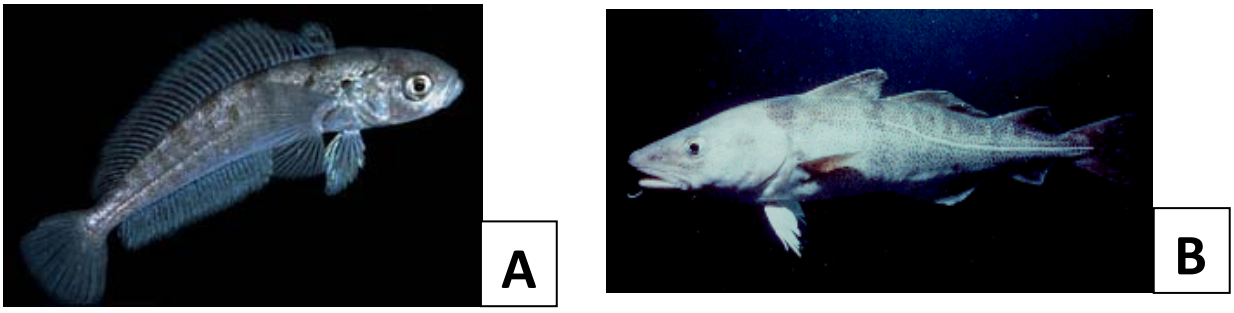

Figure 1.3 Antarctic Notothenioid *(Pagothenia borchgrevinki)* (**A**) and Atlantic Cod *(Gadus morhua)* (**B**)[39,40]

Extensive studies have elucidated the key structures of the different biological antifreezes discovered.[44,45,46,47] Currently there are five known distinct classes of antifreezes: four types of antifreeze proteins (AFP) I, II, III, IV (which are also found in insects, amphibians and plants) and one class of antifreeze glycoproteins (AFGPs), which are exclusive to fish, see Table 1.1.[48] The AFPs vary quite significantly in primary, secondary and tertiary structures. Type I AFPs

consist of alanine-rich α helices while AFP types II and III are significantly less structurally organized than type I. Type II protein complexes have a larger number of disulfide bonds, whereas type III AFPs display β-sandwich conformations. The last class of antifreezes to be discovered is type IV AFPs and these display structural similarities to type I AFPs.[49]

Table 1.1 Summary of origin, classification and key structural differences between representative antifreeze proteins and glycoproteins.[44-49]

Characteristic	AFGP	Type I AFP	Type II AFP	Type III AFP	Type IV AFP
Mass (kDa)	2.6 - 33	3.3 – 4.5	11 - 24	6.5	12
Key Properties	TAA repeat; disaccharide	Alanine-rich α-helix	Disulfide bonded	β-sandwich	Alanine rich; helical bundle
Representative Structure	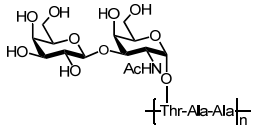				
Natural Source	Antarctic notothenioids; northern cods	Right-eyed flounders; sculpins	Sea raven; smelt; herring	Ocean pout; wolfish; eel pout	Longhorn sculpin

AFGPs, on the other hand, possess much higher structural homology between species, rendering their use for further structure activity studies more attractive.[41] Their general structure consists of repeating tripeptide units (threonyl-alanyl-alanyl) in which the secondary hydroxyl group of the threonyl residue is glycosylated to a disaccharide unit, β-D-galactosyl-(1,3)α-D-*N*-acetylgalactosamine (Figure 1.4).[50] Eight subtypes of AFGPs were isolated from various fish plasma and differ mainly by their molecular weight which reflects the number of repeating glycopeptide units.[51] The larger AFGPs (1 to 5) contain up to 50 units and are 20 kDa to 30 kDa in size. The smaller AFGPs (6 to 8) contain fewer units, with AFGP 8 **(1)** having only four, and

are <20kDa in size. It is known that the larger AFGPs possess greater TH activity than the smaller AFGPs.[51]

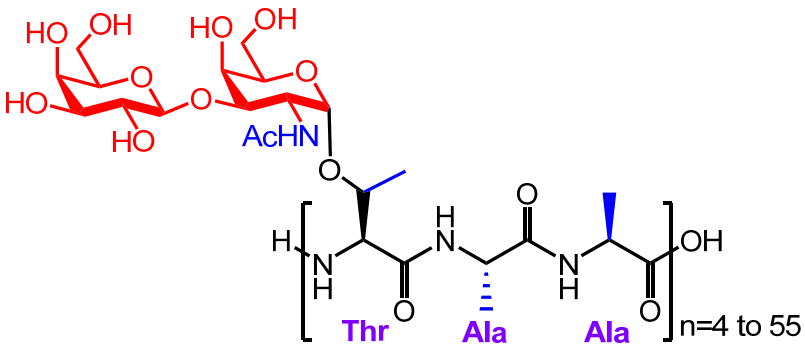

Figure 1.4 Glycopeptide repeating building block of native AFGPs.[50]

Although AFPs and AFGPs possess different structures, they exhibit similar antifreeze properties.[39,40] These properties are of great medical and industrial interest because they provide promising applications to such domains as cryosurgery, cryopreservation, food science and agriculture.[9,10,11] Unfortunately, their mode of action at the ice-water interphase is still unclear. It is generally agreed that, on a macroscopic scale, these antifreeze molecules will bind to specific faces of a growing ice crystal in order to prevent further growth.[52,53,54]

1.3.2 Physical Properties of Water and Ice

Since AF(G)Ps act to inhibit ice growth, a brief description of ice formation follows.

At standard atmospheric temperature and pressure, water is liquid and dynamic, forming reversible, yet strong intermolecular electrostatic hydrogen bonds.[55] As more energy is removed from the system, via reduced temperature, the molecules become more structured and organized. Unlike most compounds that become denser with cooling, water increases in volume to form lighter and highly structured ice.[56]

As water is cooled below its freezing point (0°C), the reversible nature of hydrogen bond formation of bulk water molecules diminishes; allowing for the formation of ice. Nucleation of small ice crystals begins around impurities, onto which subsequent water molecules bind to increase the crystal size and subsequently form solid ice.[56] Interestingly, the water surrounding newly formed ice crystals is not as dynamic as originally thought.[57,58,36] There exists a semi-ordered, nanometer thick layer of water at the interphase between solid ice and liquid water which is called the quasi-liquid layer (QLL) (Figure 1.5).[57,58,36] The thickness of the QLL is inversely dependent of the temperature, so that a thinner QLL is formed in colder temperatures.[57,58] The exact dynamic nature of this layer is uncertain, however, it is known that the QLL is more ordered than liquid water, but less than solid ice. Therefore, determining the mechanism of action of compounds that work at this ice-water interphase, such as AF(G)Ps, is difficult.

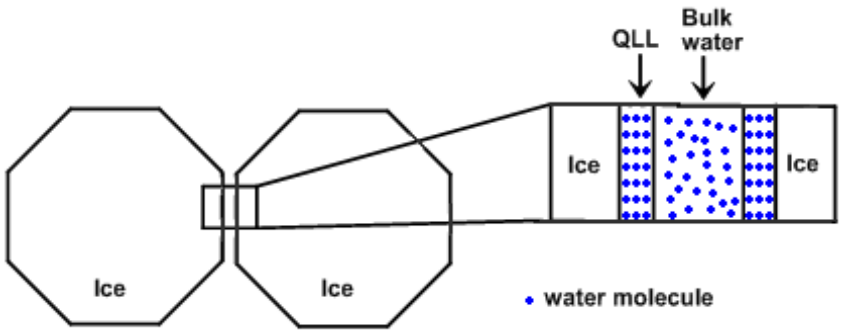

Figure 1.5 Schematic representation of the ice-water interphase with presence of a semi-ordered quasi-liquid layer (QLL) [57,58,36]

In order to increase ice crystal size, further addition of water molecules to the seed crystal is required. Addition is enthalpy dependent and is further dependent on ice structure.[56]

In standard ice formation conditions (101.1 kPa), the structure of an ice crystal is a hexagonal prism with defined faces and axes as shown in Figure 1.6.[59]

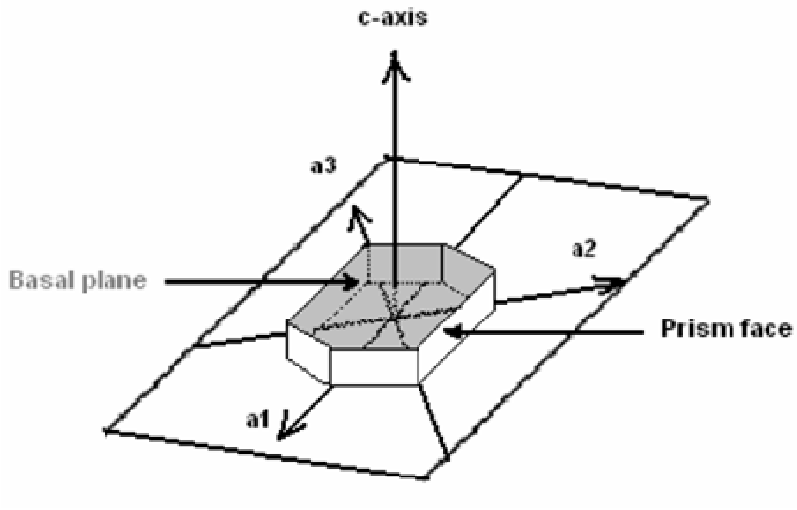

Figure 1.6 Schematic representation of the structure of an ice crystal formed in pure water[59]

The orientation of water molecules within the three dimensional lattice is two directional.[56] The water molecules along the basal face are oriented in repeated "chair-like" conformations via hydrogen bonding (Figure 1.7A).[56] In contrast, the water molecules in the prismatic face are oriented in "boat-like" conformations (Figure 1.7B).[56] The structural differences between the two faces therefore cause different enthalpic requirements for subsequent water molecules to attach to each face. Ice growth therefore occurs differently on the basal face in comparison to the prismatic face when the crystal is subjected to various ice-forming conditions.[56]

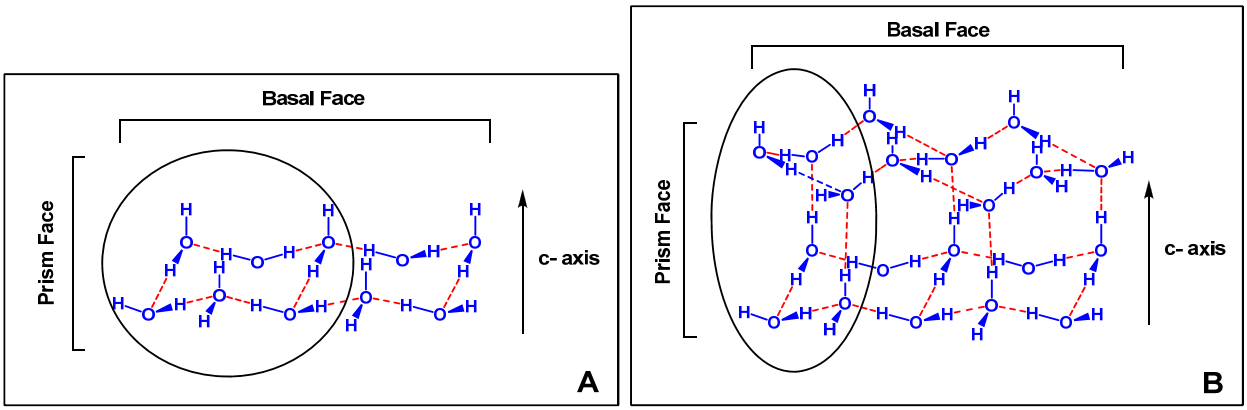

Figure 1.7 Schematic representation of the orientation of water molecules within the three dimensional ice lattice. Water molecules found on the basal face are ordered in (**A**) "chair-like" conformation and molecules found on the prismatic face are ordered in (**B**) "boat-like" conformation.[56]

As mentioned, the formation of larger ice crystals in and around the plasma membrane of cells is proposed to cause membrane damage and subsequent cell death during cryopreservation.[2,3,7] Therefore, the ability of AF(G)Ps to inhibit the growth of large ice crystals provides an interesting solution to mammalian cell cryoinjury during preservation.[60]

1.3.3 Thermal Hysteresis (TH)

As previously mentioned, when ice is formed under atmospheric conditions, small seed crystals begin to form as the temperature is lowered below the equilibrium melting/freezing point (0 °C at 101.1kPa).[56] Addition of colligative solutes (neutral or charged electrolytes) increases the enthalpy of ice formation and lowers the freezing equilibrium below 0°C.[61] As shown in Figure 1.8, the change in the melting/freezing point of separate solutions of sodium chloride, D-galactose and chicken lysozyme is proportional to the concentration of solute added, suggesting that these solutes are acting colligatively.[42,62] However, this linear (concentration-dependent freezing point depression) correlation is not observed with AFGP. This suggests that unlike the other solutes in Figure 1.8, AFGP 8 (**1**) acts non-colligatively.[42,62,63] It is important to note that

NaCl acts synergistically with AFGP to further decrease the freezing point in a non-colligative fashion which suggests that the specific structural nature of AFGP is responsible for affecting ice formation.[42,62,63] It was later revealed that all AF(G)Ps act non-colligatively and that AF(G)Ps alter the freezing point independent of the melting point in a process called thermal hysteresis (TH).[64]

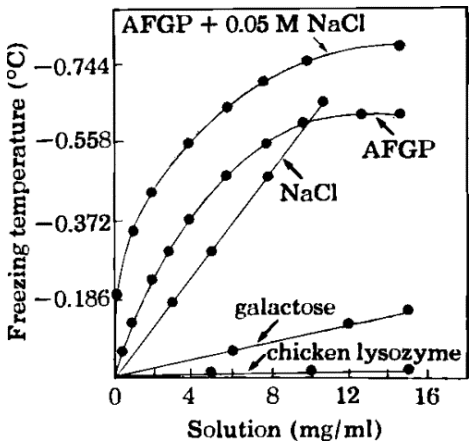

Figure 1.8 Freezing temperatures (°C) of solutions of chicken lysozyme, galactose, sodium chloride (NaCl), AFGP 8 (**1**) and AFGP 8 (**1**) with NaCl.[40,42]

Harding and coworkers theorized that AF(G)Ps bind to small seed crystals and prevent ice nucleation.[48,65,66] However, since ice crystals do form at lower temperatures in the presence of AF(G)Ps, Knight and DeVries suggested that TH occurs as a result of AF(G)Ps binding to the ice surface to inhibit further ice growth.[67,68] There are two postulated static models which illustrate how ice growth occurs in the presence of AF(G)Ps.[67,68] The first two dimensional model suggests that ice growth is prevented perpendicular to the ice surface with irreversible binding of the AF(G)P and is known as the mattress model (Figure 1.9A). The second model, known as the step pinning model (Figure 1.9B), demonstrates how AF(G)Ps inhibit ice growth on the three dimensional crystalline surface of ice.[68]

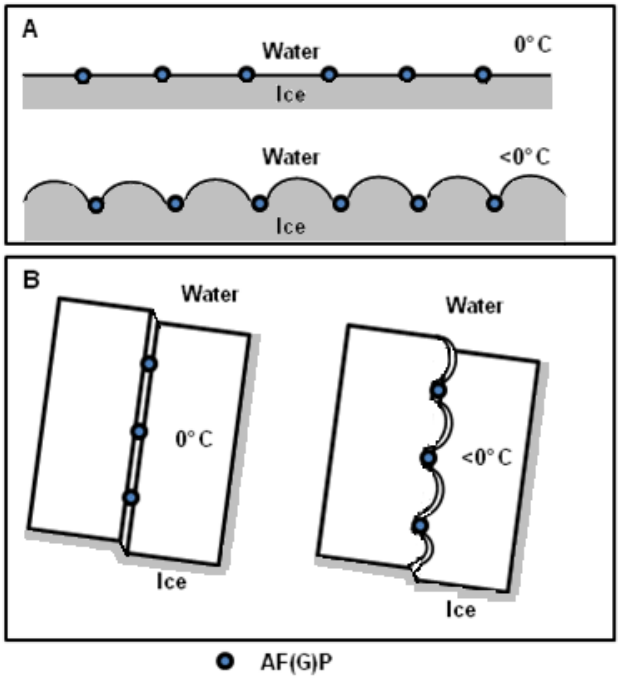

Figure 1.9 Schematic representations of (**A**) the mattress and (**B**) step pinning models of the Kelvin Effect induced by AF(G)Ps bound to the ice-water interphase.[68]

While the reversible nature of AF(G)Ps binding to the ice crystal surface is a source of debate,[65-68] arresting ice growth along the ice surface forces the addition of water molecules to the free unbound ice surfaces that are exposed between AF(G)Ps.[68] As more water molecules are added, the ice surface becomes convex which causes an increase in energy required for further addition to these convex surfaces. This process is also known as the Kelvin effect.[68] The increasing energy required to add additional water molecules to the ice surface causes a depression in the freezing point temperature while the incorporated water molecules require more energy to detach from the ice lattice. Therefore, the freezing point temperature is independent of the melting point temperature which remains at 0°C.[64] The resulting temperature difference between melting and freezing point of AF(G)P bound ice is known as the TH gap (Figure 1.10). In most AFGPs this TH gap will not exceed 1.0 °C, however, some terrestrial anthropoids have "hyperactive" AFPs that increase this gap up to 6.0 °C.[69] It is believed that

these hyperactive AFPs will bind to both prismatic and basal faces to enhance ice growth inhibition.[69] It is also noted that the TH gap will increase with greater concentrations of AF(G)Ps and that the size of an ice crystal held within a specific TH gap will remain constant.[70]

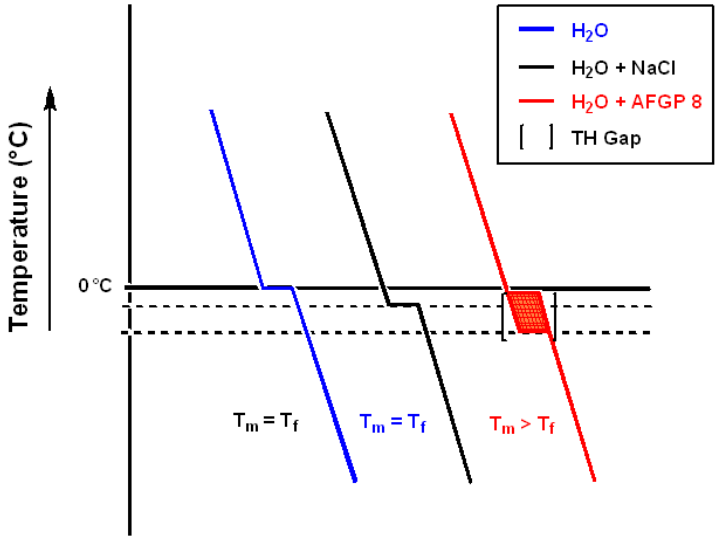

Figure 1.10 Schematic representation of thermal hysteresis of solutions of pure water, colligatively acting sodium chloride (NaCl) and AFGP 8 (**1**).[64-68]

1.3.4 Dynamic Ice Shaping (DIS)

An ice crystal's morphology in the presence of AF(G)Ps is different than crystals formed in pure water.[70] An ice crystal formed in pure water will appear circular in shape. Below the equilibrium freezing point of pure water, additional water molecules usually bind to the prismatic faces of the ice crystal as shown in Figure 1.6.[70,59] In the absence of AF(G)Ps, adhering to the basal face requires more energy, therefore ice growth is normally observed along the prismatic face to gradually form sheets of ice.[70]

It was determined by ellipsometry that AF(G)Ps bind to the prism faces to inhibit this typical prismatic face growth.[71] Since AF(G)Ps block the adhesion of water molecules to the

prism faces, the water molecules will slowly add to the basal face, resulting in the formation of hexagonal bipyramidal crystals held within the TH gap (Figure 1.11).[70,71,59]

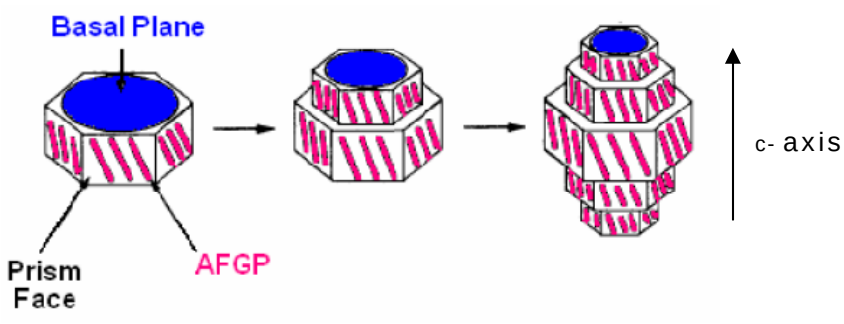

Figure 1.11 Schematic representation of the formation of bipyramidal ice crystals in the presence of AF(G)Ps[59]

Rapid or "burst" growth of ice crystals occurs along the c- axis once the TH gap is surpassed, resulting in long spicule-like structures (Figure 1.12).[71,72] The formation of spicules (below -1°C to -6°C) can cause significant structural damage to membranes and internal cell organelles, which limits AF(G)P use in cryopreservation.[6,9] Rubinsky has utilized this AF(G)P property to eradicate tumor cells in cryosurgery.[6,9]

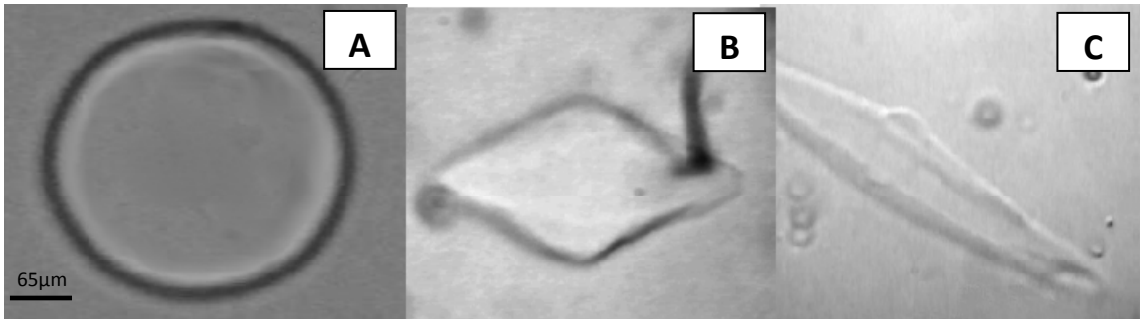

Figure 1.12 Ice crystals grown in (**A**) a sample of distilled water, (**B**) a sample of AFGP held within the thermal hysteresis (TH) gap and (**C**) a sample of AFGP in temperatures below the TH gap.[72]

1.3.5 Ice Recrystalization Inhibition (IRI)

Although DIS, resulting from uncontrolled crystal growth outside the TH gap is detrimental to the cell,[6,9] AF(G)Ps posses ice recrystallization inhibition activity which is a cell cryoprotection property.[73,74] Ice recrystallization inhibition (IRI) involves inhibiting the formation of large ice crystals when ice samples are kept frozen for long periods of time which has important applications in cell and food preservation.[10,11] Usually when ice samples containing small-sized crystals are kept at a sub-melting temperature, entropic effects will promote the formation of larger crystals at the expense of smaller crystals.[73] This thermodynamic process, called recrystallization, is driven by the overall reduction in grain boundary energy.[73,74] For example, the grain boundary of two smaller ice crystals is larger than the boundary of a larger crystal resulting from merging the two smaller crystals together.[73,74] Solutes present in the solution will normally be pushed along with the migrating grain boundaries. Interestingly, certain IRI active AFPs and AFGPs are able to dramatically limit this grain boundary migration (Figure 1.13). Therefore, ice samples containing IRI active AF(G)Ps will have small ice crystals present which is believed to reduce cell membrane damage.[20,73,74,75]

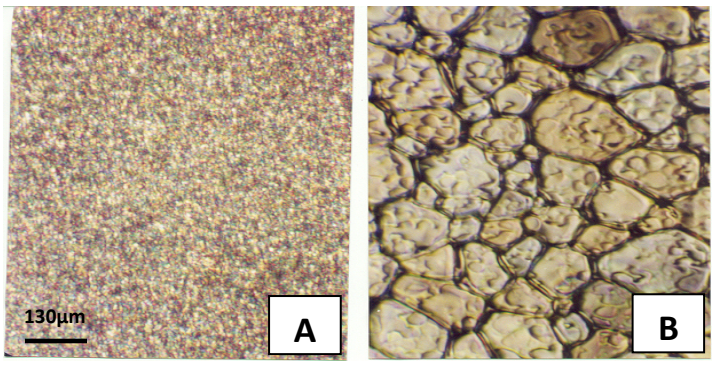

Figure 1.13 Ice crystals formed in a solution of (**A**) IRI active AFGP 8 (**1**) at 5.5 x 10^{-6} M and (**B**) IRI inactive phosphate buffered saline (PBS).[6]

Having such extraordinary properties, the direct use of AFGPs has been explored, but great limiting factors exist which prevent their use in cryopreservation. Their isolation from limited natural sources is quite laborious and costly.[60] Synthetic production of these natural AFGPs unfortunately is also quite difficult and expensive,[60] and to date only one total synthesis of AFGP 8 (**1**) has been reported by Filira *et al*.[76] The cryopreservation studies on cell, tissues and organs using AFGPs as cryoadjuvants have conflicting results. Pig oocytes, mouse embryos, carp spermatozoa and human platelet cells all had increased cell viability post cryopreservation with AFGPs.[67,77] Further studies propose that AFGPs protect the cell by stabilizing the phospholipid bilayer during thermatropic phase transition.[78] Unfortunately, high concentrations of AFGPs failed to protect an isolated rat heart during the freeze-thaw process[79] and it is believed that the DIS, which forms long "ice spicules" is causing additional cell damage.[6,40,80] Since AFGPs would be used as an alternative to cytotoxic DMSO, the newly discovered cytotoxicity of AFGP 8 (**1**) to human liver and kidney cells eliminates its possible use as a cryopreservant.[5] It was previously believed that TH, DIS and IRI were inseparable and prevented AFGP analogue production. The discovery by Sidebottom of an AFP from ryegrass (*Lolium perenne*) which exhibits IRI activity and no TH activity suggests that certain structural components of biological antifreezes impart TH and DIS while others impart IRI activity.[81] This may suggest entirely different modes of action for both TH and IRI activity.

1.4 Structure Activity Relationship Studies and Rational Design of AFGP Analogues

1.4.1 Initial Structure-Activity Studies Conducted on AF(G)Ps

Previous structure-activity studies conducted on native AFGPs concluded that the pyranose ring, hydroxyl groups (except for the C6 hydroxyl group) and cis hydroxyl groups on

the carbohydrate moiety are essential for TH activity.[82] Also, the length of AFGPs is directly proportional to TH activity with AFGP 8 (n=4) (**1**) displaying a 70% reduction in TH activity compared to AFGP 1 (n=55).[83] A comprehensive study conducted by Nishimura revealed many structural features of AFGP 8 (**1**) which are important for TH activity (Figure 1.14). It was confirmed that AFGP 8 (**1**): (a) requires a disaccharide over a monosaccharide, (b) requires an *N*-acetyl group (NAc) on the first galactose sugar, (c) requires hydrophobic alanine residues on the tripeptide chain, (d) requires the methyl group of the *O*-linked threonyl residue on the tripeptide backbone and finally (e) requires the stereochemistry of the glycosidic linkage between the saccharide and peptide backbone to be α instead of β.[84] Unfortunately, this study did not test for IRI activity.

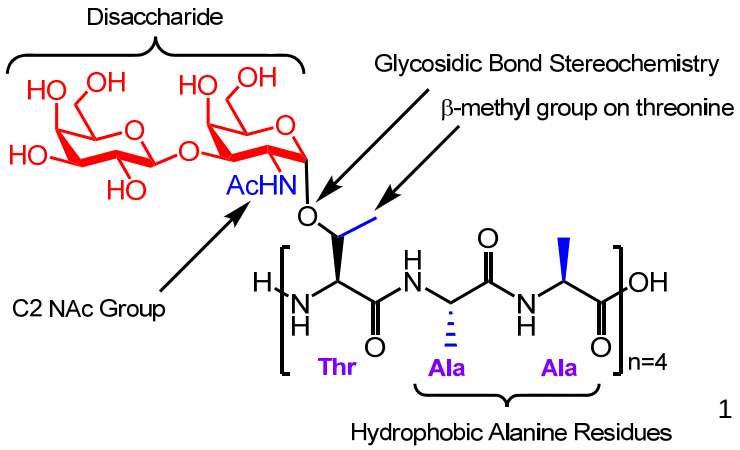

Figure 1.14 Structural components of AFGP 8 (**1**) required for TH activity[84]

1.4.2 First and Second Generation AFGP Analogues

This prompted Ben *et al*. to synthesize AFGP analogues to probe the structure activity relationship between AFGP and IRI activity.[60] An important issue faced regarding chemical synthesis of AFGP 8 (**1**) analogues is the poor stability of the galactose-threonyl *O*-linkage which can undergo acidic, basic and β-glycosidase cleavage.[85] The solution proposed by Ben *et*

al. was to change the *O*-linkage for a *C*-linkage since literature precedence indicated that glycopeptides with *C*-linkages and *S*-linkages have increased stability.[86] The chosen analogue, ((*C*-(KGG)-gal (**2**), shown below (Figure 1.15), had several modifications.[87] First, the disaccharide β-D-galactosyl-(1,3)α-D-*N*-acetylgalactosamine was shortened to one molecule of D-galactose.[87] Also, lysine replaced threonine because its functional group has approximately the same length as arginine, which will often replace threonine in the smaller native AFGPs (7 and 8).[87] Finally, glycines, which are similar in length to alanine, were used to eliminate the possibility of forming diastereoisomers during solid phase assembly.[87] Although its antifreeze activity was low (Graph 1.1),[87,88,89] this first attempt at rationally designed AFGP analogues did however set precedence for the use of the more stable *C*-linkage.

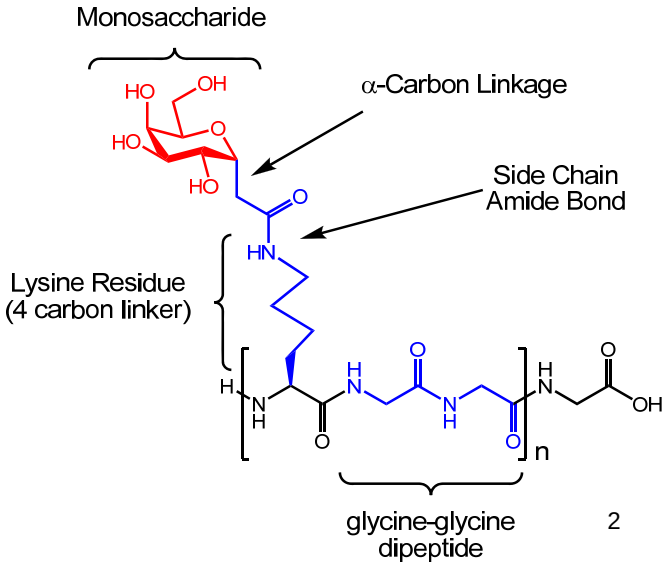

Figure 1.15 Repeating building block of first generation *C*-linked AFGP analogue ((*C*-KGG)-gal (**2**)[87]

One vital second generation *C*-linked analogue, shown in Figure 1.16, had a shortened peptide side chain with incorporation of ornithine, (*C*-OGG)-gal (**3**).[88] The antifreeze activity and cytotoxicity results of this compound were quite surprising (Graph 1.1).[87,88,89] Firstly, this

compound exhibited potent IRI activity and minor DIS. Secondly, this compound was the first to display no TH activity which suggests that TH and IRI are not directly linked and can be obtained by synthetic manipulations.[5,88] Also, several different cytotoxic tests revealed that ((*C*-OGG)-gal) (**3**) remained non-toxic to both liver and kidney cell lines at concentrations from 0.63mg/mL to 2.0 mg/mL.[5,88] Interestingly, of the two second generation analogues shown in Figure 1.16 (**3**, **4**) the more potent *C*-linked analogue (**4**) had a shorter, all aliphatic linkage between the peptide backbone due to the presence of a serine derived amino acid (Graph 1.1).[88,89] Several other *C*-linked serine analogues were prepared with increasing aliphatic chain lengths to probe the influence of the linker length on IRI activity. It was revealed that the *C*-serine analogue ((*C*-SGG)-gal) (**4**) with two methylene units provided optimal IRI activity.[90] It is still unclear exactly how length affects IRI activity. Recent studies suggest that the size of the linker is affecting the orientation of the carbohydrate in relation to the peptide backbone which governs overall hydration of the glycopeptide.[90]

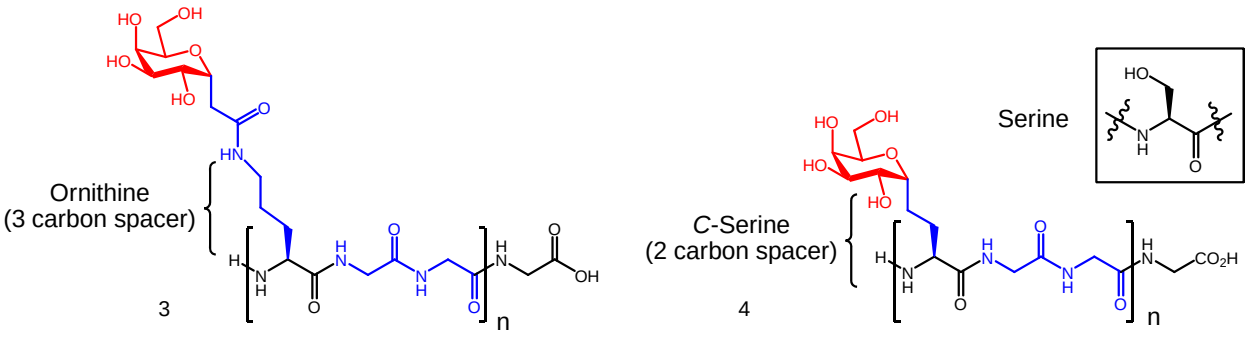

Figure 1.16 Repeating building blocks of second generation *C*-linked AFGP analogues ((*C*-OGG)-gal) (**3**) and ((*C*-SGG)-gal) (**4**)[88,89]

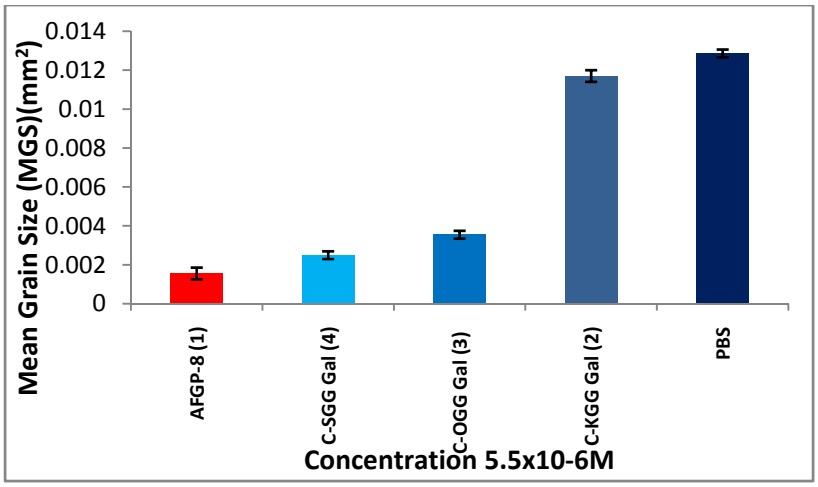

Graph 1.1 IRI activities of first and second generation AFGP analogues (**2**, **3**, **4**) compared to AFGP 8 (**1**) and phosphate buffered saline (PBS) (negative control). [87,88,89]

In a slightly different experiment, Trant and Biggs in the Ben group synthesized a series of *N*-alkyl-acetamide galactosyl derivatives which had increasing alkyl chain lengths to probe the importance of anomerically substituted alkyl chains on galactose IRI activity (Graph 1.2).[91] Interestingly, there also seemed to be an optimal alkyl chain length at which IRI activity was obtained. The propyl amide derivative, as shown in Graph 1.2, had the greatest IRI activity overall.

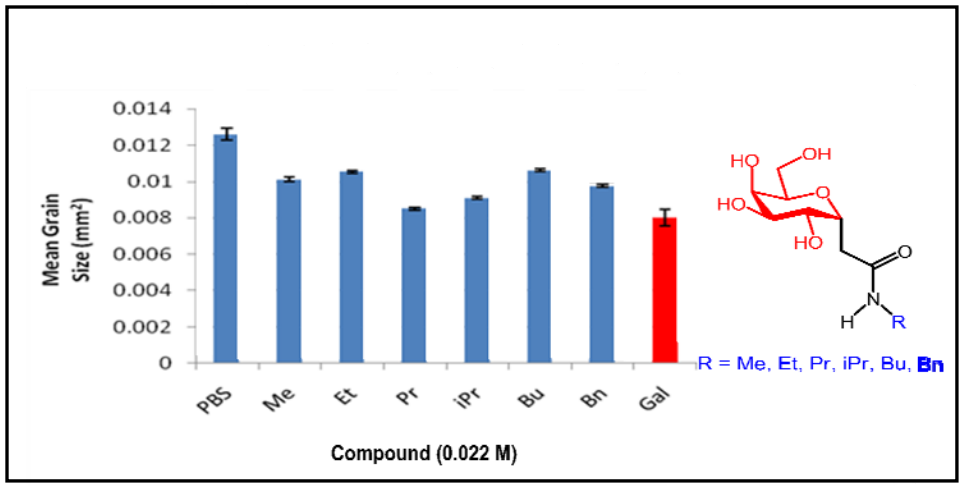

Graph 1.2 IRI activities of previously synthesized *N*-alkyl-acetamide derivatives compared to galactose and PBS[91]

In relation to the nature of the anomeric linkage, the IRI activity of a prepared *O*-linked serine analogue ((*O*-SAA)-gal) (**5**) was compared to the *C*-linked serine analogue ((*C*-SGG)-gal) (**4**).[92] The *C*-linked analogue, with the less electronegative atom in the anomeric position, had more potent IRI activity. This led Campbell to probe the influence of a less electronegative sulfur atom (in relation to the *O*-linked analogue) with the generation of stable *S*-linked serine analogues, ((CGG)-gal) (**6**) and ((CAA)-gal) (**7**) (Figure 1.17).[93] Replacing serine by cysteine on the peptide backbone afforded the desired compounds.

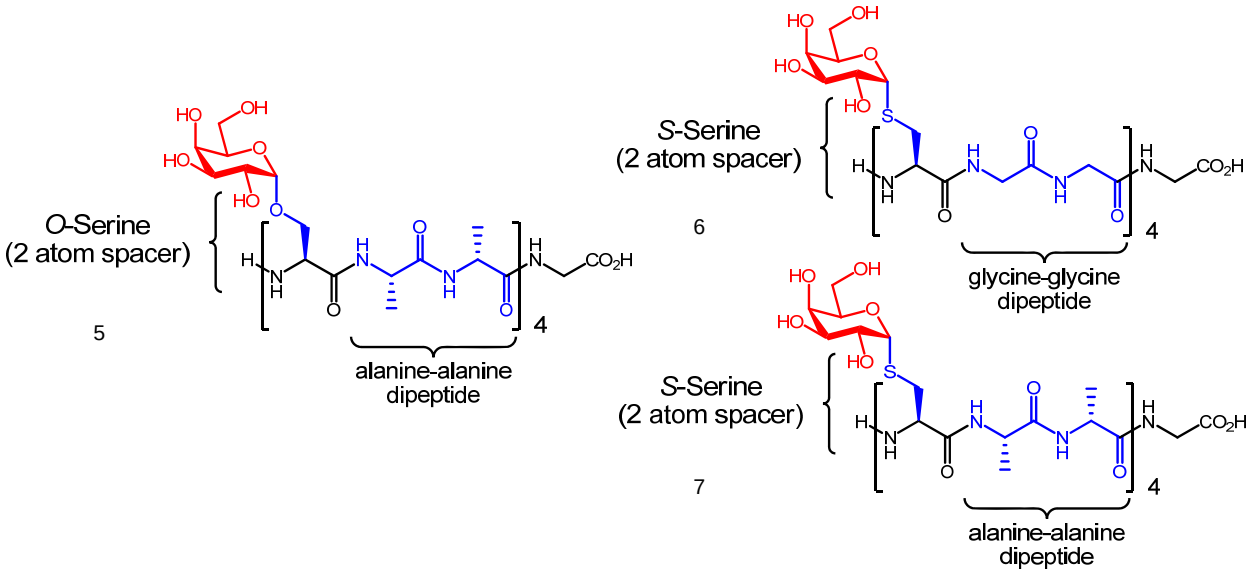

Figure 1.17 Repeating building block of *O*-linked serine analogue (**5**) and *S*-linked AFGP analogues (**6, 7**) synthesized by Campbell[92,93]

From the results it can be concluded that the larger sulfur atom at the anomeric position causes reduced IRI activity compared to the *O*-linked analogue, and has even less IRI activity compared to the *C*-linked counterpart (Graph 1.3).[93] The nature of this effect as well as the importance of the anomeric stereochemistry needs further investigation.

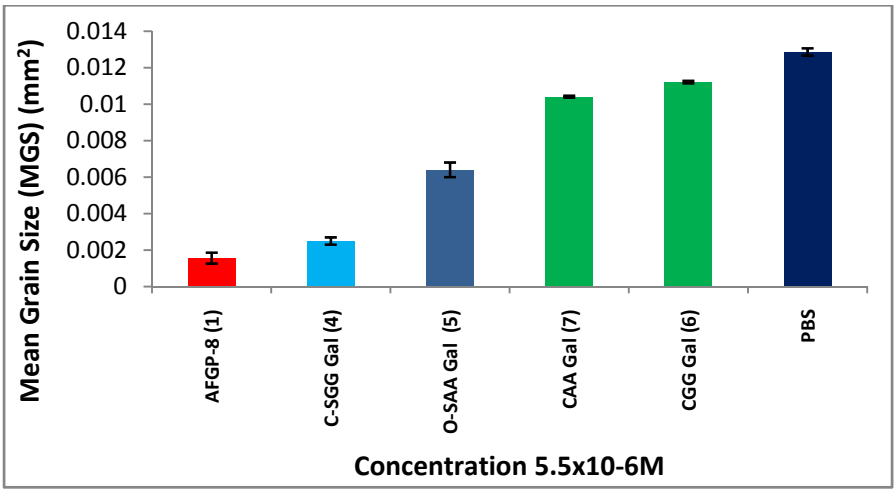

Graph 1.3 IRI activity of previously synthesized *S*-linked serine AFGP analogues (**6**, **7**) compared to *O*- and *C*-linked serine analogues (**4**, **5**), AFGP 8 (**1**) and PBS.[89, 92, 93]

1.4.3 Influence of Carbohydrate Hydration on IRI Activity of AFGP analogues

To probe the effect of the carbohydrate moiety on IRI activity, the second generation analogue ((*C*-OGG)-gal) (**3**) was further modified.[58] It was hypothesized that stereochemistry of the carbohydrate affected its hydration which is both important for cryopreservation ability and antifreeze activity.[58] Czechura *et al*. prepared four analogues of ((*C*-OGG)-gal) (**3**) which had D-galactose (Gal) (**3**), D-glucose (Glu) (**9**), D-mannose (Man) (**10**) and D-talose (Tal) (**11**) as the monosaccharide moiety attached to the peptide backbone and tested their IRI activity (Figure 1.18).[58]

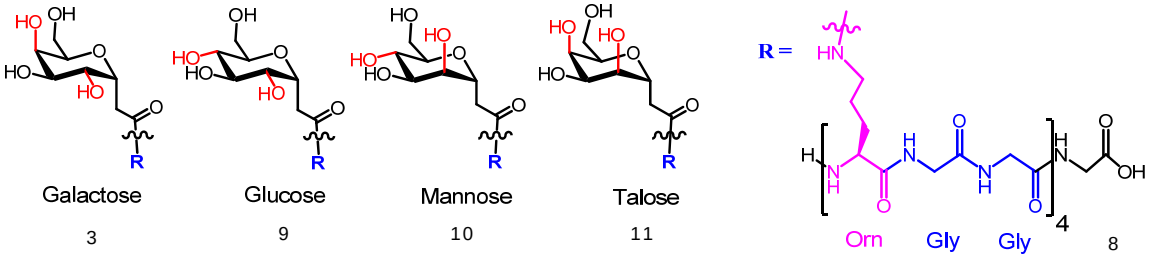

Figure 1.18 *C*-linked AFGP analogues (**3, 9-11**) previously synthesized and tested by Czechura *et al*.[58]

It was noted that increases in IRI activity, among the glycoconjugates tested, were proportional to the decreases in partial molar compressibility values for the corresponding free reducing sugars described by Galema and Høiland.[94] This parameter as defined by Galema *et al.* is a measure of how well the hydrated compound is incorporated, or "fits", into the three dimensional water network of surrounding water and was determined using molecular dynamic simulations, kinetic experiments and density and ultrasound measurements.[94] The poorer the compatibility with the surrounding water network, the poorer the compressibility of the hydrated carbohydrate (Figure 1.19).[58,94]

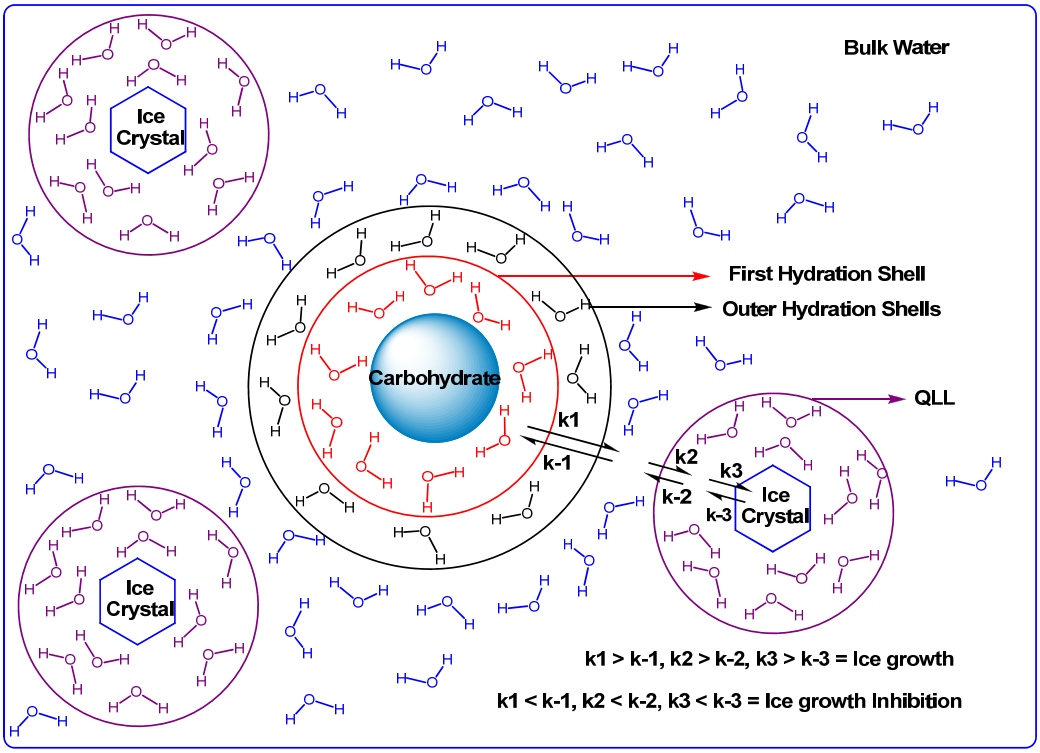

Figure 1.19 Schematic representation of the hydration layer surrounding a solute (ex. carbohydrate) in the presence of ice crystals.[58]

This will result in a larger compressibility value. The partial molar compressibilities of the four carbohydrates used in this study are shown in Graph 1.4 as a function of the IRI activity

of the glycoconjugates containing these carbohydrates.[58] It can be concluded that the higher the partial molar compressibility of the carbohydrate, which represents poorer carbohydrate compatibility with the surrounding water network, the better the IRI activity (Graph 1.4).[58]

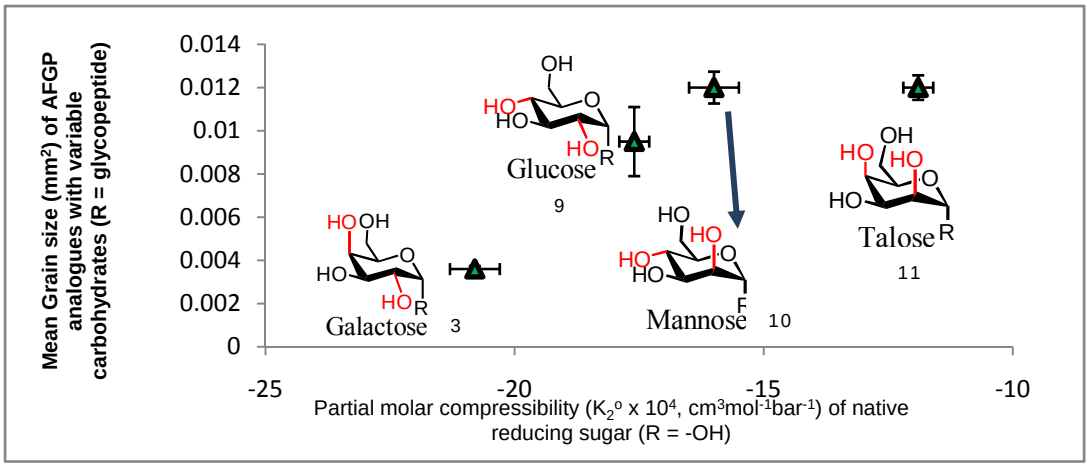

Graph 1.4 IRI activities (tested at 5.5 x 10^{-6} M) of *C*-linked AFGP analogues (**3**, **9-11**) as a function of the partial molar compressibility of their respective native free reducing sugar.[58]

This led to a new hypothesis regarding AFGP mode of action. As previously mentioned, the ice-water interphase is more complex than previously believed.[57,58,36] There exists a semi-ordered quasi- liquid layer (QLL) which is ~1nm thick at -6°C (the temperature of the IRI assay) and corresponds to three monolayers of semi-ordered water.[57,58,36] It is proposed that for larger crystals to form, water molecules from the bulk water phase must migrate to the QLL before further migrating to the ice lattice (Figure 1.19).[57,58,36] As hydration of the sugar moiety is important for activity, it is believed that instead of directly binding to the ice lattice, native AFGPs bind to the bulk water and greatly disrupts the semi-ordered nature of the QLL (Figure 1.19). [57,58,36] This results in a higher energy requirement for the disrupted and poorly ordered water molecules from the bulk water to enter the QLL and further bind to the ice lattice, resulting in ice crystal growth inhibition. Therefore, the D-galactose analogue, having the worst "fit" with the three dimensional water network provides the best IRI.[58] This study demonstrated that

carbohydrates themselves have significant IRI activity and that hydration of these carbohydrates is altering their antifreeze activity.[58] More importantly, the results were consistent with the literature which states that stereochemistry of C2 and C4 hydroxyl groups are important for hydration of carbohydrates.[94,95,96] Therefore, the specific C2 and C4 hydroxyl group stereochemistry of the galactose residue is responsible for the increased IRI activity of ((*C*-OGG)-gal) **(3)** over the other glycopeptides tested (**9-11**).[58]

Since the glycoconjugates were tested for IRI activity and compared to the hydration of the free reducing sugars, there lacked a direct comparison between the hydration parameters of the free reducing sugars to their respective IRI activity.[58,36] This led Tam *et al*. from the Ben group to further probe the link between carbohydrate hydration and IRI activity.[36] A brief discussion on carbohydrate hydration, followed by the results of this study will be presented.

1.5 Carbohydrate Hydration

As previously mentioned carbohydrates are used alone and in conjunction with DMSO and glycerol to cryopreserve cells.[15,35,37] It is theorized that since sugars do not enter the cell without active transport, they somehow affect the recrystallization of ice in and around a cell by interacting with extracellular water molecules during the freezing process.[15] Sugars, such as trehalose, were shown to inhibit ice crystal growth using transmission electron microscopy.[97] It is believed that ice growth inhibition as well as cryopreservation is correlated with the high degree of carbohydrate hydration.[36,58,94-97] The hydration of a carbohydrate is dependent on its structure, more importantly, the number of hydroxyl groups (which act either as hydrogen bond donors or hydrogen bond acceptors) and hydroxyl group stereochemistry. Several studies have elucidated key structural features which affect carbohydrate hydration. Due to steric restraints, it

is believed that equatorial hydroxyl groups are better hydrated than axial groups.[94,98] It is also believed that since intramolecular bonds form more readily than intermolecular bonds, hydrogen bond networks may be formed within the carbohydrate ring as long as they have the required stereochemistry to obtain the right hydrogen bond distance. It is believed that the C4 hydroxyl group stereochemistry greatly affects this intramolecular hydrogen bond network.[94-98] Lopez de la Paz further suggested that the electronics of the carbohydrate ring affects the nature of the hydrogen bond network such that electron poor hydroxyl groups which are next to electron withdrawing groups will act as hydrogen bond donors.[99] Galema and Høiland proposed that the distance between each adjacent hydroxyl group is the main factor affecting hydration.[94] They also proposed that the hydroxyl group stereochemistry of C2 and C4 greatly affects the carbohydrate's compatibility with the hydrogen bonded network of surrounding hydrating water molecules.[95] Mastai also concluded that as long as there are at least two hydroxyl groups spaced 4.2 to 4.5 Å apart on a carbohydrate ring, the carbohydrate is better hydrated since it matches the hydrogen bond network of surrounding water.[96] Interestingly, it was discovered that the possibility of an intramolecular hydrogen bond between the hydroxyl groups on C2 and C4 of D-talose would render these hydroxyl groups less hydrated and would contribute to the increased hydrophobicity of D-talose.[95]

1.5.1 Effect of Carbohydrate Hydration on IRI activity

In order to further link carbohydrate hydration to IRI activity, the IRI activities of several monosaccharides (**12-15**) and disaccharides (**16-20**) were compared to their published hydration number, partial molar compressibilities and partial molar volume (Table 1.2)[36,58,94]

Table 1.2 Partial molar compressibility (10^4 $K_2^o(s)$, cm^3 mol^{-1} bar^{-1}), hydration number, and partial molar volume (cm^3) of various monosaccharides and disaccharides. Errors are shown in parentheses.[36, 58, 94]

Carbohydrate	Molar Compressibility ($K_2^o(s)x10^4$, cm^3 mol^{-1} bar^{-1})[94]	Hydration Number (0.1)[94]	Partial Molar Volume (cm^3)[94]	Carbohydrate	Molar Compressibility ($K_2^o(s)x10^4$, cm^3 mol^{-1} bar^{-1})[94]	Hydration Number (0.1)[94]	Partial Molar Volume (cm^3)[94]
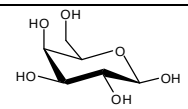 D-Galactose (**12**)	-20.8 (0.5) -20.4 (0.4)	8.7	110.2 (0.3)	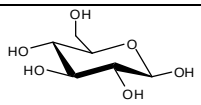 D-Glucose (**13**)	-17.6 (0.3)	8.4	111.7 (0.3)
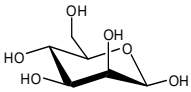 D-Mannose (**14**)	-16.0 (0.5)	8.1	111.3 (0.3)	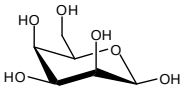 D-Talose (**15**)	-11.9 (0.3)	7.7	112.5 (0.1)
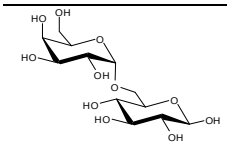 D-Melibiose (**16**)	-31.2 (1.0)	15.5	204.0 (0.2)	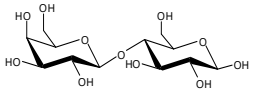 D-Lactose (**17**)	-31.1 (0.2) -30.4 (1.0)	15.3	207.6 (0.2)
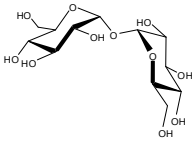 D-Trehalose (**18**)	-30.2 (0.3)	15.3	206.9 (0.5)	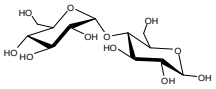 D-Maltose (**19**)	-23.7 (1.0)	14.5	208.8 (0.3)
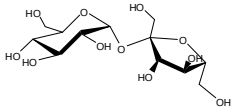 D-Sucrose (**20**)	-17.8 (0.5)	13.9	210.2 (0.3)				

The hydration number of a compound is defined as the number of hydrating water molecules which are tightly bound to the compound to form the first hydration shell.[94] This parameter is said to give a more accurate representation of the number of water molecules that

immediately surround the solute than partial molar compressibility, which expresses the compressibility of the first two hydration shells surrounding the solute.[94] Partial molar volume is a measure of the volume of the carbohydrate and first hydration shell.[94] As shown in Graph 1.5, the IRI activities of the monosaccharides (**12-15**) and disaccharides (**16-20**) listed in Table 1.2 were tested at 0.022 M and plotted as a function of their calculated hydration numbers.[36]

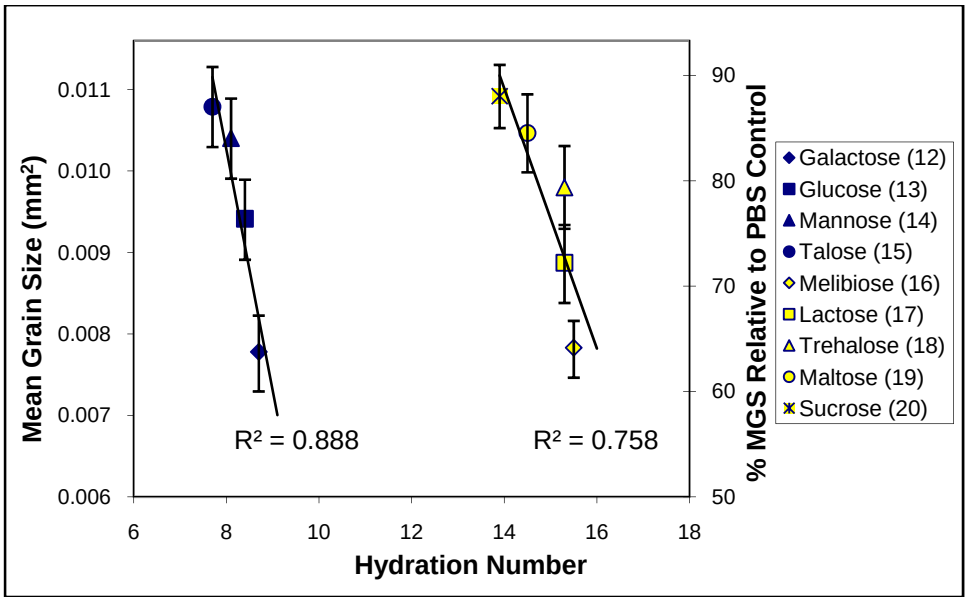

Graph 1.5 IRI activities (tested at 0.022 M) of carbohydrates (**12-20**) at 0.022 M as a function of their respective hydration number.[36]

In Graph 1.5 there are two distinct linear correlations found between IRI activity and hydration number. Just as the monosaccharides (**12-15**) alone, the disaccharides (**16-20**) increase in IRI activity as the hydration number is increased. However, if monosaccharides (**12-15**) are compared to the disaccharides (**16-20**), there is a break in the linear trend, suggesting that hydration number alone cannot accurately predict IRI activity.[36] Tam *et al*. decided to employ a similar method as Parke *et al*. who compared the taste properties of various solutes to the hydration per unit volume of the solute.[100] As shown in Graph 1.6 the IRI activities of all the saccharides (**12-20**) tested were compared to their hydration index which is derived from

dividing the hydration number of the sugar by its partial molar volume. More precisely, the hydration index is a measurement of the number of water molecules within the first hydration shell per unit volume of the solute within the first hydration shell.[36] It is apparent by the linear correlation between the hydration index and IRI activities (Graph 1.6) of all the saccharides (R= 0.791), that the hydration index more accurately predicts IRI activity than both partial molar compressibility and hydration number alone.[36] Although the hydration index accurately predicts the IRI activity of simple non-substituted carbohydrates, more studies are required to fully assess the impact of hydrophobic and hydrophilic modifications to simple carbohydrates on carbohydrate hydration and IRI activity.

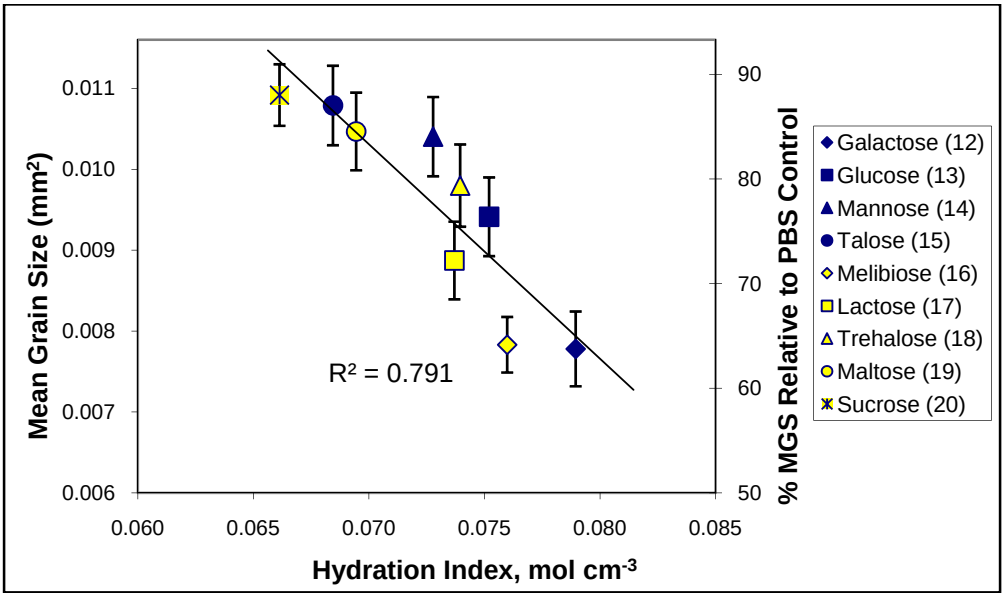

Graph 1.6 IRI activities (tested at 0.022 M) of carbohydrates (**12-20**) as a function of their respective hydration index (hydration number/partial molar volume, $mol^{1}cm^{-3}$).[36]

Since current cryopreservation studies do not address IRI activity of current cryoprotective agents, more research is required to prove that ice recrystallization inhibition improves cell viability post freeze-thaw. Also, the cytotoxicity of DMSO has detrimental results in cells and transplant recipients that are often overlooked in the literature. It is therefore

important to address cytotoxic effects of all novel cryopreserving agents prior to commercial use. Given the importance of hydrophilic and hydrophobic groups on AF(G)P activity, more research relating their specific effects on the carbohydrate moiety hydration will be explored.

References

1. (a) Can, A.; Karahuseyinoglu, S., Concise Review: Human umbilical cord stroma with regard to the source of fetus-derived stem cells. *Stem Cells* **2007**, 25, 2886-2895. (b) Kraus, K. H.; Kerker-Head, C., Mesenchymal stem cells and bone regeneration. *Veterinary Surgery,* **2006**, 35, 232-242. (c) Quevedo, H. C.; Hatzistergos, K. E.; Oskouei, B. N.; Feigenbaum, G. S.; Rodriguez, J. E.; Valdes, D.; Pattany, P. M.; Zambrano, J. P.; Hu, Q.; McNiece, I.; Heldman, A. W.; Hare, J. M., Allogeneic mesenchymal stem cells restore cardiac function in chronic ischemic cardiomyopathy via trilineage differentiating capacity. *Proc Natl Acad Sci U S A,* **2009**, 106, 14022-14027. (d) Sykova, E.; Jendelova, P.; Urdzikova, L.; Lesny, P.; Hejel, A., Bone marrow stems cells and polymer hydrogels – two strategies for spinal cord injury repair. *Cellular and Molecular Neurobiology*, 2006, 26, 1113-1129.

2. (a) Mazur, P., The role of cell membranes in the freezing of yeast and other single cells. *Ann. N. Y. Acad. Sci.* 1965, 125, 658-676. (b) Tonino, G. J. M.; Steyn-Parve, E. P., Localization of some phosphatases in yeast. *Biochim. Biophys. Acta* **1963**, 67, 453.

3. (a)Heber, U., Freezing Injury and Uncoupling of Phosphorylation from Electron Transport in Chloroplasts. *Plant Physiol.* **1967**, 42, 1343-1350. (b) Greiff, D.; Seifert, P., Cryotolerance of selected sites on the surfaces of membranes of cells: I. Mucopolysaccharides of erythrocytes. *Cryobiology*, **1968**, 4, 295-302.

4. (a) Lovelock, J.E., The haemolysis of human red blood-cells by freezing and thawing. *Biochim. Biophys. Acta.,* **1953**, 10, 414. (b) Lovelock, J.E., The mechanism of the protective action of glycerol against haemolysis by freezing and thawing.*Biochim. Biophys. Acta.,* **1953**, 11, 28.(c) Meryman, H. T.; Williams, R. J.; Douglas, M. St. J., Freezing injury from "solution effects" and its prevention by natural or artificial cryoprotection. *Cryobiology*,**1977**, 14, 287-302.

5. Liu, S.; Wang, W.; von Moos, E.; Jackman, J.; Mealing, G.; Monette, R.; Ben, R. N., *In Vitro* Studies of Antifreeze Glycoprotein (AFGP) and a *C*-Linked AFGP Analogue. *Biomacromolecules,* **2007**, 8, 1456-1462.

6. Koushafar, H.; Pham, L.; Lee, C.; Rubinsky, B., Chemical adjuvant cryosurgery with antifreeze proteins. *J. Surg. Oncol.* **1997**, 66, 114-121.

7. Mazur, P., Cryobiology: The Freezing of Biological Systems, *Science*, **1970**, 168, 939-949.

8. Scholander, P.E.; Flagg,W.; Walters, V.; Irving, L., Climatic adaptation in arctic and tropic poikilotherms. *Physiol. Zool.* **1953**, 26, 67-92.

9. (a) Rubinsky, B.; Arav, A.; DeVries, A. L., The cryoprotective effect of antifreeze glycopeptides from Antarctic fishes. *Cryobiology*, **1992**, 29, 69-79. (b) Pham, L.; Dahiya, R.; Rubinsky, B., An *in vivo* study of antifreeze protein adjuvant cryosurgery. *Cryosurgery* **1999**, 38, 169-175.

10. Wallis, J. G.; Wang, H.; Guerra, D. J., Expression of a synthetic antifreeze protein in potato reduces electrolyte release at freezing temperatures. *Plant Mol. Biol.* **1997**, 35, 323-354.

11. Griffith, M.; Ewart, K. V., Antifreeze proteins and their potential use in frozen foods. *Biotech. Adv.* **1995**, 13, 375-403.

12. (a) Roland, W.; Ring, R. A., Cold, freezing, and desiccation tolerance of the limpet *Acmaea digitalis* (Eschscholtz) *Cryobiology*, **1977**, 14, 228-235. (b) Crisp, D. J.; Davenport, J.; Gabbott, P. A., Freezing tolerance in *Balanus balanoides. Comparative Biochemistry and Physiology Part A: Physiology*, **1977**, 57,359-36.

13. Offerijns, F. G. J.; Krijnen, H. W., The Preservation of the Rat Heart in the Frozen State, *Cryobiology*, **1972**, 9,289-295.

14. Tong, M. M.; Pincock, R. E., Denaturation and reactivity of invertase in frozen solutions. *Biochemistry*, **1969**, 8, 908.

15. Mazur, P.; Farrant, J.; Leibo, S. P.; Chu, E. H. Y., Survival of hamster tissue culture cells after freezing and thawing: Interactions between protective solutes and cooling and warming rates, *Cryobiology*, **1969**, 6, 1-9.

16. Meryman, H.T., Osmotic stress as a mechanism of freezing injury, *Cryobiology*, **1971**, 8, 489-500.

17. Muldrew, K.; McGann, L. E., The Osmotic Rupture Hypothesis of Intracellular Freezing Injury. *Biophysical Journal ,* **1994,** 66, 532-541.

18. Mazur, P., The role of intracellular freezing in the death of cells cooled at supraoptimal rates. *Cryobiology*, **1977**, 14, 251-272.

19. Toner, M.; Karel, M.; Cravalho, E., Thermodynamics and kinetics of intracellular ice formation during freezing of biological cells. *J. Appl.Phys.* **1990**, 67, 1582-1593.

20. Muldrew, K.; McGann, L. E., Mechanisms of intracellular ice formation. *Biophys. J.* **1990**, 57, 525-532.

21. Salt, R. W., Survival of Frozen Fat Body Cells in an Insect, *Nature*, **1959**, 184, 1426-1427.

22. Kingery, W. D., Regelation, surface diffusion, and ice sintering. *J. Appl. Phys.* **1960**, 31, 833-838.

23. Mazur, P., Freezing of living cells: mechanisms and implications. *Am. J. Physiol. Cell Ph.*, **1984**, 247, C125-C142.

24. (a) Fahy, G. M.; MacFarlane, D. R.; Angell, C. A.; Meryman, H. T., Vitrification as an approach to cryopreservation.*Cryobiology*, **1984**, 21, 407-426. (b) Rall, W. F.; Fahy, G. M., Ice-free cryopreservation of mouse embryos at -196°C by vitrification. *Nature*, **1985**, 313, 573-575.

25. Polge, A.; Smith, A. U.; Parkes, A. S., Revival of Spermatozoa after Vitrification and Dehydration at Low Temperatures. *Nature*, **1949**, 164, 666-667.

26. Lovelock, J. E.; Bishop, M. W. H., Prevention of Freezing Damage to Living Cells by Dimethyl Sulphoxide. *Nature*, **1959**, 4672, 1394-1395.

27. Lovelock, J. E., The Protective Action of Neutral Solutes against Haemolysis by Freezing and Thawing. *Biochem. J.*, **1954**, 56, 265-270.

28. Notman, R.; Noro, M.; O'Malley, B.; Anwar, J., Molecular Basis for Dimethylsulfoxide (DMSO) Action on Lipid Membranes. *J. Am. Chem. Soc.* **2006**, 128, 13982-13983.

29. Gurtovenko, A. A.; Anwar, J., Modulating the Structure and Properties of Cell Membranes: The Molecular Mechanism of Action of Dimethyl Sulfoxide.*J. Phys. Chem. B*, **2007**, 111, 10453-10460.

30. Doebbler, G. F.; Rinfret. A. P., The influence of protective compounds and cooling and warming conditions on hemolysis of erythrocytes by freezing and thawing. *Biochim. Biophys. Acta,* **1962**, 58, 449-458.

31. Haaf, F.; Sanner, A.; Straub, F., Polymers of N-Vinylpyrrolidone: Synthesis, Characterization and Uses. *Polymer Journal*, **1985**, 17, 143–152.

32. Kahovec, J.; Fox, R. B.; Hatada, K., Nomenclature of regular single-strand organic polymers. *Pure and Applied Chemistry*, **2002**, 74, 1921–1956.

33. Farrant, J., Is there a common mechanism of protection of living cells by polyvinylpyrrolidone and glycerol during freezing? *Nature*, **1969**, 222, 1175-1176.

34. Smorag, Z.; Heyman, Y.; Garnier, V.; Gajda, B., The effect of sucrose and trehalose on viability of one- and two-cell rabbit embryos. *Theriogenology*,**1990**, 33, 741-747.

35. Sei, T.; Gonda, T.; Arima, Y., Growth rate and morphology of ice crystals growing in a solution of trehalose and water. *J.Cryst. Growth* **2002**,240, 218-229.

36. Tam R.Y.; Ferreira, S. S.; Czechura, P.; Chaytor, J. L.; Ben, R. N., Hydration Index - A Better Parameter for Explaining Small Molecule Hydration in Inhibition of Ice Recrystallization, *J. Am. Chem. Soc*. **2008**, 130, 17494–17501.

37. (a) Eroglu, A.; Bailey, S. E.; Toner, M.; Toth, T. L., Successful Cryopreservation of Mouse Oocytes by Using Low Concentrations of Trehalose and Dimethylsulfoxide. *Biol. Reprod.* **2009**, 80, 70-80. (b) Izadyar, F.; Matthijs-Rijsenbilt, J. J.; Den Ouden, K.; Creemers, L. B.; Woelders, H.; De Rooij, D. G., Development of a Cryopreservation Protocol for Type A Spermatogonia. *J. Androl.* **2002**, 23, 537-545. (c) Ma, W.; O'Shaughnessy, T.; Chang, E., Cryopreservation of adherent neuronal networks. *Neurosci. Lett.* **2006**, 403, 84-89. (d) Santos, R. R.; Tharasanit, T.; Figueiredo, J. R.; van Haeften, T.; van den Hurk, R., Preservation of caprine preantral follicle viability after cryopreservation in sucrose and ethylene glycol. *Cell Tissue Res.* **2006**, 325, 523-531. (e) Vicente, J. S.; Viudes-de-Castro, M. P., A sucrose-DMSO extender for freezing rabbit semen. *Reprod. Nutr. Dev.* **1996**, 36, 485-492. (f) Gutierrez-Perez, O.; Juarez-Mosqueda, M. D. L.; Carvajal, S. U.; Ortega, M. E. T., Boar spermatozoa cryopreservation in low glycerol/trehalose enriched freezing media improves cellular integrity. *Cryobiology* **2009**, 58, 287-292. (h) Coticchio, G.; De Santis, L.; Rossi, G.; Borini, A.; Albertini, D.; Scaravelli, G.; Alecci, C.; Bianchi, V.; Nottola, S.; Cecconi, S., Sucrose concentration influences the rate of human oocytes with normal spindle and chromosome configurations after slow-cooling cryopreservation. *Hum. Reprod.* **2006**, 21, 1771-1776. (i) Neto, V.; Buff, S.; Lornage, J.; Bottollier, B.; Guerin, P.; Joly, T., Effects of different freezing parameters on the morphology and viability of preantral follicles after cryopreservation of doe rabbit ovarian tissue. *Fertil. Steril.* **2008**, 89, 1348-1356.

38. (a) Davis, J. M.; Rowley, S. D.; Braine, H. G.; Piantadosi, S.; Santos, G. W. Clinical toxicity of cryopreserved bone marrow graft infusion. *Blood,* **1990**, 75, 781-786. (b) Liseth, K.; Abrahamsen, J. F.; Bjorsvik, S.; Grottebo, K.; Bruserud, O., The viability of cryopreserved PBPC depends on the DMSO concentration and the concentration of nucleated cells in the graft. *Cytotherapy,* **2005**, 7, 328-333.

39. Duman, J. G.; DeVries, A. L., The Role of Macromolecular Antifreeze in Cold Water Fishes. *Comparative Biochemistry and Physiology.* **1975**, 52A, 193-199.

40. Yeh, Y.; Feeney, R.E., Antifreeze proteins: structures and mechanism of action. *Chem. Rev.* **1996**, 96, 601-617.

41. (a) Scholander, P. F.; Van Dam, L.; Kanwisher, J. W.; Hammel, H. T.; Gordon, M. S.; Supercooling and osmoregulation in Arctic fish. *J. Cell Com. Physiol.* **1957**, 49, 5-24.(b) Chen, L. B.; DeVries, A. L.; Cheng, C. H. C., Convergent Evolution of antifreeze glycoproteins in Antartic notothenoid fish and Arctic cod. *Proc. Natl. Acad. Sci. USA*., **1997**, 94, 3811-3816.

42. Feeney, R. E.; Hofmann, R., Depression of freezing point by glycoproteins from an Antarctic fish. *Nature (London)* **1973**, 243, 237-238.

43. Scholander, P.F.; Maggert, J. E., Supercooling and ice propagation in blood from Arctic fish. *Cryobiology* **1971**, 8, 371-374.

44. Ananthanarayanan, V. S., Antifreeze proteins: structural diversity and mechanism of action. *Life Chem. Rep.* **1989**, 7, 1-32.

45. Scott, G. K.; Davies, P. L.; Shears, M. A.; Fletcher, G. L., Structural variations in the alanine-rich antifreeze proteins of the Pleuronectinae. *Eur. J. Biochem.* **1987**, 168, 629-633.

46. Patterson, J. L.; Duman, J. G., Purification and composition of insect antifreezes with high cysteine contents from larvae of the beetle, *Tenebrio molitor. J Exp. Zool.* **1982**, 219, 381-384.

47. Chao, H.; Sönnichsen, F. D.; DeLuca, C. I.; Sykes, B. D.; Davies, P. L., Structure-function relationship in the globular Type III antifreeze proteins identification of a cluster of surface residues required for binding to ice. *Protein Science*, **1994**, 3, 1760-1769.

48. Harding, M. M.; Anderberg, P. I.; Haymet, A. D. J., 'Antifreeze' glycoproteins from polar fish. *Eur. J. Biochem*. **2003**, 270, 1381–1392.

49. Deng, G.; Andrews, D. W.; Laursen, R. A., Amino acid sequence of a new type of antifreeze protein from the longhorn sculpin, *Myoxocephalus octodecimsponosis, FEBS Lett,* **1997**, 402, 17-20.

50. Komatsu, S. K.; DeVries, A. L.; Feeney, R. E., Studies of the structure of freezing point - depressing glycoproteins from an Antarctic fish. *J. Biol. Chem.***1970**, 245, 2909-2913.

51. Hew, C. L.; Slaughter, D.; Fletcher, G. L.; Joshi, S., Antifreeze glycoproteins in the plasma of Newfoundland Atlantic cod (*Gadus morhua). Can. J. Zool.* **1981**, 60, 348-355

52. Brown, R. A.; Yeh, Y.; Burcham, T. S.; Feeney, R. E., Direct Evidence for Antifreeze Glycoprotein Adsorption onto an Ice Surface, *Biopolymers*. **1985**, 24, 1265-1270.

53. Kuiper, M. J.; Lankin, C.; Gauthier, S. Y.; Walker, V. K.; Davies, P. L., Purification of antifreeze proteins by absorption to ice. *Biochem. Biophys. Res. Comm.* **2003**, 300, 645-648.

54. Knight, C. A., Adding to the antifreeze agenda. *Nature* **2000**,406**,** 249-251.

55. Lide, D. R., ed. (**2005**), *CRC Handbook of Chemistry and Physics* (86th ed.), Boca Raton (FL): CRC Press

56. Malenkov, G., Liquid water and ices: understanding the structure and physical properties. *J. Phys.: Condens. Matter* **2009**, *21*, 283101-283136.

57. (a) Karim, O. A.; Haymet, A. D., The ice/water interface: A molecular dynamics simulation study. *J. Chem. Phys.***1988**, 89, 6889. (b) Sadtchenko, V.; Ewing, G. E., Interfacial melting of thin ice films: An infrared study. *J. Chem. Phys.* **2002**, 116, 4686. (c) Haymet, A.D.J.; Ward, L.G.; Harding, M.M., Winter Flounder "Antifreeze" Proteins: Synthesis and Ice Growth Inhibition of Analogues that Probe the Relative Importance of Hydrophobic and Hydrogen-Bonding Interactions. *J. Am. Chem. Soc.* **1999**, 121, 941-948.

58. Czechura, P.; Tam, R. Y.; Dimitrijevic, E.; Murphy, A. V.; Ben, R. N., The Imporance of Hydration for Inhibiting Ice Recrystallization with *C*-linked Antifreeze Glycoproteins. *J. Am.Chem. Soc.* **2008**, 130, 2928-2929.

59. Hew, C. L.; Yang, D. C., Protein Interaction with ice. *Eur. J. Biochem*. **1992**, 203, 33-42.

60. Ben, R.N., Antifreeze glycoproteins-preventing the growth of ice. *Chem. Bio. Chem.* **2001**, 2, 161-166.

61. Fletcher, G. L.; Hew, C. L.; Davies, P. L., Antifreeze Proteins of Teleost Fishes *Annu. Rev. Physiol.* **2001**, 63, 359-390.

62. DeVries, A. L.; Komatsu, S. K.; Feeney, R. E., Chemical and Physical Properties of Freezing Point-Depressing Glycoproteins from Antarctic fish. *J. Biol. Chem.* **1970**, 245, 2901-2908.

63. Duman, J. G.; DeVries, A. L., Freezing resistance in winter flounder *Pseudopleuronectes americanus*. *Nature,***1975,** 247, 237-238.

64. Gibson, M.I., Slowing the Growth of Ice with Synthetic Macromolecules: Beyond Antifreeze(glyco) Proteins. *Polymer Chemistry*, **2010**, 1141-1152.

65. Wilson, P. W.; Leader, J. P., Stabilization of supercooled fluids by thermal hysteresis proteins. *Biophys. J.***1995**, 68, 2098-2107.

66. Hall, D. G.; Lips, A., Phenomenology and Mechanism of Antifreeze Peptide Activity *Langmuir*, **1999**, 15, 1905.

67. Knight, C. A.; Cheng, C. C.; DeVries, A. L., Adsorption of a-helical antifreeze peptides on specific ice crystal surface planes, *Biophys. J.* **1991**, 59, 409-418.

68. (a) Raymond, J. A.; DeVries, A. L., Adsorption inhibition as a mechanism of freezing resistance in polar fishes. *Proc. Natl. Acad. Sci. USA*. **1977**, 74, 2589-2593. (b) Knight, C. A.; DeVries, A. L.; Oolman, L. D., Fish antifreeze protein and the freezing and recrystallization of ice. *Nature (Lond.)* **1984**, 308, 295-296.

69. Graham, L. A.; Yin-Cheung, L.; Walker, V. K.; Davies, P. L., Hyperactive antifreeze protein from beetles, *Nature*, **1997**, 388, 727-728.

70. Raymond, J.A.; Wilson, P. W.; DeVries, A.L., Inhibition of growth of non-basal planes in ice by fish antifreezes. *Proc. Natl Acad. Sci. USA,* **1989**, 86, 881–885.

71. Wilson, P. W.; Beaglehole, D.; DeVries, A. L., Antifreeze glycopeptides adsorption on single crystal ice surfaces using ellipsometry. *Biophys. J.* **1993**, 64, 1878-1884.

72. Davies, P.L.; Sykes, B.D., Antifreeze proteins. *Curr. Opin. Struct. Biol.* **1997**, 7, 828–834.

73. Knight, C. A.; Wen, D.; Laursen, R. A., Nonequilibrium antifreeze peptides and the recrystallization of ice, *Cryobiology*, **1995**, 32, 23-34.

74. Knight, C. A.; Hallet, J.; DeVries, A. L., Solute effects on ice recrystallization: An assessment technique, *Cryobiology*, **1988**, 25, 55-60.

75. Larese, A.; Acker, J.; Muldrew, K.; Yang, H. Y.; McGann, L., Antifreeze protein induce intracellular nucleation, *Cryo-Lett*, **1996**, 17, 175-182.

76. Filira, F.; Biondi, L.; Scolaro, B.; Foffani, M.T.; Mammi, S.; Peggion, E.; Rocchi, R., Solid phase synthesis and conformation of sequential glycosylated polytripeptide sequences related to antifreeze glycoproteins. *Int. J. Biol. Macromol.* **1990**, 12, 41–49.

77. (a) Rubinsky,B.; Arav, A.; Mattiolo, M.; DeVries, A.L., The effect of antifreeze glycopeptides on membrane potential changes at hypothermic temperatures. *Biochem. Biophys. Res. Commun.* **1990**, 173, 1369-1374. (b) Rubinsky, B.; Arav, A.; DeVries, A.L., The cryoprotective effect of antifreeze glycopeptides from antarctic fishes. *Cryobiology* **1992**, 29, 69-79. (c) Tablin, F.; Oliver, A. E.; Walker, N. J.; Crowe, L. M.; Crowe, J. H., Membrane phase transition of intact human platelets: Correlation with cold-induced activation *J. Cell. Physiol.* **1996**, 168, 305-313.

78. Hays, L. M.; Feeney, R. E.; Crowe, J. H.; Oliver, A. E., Antifreeze glycoproteins inhibit leakage from liposomes during thermotropic phase transitions. *Proc. Natl. Acad. Sci. U.S.A.* **1996**, 93, 6835-6840.

79. (a) Mugnano, J. A.; Wang, T.; Layne, J. R.; DeVries, A. L.; Lee, R. E., Antifreeze glycoproteins promote intracellular freezing of rat cardiomyocytes at high subzero temperatures. Am. J. Physiol., **1994**, 269, R474- R479. (b) Wang, T.; Zhu, Q.; Yang, X.; Layne, J. R., Jr.; DeVries, A. L., Antifreeze Glycoproteins from Antarctic Notothenioid Fishes Fail to Protect the Rat Cardiac Explant during Hypothermic and Freezing Preservation. *Cryobiology*,**1994**, 31,185-192.

80. (a) Koushafar, H.; Rubinsky, B., Effect of antifreeze proteins on frozen primary prostatic adenocarcinoma cells. *Urology* **1997**, 49, 421-425. (b) Rubinsky, B.; DeVries, A. L., Effect of ice crystal habit on the viability of glycerol-protected red blood cells. *Cryobiology,* **1989**, 26, 580.

81 Sidebottom, C.; Buckley, S.; Pudney, P.; Twigg, S.; Jarmann, C.; Holt, C.; Telford, J.; McArthur, A.; Worrall, D.; Hubbard, R.; Lillford, P., Phytochemistry: Heat-stable antifreeze protein from grass. *Nature*, **2000**, 406, 256-257.

82. (a)Vandenheede, J.R.; Ahmed, A.I.; Feeney,R.E., Structure and role of carbohydrate in freezing point-depressing glycoproteins from an Antarctic fish. *J. Biol. Chem.* **1972**, 247, 7885–7889. (b) Ahmed, A.I.; Yeh, Y.; Osuga, D.T.; Feeney, R.E., Antifreeze glycoproteins from Antarctic fish: inactivation by borate. *J. Biol. Chem.***1976**, 251, 3033–3036. (c) Osuga, D.T.; Feather, M.S.; Shah, M.J.; Feeney, R.E., Modification of galactose and N-galactoseamine residues by oxidation of C-6 hydroxyls to the aldehydes followed by reductive amination: Model systems and antifreeze glycoproteins. *J. Prot. Chem.* **1989**, 8, 519–528.

83. Burcham, T.S.; Knauf, M.J.; Osuga, D.T.; Feeney, R.E.; Yeh, Y., Antifreeze glycoproteins: Influence of polymer length and ice crystal habit on activity. *Biopolymers,* **1984***,* 23, 1379–1395.

84. Tachibana, Y.; Fletcher, G. L.; Fujitani, N.; Tsuda, S.; Monde, K.; Nishimura, S., Antifreeze glycoproteins: Elucidation of the structural motifs that are essential for antifreeze activity, *Angew. Chem. Int. Ed.* **2004**, 43, 856-862.

85. Sjölin, P.; Kihlberg, J., Use of Fluorobenzoyl Protective Groups in Synthesis of Glycopeptides: β-Elimination of *O*-Linked Carbohydrates Is Suppressed. *J.Org. Chem.***2001**, 66, 2957-2965.

86. Marcaurelle, L. A.; Bertozzi, C. R., New Directions in the Synthesis of Glycopeptide Mimetics, *Chem. Eur. J.*, **1999**, 5, 1384-1390.

87. Eniade A.; Hauer, L.; Ben, R.N. (1999) Synthesis of a *C*-linked antifreeze glycoprotein (AFGP) mimic: Probes for investigating the mechanism of action. *Org. Lett*. **1999**, 1, 1759-1762.

88. Eniade, A.; Purushotham. M.; Ben, R. N.; Wang, W.; Horwarth, K., A serendipitous discovery of antifreeze protein-specific activity in *C*-linked antifreeze glycoprotein analogs. *Cell Biochem. Biophys.* **2003**, 38, 115-124.

89. Liu, S.; Ben, R. *C*-Linked Galactosyl Serine AFGP Analogues as Potent Recrystallization Inhibitors. *Org. Lett*. **2005**, 7, 2385-2388.

90. Tam, R.Y.; Rowley, C. N.; Petrov, I.; Zhang,T.; Afagh, N. A.; Woo T. K.; Ben, R. N., Solution Conformation of *C*-Linked Antifreeze Glycoprotein Analogues and Modulation of Ice Recrystallization, *J. Am. Chem. Soc.*, **2009**, 131, 15745-15753.

91. Trant, J. T.; Biggs, R.; Ben, R. N., unpublished results, **2009**

92. Bouvet,V., Ph.D. Dissertation, University of Ottawa, **2005**

93. Campbell, W., M. Sc. Dissertation, University of Ottawa, **2009**

94. (a) Galema, S. A.; Høiland, H. Stereochemical Aspects of Hydration of Carbohydrates In Aqueous Solutions. 3. [1]Density and Ultrasound Measurements, *J. Phys. Chem.* **1991**, *95*, 5321. (b) Høiland, H.; Hølvik, H., Partial Molar Volumes and Compressibilities of Carbohydrates in Water. *J. Solution Chem.* **1978**, 7, 587-596.

95. Dashnau, J.; Sharp, K. A.; Vanderkooi, J. M., Carbohydrate Intramolecular Hydrogen Bonding Cooperativity and Its Effect on Water Structure, *J. Phys. Chem. B.* **2005**, 109, 24152–24159.

96. Baruch, E.; Belostotskii, A. M.; Mastai, Y., Relationship between the antifreeze activities and the chemical structure of polyols. *J. Mol. Struct.* **2008**, 874, 170-177.

97. Uchida,T.; Nagayamaa, M.; Kazutoshi Goharaa, K., Trehalose solution viscosity at low temperatures measured by dynamic light scattering method: Trehalose depresses molecular transportation for ice crystal growth, *Journal of Crystal Growth*, **2009**, 311, 4747-4752.

98. (a) Uedaira, H., Uedaira H., Sugar-Water Interaction from the Diffusion Measurements. *J. Solution Chem.* **1985**, 14, 27-34. (b) Uedaira, H.; Ikura, M.; Uedaira, H., Natural-Abundance Oxygen-17 Magnetic Relaxation in Aqueous Solutions of Carbohydrates. *Bull. Chem. Soc. Jpn.* **1989**, 62, 1-4.

99. Lopez de la Paz, M.; Ellis, G.; Perez, M.; Perkins, J.; Jimenez-Barbero, J. ; Vincent, C., Carbohydrate Hydrogen-Bonding Cooperativity- Intramolecular Hydrogen Bonds and Their Cooperative Effect on Intermolecular Processes-Binding to a Hydrogen-Bond Acceptor Molecule. *Eur. J. Org. Chem.* **2002**, 840-855.

100. Parke, S. A.; Birch, G. G.; Dijk, R., Some Taste Molecules and their Solution Properties, *Chem. Senses.* **1999**, 24, 271-279.

Chapter 2: Goals and Objectives

2.1 Introduction

Current cell penetrating cryoprotective agents (CPAs) which are routinely used in literature and clinical settings (DMSO, glycerol) display significant amounts of cytotoxicity in cell line cultures, tissues and organs which renders their use problematic.[1,2,3] Alternatives to these commercially available CPAs must therefore be non-toxic to the cell and transplant recipient at physiological conditions. It has been postulated that ice recrystallization is a major source of cell damage during cryopreservation, but this assumption requires further validation.[4,5] A possible means to corroborate this hypothesis would be to directly link ice recrystallization to cell survival post-cryopreservation.

A primary focus of the Ben research group is the synthesis of novel cryoprotectants based on the chemical structure of antifreeze glycoproteins (AFGPs). It is believed that native AFGPs are responsible for survival of fish inhabiting sub-zero waters (~ -2.0 ^{o}C) via thermal hysteresis (TH) and ice recrystallization inhibition (IRI).[6,7] Unfortunately, the cryoprotective property of TH is only effective at temperatures within the TH gap, as temperatures below the TH gap induce the formation of "ice spicules" which are damaging to cell membranes and undesirable for cryopreservation in low temperatures (-78° to -196°C).[7,8,9,10,11] Therefore, it is important to synthesize analogues which exhibit strictly IRI activity and this endeavor is being further pursued in our research group. As previously demonstrated by our research group, the extent of hydration of the carbohydrate found on AFGPs affects IRI activity.[12,13] Therefore, understanding how hydration of certain small molecules affects their IRI activity will lead to the development of better ice recrystallization inhibitors and cryoprotectants.

2.2 Objective 1: Probing the Potential Relationship between IRI Activity and Cryopreservation

As mentioned previously, the cytotoxicity of penetrating DMSO is an issue which affects cell viability as well as patient health and safety.[1,2,3] As a result, non-penetrating carbohydrates have been used as potential cryoprotectant alternatives due to their endogenous nature.[14] Carbohydrates (mainly D-sucrose (**20**) and D-trehalose (**18**)) are found to improve cell viability post-thaw and are sometimes used in combination with DMSO,[15] glycerol,[16] or 1,2-propanediol.[17] However, contradicting results have also emerged, where the addition of carbohydrates in some studies actually lowers cell viability or gives no additional benefit compared to controls.[18] Unfortunately, the exact nature by which carbohydrates act as cryoprotectants is unclear.

Given that simple carbohydrates have recently been shown to act as ice recrystallization inhibitors,[12,13] one possible mode of cryoprotection by carbohydrates may be by preventing ice recrystallization, which is believed to be a significant cause of cell injury.[4,5] To determine how carbohydrates affect cell viability post thaw, it is necessary to also assess their cytotoxicity under physiological conditions. This will establish a correlation between the IRI activity of carbohydrates and their cytotoxicity and cryopreservation ability. Towards this end, a series of monosaccharides (**12**, **13**) and disaccharides (**16-18**, **20**) (Figure 2.1) will be tested for cytotoxic effects (MTT assay)[7] in a transformed human liver cell line (WRL-68) using three concentrations (0.022 M, 0.2 M and 0.5 M). The lower concentrations (0.022 M, 0.2 M) will allow direct comparison to IRI activity measurements that will be taken of these carbohydrates and the higher concentration (0.5 M) resembles the concentrations of carbohydrates used in standard cryopreservation protocols.[14-17] The results will be compared to the IRI activities of their respective concentrations and also compared to the IRI activity and cytotoxic effects of 2.5 % and 5 % DMSO which represent the positive controls.

It was determined by Tam *et al*. that low concentrations of DMSO (~3%) are as effective at inhibiting ice recrystallization as 0.022 M D-galactose (**12**).[13] Also it has been reported that concentrations less than 10% are effective at cryopreserving cells.[3] Thus, the fact that DMSO has concentration dependent IRI activity sets the precedence for testing the hypothesis that cryoprotectants function by limiting ice recrystallization. Consequently, a series of monosaccharides (**12**, **13**) and disaccharides (**16-18**, **20**) (Figure 2.1) will be tested at concentrations of 0.022 M, 0.2 M and 0.5 M for their ability to cryopreserve WRL 68 cells. The resulting total cell viability will be compared to the IRI activity of the respective carbohydrate concentrations and compared to 2.5 % and 5 % DMSO which are used as positive controls.

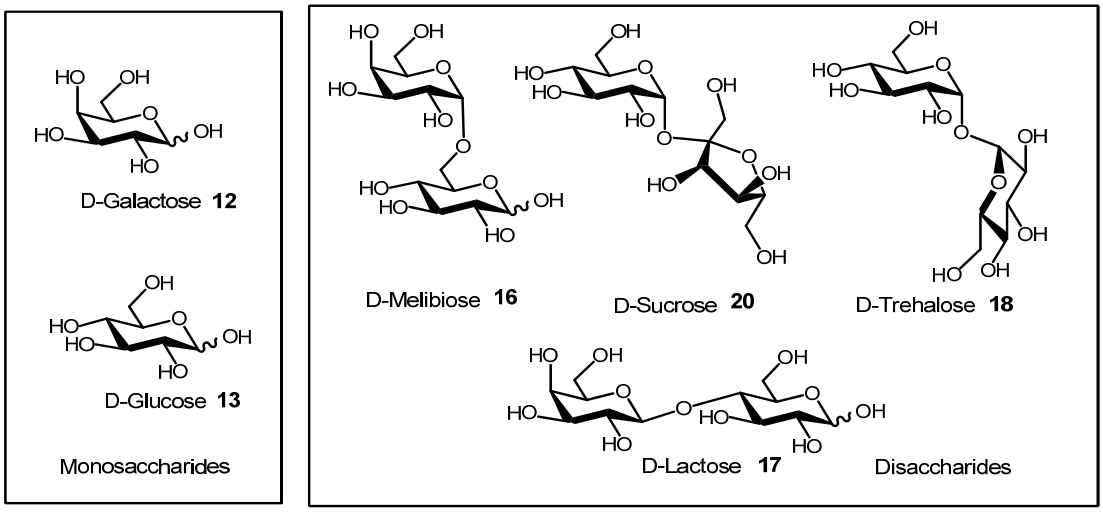

Figure 2.1 Structure of monosaccharides (**12, 13**) and disaccharides (**16 - 18, 20**) undergoing cytotoxicity, cryopreservation ability and IRI activity testing

As previously discovered by Tam *et al*., the hydration index of various commercially available mono- and disaccharides correctly predicts their respective IRI activity at 0.022 M.[13] To probe if the hydration parameter can effectively predict the IRI activity of carbohydrate

concentrations higher than 0.022 M, carbohydrates (**12**, **13**, **16 - 18**, **20**) (Figure 2.1) will be tested at 0.22 M.

The following goals provide a brief summary of this research objective:

1. Assess the IRI activity of monosaccharides (**12**, **13**) and disaccharides (**16-18**, **20**) at both 0.022 M and 0.22 M concentrations to test the hydration index model.

2. Assess the cytotoxicity of 2.5 % DMSO, 5 % DMSO, monosaccharides and disaccharides at 0.022 M, 0.2 M and 0.5 M concentrations.

3. Assess the cryopreservation ability of 2.5% DMSO, 5% DMSO, monosaccharides and disaccharides at 0.022 M, 0.2 M and 0.5 M concentrations.

4. Assess whether there are correlations between cytotoxicity and IRI activity, as well as cryopreservation ability and IRI activity of these carbohydrates and DMSO.

2.3 Objective 2: Probing the Importance of Hydrophilicity and Hydrophobicity at Non Anomeric Positions of D-Galactose on IRI Activity

As mentioned in the previous chapter, the exact mode of action for ice-recrystallization inhibition is unclear, and recent evidence suggests that its mechanism is different than thermal hysteresis.[13] For example, the mechanism of action for TH is hypothesized to be caused by binding of the antifreeze molecule to the ice surface.[19] Braslavsky has shown (Figure 2.2) with green fluorescent bound AFPs that ice binding occurs in a semi-permanent fashion (involving both irreversible and reversible hydrogen bonding).[20] However, recent work by Tam *et al*. (using simple carbohydrates which have no TH activity) suggests that the mechanism of action of IRI does not involve direct ice binding, but occurs at the ice-liquid interface.[13]

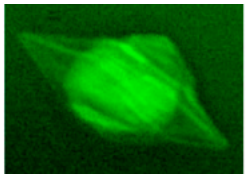

Figure 2.2 Green Fluorescent Labeled AFP III bound to Ice[20]

Furthermore, several studies have probed whether hydrophilic and hydrophobic groups of AF(G)Ps are essential for ice binding and TH activity.[21-24] For example, studies have suggested that the hydrophilic polar groups of AFGP 8 (**1**) and AFP I are incorporated into the ice lattice so that the amount of hydrogen bonding is sufficient for irreversible hydrogen bonding to the ice lattice.[21] In addition, recent studies by Mastai and DeVries have also suggested that ice binding is favoured due to the matching distance between hydroxyl groups (~4 -4.5 Å) found on AF(G)Ps and the oxygen spacing within the three dimensional water network of ice.[22] However, structural degradation and point mutation studies suggest that hydrophobic structures on AF(G)Ps are also important for ice lattice binding.[23,24] Sönnichsen *et al*. studied the solution structure of AFP III and revealed that although the polar groups are sufficiently spaced to allow binding to the ice lattice, these binding sites are sterically hindered and thus inhibits hydroxyl group ice binding.[24] They propose that hydrophobic ice-protein interactions are accounting for ice binding in the case of AFP III.[24] Unfortunately, these studies did not address IRI activity, and since it is proposed that the mechanisms of TH and IRI may be different, the importance of hydrophobic and hydrophilic effects in IRI activity must be determined.

Initial work conducted by Czechura and Tam linked the hydration parameters of AFGP analogues (**3**, **9-11**) and carbohydrates (**12-20**) to their respective IRI activity.[12,13] This was accomplished by comparing IRI activity to partial molar compressibility and it was demonstrated that a carbohydrate with a more negative partial molar compressibility value (representing a

poorer fit with the three dimensional bulk water network), had better IRI activity. Furthermore, carbohydrates with a higher hydration index (such as D-galactose (**12**), 0.078 mol·cm^{-1}), which represents the density of tightly bound water molecules surrounding the carbohydrate,[25] also have higher IRI activity compared to carbohydrates with lower hydration indices (such as D-talose (**15**), 0.068 mol·cm^{-1}). Carbohydrates with higher hydration indices will therefore better disrupt the flow of water molecules from the bulk water environment to the growing ice lattice and cause greater IRI (Figure 2.3).[12,13] However, the exact mechanism by which these water molecules tightly bind to D-galactose (**12**), and how this affects IRI activity, is uncertain. It was previously demonstrated that the stereochemistry of C2 and C4 hydroxyl groups of galactose greatly affects its hydration and is important for its potent IRI activity.[14,25] How these hydroxyl groups affect hydration is unclear, but it is proposed that intramolecular hydrogen bonding, especially between adjacent hydroxyl groups, affects the carbohydrate's hydration and fit into the three dimensional hydrogen bonded network of water.[14, 25]

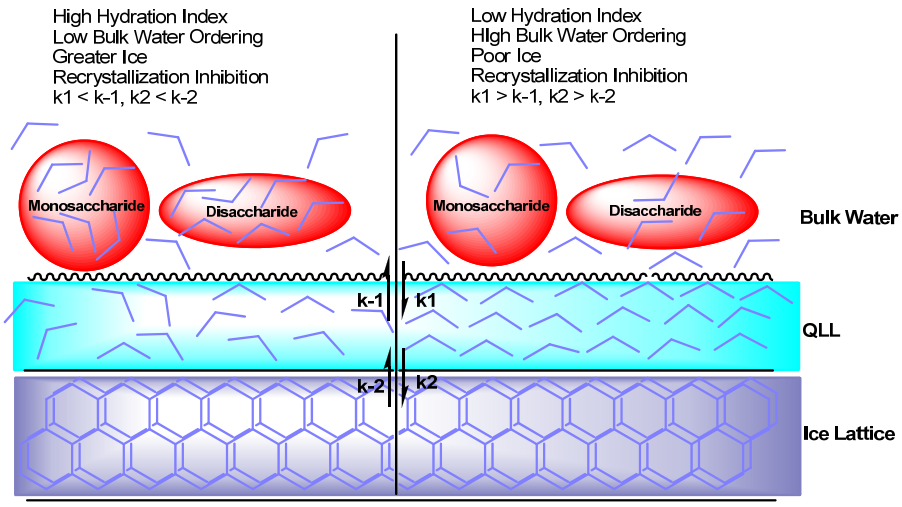

Figure 2.3 Schematic representation of the effect of the hydration index of mono- and disaccharides on IRI activity[13]

To further probe the importance of the hydrogen bond donor ability of each hydroxyl group on the galactose ring, Chaytor synthesized and tested a series of *C*-linked methylated galactose derivatives (**21-24**) shown in Figure 2.4.[26]

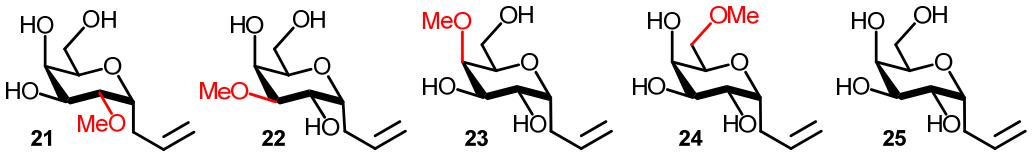

Figure 2.4 Structure of methoxy α-*C*-allyl galactose regioisomers (**21-24**) and α-*C*-allyl galactose (**25**) previously synthesized and tested for IRI activity[26]

It was rationalized that each hydroxyl group on the pyranose ring was increasing hydration by acting either as a hydrogen bond donor and/or a hydrogen bond acceptor. Replacing each hydroxyl group with a methoxy group removes its hydrogen bond donor ability while still retaining its hydrogen bond acceptor ability.[27] Therefore, testing these methoxy compounds provides insight into the importance of hydrogen bond acceptor ability on IRI activity. The results presented in Graph 2.1 provide some interesting conclusions.[26] First, from the hydration index, it is hypothesized that the more hydrophobic methoxy group would be less hydrated than a hydroxyl group.[26] This would result in more ordered and less disrupted bulk water molecules and produce poorer IRI activity. The results are consistent with this hypothesis. Secondly, the results suggest that the hydrogen bond donor ability of a hydroxyl group may be a more important factor than the acceptor ability of the methoxy group for IRI activity since these compounds are IRI inactive.[26] Finally, the fact that systematic replacement of each hydroxyl group on galactose by a methoxy group resulted in loss of IRI activity suggests that C2 and C4 stereochemistry may not be as important as originally proposed.[26] However, these results also raise questions which need addressing. The first question involves determining if removing both

hydrogen bond donor and hydrogen bond acceptor ability of the hydroxyl groups on galactose will cause a greater decrease in IRI activity. Also, it is uncertain if the presence of the allyl chain at the C1 position on these methoxy derivatives is causing an effect on IRI activity and therefore modifications to the anomeric position of galactose must be separately addressed.

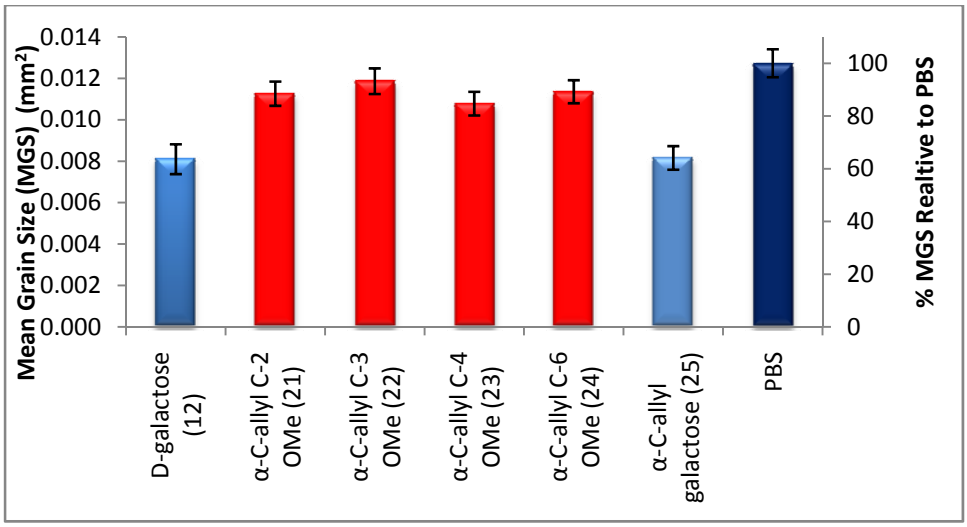

Graph 2.1 IRI activities at 0.022 M of α-*C*-allyl-D-galactose (25) and methoxy α-*C*-allyl-D-galactoses (**21-24**) relative to D-galactose (**12**)[26]

To address these questions a series of deoxy galactose derivatives (**26-29**) and α-*C*-linked deoxy galactose derivatives (**30-33**) will be synthesized and tested for IRI activity (Figure 2.5). 2-Deoxy galactose (**34**) was previously tested for IRI activity by Ferreira and had reduced IRI activity compared to D-galactose.[28] Complete removal of the hydroxyl group eliminates issues involving stereochemistry and eliminates complete hydrogen bond donor and acceptor ability at each specific location on the galactose ring. Based on the results reported by Chaytor, it is hypothesized that removing the hydrogen bond acceptor ability of the hydroxyl group would cause a further decrease in IRI activity compared to the methoxy group derivatives since it is speculated that hydrogen bonding to each hydroxyl group is important for IRI activity. Also,

based on the results of Chaytor, it is believed that the regiochemistry of the deoxy compounds (**26-34**) will not affect IRI activity.

The synthesis of both α-*C*-allyl substituted (**26-29**) and free OH deoxy galactosyl derivatives (**30-33**) will probe whether there is a steric or electronic effect caused by the added α-*C*-allyl group which may be affecting the IRI activity of these galactose derivatives. Since α-*C*-allyl-D-galactose is reported to have similar IRI activity as D-galactose (see Section 2.4)[13], it is hypothesized that both deoxy galactose regioisomers (**26-29, 34**) and α-*C*-linked deoxy galactose regioisomers (**30-33**) will have the same IRI activity. Therefore, in order to prove or disprove the hypotheses proposed, compounds **26-33** must be synthesized and tested for IRI activity.

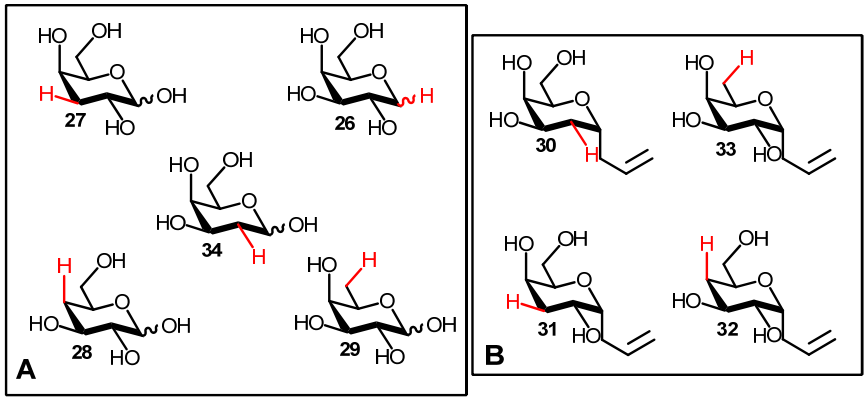

Figure 2.5 Structure of target (**A**) deoxy regioisomers (**26-29**) and (**B**) deoxy α-*C*-allyl galactose regioisomers (**30-33**).

In a related study, Ferreira tested the IRI activity of various C2 functionalized galactosyl derivatives (Graph 2.2) which had varying size and hydrophilicity.[28] The following IRI activity trend was observed: presence of C2 hydroxyl group had the highest IRI activity followed by, galactoazide (**35**), galactoamine (**36**) and *N*-acetyl-galactoamine (**37**). To explain the observed trend, Ferreira proposed that both the azide (**35**) and amine (**36**) would be highly solvated since the azide (**35**) would exist as a zwitterion in solution, while the amine (**36**) would be protonated

(NH_3^+).[28] Being more highly solvated, the azide zwitterion would further disrupt the three dimensional hydrogen bond network surrounding the solute, causing enhanced ice recrystallization inhibition. The increased size of the *N*-acetyl group and loss of hydrogen bond donor ability would reduce the hydration indices of *N*-acetyl-galactosamine (**37**) and 2-deoxy-galactose respectively (**34**).[28]

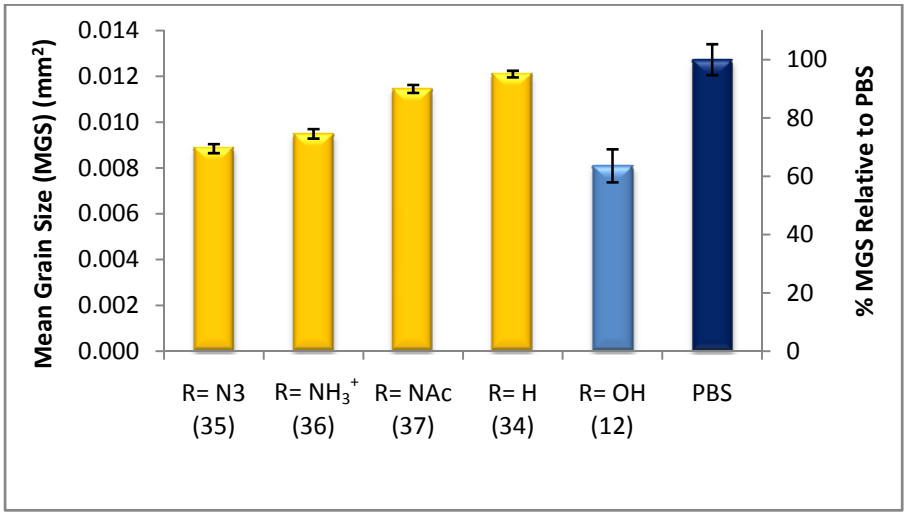

Graph 2.2 IRI activities of C2 functionalized galactosyl derivatives (**34-37**) previously tested by Ferreira at 0.022 M[28]

However, since this study only addressed the C2 position, a series of azide (**38-40**) and amine (**41-43**) functionalized free reducing galactosyl derivatives will also be synthesized and tested for IRI activity (Figure 2.6) to determine the regioelectronic effect of these functional groups on IRI activity. The synthesis will involve formation of the azide derivatives which will be further reduced to the amines.

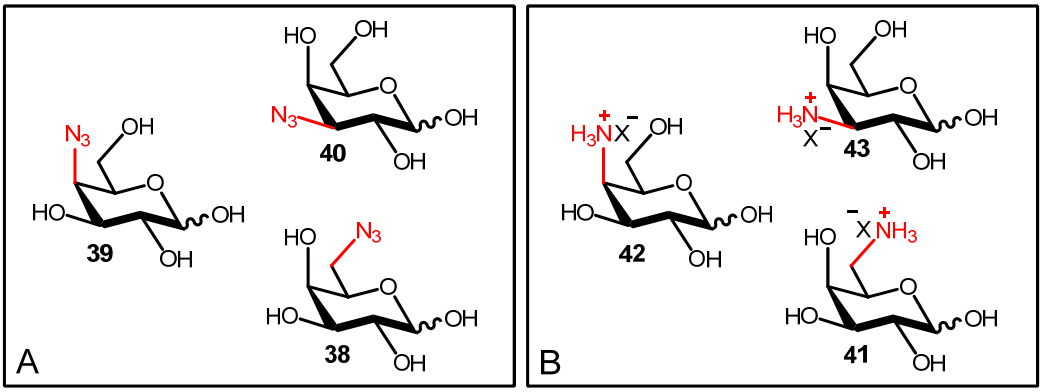

Figure 2.6 Structure of target (**A**) azide (**38-40**) and (**B**) amine (**41-43**) galactose regioisomers

From the results of Chaytor, it is hypothesized that regiochemistry of the azide and amine derivatives will not significantly alter IRI activity. Also, from the results of Ferreira, it is believed that both the azide and amine derivatives will have reduced IRI activity compared to the hydroxyl group containing counterparts. Finally, based on the results shown in Graph 2.2, addition of an azide group instead of an amine is believed to increase IRI activity of the carbohydrate.

The following goals provide a brief summary of this research objective:

1. Synthesize and test the IRI activity of free hydroxyl deoxy galactosyl pyranosides (**26-29**) to gain insight into the effect of hydroxyl group presence, hydrogen bond donor and acceptor ability, and regiochemistry on IRI activity.

2. Synthesize and test the IRI activity of α-*C*-allyl deoxy galactosyl pyranosides (**30-33**) to determine the effect of the α-*C*-allyl anomeric substituent on the IRI activity of galactose.

3. Synthesize and test the IRI activity of azide and amine galactosyl pyranosides (**38-43**) to determine their regioelectronic effect on IRI activity.

2.4 Objective 3: Probing the Effect of Sulfur Substitution at the Anomeric Linkage of Galactose Derivatives on IRI Activity

The importance of the anomeric linkage stereochemistry in AFGP 8 (**1**) activity was previously reported by Nishimira.[29] It was determined that α-configurations conferred better TH activity than the β configuration.[29] However, this study did not test for IRI activity. Therefore, several allyl (**25**, **44**) and methoxy (**45**, **46**) galactosyl derivatives having both α and β configuration were synthesized by Tam *et al*. and Chaytor and tested for IRI activity (Graph 2.3).[13,26] It was determined that the α-configuration imparts slightly greater IRI activity over the β configuration in these galactopyranosyl derivatives. As shown in Graph 2.3, the IRI activities of both the β-methoxy and β-allyl galactosides (**44**, **46**) are lesser compared to their respective α counterparts (**25**, **45**).[13,26] Interestingly, in the presence of the more electronegative atom (oxygen), the methoxy derivatives had poorer activity compared to the *C*-linked allyl derivatives.

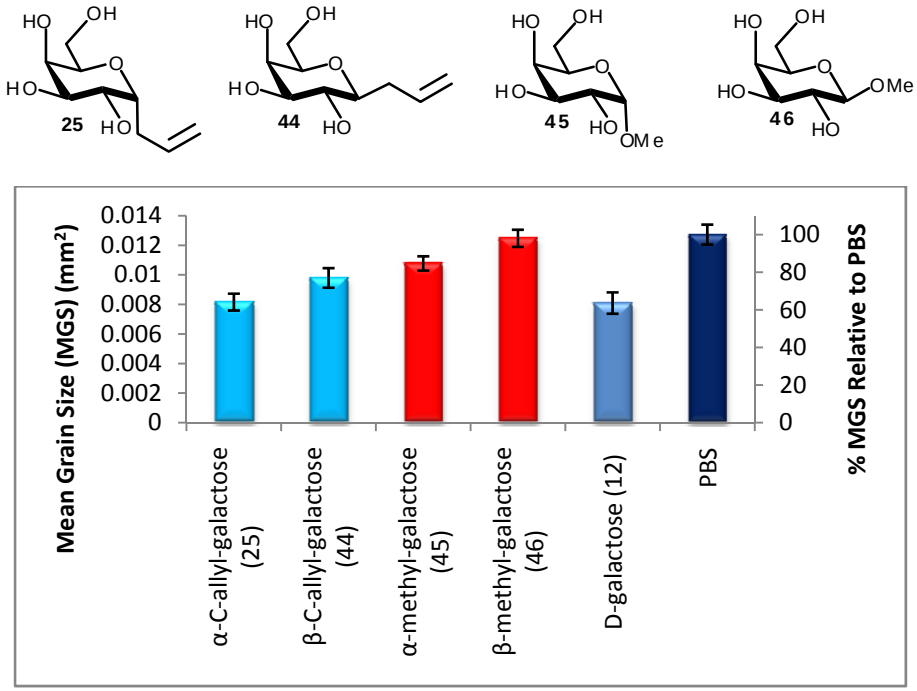

Graph 2.3 IRI activities of α and β allyl and methoxy galactosyl derivatives (**25**, **44-46**) previously synthesized and tested by Tam *et al.* and Chaytor at 0.022 M[12,13,26]

Further varying the nature of the anomeric atom in *C*-serine AFGP analogues (**4-7**) dramatically modified their IRI activity.[6] It was revealed that the more electronegative atom (oxygen) ((*O*-SAA)-gal) (**5**) gave poorer activity than the *C*-linked analogue ((*C*-SGG)-gal) (**4**) (Graph 1.3, p. 27)[6,30] which led Campbell to further investigate the importance of this anomeric position.[31] Since both carbon and sulfur carbohydrate linkages are more stable and easier to synthesize than oxygen derivatives, sulfur α- linked analogues ((CGG)-gal) (**6**) and ((CAA)-gal) (**7**) were prepared (Figure 1.17, p. 26) and tested (Graph 1.3, p. 27) for IRI activity.[31] The results suggest that presence of a more electronegative atom at the anomeric position is negatively affecting the overall IRI activity of these analogues (compared to *C*-serine (**4**)). In addition, the more hydrophobic groups (alanine) (**7**) in the peptide backbone resulted in no change in IRI activity compared to the glycine containing analogue (**6**).[31] Unfortunately the stereochemistry of these analogues was not varied and must be further investigated.

In an attempt to understand the effect of hydrophobic alkyl groups at the C1 position of galactose on its IRI activity, a series of *N*-alkyl acetamide galactopyranosyl derivatives which had increasing alkyl chain lengths were synthesized (Graph 1.2, p. 25).[32] Interestingly, there seemed to be an optimal alkyl chain length at which IRI activity was obtained, which is consistent with recent results reported by Tam *et al*.[33] The propyl amide derivative, as shown in Graph 1.2, has the greatest IRI activity overall, however, the nature of this effect is also not known and needs further investigation.

Since glycopeptides are unfortunately difficult and costly to synthesize,[29] quick generation of a library of structurally different galactosyl derivatives which display IRI activity will accelerate the structure activity relationship studies on the carbohydrate component in AFGPs. Therefore, a series of α- and β-*S*-linked galactosyl derivatives (**47-56**), shown in Figure

2.7, will be synthesized and tested for their IRI activity to determine the influence of the following three structural modifications on IRI activity:

1- Addition of the larger sulfur atom at the anomeric position.

2- Stereochemistry of the anomeric position in the presence of sulfur as the linker atom.

3- Increased hydrophibicity caused by the addition of various *S*-alkyl chains at the C1 position of galactose.

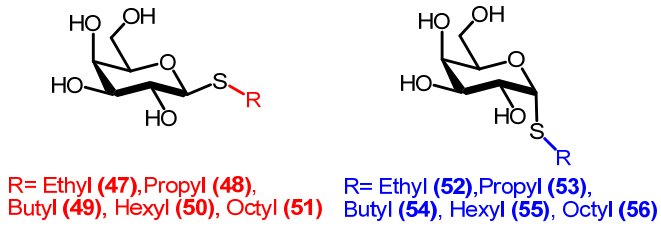

Figure 2.7 Structures of target β-thioalkyl galactoside derivatives (**47-51**) and α-thioalkyl galactoside derivatives (**52-56**).

From the previously described structure activity relationship studies on AFGPs analogues and galactose pyranosides, it is believed that the α-*S*-linked galactosides (**52-56**) will have greater IRI activity than their β-linked counterparts. Also, based on the hydration index proposed by Tam *et al*. it is hypothesized that increases in the hydrophobic nature of a carbohydrate will result in a reduced hydration index and reduced IRI activity. Therefore increasing the alkyl chain length in the β- and α-thioalkyl galactoside derivatives (**47-56**) is believed to further decrease the IRI activity of these galactosyl derivatives.

References

1. Davis, J. M.; Rowley, S. D.; Braine, H. G.; Piantadosi, S.; Santos, G. W., Clinical toxicity of cryopreserved bone marrow graft infusion. *Blood,* **1990**, 75, 781-786

2. Elmoazzen, H. Y.; Poovadan, A.; Law, G. K.; Elliott, J. A. W.; McGann, L. E.; Jomha, N. M., Dimethyl sulfoxide toxicity kinetics in intact articular cartilage. *Cell Tissue Bank,* **2007**, 8, 125-133.

3. Liseth, K.; Abrahamsen, J. F.; Bjorsvik, S.; Grottebo, K.; Bruserud, O., The viability of cryopreserved PBPC depends on the DMSO concentration and the concentration of nucleated cells in the graft. *Cytotherapy,* **2005**, 7, 328-333.

4. Fowler, A.; Toner, M., Cryo-Injury and Biopreservation. *Ann. NY Acad. Sci.* **2006**, 1066, 119-135.

5. Mazur, P., Principles of cryobiology. In: Life in The Frozen State. Fuller BJ, Lane N, Benson EE, eds. **2004**, Boca Raton, FL: CRC Press. p. 3–65.

6. Liu, S.; Ben, R., *C*-Linked Galactosyl Serine AFGP Analogues as Potent Recrystallization Inhibitors. *Org. Lett*. **2005**, 7, 2385-2388.

7. Liu, S.; Wang, W.; von Moos, E.; Jackman, J.; Mealing, G.; Monette, R.; Ben, R. N., *In Vitro* Studies of Antifreeze Glycoprotein (AFGP) and a *C*-Linked AFGP Analogue. *Biomacromolecules,* **2007**, 8, 1456-1462.

8. Koushafar, H. ; Pham, L.; Lee, C.; Rubinsky, B., Chemical adjuvant cryosurgery with antifreeze proteins. *J. Surg. Oncol.* **1997**, 66, 114-121.

9. Mugnano, J. A.; Wang, T.; Layne, J. R.; DeVries, A. L.; Lee, R. E., Antifreeze glycoproteins promote intracellular freezing of rat cardiomyocytes at high subzero temperatures. Am. J. Physiol., **1994**, 269, R474- R479.

10. Wang, T.; Zhu, Q.; Yang, X.; Layne, J. R., Jr.; DeVries, A. L., Antifreeze Glycoproteins from Antarctic Notothenioid Fishes Fail to Protect the Rat Cardiac Explant during Hypothermic and Freezing Preservation. Cryobiology, **1994**, 31, 185-192.

11. Yeh, Y.; Feeney, R. E., Antifreeze Proteins: Structures and Mechanisms of Function. *Chem Rev.,* **1996**, 96, 601-607.

12. Czechura, P.; Tam, R.Y.; Dimitrijevic, E; Murphy, A.V; Ben, R. N., The Importance of Hydration for Inhibiting Ice Recrystallization with *C*-Linked Antifreeze Glycoproteins, *J. Am. Chem. Soc.*, **2008,** 130, 2928-2929.

13. Tam R.Y.; Ferreira, S. S.; Czechura, P.; Chaytor, J. L.; Ben, R. N., Hydration Index - A Better Parameter for Explaining Small Molecule Hydration in Inhibition of Ice Recrystallization, *J. Am. Chem. Soc*. **2008**, 130, 17494–17501.

14. Dashnau, J.; Sharp, K. A.; Vanderkooi, J. M., Carbohydrate Intramolecular Hydrogen Bonding Cooperativity and Its Effect on Water Structure, *J. Phys. Chem. B* **2005**, 109, 24152–24159.

15. (a) Eroglu, A.; Bailey, S. E.; Toner, M.; Toth, T. L., Successful Cryopreservation of Mouse Oocytes by Using Low Concentrations of Trehalose and Dimethylsulfoxide. *Biol. Reprod.* **2009**, 80, 70-80. (b) Izadyar, F.; Matthijs-Rijsenbilt, J. J.; Den Ouden, K.; Creemers, L. B.; Woelders, H.; De Rooij, D. G., Development of a Cryopreservation Protocol for Type A Spermatogonia. *J. Androl.* **2002**, 23, 537-545. (c) Ma, W.; O'Shaughnessy, T.; Chang, E., Cryopreservation of adherent neuronal networks. *Neurosci. Lett.* **2006**, 403, 84-89. (d) Petrenko, Y. A.; Jones, D. R. E.; Petrenko, A. Y., Cryopreservation of human fetal liver hematopoietic stem/progenitor cells using sucrose as an additive to the cryoprotective medium. *Cryobiology,* **2008**, 57,195-200. (e) Santos, R. R.; Tharasanit, T.; Figueiredo, J. R.; van Haeften, T.; van den Hurk, R., Preservation of caprine preantral follicle viability after cryopreservation in sucrose and ethylene glycol. *Cell Tissue Res.* **2006**, 325, 523-531. (f) Vicente, J. S.; Viudes-de-Castro, M. P., A sucrose-DMSO extender for freezing rabbit semen. *Reprod. Nutr. Dev.* **1996**, 36, 485-492.

16. (a) Gutierrez-Perez, O.; Juarez-Mosqueda, M. d. L.; Carvajal, S. U.; Ortega, M. E. T., Boar spermatozoa cryopreservation in low glycerol/trehalose enriched freezing media improves cellular integrity. *Cryobiology* **2009**, 58, 287-292. (b) Hu, J.-H.; Li, Q.-W.; Jiang, Z.-L.; Yang, H.; Zhang, S.-S.; Zhao, H.-W., The Cryoprotective Effect of Trehalose Supplementation on Boar Spermatozoa Quality. *Reprod. Dom. Anim.* **2009**, 44, 571-575.

17. (a) Coticchio, G.; De Santis, L.; Rossi, G.; Borini, A.; Albertini, D.; Scaravelli, G.; Alecci, C.; Bianchi, V.; Nottola, S.; Cecconi, S., Sucrose concentration influences the rate of human oocytes with normal spindle and chromosome configurations after slow-cooling cryopreservation. *Hum. Reprod.* **2006**, 21, 1771-1776. (b) Neto, V.; Buff, S.; Lornage, J.; Bottollier, B.; Guerin, P.; Joly, T., Effects of different freezing parameters on the morphology and viability of preantral follicles after cryopreservation of doe rabbit ovarian tissue. *Fertil. Steril.* **2008**, 89, 1348-1356.

18. (a) Holovati, J. L.; Gyongyossy-Issa, M. I. C.; Acker, J. P., Effects of trehalose-loaded liposomes on red blood cell response to freezing and post-thaw membrane quality. *Cryobiology* **2009**, 58, 75-83. (b) Son, J. H.; Kim, K.-H.; Nam, Y.-K.; Park, J.-K.; Kim, S.-K., Optimization of cryoprotectants for cryopreservation of rat hepatocyte. *Biotechnol. Lett.* **2004**, 26, 829-833. (c) Valente, S. S.; Pereira, R. M.; Baptista, M. C.; Marques, C. C.; Vasques, M. I.; Silva Pereira, M. V. C.; Horta, A. E. M.; Barbas, J. P., In vitro and in vivo fertility of ram semen cryopreserved in different extenders. *Anim. Reprod. Sci.* **2010**, 117, 74-77.

19. Raymond, J. A.; DeVries, A. L., Adsorption inhibition as a mechanism of freezing resistance in polar fish, *Proc. Nat. Acad. Sci. USA*, **1977**, 74, 2589-2593.

20. Pertraya, N; Marshall, C. B.; DiPrinzio, C. L.; Wilen, L.; Thomson, E. S.; Wettlaufer, J. S.; Davies, P. L.; Braslavsky, I., Fluorescence Microscopy Evidence for Quasi-Permanent Attachment of Antifreeze Proteins to Ice Surfaces. *Biophys. J.* **2007**, 92, 3663-3673.

21. (a) Knight, C. A.; Driggers, E.; DeVries, A. L., Adsorption to ice of fish antifreeze glycopeptides 7 and 8. *J. Biophys*., **1993**, 64, 252-259. (b) DeVries, A. L.; Komatsu, S. K.; Feeney, R. E., Chemical and Physical Properties of Freezing Point-Depressing Glycoproteins from Antarctic Fish. *J. Biol. Chem.***1970**, 245, 2901-2908. (c) Wen, D.; Laursen, R. A., Structure-Function Relationships in an Antifreeze Polypeptide: The role of neutral, polar amino acids. *J. Biol. Chem.* **1992**, 267, 14102-14108. (d) Madura, J. D.; Wierzbicki,A.; Harrington, J. P.; Maughon, R. H.; Raymond, J. A.; Sikes, C.S., Interactions of the D- and L-Forms of Winter Flounder Antifreeze Peptide with the {201} Planes of Ice. *J. Am. Chem. Soc.* **1994**,116, 417-418.

22. (a) Baruch, E.; Belostotskii, A. M.; Mastai, Y., Relationship between the antifreeze activities and the chemical structure of polyols. *J. Mol. Struct.***2008**, 874, 170-177. (b) DeVries, A. L.; Price, T. J., Role of Glycopeptides and Peptides in Inhibition of Crystallization of Water in Polar Fish [and Discussion]. *Philosophical Transactions of the Royal Society B*, **1984**, 304, 575-588.

23. (a) Chakrabartty, A.; Yang, D. S. C.; Hew, C. L., Structure-Function Relationship in a Winter Flounder Antifreeze Polypeptide: II. Alteration of the component growth rates of ice by synthetic antifreeze polypeptides. *J. Biol. Chem.* **1989**, 264, 11313-11316. (b) Yang, D. S. C.; Sax, M.; Chakrabartty, A.; Hew, C. L., Crystal Structure of an antifreeze polypeptide and its mechanistic implications. *Nature*, **1988**, 333, 232-237. (c) Chao, H.; Housten, M. E. J.; Hodges, R. S.; Kay, C. M.; Sykes, B. D.; Loewen, M. C.; Davies, P. L.; Sönnichsen, F. D., A Diminished Role for Hydrogen Bonds in Antifreeze Protein Binding to Ice. *Biochemistry*, **1997**, 36, 14652-14660. (d) Zhang, W.; Laursen, R. A., Structure-Function Relationships in a Type I Antifreeze Polypeptide: The role of threonine methyl and hydroxyl groups in antifreeze activity. *J. Biol. Chem.***1998**, 273, 34806-34812.

24. Sönnichsen, F. D.; DeLuca, C. I.; Davies, P. L.; Sykes, B. D., Refined solution structure of type III antifreeze protein: hydrophobic groups may be involved in the energetics of the protein-ice interactions. *Structure*, **1996**, 4, 1325-1337.

25. Galema, S. A.; Høiland, H. Stereochemical Aspects of Hydration of Carbohydrates In Aqueous Solutions. 3. ^{1}Density and Ultrasound Measurements, *J. Phys. Chem.* **1991**, *95*, 5321.

26. Chaytor, J. L., Ph.D. Dissertation, University of Ottawa, **2010**

27. Marcin Palusiak,M.; Grabowski, S. J., Methoxy group as an acceptor of proton in hydrogen bonds. *Journal of Molecular Structure*, **2002**, 642, 97-104.

28. Ferreira, S. S., M. Sc. Dissertation, University of Ottawa, **2009**

29. Tachibana, Y.; Fletcher, G. L.; Fujitani, N.; Tsuda, S.; Monde, K.; Nishimura, S. –I., Antifreeze Glyoproteins: Elucidation of the Structural Motifs that are Essential for Antifreeze Activity. *Angew. Chem. Int. Ed.* **2004**, 43, 856-862.

30. Bouvet, V., Ph.D. Dissertation, University of Ottawa, **2005**

31. Campbell, W., M. Sc. Dissertation, University of Ottawa, **2009**

32. Trant, J. T.; Biggs, R.; Ben, R. N., unpublished results, **2009**

33. Tam, R.Y.; Rowley, C. N.; Petrov, I.; Zhang, T.; Afagh, N. A.; Woo T. K.; Ben, R. N., Solution Conformation of C-Linked Antifreeze Glycoprotein Analogues and Modulation of Ice Recrystallization, *J. Am. Chem. Soc.*, **2009**, 131, 15745-15753.

Chapter 3: Assessing the Potential Link between Cryopreservation Ability and IRI Activity of Simple Mono- and Disaccharides

3.1 Introduction

Recrystallization has been extensively studied in the metallurgical and material sciences.[1] It is believed that ice recrystallization inside and around a frozen cell causes significant cell damage during cryopreservation.[2,3] The fact that fish dwelling in sub-zero temperatures experience freeze-protection due to the production of IRI-active AFGPs suggests there is a link between IRI and cryoprotection.[4] However, more studies are required in order to confidently link ice recrystallization to cellular damage after the freeze/thaw process.

It has been noted that the hydration of the carbohydrate moiety on the previously synthesized AFGP analogues (**3**, **9-11**) (Figure 1.18, p. 27, Graph 1.4, p. 29) affects IRI activity and that simple mono- and disaccharides, as well as DMSO, also exhibit IRI activity.[5] The fact that DMSO and simple sugars are frequently used as cryoprotectants,[6] sets precedence for assessing whether there is a link between IRI activity and cryopreservation ability. Using these small molecules will provide insight into the cryoprotective mode of action of AFGP and other similar cryoprotectants (such as DMSO and carbohydrate derivatives).

3.2 Assessing the Effects of Concentration on IRI Activity of Simple Mono- and Disaccharides

As previously mentioned, Tam *et al*. tested the IRI activity of monosaccharides (D-galactose (**12**), D-glucose (**13**), D-mannose (**14**) and D-talose (**15**)), and disaccharides (D-melibiose (**16**), D-lactose (**17**), D-trehalose (**18**) and D-sucrose (**20**)) at 0.022 M.[5] They proposed that the hydration index (hydration number per unit volume)[7] of these sugars could easily predict their relative IRI activities. Initially, we tested the IRI activity using the same method as before but with a higher concentration (0.22 M) in order to reflect concentrations used in

cryopreservation protocols[2,8] and to further probe the predictive power of the hydration index at higher concentrations (Graph 3.1). Although common carbohydrate concentrations found in the literature exceed 0.22 M, higher concentrations were too viscous to be accurately tested.[6]

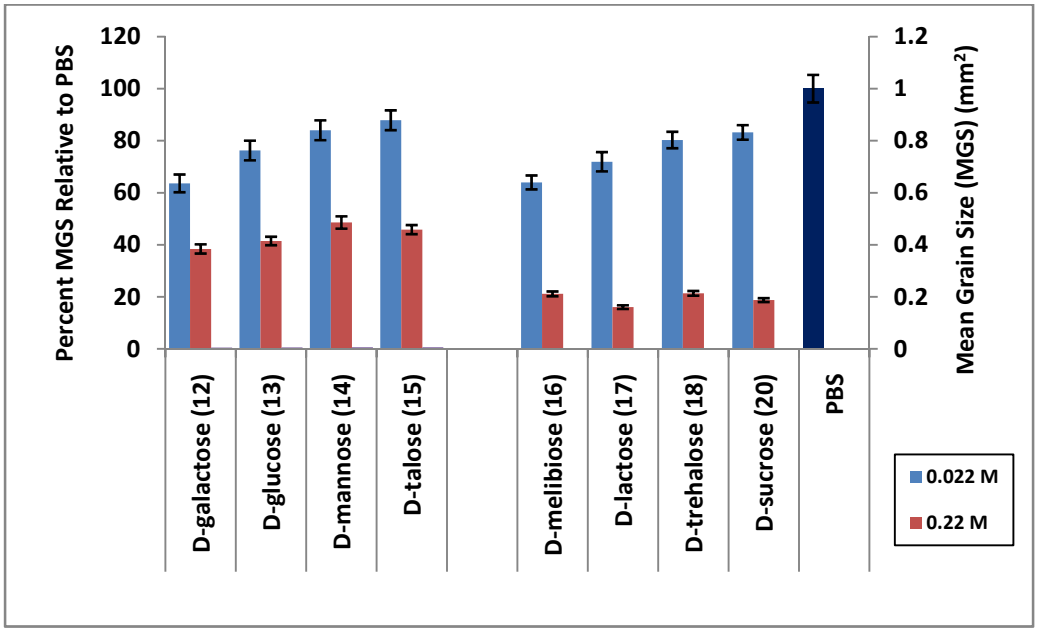

Graph 3.1 Ice recrystallization inhibition activity (% Mean Grain Size (MGS) relative to PBS) of mono- and disaccharides (**12-18**, **20**) tested at concentrations of 0.022 M (blue bars) and 0.22 M (red bars).

From Tam *et al.*, it was shown that IRI activity correlates well with the calculated hydration indices of the mono- and disaccharides at concentrations of 0.022 M.[5] D-Galactose (**12**) and D-melibiose (**16**) were the most IRI active (mean grain size, MGS, compared to PBS) mono- and disaccharides respectively at 0.022 M and possessed similar IRI activities as predicted by their hydration indices.[5]

At 0.22 M, the monosaccharides displayed greater IRI activity (about twice as effective as 0.022 M) and still maintained the same trend, with D-galactose **(12)** having the best IRI activity and D-talose **(15)** having the worst. However, the relative IRI activities of disaccharides at 0.022 M are different than at 0.22 M. At the higher concentration, all disaccharides show

similar IRI activities and are all, in general, about 50 % more active than 0.22 M monosaccharides. Also, D-lactose **(17)** has slightly better IRI activity compared to the other disaccharides tested. Interestingly, the hydration index does not predict these results, suggesting that carbohydrate concentration plays a more significant role in determining carbohydrate IRI activity.[5] In fact, if the hydration indices were correct predictors of IRI activity, D-galactose **(12)** and D-melibiose **(16)** would have the same IRI activity, irrespective of their concentrations.[5]

One reason which may explain why the hydration index fails to predict the IRI activity of carbohydrates at higher concentrations is that the compressibility co-efficient used to calculate the hydration index was derived for solutions at infinite dilution.[7] Thus, at high carbohydrate concentrations, infinite dilution cannot be considered, which prevents the use of the hydration index parameter. At these higher concentrations, interactions between the carbohydrate structures in solution (such as intermolecular hydrogen bonds) may affect their individual hydration which minimizes the effect of hydration on IRI activity.

3.3 IRI Activity of DMSO, Carbohydrates and DMSO/Carbohydrate Concentrations

Since DMSO, a commonly used cryoprotectant (in concentrations ranging from 10 to 20 %),[9,10] has effective IRI activity (at a concentration of 4 %),[5] and is sometimes used in conjunction with carbohydrates during cryopreservation protocols,[6] we wished to compare the IRI activity of solutions of DMSO and DMSO with carbohydrates to carbohydrates alone. Concentrations higher than 5 % DMSO could not be used since large portions of the ice wafer (used for the IRI assay) remained unfrozen. In addition, Liseth *et al*. have reported that concentrations lower than 10 % DMSO are effective cryprotectants[10]. Therefore, as shown in Graph 3.2, we tested the IRI activity of 2.5 % and 5 % DMSO solutions. We also tested the IRI

activity of mixtures of mono- (D-galactose (**12**)) and disaccharides (D-melibiose (**16**) and D-sucrose (**20**)) with varying concentrations of DMSO. D-Galactose (**12**) was chosen since it is the monosaccharide with the best IRI activity at both 0.022 M and 0.22 M, similar to D-melibiose (**16**) which was the best disaccharide at 0.022 M. D-Sucrose (**20**) was chosen since it has the worst IRI activity of the disaccharides at 0.022 M and was used for comparison.

From the results (Graph 3.2) it is apparent that both 2.5 and 5 % DMSO exhibit IRI activity and that a 5 % DMSO solution is approximately 50 % more effective at inhibiting ice recrystallization than a 2.5 % solution. Compared to the carbohydrates, 2.5 and 5 % DMSO solutions have similar IRI activity to 0.022 M and 0.22 M D-galactose (**12**) respectively. Also, a 2.5 % DMSO solution is more effective than 0.022 M D-sucrose (**20**). Interestingly, the IRI activity of 0.022 M D-galactose (**12**) remains relatively unchanged with addition of 2.5 % DMSO. In contrast, addition of 2.5 % DMSO to 0.022 M disaccharides (D-melibiose (**16**) and D-sucrose (**20**)) increases the IRI activity of the carbohydrate mixture to about the same activity as 2.5 % DMSO alone. Further addition of DMSO from 2.5 to 5 % causes an additional improvement in IRI activity for all three sugars at 0.022 M, such that the activities closely ressemble 5 % DMSO. Both 2.5 % and 5 % DMSO solutions are quite concentrated (0.350 and 0.700 M respectively) in relation to the amount of carbohydrate added (0.022 M). It may be possible that the higher concentrations of DMSO are negating (or masking) the IRI activity of these sugars, therefore producing IRI activities similar to DMSO solutions alone.

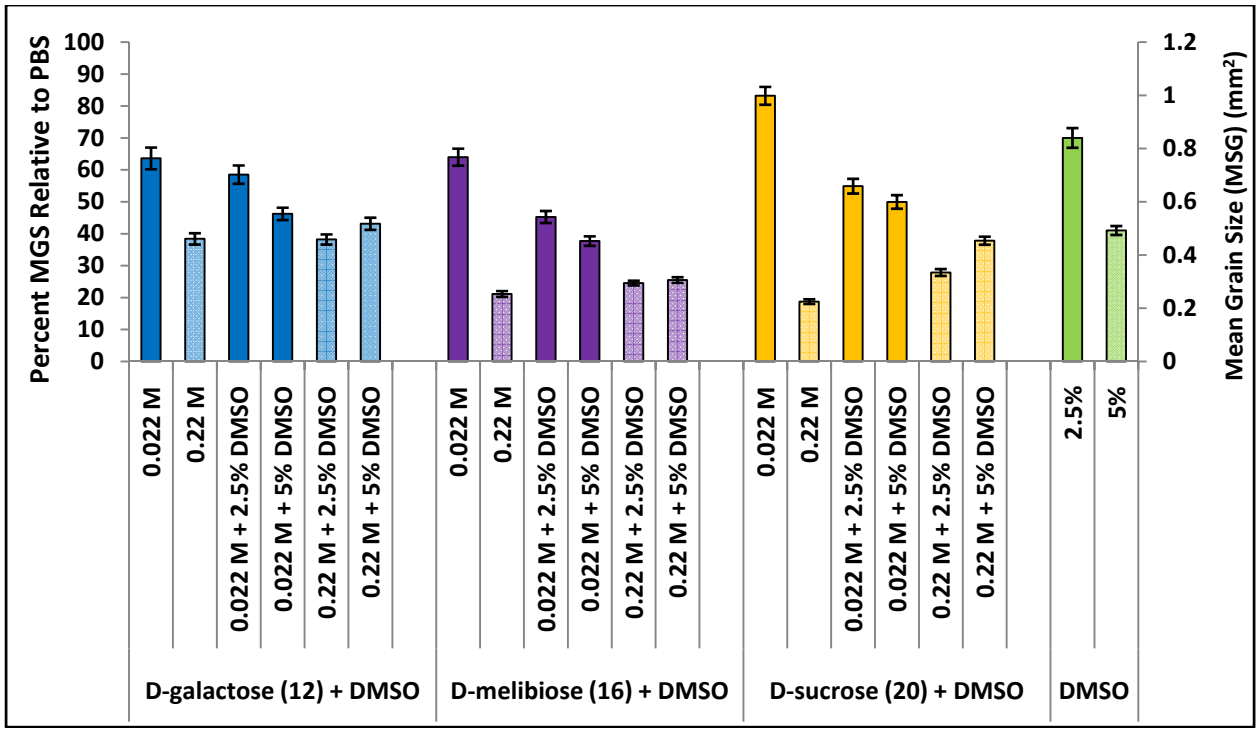

Graph 3.2 Ice recrystallization inhibition activities of a series of mono- and disaccharides (**12**, **16**, **20**) combined with 2.5 and 5.0 % DMSO.

With 0.22 M solutions of the reducing sugars (D-galactose (**12**) and D-melibiose (**16**)), the % MGS relative to PBS decreases slightly (4.9 and 0.9 % respectively) with addition of 5 % DMSO. More importantly, there is a larger decrease (10 %) in % MGS relative to PBS as 5 % DMSO is added to 0.22 M D-sucrose (**20**) solution. Therefore, it appears that DMSO has a synergistic effect with 0.022 M solutions of D-sucrose (**20**), D-galactose (**12**) and D-melibiose (**16**), but an antagonistic effect with higher concentrations of these carbohydrates. An explanation as to why addition of DMSO negatively affects the IRI activity of these 0.22 M carbohydrate solutions, is that the increased concentration of carbohydrate is no longer soluble in these solutions of highly concentrated DMSO, since carbohydrate solubility in DMSO is lower than in water.[11] Also, it seems that the IRI activity of the only non-reducing sugar tested (D-sucrose (**20**)) is more strongly affected by the addition of DMSO than the other reducing sugars

(D-galactose (**12**) and D-melibiose (**16**)). Further investigations are required to determine if and how the non-reducing ability of D-sucrose (**20**) is a major factor affecting its IRI activity in the presence of DMSO. While the nature of these effects needs to be investigated further, these results suggest that, based upon IRI activity alone, addition of DMSO is not required when 0.22 M D-sucrose (**20**) is used to inhibit ice recrystallization.

It is also apparent that a combination of 2.5 % DMSO with 0.22 M D-galactose (**12**) is as effective as a 5 % DMSO solution alone. Since DMSO is cytotoxic,[10] lowering the DMSO concentration in combination with low concentrations of carbohydrate (≤ 0.22 M) is better than using higher concentrations of DMSO alone. If IRI activity is a predictor of cryopreservation ability, a 0.22 M D-galactose (**12**) solution could effectively replace 5 % DMSO in cell preservation protocols and may result in less cytotoxicity post freeze-thaw. However, this last effect (cytotoxicity) must first be determined.

3.4 Assessing Cytotoxicity of Simple Mono- and Disaccharides

To test for potential cytotoxic effects that carbohydrates may have on cells, von Moos and Guolla tested cytotoxic effects (at physiological temperatures, 37°C) of three concentrations (0.022, 0.2 and 0.5 M) of carbohydrates (**12**, **13**, **16-18**, **20**) (Figure 2.1, p. 46) along with 2.5 and 5 % DMSO in a single human embryonic liver cell line (WRL 68) using a conventional MTT assay.[12] As mentioned, this assay screened for mitochondrial function by determining the amount of formazan reduced by the mitochondrial and cytosolic enzymes which use cellular reducing equivalents (i.e. NADH, NADPH, or succinate), (see Figure 3.1).

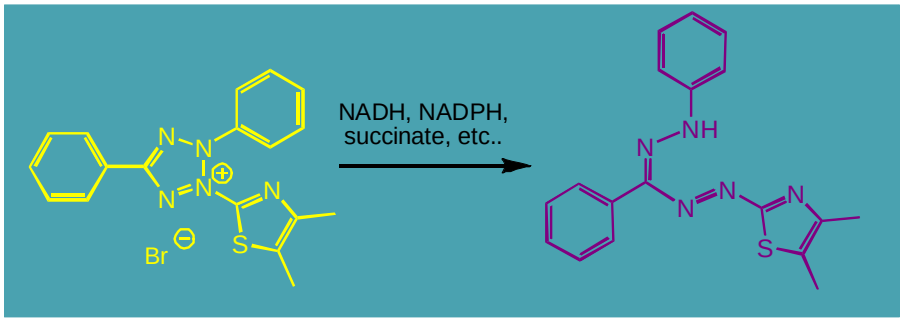

Figure 3.1 Structures of oxidized (a yellow tetrazole) and reduced (purple formazan) MTT (3-(4,5-dimethylthiazol-2-yl)-2,5-diphenyltetrazolium bromide) in the cell viability colorimetric assay[12]

From the results shown in Graph 3.3, it is apparent that all carbohydrates (**12**, **13**, **16-18**, **20**) display mild cytotoxicity which increases with concentration. Also, cell viability following exposure to 0.022 and 0.2 M carbohydrates is approximately equal to that with 2.5 and 5 % solutions of DMSO respectively. However, there is a significant decrease in cell viability for the disaccharides (**16-18**, **20**) at 0.5 M compared to the other concentrations, while only a slight decrease is observed for the monosaccharides at 0.5 M relative to 0.2 M. While the reason why these higher concentrations of disaccharides show greater cytotoxicity than the higher concentrations of monosaccharides is unclear, it may be due to increased size or number of hydroxyl groups which is affecting the osmotic pressure and water efflux across the cellular membrane. It has been reported that D-sucrose (**20**) does not internalize into the cell at 37°C.[13] Also, it has been reported that cells exposed to carbohydrate concentrations which exceed 0.1 M will undergo significant cellular damage due to the formation of Schiff bases from glycation, even at physiological temperatures.[14] Although the nature of this effect needs further investigation, glycation can only occur if the cell is exposed to reducing carbohydrates[15] and since both non-reducing disaccharides (D-sucrose (**20**) and D-trehalose (**18**)) and reducing disaccharides (D-melibiose (**16**) and D-lactose (**17**)) have the same magnitude of cytotoxicity at

all concentrations tested, the cytotoxic effects from formation of Schiff bases may not be the dominant factor causing poor cell viability.

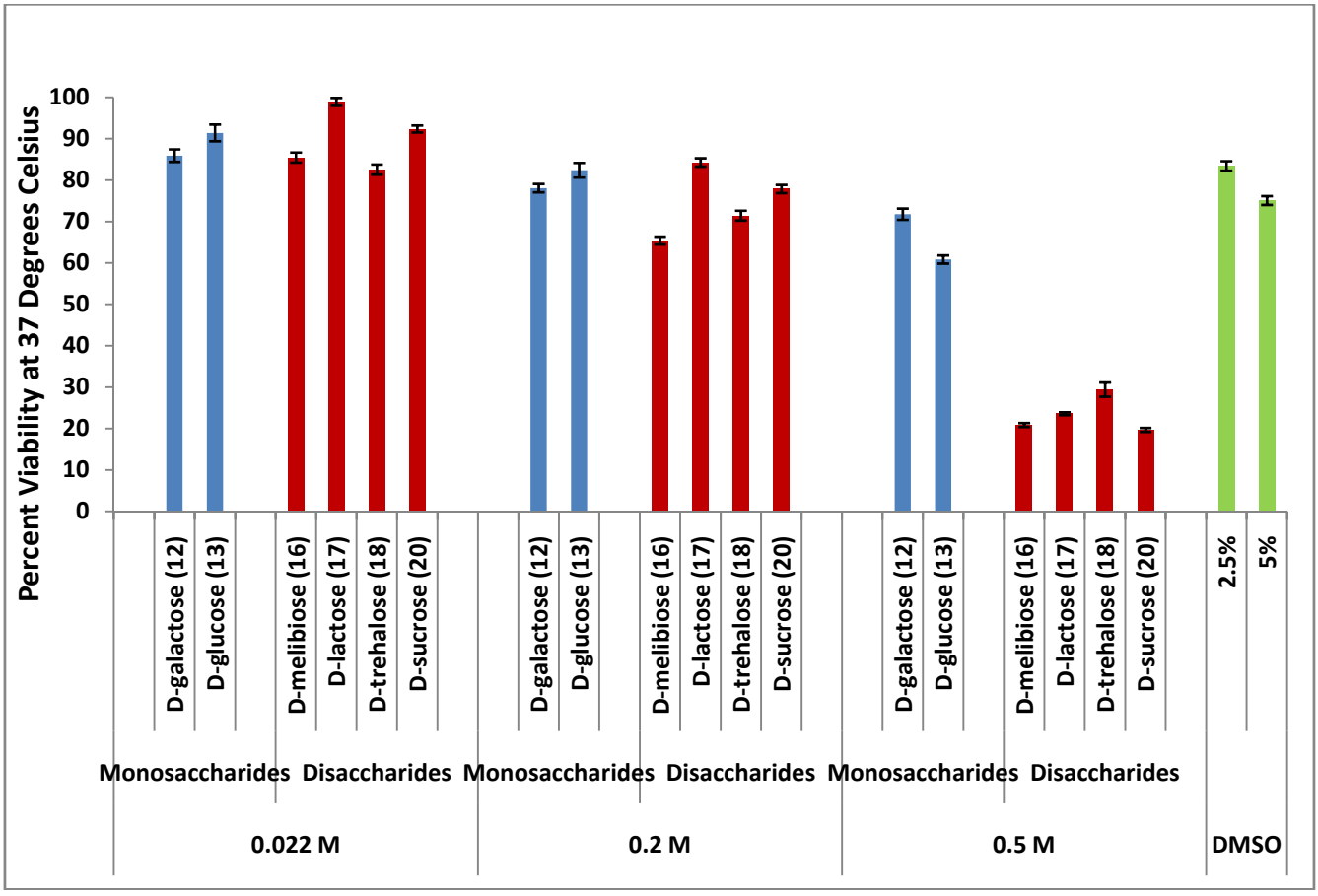

Graph 3.3 Recorded percent viabilities of WRL-68 cells incubated at physiological temperature (37°C) with a series of carbohydrates (**12**, **13**, **16-18**, **20**) and DMSO.

3.5 Assessing Cryopreservation Ability of Simple Mono- and Disaccharides which Display IRI Activity

Since carbohydrates **12**, **13**, **16-18** and **20** as well as DMSO have similar cytotoxicity profiles, the next step was to probe their cryoprotection profiles which was conducted by Wu and von Moos using a flow cytometer and the same cell line (WRL-68) as the previous cytotoxicity testing. It was crucial to use the same human embryonic liver cell line since previous studies conducted on cryoprotective agents lacked the consistency of a systematic scan in a single cell

line. This is therefore the first study of its kind to assess cytotoxicity and cryoprotective ability of mono- and disaccharides (**12**, **13**, **16-18**, **20**) in a single cell line. Therefore, the same carbohydrates and concentrations were used to cryopreserve the WRL-68 cells using a standard freezing protocol which consisted of cooling the cells to -80°C at a rate of 1°C/min followed by transfer to liquid nitrogen (-196°C) for seven days. After a week of cold incubation, the cells were quickly thawed and an apoptosis (programmed cell death) marker (Annexin V)[16] as well as a cell viability marker (7-AAD)[17] were added to the cell suspension before measuring the fluorescence of each cell using flow cytometry. How these markers (Annexin V and 7-AAD (or 7-Aminoactinomycin D)) bind to the apoptotic and necrotic cell is shown in Figure 3.2. It is reported that as a cell undergoes apoptosis, phosphatidylserine fatty acids will accumulate at the surface of the extracellular membrane.[16] Annexin V will strongly bind to the negatively charged end of the fatty acid which indicates early signs of apoptosis (early apoptosis cell fraction).[16] As the cell membranes become more compromised during the cell death process, this barrier can no longer inhibit the infiltration of exterior particulates. 7-AAD which is a double strand DNA intercalator will bind to exposed DNA which indicates the late stage of the apoptosis pathway (late apoptosis cell fraction).[16,17] However, it may be possible that cell membrane damage occurs during or after the freeze-thaw cycle so that Annexin V binding does not occur. In this case 7-AAD binds to exposed double stranded DNA and indicates complete cell death (necrotic cell fraction).[16,17] Therefore, from the results of a flow cytometer scan, only the cells which have no Annexin V and 7-AAD binding are considered fully viable cells.

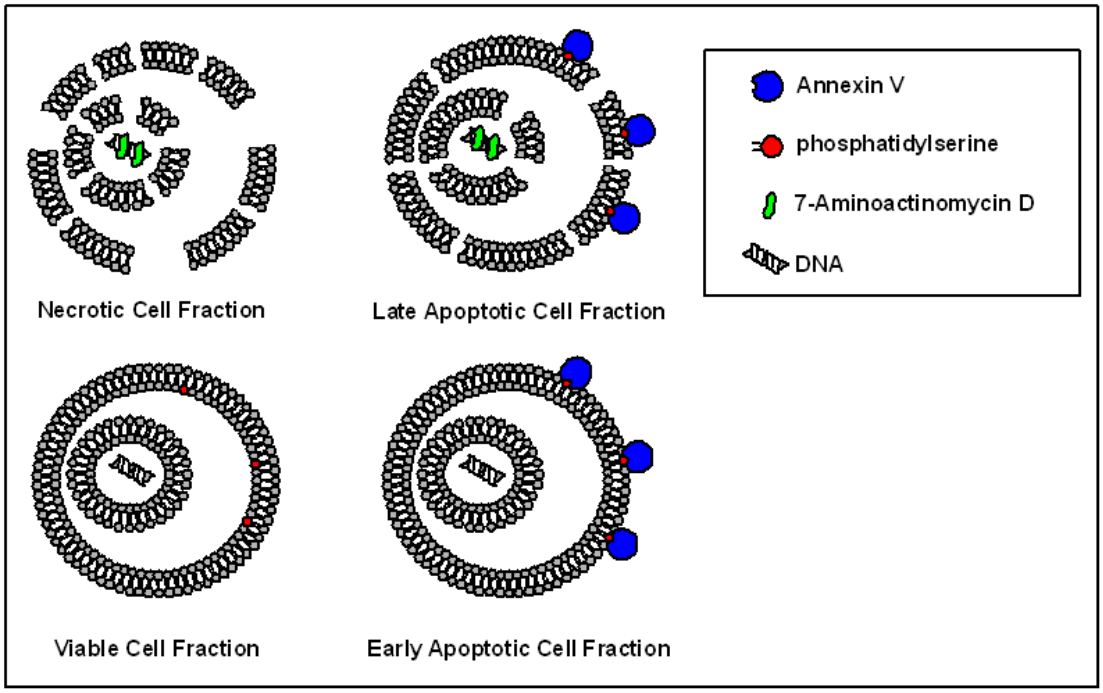

Figure 3.2 Schematic representation of Annexin V and 7-AAD binding to viable, early apoptotic, late apoptotic and necrotic cells.[16,17]

The percent of viable cells following cryopreservation with various carbohydrates and carbohydrate concentrations is plotted in Graph 3.4 with 2.5 and 5 % DMSO. Upon initial analysis, it is clear that a 0.022 M concentration of all carbohydrates (**12**, **13**, **16-18**, **20**) results in poor cryoprotection. It is also noted that beyond 0.2 M, very little additional cryoprotection is confered to WRL-68 cells. Since 0.5 M disaccharides are more toxic to the cell at physiological temperatures, these results indicate that a smaller concentration than those used in literature is sufficient to cryopreserve cells. If these results are compared to DMSO, it seems that 2.5 and 5 % DMSO corresponds to 0.022 and 0.2 M D-galactose (**12**) respectively. Interestingly, when comparing the cytotoxicity (Graph 3.3) data to this new data (Graph 3.4) we see a change in the general trend. It is proposed that compounds which are cytotoxic to human embryonic liver cells at physiological conditions confer better cryoprotection during cryopreservation in the presence of these same compounds.

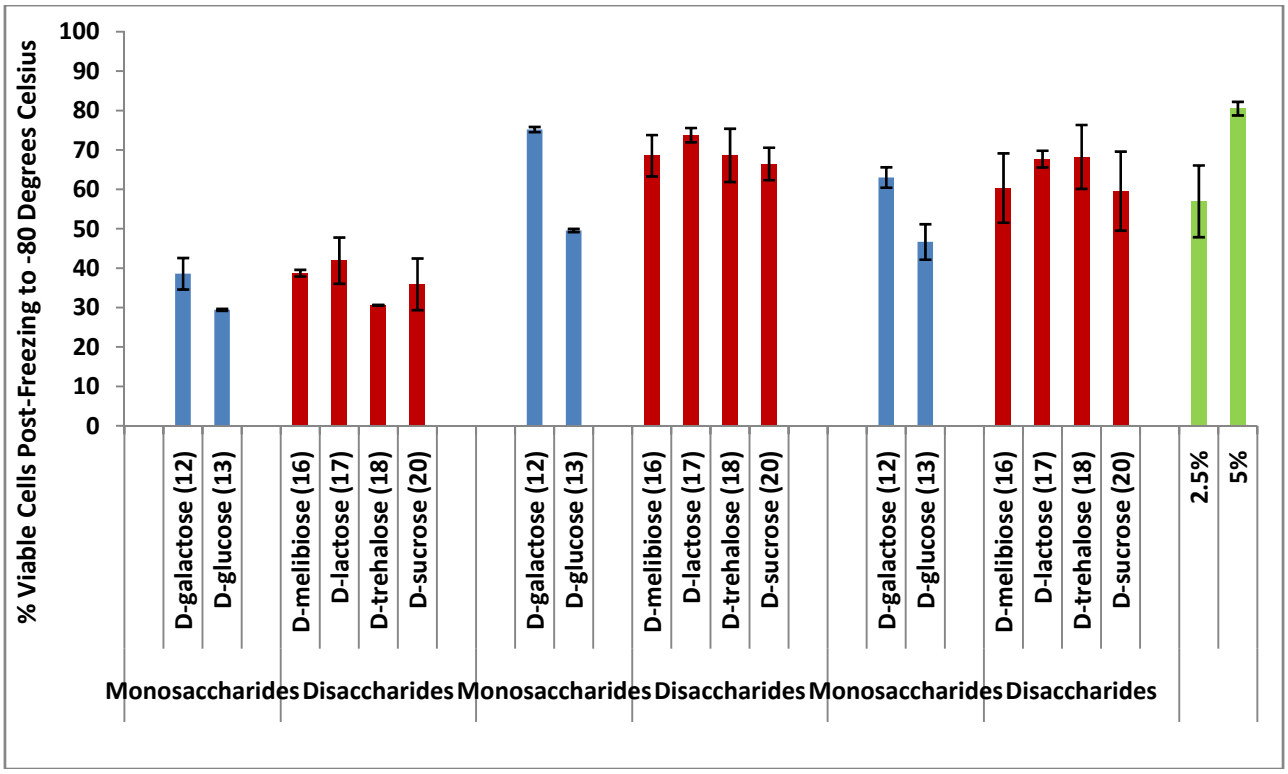

Graph 3.4 Recorded percent viabilities of WRL-68 cells cryopreserved (-198°C) with a series of carbohydrates (**12**, **13**, **16-18**, **20**) and DMSO.

3.6 Determining whether there is a link between IRI activity and cryopreservation ability

To verify this hypothesis, the results were further analyzed to identify any possible trends between cytotoxicity or cell viability post cryopreservation and IRI activity of these carbohydrates and DMSO. The cell viability recorded (at 0.022 M and 0.2 M) in Graph 3.3 was plotted against the IRI activity of the respective sugars at concentrations of 0.022 M and 0.22 M. The IRI activity of carbohydrates at 0.5 M could not be assessed due to large unfrozen portions in the ice wafer. The results plotted in Graph 3.5 show a positive slope between the two parameters with low R^2 value (0.54) which suggests there is a weak correlation between IRI activity and cytotoxicity. However, there are two distinct groupings found on the graph. First, the carbohydrates with poorer IRI activity (0.022 M concentrations) are grouped on the right along with 2.5 % DMSO and correspond to a high cell viability post 24 h exposure. Secondly,

the carbohydrates with greater IRI activity (0.22 M concentrations) are grouped on the left hand side along with 5 % DMSO and correspond to a low cell viability post 24 h exposure. These results suggest that higher concentrations of carbohydrates are less toxic to the human embryonic liver cell.

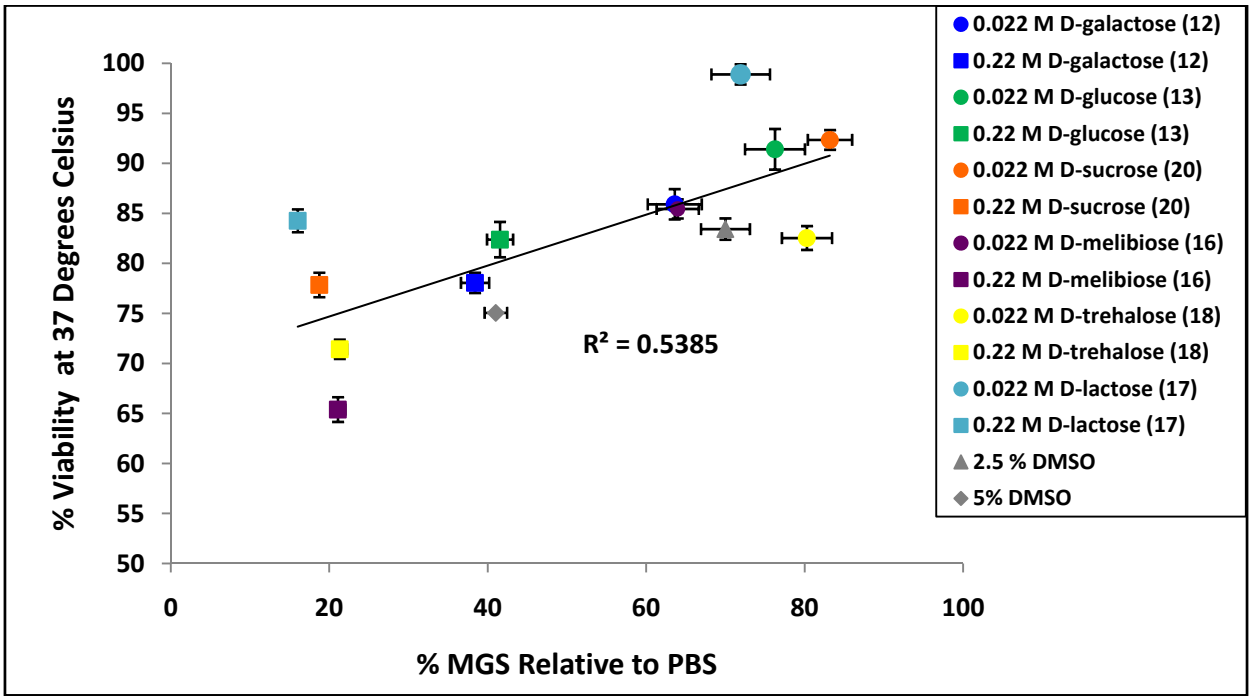

Graph 3.5 Comparison of recorded percent cell viabilities (y-axis) of WRL-68 cells incubated at physiological temperature with a series of carbohydrates (**12, 13, 16-18, 20**) and DMSO in relation to their respective IRI activities (x-axis).

Graph 3.6 represents the viable cell fraction post- cryopreservation in the presence of various carbohydrates as a function of their respective IRI activities. From an initial analysis, it is clear that the sign of the slope of regression changes between Graph 3.5 and Graph 3.6. It is important to note that sugars displaying poor IRI activity confer poor cryopreservation protection whereas sugars with greater IRI activity provide greater cryoprotection. More importantly, the R^2 value is much higher (0.85) suggesting there is a stronger correlation between IRI activity and cryopreservation ability of a given carbohydrate than between IRI activity and cytotoxicity. This

is therefore the first study to prove that the IRI activity of a given compound can be used as a predictor of its cryopreservation ability.

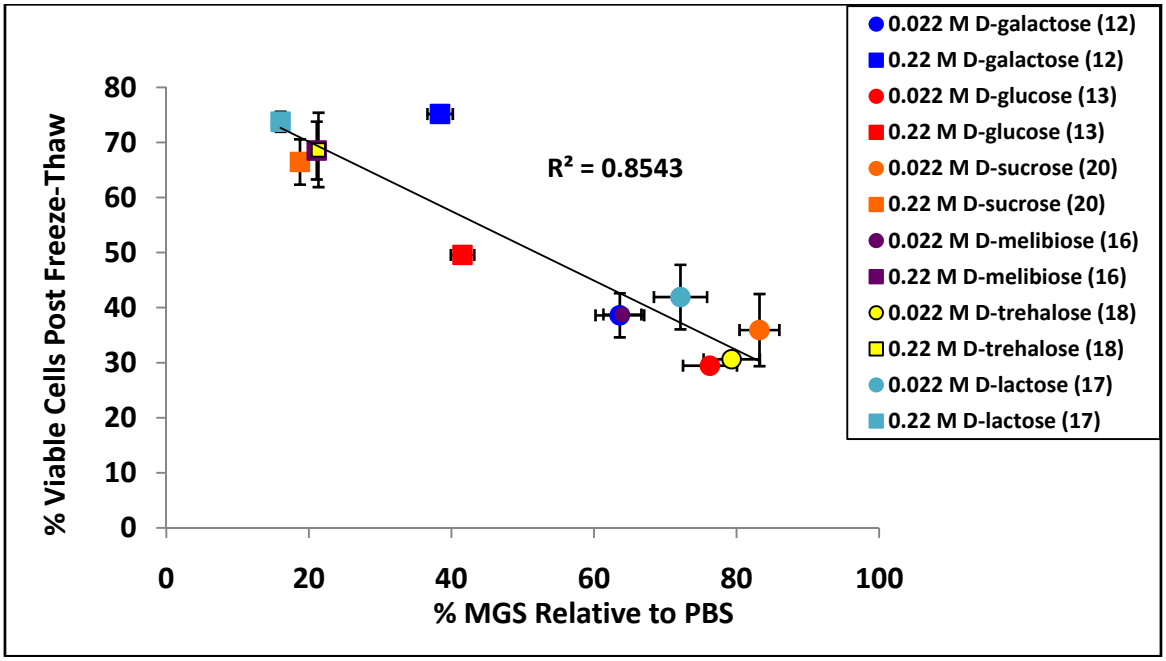

Graph 3.6 Comparison of recorded percent cell viabilities (y-axis) of WRL-68 cells cryopreserved with a series of carbohydrates (**12**, **13**, **16-18**, **20**) and DMSO in relation to their respective IRI activities (x-axis).

Since cytotoxicity of currently used cryoprotectants is an issue that needs addressing,[10] the best cryoprotectants will have a balance between cytotoxicity and cryopreservation ability. If the cell viabilities of both the cytotoxicity and cryopreservation studies are tabulated (Table 3.1), it is apparent that D-galactose (**12**) is the best cryoprotectant since it has relatively low cytotoxicity at physiological temperatures, high cryopreservation ability and the difference between these two results varies very little compared to the other saccharides tested.

Table 3.1 Differences between recorded cell viabilities obtained from cytotoxicity and cryopreservation ability testing of WRL 68 cells treated with a series of carbohydrates (**12**, **13**, **16-18**, **20**) and DMSO. Errors (Standard Error of the Mean, SEM) are shown in parentheses.

Concentration	Carbohydrate or Cryoprotectant	Cell Viability at 37°C (%)	Cell Viability Post Freeze-Thaw (%)	Difference
0.022 M	**D**-galactose **(12)**	**85.9 (1.5)**	**38.6 (4.0)**	**47.3**
	D-glucose **(13)**	**91.4 (2.0)**	**29.4 (0.3)**	**62.0**
	D-melibiose **(16)**	**85.4 (1.2)**	**38.8 (0.8)**	**47.0**
	D-lactose **(17)**	**98.9 (1.0)**	**41.9 (5.9)**	**57.0**
	D-trehalose **(18)**	**82.5 (1.2)**	**30.6 (1.2)**	**51.9**
	D-sucrose **(20)**	**92.4 (0.8)**	**35.9 (0.9)**	**56.4**
0.22 M	**D**-galactose **(12)**	**78.0 (1.0)**	**75.2 (0.7)**	**2.9**
	D-glucose **(13)**	**82.4 (1.8)**	**49.6 (0.4)**	**32.8**
	D-melibiose **(16)**	**65.4 (1.0)**	**68.6 (5.2)**	**3.2**
	D-lactose **(17)**	**84.3 (1.0)**	**73.8 (1.8)**	**10.5**
	D-trehalose **(18)**	**71.4 (1.2)**	**68.6 (6.8)**	**2.8**
	D-sucrose **(20)**	**77.8 (1.0)**	**66.5 (4.1)**	**11.4**
2.5 %	**DMSO**	**83.4 (1.1)**	**57.0 (9.1)**	**26.4**
5 %		**75.1 (1.1)**	**80.5 (1.7)**	**5.4**

Interestingly, in Graph 3.6, D-galactose (**12**) seems to be an outlier among the other sugars tested since it sits just above the line of regression. When plotted along with 2.5 and 5 % DMSO (Graph 3.7), both the results of these DMSO concentrations sit above the line of regression. Interestingly, 5 % DMSO is in the same region as 0.22 M D-galactose (**12**). Also, when results from addition of 5 % DMSO to solutions of 0.022 and 0.22 M D-galactose (**12**) and D-sucrose (**20**) are introduced into the graph, these results also cluster around 0.22 M D-galactose (**12**). This produces an interesting result that needs further investigation. Given that 0.22 M D-galactose (**12**) is almost equally as effective but is less toxic then 5 % DMSO, it suggests that D-galactose (**12**) at 0.2 M may be used alone for cell cryopreservation.

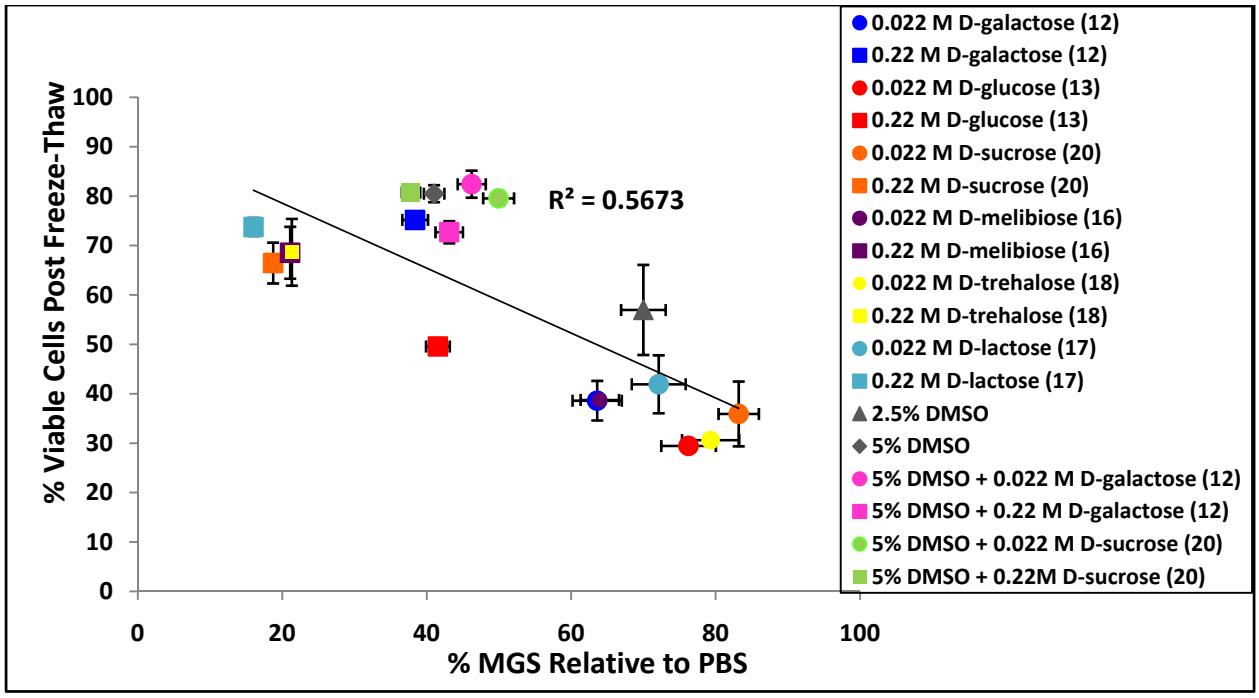

Graph 3.7 Comparison of recorded percent cell viabilities (y-axis) of WRL-68 cells cryopreserved with a series of carbohydrates (**12**, **13**, **16-18**, **20**), DMSO and combinations of **12** and **20** with 5 % DMSO in relation to their respective IRI activities (x-axis).

An explanation as to why D-galactose (**12**) is less toxic and the better cryoprotectant (among the other IRI active sugars tested) may be because it is being internalized in the cell via the asialyglycoprotein receptor (ASGPr) which is found on the surface of liver cells.[18] ASGPrs are known to readily internalize D-galactose (**12**) and D-galactose (**12**) containing compounds into liver cells within minutes.[18] This internalization may reduce cell death at physiological temperatures by reducing the development of strong osmotic pressure across the cellular membrane which would normally occur when high concentrations of non-permeable solutes are introduced to the extracellular environment.[13] Also, although all the sugars tested at 0.22 M posses potent IRI activity which would inhibit extracellular ice recrystallization due to their non-permeable nature, the internalization of D-galactose (**12**) would inhibit internal ice recrystallization which is believed[2,3] to be more strongly influencing cell viability than external

ice recrystallization. Finally, the fact that D-galactose (**12**) and DMSO have potent IRI activity and are proposed to internalize into cells[18,19] may account for their increased cell viability post freeze-thaw. Recent preliminary studies by Leclere and Tam in the Ben group have shown that D-galactose (**12**) is more cytotoxic to kidney cells (HEK 293) than WRL-68 cells. This is believed to be due to the inability of D-galactose (**12**) to internalize (Graph 3.8) into HEK 293 cells. Although more trials are required, addition of DMSO to D-galactose (**12**) was shown to increase cell viability post freeze-thaw in this cell line (HEK 293), however, it is unclear whether DMSO is directly increasing internalization of D-galactose (**12**) and increasing its cryoprotective ability. Therefore, more work is needed and is currently ongoing to determine the effect of internalization of ice-recrystallization inhibitors on cell viability.

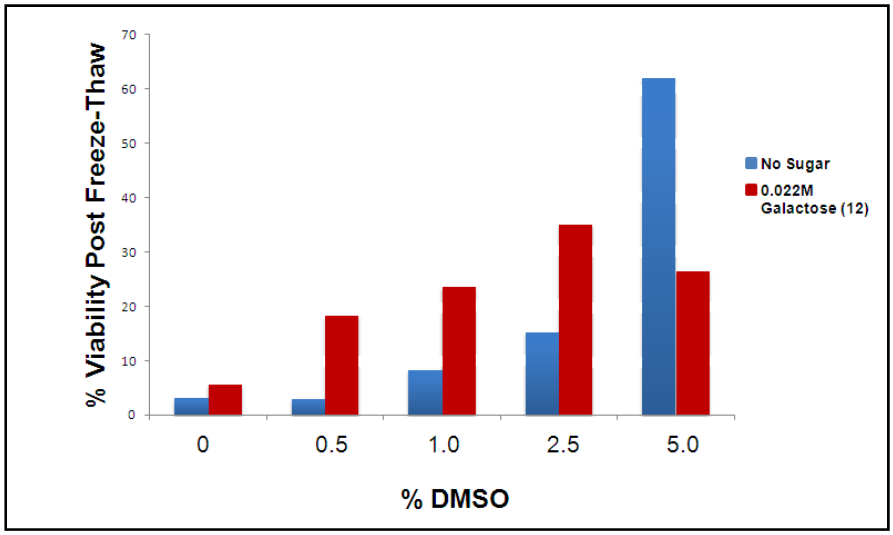

Graph 3.8 Recorded cell viabilities of HEK-293 cells cryopreserved with various combinations of 0.22 M D-galactose (**12**) and DMSO[2]

3.7 Summary

In summary, it was determined that the hydration index fails to correctly predict the IRI activity of higher concentrations (0.22 M) of disaccharides. The nature of this effect is unclear and needs further investigation. The IRI activity of 0.022 M and 0.22 M D-galactose (**12**) corresponds to the IRI activity of 2.5 and 5 % DMSO respectively. When carbohydrates (D-galactose (**12**), D-sucrose (**20**) and D-melibiose (**16**)) were tested with 2.5 and 5 % DMSO, it was determined that addition of DMSO to 0.022 M D-galactose (**12**), D-sucrose (**20**) and D-melibiose (**16**) improved their IRI activity. However, when DMSO is added to higher concentrations (0.22 M) of these sugars, their IRI activity worsens. It may be that saturation effects or reduced solubility[11] are accounting for this drop in IRI activity since 2.5 and 5 % DMSO are quite concentrated (0.35 and 0.7 M respectively) in relation to the carbohydrates (0.022 M and 0.22 M). Therefore, to further investigate these effects, lower concentrations of DMSO must be tested alone and in combination with these carbohydrates.

Since DMSO is toxic,[10] determining the cytotoxicity profiles of these IRI active carbohydrates was conducted. It was determined that low concentrations of carbohydrates (0.022 M) and DMSO (2.5 %) display poor IRI activity yet have low cytotoxic effects in human embryonic liver cells. With higher concentrations (0.2 M carbohydrate and 5 % DMSO), however, cytotoxicity and IRI activity increased, suggesting that these two properties increase with concentration. Disaccharides at 0.5 M displayed abnormally high cytotoxic effects and although future studies are required to determine the source of this effect, it is suggested that osmotic shock is accounting for increased cytotoxicity.

Since the main goal of this research was to determine if there was a link between IRI activity and improved cell viability post cryopreservation, the cryopreservation ability of these

carbohydrates was assessed and compared to 2.5 and 5 % DMSO. It was determined that higher concentrations of carbohydrates (0.2 M) and 5 % DMSO, which had greater IRI activity, had improved cell viability post freeze-thaw compared to lower concentrations (0.022 M carbohydrate and 2.5 % DMSO). Also, concentrations above 0.2 M conferred little additional improvement in cell viability. Since cytotoxicity of currently used cryoprotective agents is an issue in research and clinical settings, using a cryoprotectant which has low cytotoxicity and high cryopreservation ability would be ideal.[10] From our research, it is clear that the best cryoprotectant, such as 0.2 M D-galactose (**12**) in this study, will have a balance between cytotoxicity and cryopreservation ability. Since 0.2 M D-galactose (**12**) was as effective as 5 % DMSO and has less cytotoxicity, using this carbohydrate alone for cryopreservation of human embryonic liver cells would be recommended.

The reason D-galactose (**12**) has lower cytotoxicity and improved cryopreservation activity is proposed to be due to its internalization within the liver cells via ASGPrs.[18] Further investigation is required to prove this hypothesis.

Although cytotoxicity must also be assessed prior to using any new compound as a cryoprotectant, this is the first study to prove that improved cell viability post cryopreservation is linked to IRI activity and encourages the development of new cryoprotectants based on this parameter.

References

1. (a) Huige, N. J. J.; Thijssen, H. A. C., Production of large crystals by continuous ripening in a stirrer tank. *J. Cryst. Growth.* **1972**, 13/14, 483-487. (b) Inada, T.; Modak, P. R., Growth control of ice crystals by poly(vinyl alcohol) and antifreeze protein in ice slurries. *Chem. Eng. Sci*. **2006**, 61, 3149-3158. (c) Knight, C. A.; Wen, D.; Laursen, R. A., Nonequilibrium Antifreeze Peptides and the Recrystallization of Ice. *Cryobiology* **1995**, 32, 23-34. (d) Pronk, P.; Ferreira, C. A. I.; Witkamp, G. J., A dynamic model of Ostwald ripening in ice suspensions. *J. Cryst. Growth*, **2005**, 275, e1355-e1361.

2. Fowler, A.; Toner, M., Cryo-Injury and Biopreservation. *Ann. NY Acad. Sci.* **2006**, 1066, 119-135.

3. Mazur, P., Principles of cryobiology. In: Life in The Frozen State. Fuller BJ, Lane N, Benson EE, eds. **2004**, Boca Raton, FL: CRC Press. p. 3–65.

4. (a) Liu, S.; Ben, R., *C*-Linked Galactosyl Serine AFGP Analogues as Potent Recrystallization Inhibitors. *Org. Lett*. **2005**, 7, 2385-2388.

5. Tam R.Y.; Ferreira, S. S.; Czechura, P.; Chaytor, J. L.; Ben, R. N., Hydration Index - A Better Parameter for Explaining Small Molecule Hydration in Inhibition of Ice Recrystallization, *J. Am. Chem. Soc*. **2008**, 130, 17494–17501.

6. (a) Eroglu, A.; Bailey, S. E.; Toner, M.; Toth, T. L., Successful Cryopreservation of Mouse Oocytes by Using Low Concentrations of Trehalose and Dimethylsulfoxide. *Biol. Reprod.* **2009**, 80, 70-80. (b) Izadyar, F.; Matthijs-Rijsenbilt, J. J.; Den Ouden, K.; Creemers, L. B.; Woelders, H.; De Rooij, D. G., Development of a Cryopreservation Protocol for Type A Spermatogonia. *J. Androl.* **2002**, 23, 537-545. (c) Ma, W.; O'Shaughnessy, T.; Chang, E., Cryopreservation of adherent neuronal networks. *Neurosci. Lett.* **2006**, 403, 84-89. (d) Petrenko, Y. A.; Jones, D. R. E.; Petrenko, A. Y., Cryopreservation of human fetal liver hematopoietic stem/progenitor cells using sucrose as an additive to the cryoprotective medium. *Cryobiology*, **2008**, 57,195-200. (e) Santos, R. R.; Tharasanit, T.; Figueiredo, J. R.; van Haeften, T.; van den Hurk, R., Preservation of caprine preantral follicle viability after cryopreservation in sucrose and ethylene glycol. *Cell Tissue Res.* **2006**, 325, 523-531. (f) Vicente, J. S.; Viudes-de-Castro, M. P., A sucrose-DMSO extender for freezing rabbit semen. *Reprod. Nutr. Dev.* **1996**, 36, 485-492.

7. (a) Galema, S. A.; Høiland, H., Stereochemical Aspects of Hydration of Carbohydrates In Aqueous Solutions. 3. ^{1}Density and Ultrasound Measurements, *J. Phys. Chem.* **1991**, *95*, 5321. (b) Høiland, H.; Hølvik, H. Partial molal volumes and compressibilities of carbohydrates in water. *J. Solution Chem.* **1978**, 7, 587-596.

8. (a) Hossain, A. M.; Osuamkpe, C. O., Sole Use of Sucrose in Human Sperm Cryopreservation *Arch. Andrology* **2007**, 53, 99-103. (b) Eroglu, A.; Russo, M. J.; Bieganski, R.; Fowler, A.; Cheley, S.; Bayley, H.; Toner, M., Intracellular trehalose improves the survival of cryopreserved mammalian cells. *Nat. Biotechnol*. **2000**, 18, 163-167. (c) Terry, C.; Dhawan, A.; Mitry, R. R.; Lehec, S. C.; Hughes, R. D., Preincubation

of rat and human hepatocytes with cytoprotectants prior to cryopreservation can improve viability and function upon thawing. *Liver Transplant.* **2005**, 11, 1533-1540.

9. Davis, J. M.; Rowley, S. D.; Braine, H. G.; Piantadosi, S.; Santos, G. W. Clinical toxicity of cryopreserved bone marrow graft infusion. *Blood*, **1990**, 75, 781-786.

10. Liseth, K.; Abrahamsen, J. F.; Bjorsvik, S.; Grottebo, K.; Bruserud, O., The viability of cryopreserved PBPC depends on the DMSO concentration and the concentration of nucleated cells in the graft. *Cytotherapy*, **2005**, 7, 328-333.

11. (a) Liu,Q.; Janssen, M. H. A.; van Rantwij, F.; Sheldon, R. A., Room-temperature ionic liquids that dissolve carbohydrates in high concentrations, *Green Chemistry*, **2005**, 7, 39-42.(b) Balakin, K.V.; Savchuk, N.P.; Tetko, I.V., In silico approaches to prediction of aqueous and DMSO solubility of drug-like compounds: Trends, problems and solutions. *Current Medicinal Chemistry*, **2006**, 13, 223-241.

12. (a) Liu, S.; Wang, W.; von Moos, E.; Jackman, J.; Mealing, G.; Monette, R.; Ben, R. N., *In Vitro* Studies of Antifreeze Glycoprotein (AFGP) and a *C*-Linked AFGP Analogue. *Biomacromolecules*, **2007**, 8, 1456-1462. (b) Mosmann, T., Rapid colorimetric assay for cellular growth and survival: Application to proliferation and cytotoxicity assays. *J. Immunol. Methods.* **1983**, 65, 55-63.

13. (a) Mazur, P.; Farrant, J.; Leibo, S. P.; Chu, E. H Y., Survival of hamster tissue culture cells after freezing and thawing: Interactions between protective solutes and cooling and warming rates, *Cryobiology*, **1969**, 6, 1-9. (b) Meryman, H.T., Osmotic stress as a mechanism of freezing injury, *Cryobiology*, **1971**, 8, 489-500.

14. (a) Brown, M. R.; Keith, T. J.; Knull, H. R., Nonenzymatic incorporation of glucose and galactose into brain cytoskeletal proteins *in vitro*. *Neurochem. Int.* **1992**, 21, 177-183. (b) Schliess, F.; Haussinger, D., The Cellular Hydration State: A Critical Determinant for Cell Death and Survival. *Biol. Chem.* **2002**, 383, 577-583.

15. Bunn, H. F.; Higgins, P. J., Reaction of monosaccharides with proteins: possible evolutionary significance. *Science* **1981**, 213, 222-224.

16. (a) Koopman, G.; Reutelingsperger, C. P.; Kuijten, G. A.; Keehnen, R. M.; Pals, S. T.; van Oers, M. H., Annexin V for flow cytometric detection of phosphatidylserine expression on B cells undergoing apoptosis. *Blood* **1994**, 84, 1415–1420. (b) Vermes, I.; Haanen, C.; Steffens-Nakken, H.; Reutelingsperger, C., A novel assay for apoptosis—flow cytometric detection of phosphatidylserine expression on early apoptotic cells using fluorescein labelled Annexin V. *J Immunol Methods*, **1995**, 184, 39-51.

17. (a) Liu, X.; Chen, H.; Patel, D., Solution structure of actinomycin-DNA complexes: drug intercalation at isolated G-C sites. *J Biomol NMR*, **1991**, 1, 323–347 (b) Latt, S., Fluorescent probes of chromosome structure and replication. *Can J Genet Cytol*, **1977**, 19, 603–623.

18. (a) Ashwell, G.; Harford, J., Carbohydrate-Specific Receptors of the Liver *Ann. Rev. Biochem.* **1982**, 51, 531-554. (b) Ashwell, G..; Morell, A. G., The role of surface carbohydrates in the hepatic recognition and transport of circulating glycoproteins. In: A Meister, Editor, *Advances in Enzymology* Vol. 41, John Wiley & Sons, New York (**1974**), pp. 99–128.

19. (a) Meryman, H.T., Modified model for the mechanism of freezing injury in erythrocytes. *Nature* **1968**, *218*, 333-336..

20. Leclere, M.; Tam, R. Y.; Ben, R. N., unpublished results, **2010**.

Chapter 4- Synthesis and IRI Activity of Galactose Derivatives

4.1 Introduction

A goal of the Ben lab is to improve the IRI activity of galactose and galactose-containing AFGPs, as it has been shown that these compounds are the most IRI-active compared to other carbohydrates.[1] From previous work conducted by Czechura *et al*.[1], it was demonstrated that the large negative partial molar compressibility value for D-galactose (**12**) correlates with the ability of this compound to inhibit ice recrystallization. It was subsequently hypothesized that this was due to a "poor fit" of the hydrated solute within the three-dimensional hydrogen bonding network of surrounding bulk water. This "poor fit" disrupts the ordering of bulk water and decreases the ability of the bulk water molecules to incorporate into the ice lattice (Figure 1.19, p. 28).[1] The "poor fit" of hydrated D-galactose (**12**) was presumed to be due to the hydroxyl group stereochemistry of the carbohydrate ring, with C2 and C4 stereochemistry being the most important.[1,2,3] It was hypothesized that the better the compatibility of the C2 and C4 hydroxyl groups with the surrounding water network, the more hydrated the carbohydrate will become and in turn, the larger the disruption of the surrounding bulk water. This hypothesis was validated, when the IRI activity of various commercially available mono- and disaccharides with different hydroxyl stereochemistries was assessed and it was demonstrated by Tam *et al*. that the ratio of tightly bound hydrating water molecules per partial molar volume of carbohydrate (or hydration index) could predict IRI activity (Figure 2.3, p. 49).[4] Carbohydrates that have a larger hydration index (large ratio of water molecules per solvated carbohydrate ring) possess better IRI activity.[4]

From this work, it was clear that the stereochemistry of the carbohydrate hydroxyl groups has an important role in dictating dynamics of surrounding water molecules. However, how this

occurs is uncertain. One possibility is that specific hydroxyl groups of the carbohydrate are able to form favourable interactions with surrounding water molecules to prevent their addition to the ice lattice.[1,2,4,5] Thus, it is prudent to study how structural changes in galactose (such as its stereochemistry and hydrophilicity), which certainly affect hydration, will influence IRI activity. To this end, we synthesized a series of galactopyranose derivatives (deoxy, azide, amine and thioalkyl galactosides) having very different hydrophilic properties and assessed their ability to inhibit ice recrystallization.

4.2 Preparation and IRI activity of deoxy and deoxy-α-C-allyl-D-galactosides

To study the effect of the hydrogen bond donating ability of the hydroxyl groups of galactose on IRI activity, Chaytor had previously prepared regioisomers of methoxy α-*C*-allyl galactose (**21-24**) (Figure 2.4, p. 50).[6] Methylation of specific hydroxyl groups in the galactopyranose residue removes their ability to act as a hydrogen bond donor. Since all these methoxy derivatives lacked IRI activity yet retained the ability to function as a hydrogen bond acceptor,[7] it was proposed that the ability of each hydroxyl group to act as a hydrogen bond donor was important for IRI activity.[6]

The next logical step was to systematically remove the hydroxyl groups on the galactose derivative to prevent them from functioning as hydrogen bond donors and acceptors. Consequently, the synthesis of a series of deoxy galactopyranoses (**26-29**, **34**) (Figure 2.5, p. 52) was attempted. 2-Deoxy-D-galactose (**34**) and 6-deoxy-D-galactose (D-fucose) (**29**) were commercially available and purchased from TCI America. As previous results by Chaytor contained α-*C*-allyl substituents, deoxy galactopyranose derivatives with anomeric substituents identical to that used by Chaytor had to also be synthesized (**30-33**).[6]

4.2.1 Preparation of 1-deoxy-D-galactose (26)

As outlined in the scheme below (Scheme 4.1), the initial formation of 2,3,4,6- tetra-*O*-acetyl galactosyl bromide (**58**) was achieved by reacting D-galactose pentaacetate with a 33% solution of hydrogen bromide in acetic acid.[8]

Scheme 4.1 Synthesis of 1-deoxy-D-galactose (**26**)

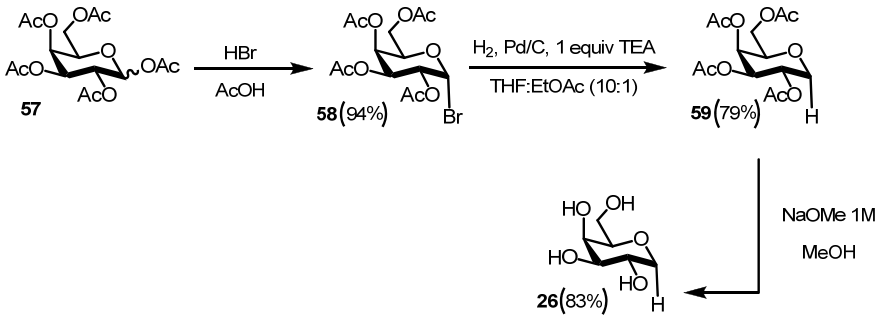

Reduction of the carbon-bromine (C-Br) bond in **58**, was attempted using two different hydrogenolysis conditions.[9-11] In the first attempt a reduction of the carbon halogen bond using 1 equivalent of tributyltin hydride (Bu_3SnH), catalytic 1,1-azobisisobutyronitrile (AIBN) and heat (80°C) was employed.[9,10] Unfortunately, this reaction yielded only starting material. However, reduction using hydrogenation over 10% palladium on carbon (Pd/C), in the presence of a stoichiometric amount of triethylamine (TEA) furnished **59** in 79 % yield.[11] TEA is an important reagent in this reaction because it neutralizes the formation of hydrogen bromide (HBr) which is known to remain adsorbed onto the Pd/C surface following halogen reductions and poisons the catalyst.[12,13] Under these conditions, a triethylammonium bromide salt is formed and the palladium catalyst is regenerated.[13]

The resulting 1-deoxy-2,3,4,6-tetra-*O*-acetyl-D-galactose (**59**) was deprotected using sodium methoxide in methanol[14] and recrystallization from ethanol afforded 1-deoxy-D-galactose (**26**) in 61 % overall yield.

4.2.2 Preparation of 3-deoxy-D-galactose (27)

Several attempts were employed to synthesize 3-deoxy-D-galactose (**27**). The challenge in the synthesis of this compound was the accessibility of the free hydroxyl at the C3 position of galactose. Unfortunately, only one route was partly successful, producing the late-stage intermediate 3-deoxy-thiophenyl-β-D-galactose (**68**) which required final deprotection. The first synthetic approach is outlined below.[15]

Scheme 4.2 First attempted synthesis of 3-deoxy-D-galactose (**27**)

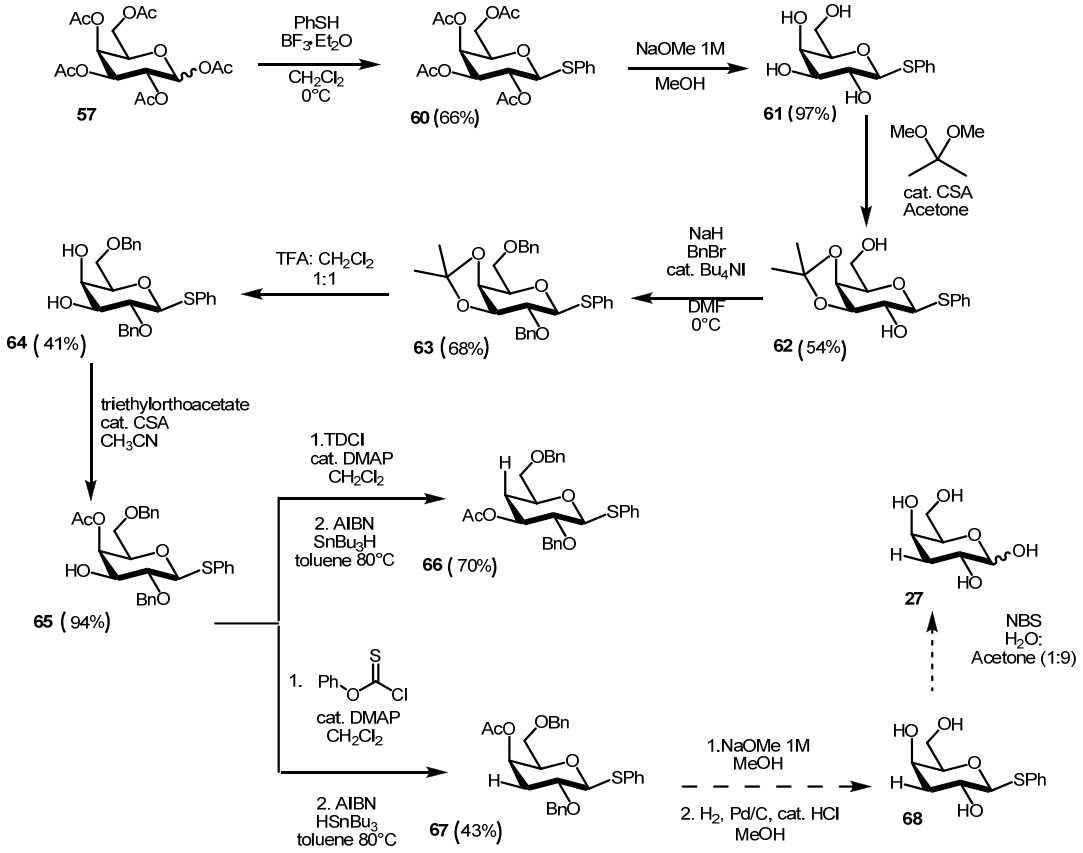

Formation of 4-*O*-acetyl-2,6-*O*-benzyl-1-thiophenyl-β-D-galactopyranoside (**65**, Scheme 4.3) was carried out according to the literature procedure reported by Janczuk and Wang.[15] This route began with the generation of 1-thiophenyl-2,3,4,6-tetra-*O*-acetyl-D-galactose (**60**) from commercially available β-D-galactose pentacetate (**57**) using trifluoroborane diethyl etherate as the Lewis acid activator.[16] The anomeric thiophenyl galactopyranose (**60**) was then deprotected using 1 M sodium methoxide,[14] to furnish **61** which was purified by recrystallization from a mixture of methanol, ethyl acetate and ether in 97 % yield.

The next step involved installation of the 3,4-*O*-isopropyl group under thermodynamic conditions. [17-20] Benzylation of the alcohols at C2 and C6 of **63** was performed using sodium hydride, benzyl alcohol and a catalytic amount of tetrabutylammonium iodide.[18] Subsequent cleavage of the isopropylidene protecting group under acidic conditions furnished the C3 and C4 diol **64** in 41 % yield.[19] Selective acetylation of position C4 of galactose was then accomplished using triethylorthoacetate and catalytic amounts of camphor sulfonic acid (CSA) in acetonitrile.[20,21] The mechanism of this reaction is presented in Figure 4.1.[20] Upon addition of acid, the dioxolenium intermediate **A** is formed.[20] Hydration occurs from the least hindered face of intermediate **A**, to form the hemi-ortho ester intermediate **B** after proton transfer.[20] Selective opening of intermediate **B** with the assistance of two primary stereoelectronic effects affords the major product (**65**).[20]

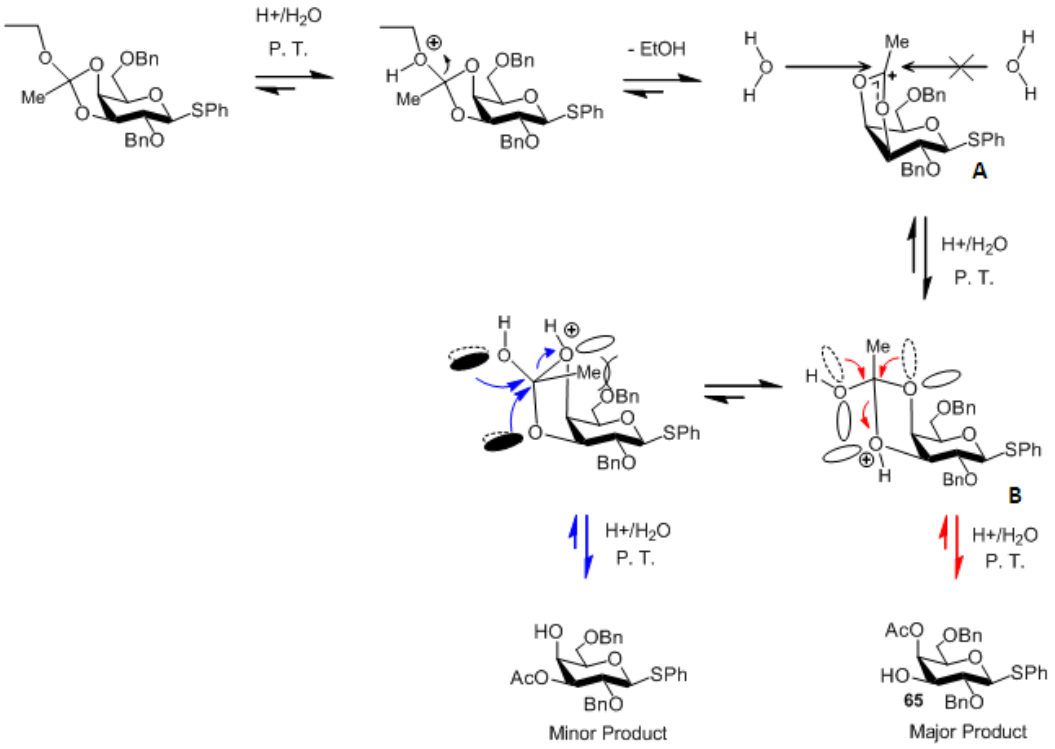

Figure 4.1 Regioselective opening of hemi-ortho ester.[20]

At this stage, the deoxygenation of position C3 of **65** was required. A Barton McCombie deoxygenation was subsequently attempted.[22] In this reaction, the C3 free hydroxyl group is converted into a thioester using *N*,*N*'-thiocarbonyldiimidazole (TCDI) which is removed by radical-initiated cleavage. The resulting carbon-centred radical is then quenched.[22] Although the deoxygenation step was proficient, analysis of the reaction mixture indicated that the acetyl group at position C3 migrated to C4. The ^{1}H COSY NMRs of the undesired (**66**) and desired (**67**) deoxygenation products are shown below (Figure 4.2A and 4.2B, respectively).

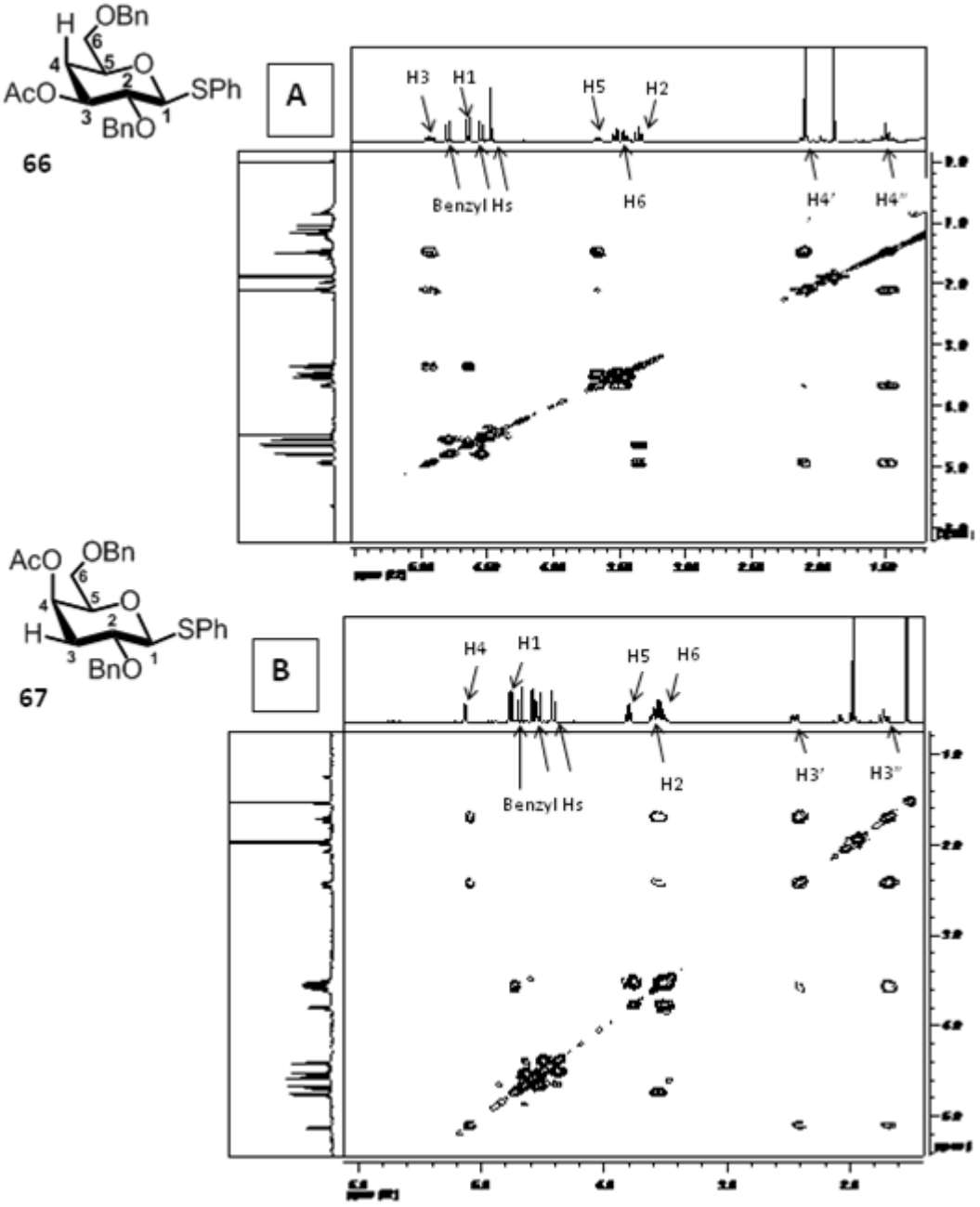

Figure 4.2 Deoxygenation regioisomers (**66, 67**) afforded using (**A**) *N*,*N*'-thiocarbonyldiimidazole and (**B**) phenyl chlorothionoformate

A similar result was reported by Mulard *et al*. who observed benzoyl group migration from C4 to C3 using the same reaction conditions.[23] To remedy this problem, phenyl chlorothionoformate was used instead of TDCI (Figure 4.3).[15] Although deoxygenation of

position C3 was successful, the synthetis needed to be repeated due to an insufficient amount of 3-deoxy-4-*O*-acetyl-2,6-*O*-benzyl-1-thiophenyl-β-D-galactopyranoside (**67**).

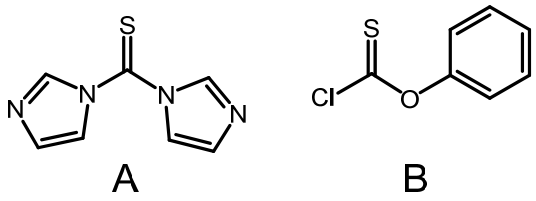

Figure 4.3 Structures of (A) *N*,*N*'-thiocarbonyldiimidazole (TDCI) and (B) phenyl chlorothionoformate

In order to increase the overall yield of 3-deoxy-D-galactose (**27**), the benzyl protecting groups at positions 2 and 6 were replaced by acetyl groups. This would reduce the number of deprotection reactions following deoxygenation of position C3. Since literature precedent existed for the generation of 2,6-*O*-acetyl-3,4-*O*-isopropyl-1-thiophenyl-β-D-galactopyranoside (**69**)[24] a slightly modified reaction sequence was attempted as outlined in Scheme 4.3.

Scheme 4.3 Attempted synthesis of 3-deoxy-D-galactose (**27**)

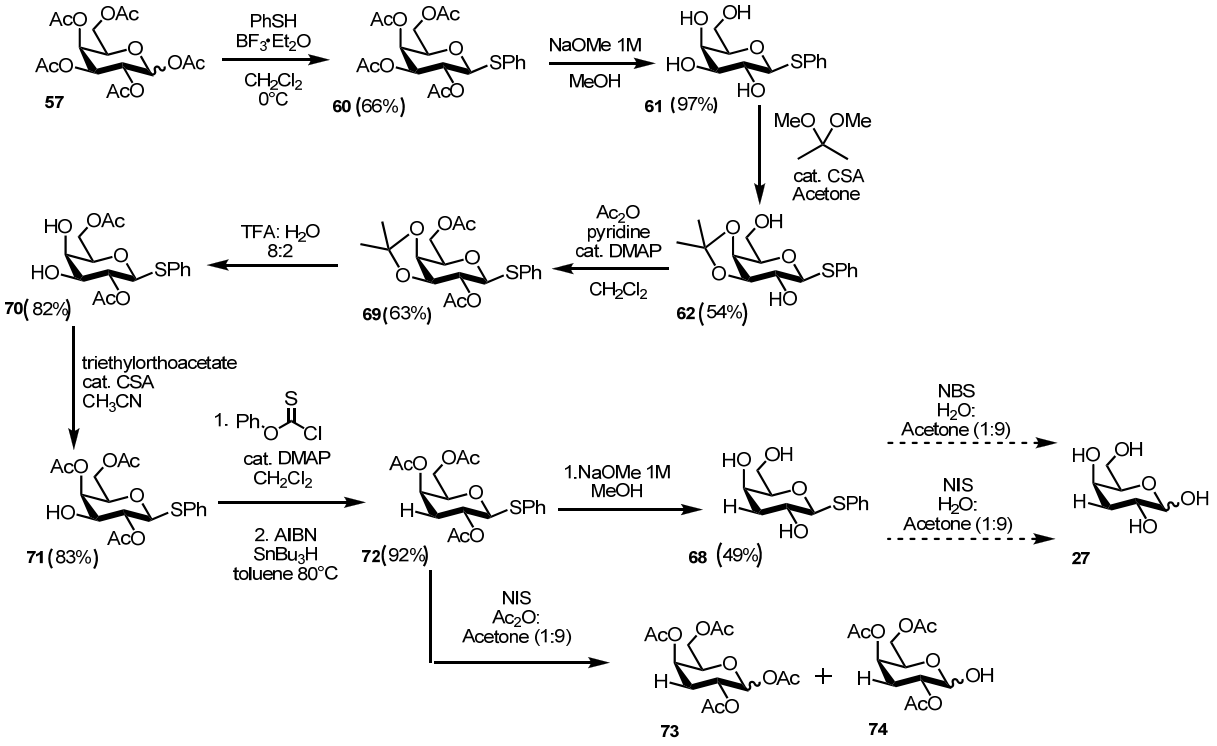

3-Deoxy-2,4,6-tri-*O*-acetyl-1-thiophenyl-β-D-galactose (**72**) was obtained in 14 % overall yield over seven steps.[15-18,21,22] 3-Deoxy-D-galactose (**27**) could not be successfully synthesized since removal of the thiophenyl group proved more difficult than initially anticipated. Use of 5 equivalents of *N*-bromosuccinimide (NBS) in an acetone: water (9:1) mixture afforded a mixture of product and starting material. However, using *N*-iodosuccinimide (NIS) thin layer chromatography analysis indicated that the starting material was fully consumed.[25] Unfortunately, it was not possible to retrieve the desired compound (**27**). Upon re-evaluation of this final step, acetic anhydride replaced water in order to form the C1 acetyl group (**73**). It was anticipated that addition of the acetyl group would ease purification by changing polarity of the product. However, this modification did not provide the desired result and again a complex mixture, including anomeric acetate (**73**) and hydroxyl (**74**), was obtained. Due to time constraints, 3-deoxy-2,4,6-tri-*O*-acetyl-1-thiophenyl-β-D-galactose (**72**) was deprotected[14] and purified via reverse phase HPLC. The resulting 3-deoxy-1-thiophenyl-β-D-galactose **68** (6 % overall yield over eight steps) was tested for IRI activity.

4.2.3 Preparation of 4-deoxy-D-galactose (28)

To selectively deoxygenate the C4 position of galactopyranose we employed a similar approach to that described in Section 4.1.1 where conversion of the C4 hydroxyl group into a halogen was followed by reduction to afford the desired compound (Scheme 4.4).[11]

Initial reaction of D-galactose (**12**) with 6.0 equivalents of pivaloyl chloride and pyridine provided a mixture of 1,2,3,4,6-penta-*O*-pivaloyl-β-D-galactose (52 %), 1,2,3,6-tetra-*O*-pivaloyl-β-D-galactose (41 %) and 1,3,6- di-*O*-pivaloyl-β-D-galactose (7.4 %). This mixture was separated by column chromatography.[26] Upon isolation of 1,2,3.6-tetra-*O*-pivaloyl-β-D-galactose (**75**), the C4 free hydroxyl group was substituted with iodine with inversion of

configuration using a Garegg iodination, providing 4-iodo-1,2,3.6-tetra-*O*-pivaloyl-β-D-glucopyranose (**76**) in 88% yield.[27]

Scheme 4.4 Synthesis of 4-deoxy-D-galactose (**28**)

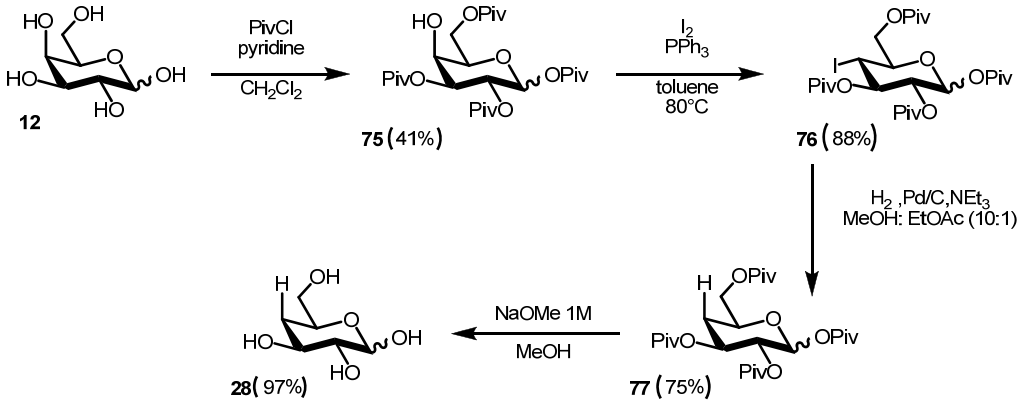

Intermediate 7**6** then underwent the same reduction protocol as described in the synthesis of 1-deoxy-2,3,4,6,-tetra-*O*-acetyl-D-galactose (**59**) followed by deprotection using 1M sodium methoxide[14] to afford 4-deoxy galactose (**28**) in 26 % overall yield.[11] Longer reaction times were required due to the catalyst's increased affinity for iodine over bromine. This has been previously reported by Tundo and Ambroise.[12,13] The iodine occupies more catalytic sites for a longer period of time than a bromine atom, explaining the slower reaction rate for the iodine reaction.[12,13]

4.2.4 Preparation of 2-deoxy-C-allyl-α-D-galactose (30), 4-deoxy-C-allyl-α-D-galactose (32) and 6-deoxy-C-allyl-α-D-galactose (33)

Syntheses of the anomeric α-*C*-allyl derivatives of 2-deoxy (**30**), 4-deoxy (**32**), and 6-deoxy (**33**) galactopyranose were accomplished via stereoselective allylation of their respective *O*-glycoside precursors (Scheme 4.5).[28] In general, the *O*-glycosyl derivatives (**28**, **29**, **34**) were

esterified (either acetylated or pivalated) from their free hydroxyl precursors. Subsequent allylation at the anomeric position using anhydrous acetonitrile, allyl-trimethylsilane and boron trifluoride diethyl etherate as Lewis acid afforded the corresponding *C*-allyl glycosides in 9:1 α:β stereoselectivity.[28]

Scheme 4.5 Synthesis of 2-,4- and 6-deoxy α-*C*-allyl-D-galactoses (**30, 32, 33**)

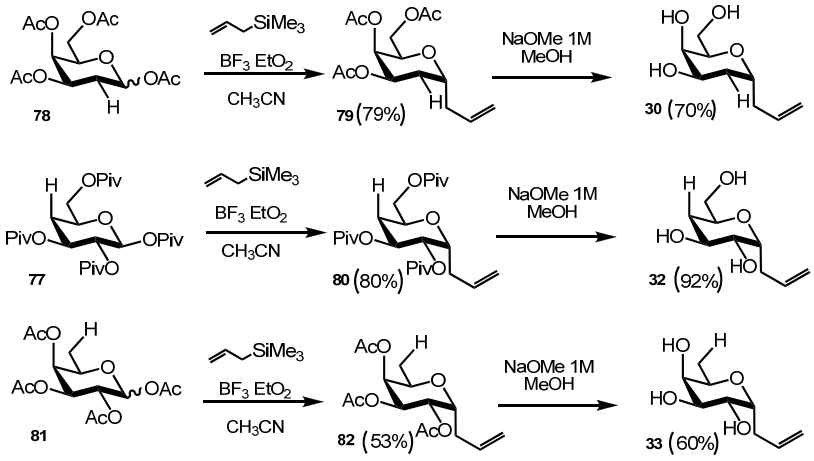

The two diastereoisomers obtained were separated using flash column chromatography and further deprotection using 1 M sodium methoxide[14] followed by recrystallization from EtOH afforded the desired α-*C*-allyl derivatives (**30**, **32**, **33**).

4.2.5 Preparation of 3-deoxy-C-allyl-α-D-galactose (31)

As with the synthesis of 3-deoxy galactopyranose (**27**), the synthesis of 3-deoxy-*C*-allyl-α-galactopyranose (**31**) was the most challenging of this series of analogues. Thus, preparation of 3-deoxy-*C*-allyl-α-D-galactose (**31**) could not be completed due to time constraints. Unlike the other deoxy α-*C*-allyl compounds (**30**, **32**, **33**), the strategy used to synthesize this compound, as depicted in Scheme 4.6, installs the anomeric α-*C*-allyl moiety prior to selective deoxygenation of the C3 hydroxyl group.[28]

Scheme 4.6 Synthesis of 3-deoxy-*C*-allyl-α-D-galactose (**31**).

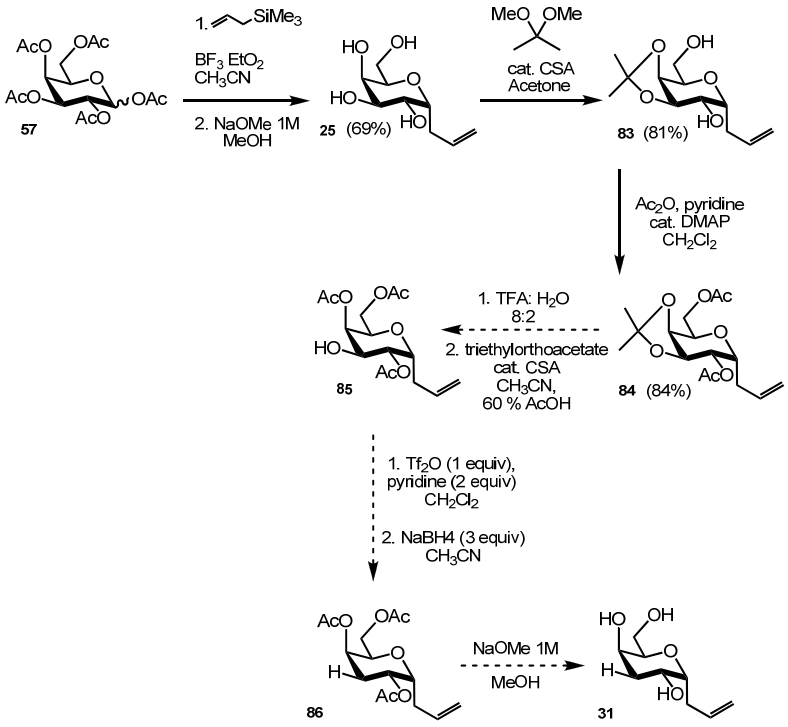

Following addition of the anomeric α-allyl group (**25**), protecting group manipulations identical to those used in the synthesis of 3-deoxy-D-galactose (**27**) afforded product **84** in 84% yield.[15,28] Further deprotection and selective acetylation of **84** will provide compound **85** which requires subsequent deoxygenation and deprotection as outlined in Scheme 4.6 in order to obtain the desired product (**31**).[15,28-30]

4.2.6 Assessment of IRI activity of 1,2,4,6-deoxy galactopyranosides (26, 28, 29, 34) and C-allyl 2,4,6-deoxy galactopyranosides (30, 32, 33)

The IRI activity of the deoxy galactopyranoses (**26**, **28**, **29**, **34**) and the α-*C*-allyl deoxy galactopyranoses (**30**, **32**, **33**) were analyzed and presented in Graph 4.1 (red and yellow bars, respectively). From these results, it is apparent that there is a dramatic decrease in the IRI activity of these compounds compared to native D-galactose and α-C-allyl D-galactose (blue

bars).[1,4] Also, as the deoxy galactopyranoses (**26**, **28**, **29**, **34**) and the α-*C*-allyl deoxy galactopyranoses (**30**, **32**, **33**) have similarly reduced IRI activity compared to D-galactose (**12**) and α-*C*-allyl-D-galactose (**25**), it is concluded that the α-*C*-allyl substituent does not interfere with the IRI ability of D-galactose and its derivatives. Of the deoxy derivatives synthesized and tested, only the 6-deoxy derivative (D-fucose) has slightly increased IRI activity compared to the PBS negative control. The reason for this is currently unknown and will require further investigation.

From these results, we conclude that the ability of a hydroxyl group to serve as a hydrogen bond donor or acceptor at positions 1-, 2-, 4- and 6- of the pyranose ring plays a large role in affecting the IRI activity of galactopyranosides. As it was previously hypothesized that IRI activity is dependent upon a carbohydrate's hydration properties,[1,4] the current results suggest that replacing a hydroxyl group by a proton at positions 1-, 2-, 4- and 6- of the pyranose ring may reduce the ability of the carbohydrate to hydrate in a favourable manner to inhibit ice growth. Similar results and conclusions were reported by Chaytor, who demonstrated that the IRI activity of various methoxy α-*C*-allyl galactopyranosides (Chapter 2, and Graph 4.1, green bars) had reduced IRI activity compared to α-C-allyl galactose.[6] Chaytor concluded that the presence of methoxy groups in these analogues (which removes the hydrogen donor ability at the substituted position) may reduce hydration of these derivatives.[6]

Czechura *et al*. had previously suggested that the relative hydroxyl stereochemistries at the C2 and C4 positions of monosaccharide derivatives modulate IRI activity.[1] However, as we observed a similar decrease in IRI activity for 1-, 2-, 4- and 6- deoxy galactopyranosyl derivatives (**26**, **28**, **29**, **34**), our results indicate that varying the substituents at positions other than C2 and C4 in the pyranose ring also significantly affects IRI activity.

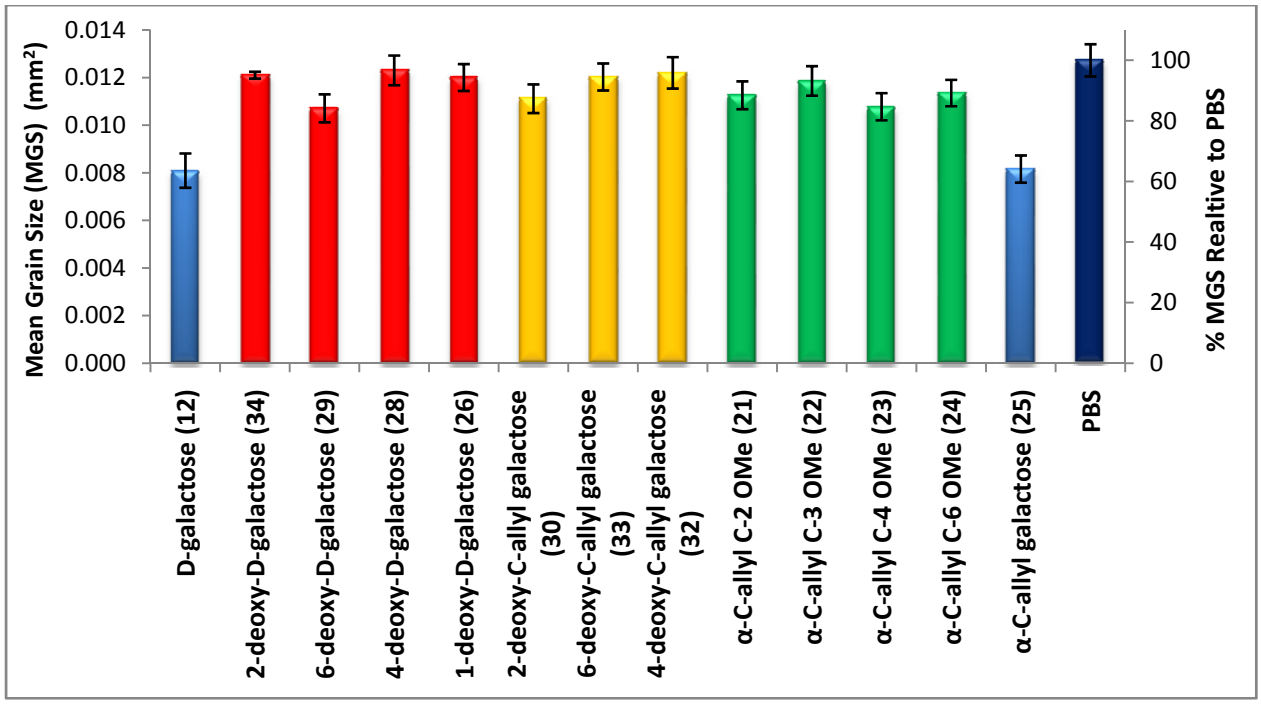

Graph 4.1 IRI activities of deoxy D-galactoses (**26**, **28**, **29**, **34**) and deoxy α-*C*-allyl-D-galactoses (**30**, **32**, **33**) in comparison to D-galactose (**12**), α-*C*-allyl-D-galactose (**25**) and methoxy α-*C*-allyl-D-galactoses (**21-24**) previously tested. Carbohydrates tested at 0.022 M[4,6]

In order to demonstrate that the overall hydration of a carbohydrate is related to its ability to inhibit ice recrystallization, Tam *et al*. had previously observed that the IRI activity of carbohydrates is directly proportional to their hydration index, which is the number of water molecules bound to the solute (hydration number) per molar volume of the hydrated solute.[4] Therefore, we were interested in determining if this correlation would also be observed for our deoxy galactopyranosides. Unfortunately, as hydration numbers from literature for these deoxy derivatives (**26**, **28**, **29**, **30**, **32- 34**) are unavailable,[2,3] a direct correlation of the IRI activities of these derivatives to their respective hydration indices is not possible. However, Parke has previously reported the hydration number and partial molar volume for L-fucose (**87**), which is the enantiomer of 6-deoxy D-galactopyranose.[31]

The relationship between the hydration parameters of D- and L-fucose and their ability to inhibit ice recrystallization is expected to be the same as ice lacks chirality. This hypothesis was recently validated by Capicciotti, who demonstrated that the IRI activities of D-galactose (**12**) and L-galactose (**88**) are identical, Graph 4.2.[4,32]

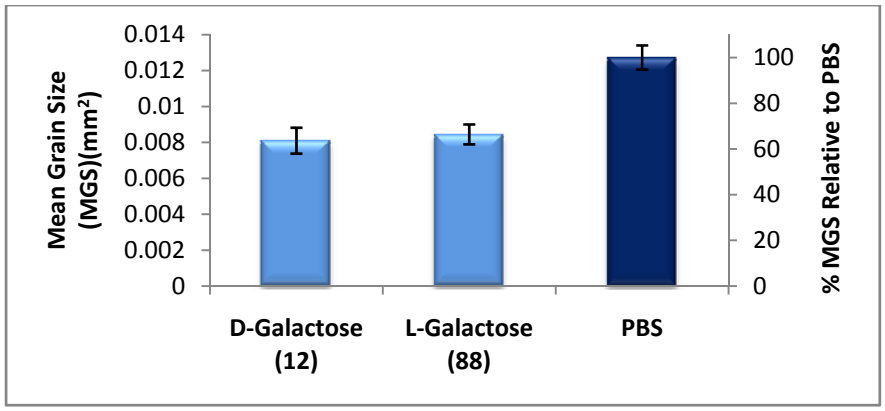

Graph 4.2 IRI activities of D-galactose (**12**) and L-galactose (**88**) tested at 0.022 M[4,32]

Therefore the hydration parameters of L-fucose could be used to effectively predict those of D-fucose. The hydration values of L-fucose obtained from Parkes were tabulated with those of simple mono- and disaccharides which were previously tested by Tam *et al*. and compared to their respective IRI activities tested at 0.022 M (Table 4.1).[4,31]

Table 4.1 Calculated hydration indices and IRI activities (% Mean Grain Size relative to PBS) of various mono- and disaccharides using partial molar volume and hydration numbers obtained by Parke.[4,31] Errors are shown in parentheses.

	Parke Hydration Measurements[31]		**Hydration Index**	**IRI activity tested at 0.022M**
Carbohydrate	Partial Molar Volume (cm^3) (0.01)	Hydration Number (0.1)	($mmol^1cm^{-3}$) (1)	% Mean Grain Size (MGS) relative to PBS
D-Galactose (**12**)	109.69	8.91	81	63.6 (5.7)
L-Fucose (87)	**108.05**	**9.17**	**85**	**91.0 (4.6)**
D-Glucose (**13**)	111.34	8.63	78	76.3 (5.0)
D-Mannose (**14**)	111.18	8.35	75	84.0 (4.4)
D-Lactose (**17**)	208.37	15.87	76	71.9 (3.7)
D-Maltose (**19**)	217.39	14.27	66	84.5 (3.6)
D-Sucrose (**20**)	210.79	14.49	69	83.2 (2.8)

In general, the hydration indices of the mono- and disaccharides calculated from the hydration parameters obtained from Parke fit the correlation proposed by Tam *et al*., such that hydration index is directly proportional to IRI activity.[4,31] However, the hydration index calculated for L-fucose (**87**) is higher than D-galactose (**12**) (Table 4.1), suggesting that fucose is more hydrated and should be more IRI-active than galactose.[4,31] From Graph 4.1, the contrary is observed and fucose is a worse ice recrystallization inhibitor compared to galactose. The reason for the anomalous nature of fucose is unclear. It is therefore imperative to experimentally determine the hydration indices of other deoxy galactopyranosyl regioisomers (**26-29**, **34**) before any conclusions are proposed regarding the ability of hydration indices to predict the IRI activity of these deoxy compounds.

4.2.7 IRI assessment of 3-deoxy-thiophenyl-D-galactose (68)

Unfortunately, due to time constraints, synthesis of the desired free reducing 3-deoxy-D-galactose derivative (**27**) was not completed (Scheme 4.3).[17-25] However, as our goal was to determine the effect of removal of the C3 hydroxyl group on IRI activity, we compared the IRI

activity of the advanced intermediate obtained (3-deoxy-β-thiophenyl-D-galactose, (**68**)) with that of β-thiophenyl-D-galactose (**61**). IRI assay analyses indicate that 3-deoxy-β-thiophenyl-D-galactose (**68**) (Graph 4.2, purple bar) has IRI activity that is nearly identical to β-thiophenyl-D-galactose (**61**),[6] α-C-allyl- D-galactose (**25**) and D-galactose **(12)**[4] (Graph 4.2, blue bars). This is surprising since previous results (Graph 4.1) demonstrated that 3-methoxy-α-*C*-allyl galactose (**22**) possessed similar IRI activity to α-*C*-allyl methoxy regioisomers (**21-24**),[6] and decreased activity compared to α-*C*-allyl D-galactose. Therefore, it was initially anticipated that the IRI activity of 3-deoxy-β-thiophenyl-D-galactose (**68**) would be similar to that of the other deoxy galactosides (**26**, **28**, **29**, **34**). As the 3-deoxy-thiophenyl-galactopyranose derivative unexpectedly possesses potent IRI activity, throughout analysis of the data presented in Graphs 4.1 and 4.2 was required in order to determine a reasonable explanation.

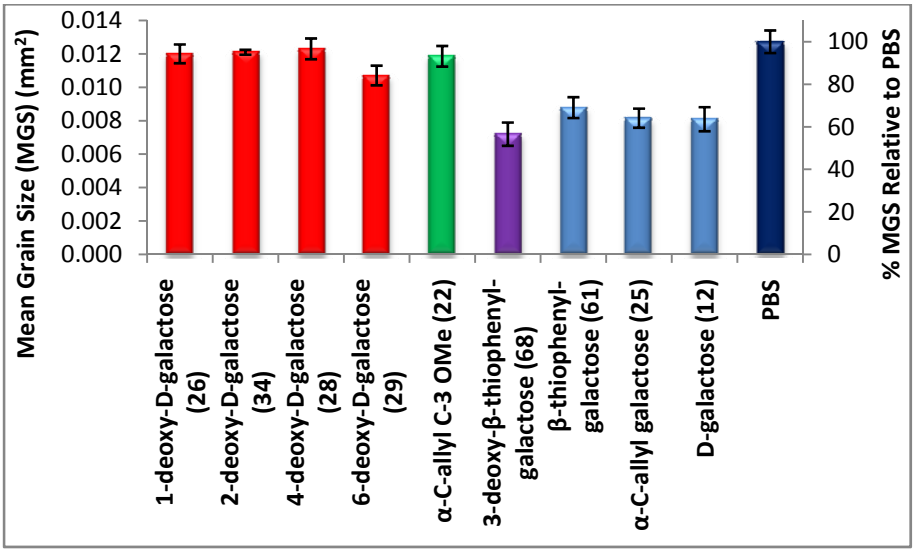

Graph 4.3 IRI activities of 1-,2-,4- and 6-deoxy-D-galactoses (**26**, **28**, **29**, **34**) , 3-deoxy-β-thiophenyl-D-galactose (**68**), β-thiophenyl-D-galactose (**61**), 3-methoxy α-*C*-allyl-D-galactose (**22**), α-*C*-allyl-D-galactose (**25**), and D-galactose (**12**).[4,6]

In order to consider the effect of C3 hydroxyl group modifications on IRI activity, C3-OH substitution products (i.e. **22**, **27**, **31** and **68**) were compared to their galactopyranose

controls, bearing the same anomeric substituent (**12**, **25**, **61**). Their structures are presented in Figure 4.4. The use of these appropriate control compounds enables the delineation in the differences in IRI activity caused by the C3 position. Unfortunately, compounds **27** and **31** have not yet been synthesized, and thus a direct comparison between these compounds cannot be currently assessed.

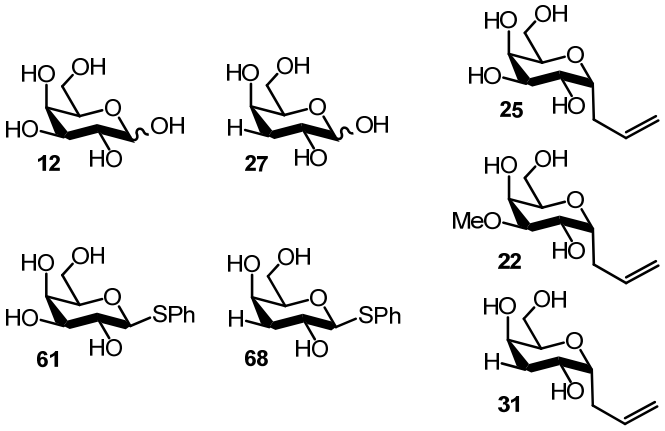

Figure 4.4 Structures of C3 substituted galactopyranosyl derivatives and their corresponding galactopyranose derivatives[4,6]

When comparing the structures and IRI activities of 3-methoxy-α-*C*-allyl-galactose (**22**) and α-*C*-allyl-galactose (**25**), loss of the hydrogen donor ability of C3 hydroxyl group eliminates IRI activity, and it was speculated that hydroxyl group methylation reduced the overall hydration of the carbohydrate.[6] In contrast to the deoxy compounds presented in Graph 4.1, substitution of the C3 hydroxyl group with a proton in β-thiophenyl-D-galactose (**68**) (which should reduce overall hydration of the compound) resulted in slightly increased IRI activity compared to β-thiophenyl-D-galactose (**61**). From this interesting result, which is contrary to our initial hypothesis, we believe there are factors other than total number of hydroxyl groups per molar volume (hydration index) that govern IRI activity in these galactopyranosyl derivatives.[4] One

such factor may involve interactions between an intramolecular hydrogen bond network within the pyranose ring and surrounding water molecules.

Simons *et al*. proposed that hydration of a carbohydrate may be governed by the strength of the hydrogen bond network in the pyranose ring.[33] This hypothesis was postulated based on energy differences observed from incorporation of a single water molecule within the intramolecular hydrogen bond network of the pyranosyl ring.[33] In their work, the lowest energy states of non-hydrated and monohydrated β-phenyl-D-galactose were calculated using infrared (IR) measurements and density functional theory (DFT) (Figure 4.5).[33] It was concluded that incorporation of the first water molecule occurs between the weakest intramolecular hydrogen bond in order to limit disruption of this intramolecular hydrogen bond network.[33] For example, the first water molecule insertion in β-phenyl-D-galactose occurs between the OH6- cyclic oxygen hydrogen bond.[33] Therefore, hydroxyl groups involved in weaker intramolecular hydrogen bonds within the pyranose ring will be more hydrated than hydroxyl groups with stronger intramolecular hydrogen bonds.[33] Similarly, carbohydrates that have overall weaker intramolecular hydrogen bonds will be more hydrated than those with stronger bonds.[33]

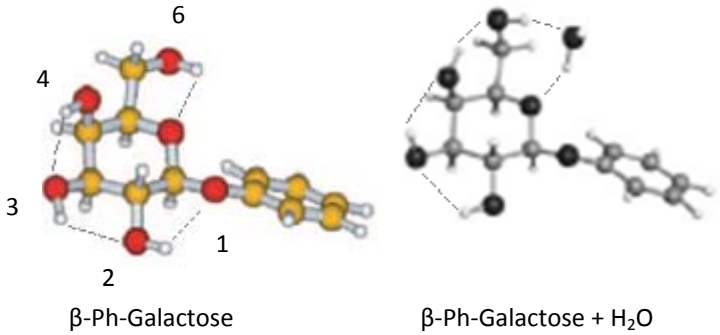

Figure 4.5 Lowest energy states calculated for incorporation of a single water molecule into the OH6-cyclic oxygen hydrogen bond of β-phenyl-D-galactose[33]

Recent preliminary studies by Tam *et al*. suggest that intramolecular bond strength indirectly correlates to IRI activity. Tam observed, through molecular dynamic (MD) simulations, that IRI-active AFGP and *C*-linked analogues contain a weaker hydrogen bond between OH4 and O6.[34] It was hypothesized that weaker intramolecular hydrogen bond networks will enable greater interaction with bulk water. This subsequently increases the entropy of bulk water, and hinders their transfer into the ice lattice.[4,34] Unfortunately it is difficult to assess the strength of the internal hydrogen bond network formed in these galactopyranosides by simply comparing their structures. Also, it is unclear how the anomeric substituents of these derivatives affect the overall hydrogen bond network strength. This renders the comparison of intramolecular bond strength to IRI activity difficult. Therefore, while literature precedent indicates that intramolecular hydrogen bond disruption and IRI activity may be related,[33,34] it is difficult to validate this hypothesis based on the results obtained in this study. It would be of interest to conduct studies which address the effect of intramolecular hydrogen bond strength on IRI activity be conducted in order to investigate this hypothesis.

Finally, as the relationship between the β-thiophenyl group at the anomeric position and the IRI activity of 3-deoxy-β-thiophenyl-D-galactose (**68**) is not understood, it is important to synthesize the remaining deoxy β-thiophenyl-D-galactose regioisomers to determine if they all have similar IRI activity due to the presence of this anomeric substituent.

4.3 Preparation and IRI analysis of azide and amine galactosides

From previous work by Ferreira, it was observed that substitution of the C2 hydroxyl group of galactose with an azide or amine afforded a slight decrease in IRI activity (compared to native galactose) than substitution with a hydrogen atom. (Graph 2.2, p. 53).[35] Interestingly, the

azide compound was found to have slightly better IRI activity than the amine derivative.[35] Azides exist as a zwitterion, whereas amines are positively charged at the pH of our IRI assay conditions (pH 7.4).[36] It was hypothesized that the zwitterionic nature of the azide permitted it to interact with a larger number of water molecules as it would be highly solvated and this would increase the degree to which bulk water was disordered, resulting in higher IRI activity.[35] In order to test this hypothesis, the syntheses of azido- and amino- galactopyranoside regioisomers were attempted (**38-43**) (Figure 2.6, p. 54).

4.3.1 Preparation of 6-deoxy-6-amino-D-galactose (38)

The synthesis of 6-deoxy-6-azido-D-galactose (**38**) from commercially available D-galactose was achieved in 41 % overall yield following the procedure of Yang and Thorson (Scheme 4.7).[37] D-Galactose was first selectively protected with 1,2- and 3,4-*O*-acetonides in 66 % yield under thermodynamic conditions (**89**).[38] The free C6 hydroxyl group was then converted to a leaving group using 1.0 equivalent of para-toluene sulfonyl chloride in anhydrous pyridine,[37] followed by immediate reaction with sodium azide to afford the C6-azide (**90**) in 96 % yield.[37] Deprotection of the acetonides was achieved under acidic conditions, and the desired free reducing azide (**38**) was obtained by recrystallization from hot ethanol.[37]

Scheme 4.7 Synthesis of 6-deoxy-6-amino-D-galactose (**41**)

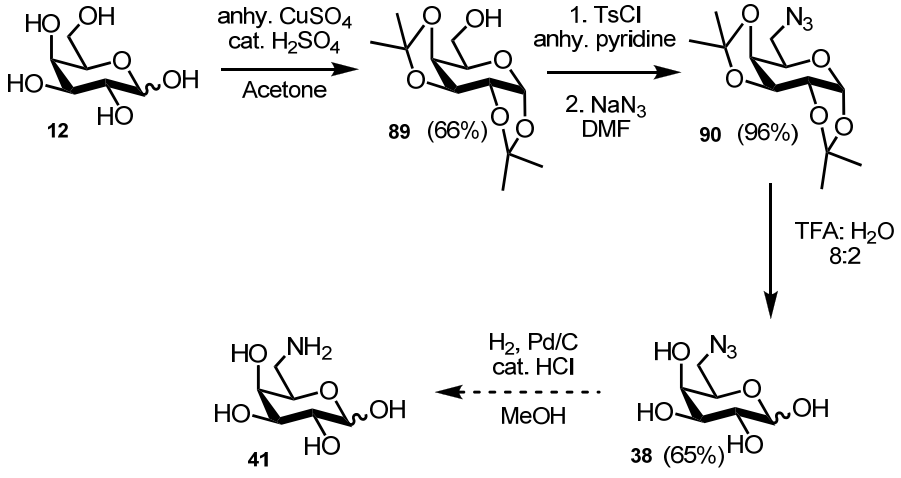

Generation of the amine (**41**) was achieved via hydrogenolysis of the azide (**38**) in the presence of a catalytic amount of hydrochloric acid.[37] Unfortunately the amine was impure following neutralization with basic Dowex 1X8 resin and C18 solid phase extraction column purification. Therefore, it could not be tested for IRI activity. Due to time constraints, the synthesis of amine **41** was not successfully accomplished.

4.3.2 Preparation of 4-deoxy-4-amino-D-glucose (93) and 4-deoxy-4-amino-D-galactose (42)

Incorporation of an azide functionality at the C4 position of galactose in the proper axial configuration was achieved from double inversion of stereochemistry of the C4 position on 1,2,3,6-tetra-*O*-pivaloyl-β-D-galactose (**75**).[39] This starting material was chosen because 1,2,3,6-tetra-*O*-pivaloyl-β-D-galactose (**75**) could be readily obtained in one step from D-galactose using 6.0 equivalents of pivaloyl chloride.[26] Inversion of stereochemistry at the C4 position was envisioned to be achieved by conversion of the free C4 hydroxyl group into a leaving group (triflate) followed by an S_N2 reaction with the desired nucleophile.[37] However, as it was uncertain whether the size of the pivaloyl protecting groups would interfere with the

displacement of the triflate, initial testing of incorporation of an azide group to the C4 position (Scheme 4.8) was conducted using 1,2,3,6-tetra-*O*-pivaloyl-β-D-galactose (**75**). The free hydroxyl group was converted to the triflate using 1.1 equivalents of triflic acid in excess pyridine. The triflate was immediately reacted with sodium azide to afford 4-azido-1,2,3,6-tetra-*O*-pivaloyl-β-D-glucose (**91**) in 96 % yield.[37] The high yield obtained demonstrated that the pivaloyl groups do not interfere with the approach of the azide anion. The next step was to attempt the double inversion of stereochemistry of position C4 on galactose, as described in Scheme 4.9.

Scheme 4.8 Attempted synthesis of 4-deoxy-4-amino-D-glucose (**93**)

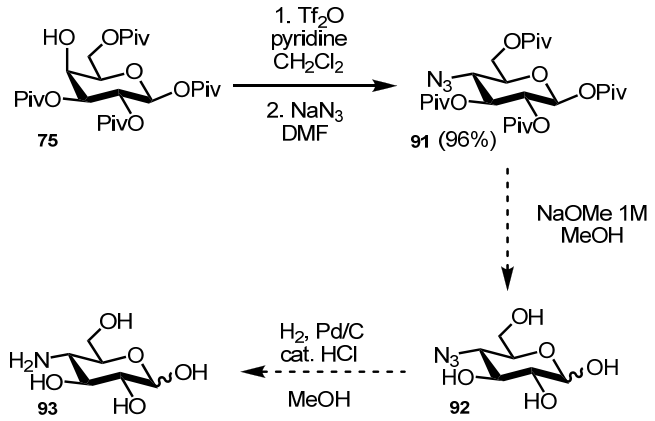

Scheme 4.9 Attempted synthesis of 4-deoxy-4-amino-D-galactose (**42**)

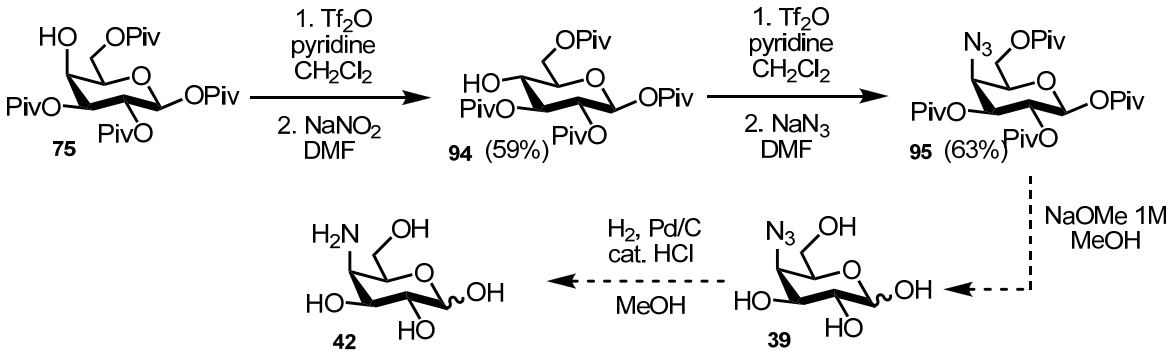

To generate the desired galactose isomer, the axial C4 hydroxyl group of 1,2,3,6-tetra-*O*-pivaloyl-β-D-galactose (**75**) was first converted to a triflate, and displaced with inversion of stereochemistry using sodium nitrite followed by aqueous work up to afford the glucopyranose derivative (**94**) in 59 % yield.[39] Subsequent triflation of the C4 hydroxyl group of 1,2,3,6-tetra-*O*-pivaloyl-β-D-glucose (**94**) followed by triflate displacement (with inversion of stereochemistry) using sodium azide[37] afforded 4-deoxy-4-azido-1,2,3,6-tetra-*O*-pivaloyl-β-D-galactose (**95**) in 63% yield.

From the results of Tam *et al*. described earlier, it was demonstrated that galactose possesses greater IRI activity than glucose.[4] It was hypothesized that the hydroxyl group stereochemistry of position C4 affects IRI activity.[2,4] Since the structures of 4-azido-D-glucose (**92**) and 4-azido-D-galactose (**39**) are C4 epimers, it would be interesting to compare their IRI activities relative to those of galactose and glucose. Therefore, deprotection of 4-azido-1,2,3,6-tetra-*O*-pivaloyl-β-D-glucose (**91**) and 4-azido-1,2,3,6-tetra-*O*-pivaloyl-β-D-galactose (**95**) was attempted using the various basic conditions presented in Table 4.2.[14, 40] Unfortunately, unlike 4-deoxy-1,2,3,6-tetra-*O*-pivaloyl-β-D-galactose (**77**), unreacted starting material and complex mixtures were recovered instead of the desired products (**92, 39**).

Table 4.2 Attempted deprotection of 4-azido-4-deoxy-1,2,3,6-tetra-*O*-pivaloyl-β-D-glucose (**91**) and galactose (**95**) under various basic conditions[14,40]

Starting Material	Product	Basic Reagent	Solvent	Temperature*	Reaction Time	Yield**
(**91**, **95**)	(**92**, **39**)	1M NaOMe[14]	MeOH	Sonicate at RT	1hr	RSM
(**91**, **95**)	(**92**, **39**)	1M NaOMe[14]	MeOH	Sonicate at RT	4hrs	RSM
(**91**, **95**)	(**92**, **39**)	1M tBuOK[40]	H_2O	RT	1 day	Complex Mixture
(**91**, **95**)	(**92**, **39**)	1M NaOMe[14]	MeOH	RT	5 days	RSM
(**91**, **95**)	(**92**, **39**)	1M NaOMe[14]	MeOH	80°C reflux	1 day	RSM
(**91**, **95**)	(**92**, **39**)	1M NaOMe[14]	MeOH	110°C reflux	2 days	Complex Mixture

*RT= Room Temperature, **RSM= Recovered Starting Material

The reason the deprotection of **91** and **95** was unsuccessful is uncertain. It was previously suggested that sterics reduce the hydrolysis rate of pivaloyl groups.[41] As an azide is larger than a hydrogen, it may be possible that the size of the azide group is inhibiting hydrolysis of the pivaloyl groups in compounds **91** and **95** while the hydrogen atom in the deoxy compound (**77**) is small enough to avoid interfering with the deprotection process.

Since removal of the pivaloyl groups was problematic, an alternative synthetic route (which does not employ pivaloyl protecting groups) is provided in Scheme 4,10. In this proposed synthesis, the 4-azido-galactose derivative (**100**) would be obtained from a single azide displacement[37] of a C4 triflate on the glucose precursor **99**. Compound **99** would be obtained from D-glucose (**13**) via protecting group manipulations involving addition of a 4,6 benzylidene acetal followed by acetyl group protection of hydroxyl groups at C1, C2 and C3.[42] The benzylidene acetal (**97**) would be cleaved under acidic conditions, affording the free C4 and C6 hydroxyl groups (**98**)[42] and the C6 hydroxyl would be converted to a silyl ether using *tert*-

butyldimethylsilyl chloride (TBDMSCl) and imidazole (**99**).[43] Triflation, followed by azide substitution at C4 would yield the desired azide galactopyranosyl regioisomer (**100**)[37] and deprotection with *tert*-butylammonium fluoride[43] and sodium methoxide[14] would afford the desired free reducing azide (**39**) which upon further hydrogenation[37] would afford the corresponding amine (**42**).

Scheme 4.10 Revised route for synthesis of 4-deoxy-4-azido-D-galactose (**39**) and 4-deoxy-4-amino-D-galactose (**42**) [37, 42, 43]

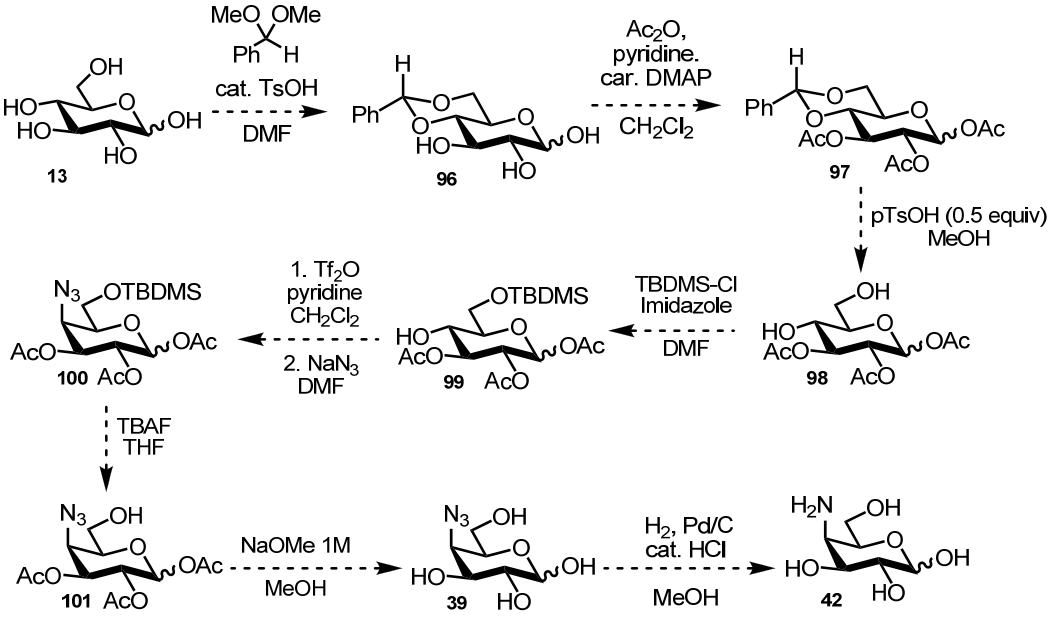

4.3.3 IRI assessment of 6-deoxy-6-azido-D-galactose (38)

The IRI activity of 6-azido galactose (**38**) at 0.022 M (Graph 4.4, purple bar) was plotted with the previously determined IRI activities of 2-azido- (**35**), 2-deoxy- (**34**) and 6-deoxy-galactose (**29**). [35]

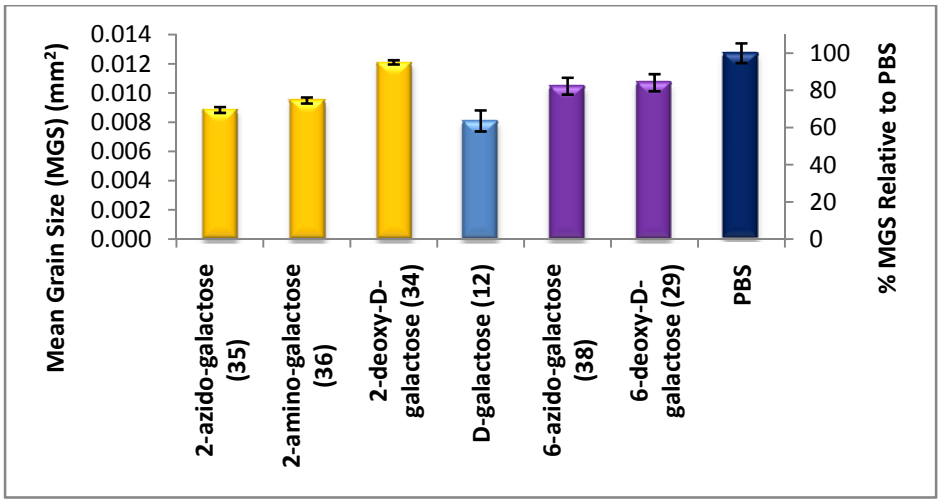

Graph 4.4 IRI activities of azide and amine galactose derivatives (**35**, **38**), D-galactose (**12**), 2-deoxy galactose (**34**) and 6-deoxy galactose (**29**),at 0.022 M.[1,35]

It is observed that the 6-azido compound (**38**) has similar activity to 6-deoxy galactose (**29**), and both are worse than native D-galactose. This result reinforces the notion that removing a single hydroxyl group has a detrimental effect on IRI activity. It was previously reported that the IRI activity of the C2-azide (**35**) is comparable to native D-galactose (**12**) and is slightly better than the C2-galactosamine derivative (**34**).[35] It is interesting to note that this C2-azide (**35**) also has greater IRI activity than the C6 azide regioisomer (**38**). This difference in IRI activity also suggests that the regiochemistry of the azide functional group affects IRI activity.

As it is postulated that the extent of hydration of a solute affects its IRI activity,[1,4] Ferreira suggested that C2 azide (**35**) has greater IRI activity than C2 amine (**36**) because the former is more hydrated than the latter.[35] Unfortunately, given the lack of data from these preliminary results, it is crucial that more azide and amine regioisomers be synthesized in order to gain more insight into the nature of the effect of these amine and azide functionalities on the IRI activity of galactose.

4.4 Influence of anomeric thioalkylation of galactose on IRI activity

Chaytor and Tam *et al*. previously tested the IRI activities of anomeric α- and β- *O*-methoxy[6] (**45**, **46**) and α- and β-allyl *C*-galactopyranoosyl derivatives[4] (**25**, **44**). Overall, as shown in Graph 2.3 (p. 56) the α-anomers (**25**, **45**) appeared to have increased IRI activity compared to the β anomers (**44**, **46**).[4,6] Interestingly, the analogue with an electronegative oxygen atom in the α-configuration (**45**) is a poorer ice recrystallization inhibitor compared to the α-*C*-linked allyl derivative (**25**).[4,6]

Campbell further investigated the glycosidic nature of antifreeze glycoprotein analogues. Syntheses and IRI analyses of glycopeptide analogues containing an anomeric sulfur atom in the α-configuration ((CGG)-gal) (**6**) and ((CAA)-gal) (**7**) (Figure 1.17, p. 26) revealed that presence of the larger anomeric sulfur atom decreases the overall IRI activity of these analogues compared to their carbon analogues (Graph 1.3, p. 27).[44] Unfortunately, the relationship between the anomeric stereochemistry of these thioalkyl analogues and IRI activity was not assessed.

In addition, previous IRI assay results for a series of *N*-alkyl acetamide galactosyl derivatives (which contain alkyl chains of various lengths) demonstrated that an analogue consisting of a propyl group yielded the greatest IRI activity (Graph 1.2, p. 25).[45]

Therefore, to further investigate the influence of alkyl chain length and anomeric stereochemistry on IRI activity, we attempted the synthesis of a series of α- and β-thioalkylgalactosides with varying alkyl chain lengths (**47-56**) (Figure 2.7, p. 57).

4.4.1 Preparation of β-thioalkylgalactosides (47-51)

The general procedure outlined in Scheme in 4.11 involves generation of the oxocarbenium ion of 2,3,4,6-tetra-*O*-acetyl-D-galactose using boron trifluoride diethyl etherate as activating Lewis acid followed by thiolation with the desired alkylthiol to form the corresponding β-thioalkylgalactoside[15] which is further deprotected using sodium methoxide and recrystallized from hot hexanes and ethanol or ether.[14]

Scheme 4.11 Synthesis of β-thioalkylgalactosides (**48**-**51**)

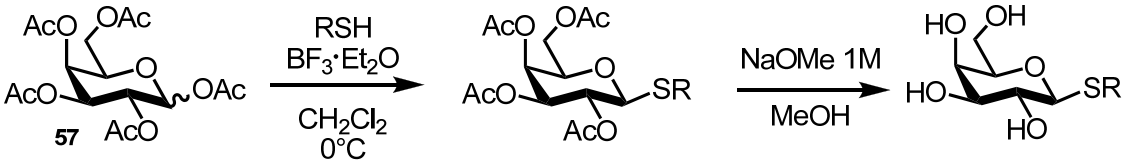

R= Propyl **(48)**,
Butyl **(49)**, Hexyl **(50)**, Octyl **(51)**

The non-optimized overall yields obtained are presented in Table 4.3. Unfortunately, β-ethylthiogalactose (**47**) was not purified enough for IRI testing.

Table 4.3 Structures and non-optimized yields of synthesized β-thioalkyl galactosides.

Compound	Structure	Yield (%)
Propyl-thio-β-D-galactose (**48**)	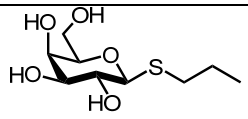	42
Butyl-thio-β-D-galactose (**49**)	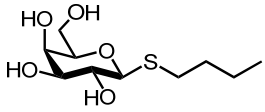	71
Hexyl-thio-β-D-galactose (**50**)	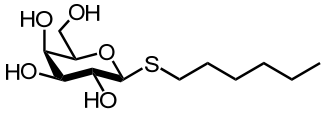	12
Octyl-thio-β-D-galactose (**51**)	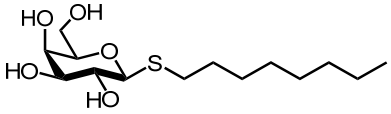	27

4.4.2 Preparation of α-thioalkylgalactosides (52-56)

Time constraints limited the synthesis and purification of these α-thiogalactoses and therefore no compounds were generated for IRI testing. However, the general procedure to be used to prepare the α-alkylthiogalactosides is outlined in Scheme 4.12. Initial preparation of β-galactosyl chloride (**102**) following the procedure by Ibatullin and Selivanov[46] is envisioned to be followed by base mediated nucleophilic displacement of the chloride atom by various alkylthiols to afford the corresponding α-alkylthiogalactosides[18] (**52-56**) which would be further deprotected using sodium methoxide[14] and recrystallized from hot hexanes and ethanol or ether.

Scheme 4.12 Synthesis of α-thioalkylgalactosides (**52-56**)

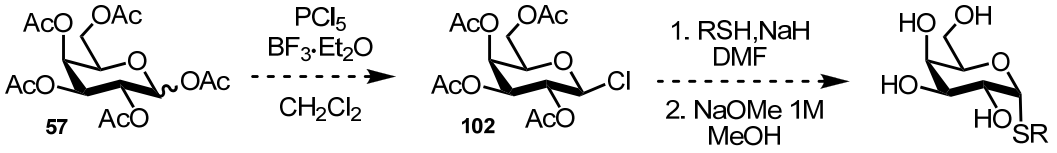

R= Ethyl **(52)**,Propyl **(53)**,
Butyl **(54)**, Hexyl **(55)**, Octyl **(56)**

4.4.3 IRI assessment of β-thioalkyl galactosides

The IRI activities of the synthesized and purified β-thiolgalactosides (**48**, **49**) were plotted with those of D-galactose (**12**), β-thiophenyl-D-galactose (**61**) and β-*C*-allyl-D-galactose (**44**) (Graph 4.5)[4,6]

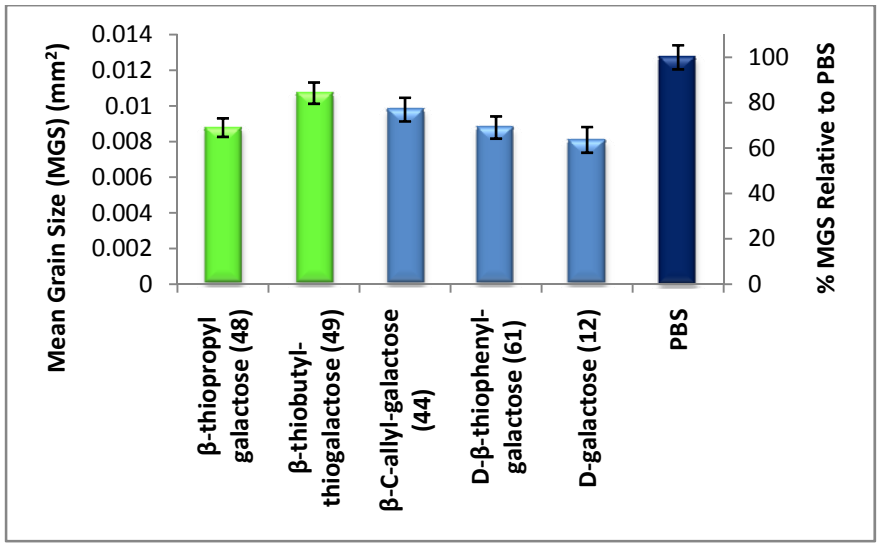

Graph 4.6 IRI activities of β-thiolalkyl galactosides (**48**, **49**) β-thiophenyl galactose (**61**), D-galactose (**12**) and β-*C*-allyl-D-galactose (**44**), at 0.022 M.[4,6]

Initially it was hypothesized that incorporation of longer alkyl chains would reduce the hydration index (number of hydrated water molecules per unit volume) of these galactose derivatives since it has been reported that hydrophobic surfaces are less hydrated than hydrophilic surfaces.[5,47] As it has been demonstrated that the hydration index of a solute is directly proportional to its IRI activity,[4] the results of β-alkyl thiogalactoses (**48**, **49**) obtained corroborate this hypothesis since the longer butyl analogue (**49**) is less IRI-active than the propyl analogue (**48**). However, the fact that a hydrophobic group such as a propyl chain (**48**), has similar IRI activity to D-galactose (**12**) and β-thiophenyl-D-galactose (**61**) is counterintuitive. Thus, given the lack of data, more testing is required in order to determine what factors are responsible for these results.

The insoluble nature of β-thiohexyl galactose (**50**) prevented IRI activity testing at 0.022 M. Therefore, to determine the effective concentration of β-thiohexyl galactose (**50**) dissolved in the 0.022 M sample, a second sample of (**50**) was prepared at the same concentration, passed

through a C-18 solid-phase extraction column to remove the buffer salts and freeze-dried to determine the actual amount of solute dissolved. A total of 2.1 mg of compound (**50**) was recovered from an initial sample of 4.0 mg, suggesting that only half of the solute was actually dissolved. To confirm that the effective concentration was 0.011 M, another sample of (**50**) at 0.011 M was also prepared and tested for IRI activity. It was demonstrated in Graph 4.6 that both 0.022 M and 0.011 M solutions of (**50**) have identical IRI activity despite the presence of undissolved particulate in the former. These results suggest that IRI activity is dependent on the effective soluble concentration of the carbohydrate.

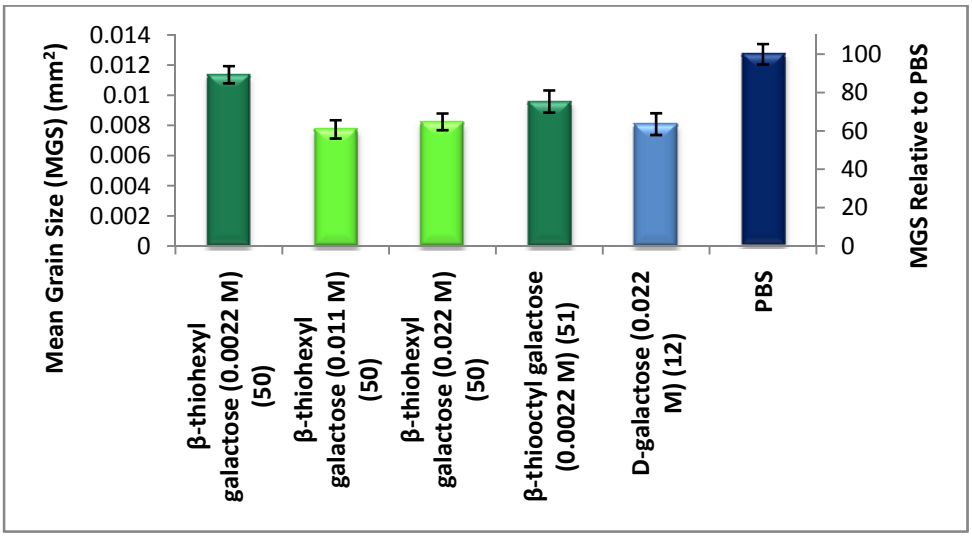

Graph 4.6 IRI activities of β-thiohexylgalactoside (**50**), β-thiooctylgalactoside (**51**) and D-galactose (**12**).[1]

Solubility issues were also present during the sample preparation of 0.022M β-thiooctyl galactoside (**51**). Therefore, β-thiooctyl-galactose (**51**) and β-thiohexyl-galactose (**50**) were tested at 0.0022 M to enable a comparison of their IRI activities. Graph 4.6 shows that β-thiooctylgalactoside (**51**) is a slightly better ice recrystallization inhibitor than the shorter hexyl analogue, which is opposite to the results observed in Graph 4.5, whereby the shorter propyl

analogue was more active than the longer butyl analogue. Thus, from these contradicting results, it is unclear how the increase in hydrophobicity of the anomeric subsituents influences IRI activity, and further studies are required.

4.5 Summary

From the results obtained by Tam and Chaytor, it was initially believed that loss of any hydroxyl group within the pyranose ring of D-galactose (**12**) would result in complete loss of IRI activity since this modification would reduce the overall hydration of this carbohydrate.[4,6] The results of Graph 4.1 corroborate this hypothesis in that all the deoxy-D-galactosyl pyranosides (**26**, **28**, **29**, **34**) and deoxy-α-*C*-allyl-D-galactosyl pyranosides (**30**, **32**, **33**) have dramatically reduced IRI activity compared to D-galactose. It is important to note that both deoxy-D-galactosyl pyranosides (**26**, **28**, **29**, **34**) and deoxy-α-*C*-allyl-D-galactosyl pyranosides (**30**, **32**, **33**) have similar IRI activities which demonstrates that the α-*C*-allyl moiety is not affecting the IRI activity of these compounds. Interestingly, 6-deoxy-D-galactose (**29**) has slightly better IRI activity than 1-, 2-, 4-deoxy galactosides (**26**, **28**, **34**). Although the reason for this increase in activity is unknown, we wished to correlate the results of Graph 4.1 to the hydration indices of these galactopyranoside derivatives as it was previously demonstrated that the hydration index of a particular carbohydrate correctly predicts its IRI activity at 0.022 M.[4] The fact that the calculated hydration index of 6-deoxy galactose (**29**) failed to predict its IRI activity provides the first result which is not consistent with the hydration index model.[4] Therefore more studies which address the significance of this data point are required.

As mentioned in sections 4.2.2 and 4.2.5, the full set of deoxy galactoside regioisomers was not complete as 3-deoxy-D-galactose (**27**) and 3-deoxy-α-*C*-allyl-D-galactose (**31**) were not obtained. Therefore the late-stage intermediate 3-deoxy-β-thiophenyl-D-galactose (**68**) was

tested for IRI activity and compared to β-thiophenyl galactose (**61**). As it was predicted that **68** would have identical IRI activity to that of the other deoxy galactosides (**26**, **28**, **29**, **34**),[6] the fact that **68** has IRI activity that is comparable to D-galactose (**12**) and β-thiophenyl galactose (**61**) is a very interesting and unexpected result which needs further investigation. Upon reviewing the literature, [4,33,34] it is hypothesized that carbohydrates which display weaker intramolecular hydrogen bonds will be more hydrated since their hydroxyl groups will be more able to interact with surrounding water molecules.[4,33,34] Being more hydrated, these carbohydrates will cause a larger disruption in bulk water ordering and therefore have increased IRI activity. Unfortunately it is difficult to determine if there is a link between intramolecular bond strength and IRI activity based on the results of this study since the strength of the intramolecular hydrogen bonds and the extent of hydration of these carbohydrates was not determined.

The preliminary results from the testing of synthesized azide and amine galactopyranoside regioisomers (**38-43**) do not provide sufficient information to draw any major conclusions regarding the effect of these functionalities on IRI activity (Graph 4.4). However, it is interesting to note that 2-deoxy-D-galactose (**34**) has poorer activity than 2-azido-D-galactose (**35**), while 6-deoxy-D-galactose (**29**) and 6-azido-D-galactose (**38**) have similar activity. Also, 2-azido-D-galactose (**35**) has slightly better activity than 6-azido-D-galactose (**38**). These results may suggest that differences in the hydration and regiochemistry of the azide, amine and hydroxyl functionalities are factors affecting IRI activity.

When comparing the IRI activities of β-thiopropyl-D-galactose (**48**) and β-thiobutyl-D-galactose (**49**) (Graph 4.5), it was noted that as the alkyl chain length increased, the IRI activity decreased for these compounds (**48** and **49**) at 0.022 M. This is in accordance with the hypothesis that hydrophobic groups decrease the IRI activity of galactose derivatives.[4,47] Interestingly, IRI

assay analyses for β-thiohexyl-D-galactose (**50**) and β-thiooctyl-D-galactose (**51**) at a more diluted concentration (0.0022 M) revealed that the longer octyl analogue was more potent than the hexyl analogue (Graph 4.6).

References

1. Czechura, P.; Tam, R.Y.; Dimitrijevic, E; Murphy, A.V; Ben, R. N., The Importance of Hydration for Inhibiting Ice Recrystallization with C-Linked Antifreeze Glycoproteins, *J. Am. Chem. Soc.*, **2008,** 130 (10) 2928-2929.

2. Galema, S. A.; Høiland, H. Stereochemical Aspects of Hydration of Carbohydrates In Aqueous Solutions. 3. [1]Density and Ultrasound Measurements, *J. Phys. Chem.* **1991**, *95*, 5321.

3. Galema, S. A.; Howard, E.; Engberts, J. B. F. N.; Grigera, J. R., The effect of stereochemistry upon carbohydrate hydration. A molecular dynamics simulation of β-D-galactopyranose and (α,β)- D-talopyranose, *Carbohydr. Res.***1994**, *265*, 215-225.

4. Tam R.Y.; Ferreira, S. S.; Czechura, P.; Chaytor, J. L.; Ben, R. N., Hydration Indexs - A Better Parameter for Explaining Small Molecule Hydration in Inhibition of Ice Recrystallization, *J. Am. Chem. Soc*. **2008**, 130, 17494–17501.

5. Dashnau, J.; Sharp, K. A.; Vanderkooi, J. M., Carbohydrate Intramolecular Hydrogen Bonding Cooperativity and Its Effect on Water Structure, *J. Phys. Chem. B* **2005**, 109, 24152–24159.

6. Chaytor, J. L., PhD Dissertation, University of Ottawa, **2010**.

7. Marcin Palusiak,M.; Grabowski, S. J., Methoxy group as an acceptor of proton in hydrogen bonds. *Journal of Molecular Structure*, **2002**, 642, 97-104.

8. Malkar, N. B.; Lauer-Fields J. L.; Fields, G. B, Convenient synthesis of glycosylated hydroxylysine derivatives for use in solid-phase peptide synthesis, *Tetrahedron Letters*, **2000**, 1137–1140.

9. Malmberg, J.; Mani, K.; Säwén, E.; Wirén, A.; Ellervik, U., Synthesis of aromatic *C*-xylosides by position inversion of glucose, *Bioorg. Med. Chem.*, **2006**, 6659-6665.

10. Ella-Menye, J.-R.; Nie, X.; Wang, G, Synthesis of octahydropyrano[3,2-*b*]pyrrole-2-carboxylic acid derivatives from D-mannose, *Carbohydr. Res.*, **2008**, 1743-1753

11. Zhang, Z; Magnusson, G., Synthesis of double-chain bis-sulfone neoglycolipids of the 2'-, 3'-, and 6'-deoxyglobotrioses, *J. Org. Chem.*, **1995**, 7304-7315.

12. Marques, C. A.; Maurizio Selva, M.; Tundo, P., Facile hydrodehalogenation with hydrogen and Pd/C catalyst under multiphase conditions, *J. Org. Chem.,* **1993,** 5256-5260.

13. Yves Ambroise, Y.; Mioskowski, C.; Djéga-Mariadassou, G.; Rousseau, B., Consequences of affinity in heterogeneous catalytic reactions: highly chemoselective hydrogenolysis of iodoarenes, *J. Org. Chem.,* **2000**, 7183-7186.

14. Zemplen, G.; Kunz, A., *Chem. Ber.*, **1923**,1705.

15. Janczuk, A. J.; Zhang, W.; Andreana, P. R.; Warrick, J.; Wang P. G, The synthesis of deoxy-α-Gal epitope derivatives for the evaluation of an anti-α-Gal antibody binding, *Carbohydr. Res.,* **2002,** 337, 1247-1259.

16. Ohlsson, J.; Magnusson, G., Galabiosyl donors; efficient synthesis from 1,2,3,4,6-penta-*O*-acetyl-β-D-galactopyranose. *Carbohydr. Res.*, **2000**, 329, 49-55.

17. Catelani, G.; Colonna, F.; Marra, A., An improved preparation of 3,4-*O*-isopropylidene derivatives of α- and β- D-galactopyranosides, *Carbohydr. Res.,* **1988,** 182, 297-300.

18. Boulineau, F. P.; Wei, A., Mirror-Image Carbohydrates: Synthesis of the Unnatural Enantionmer of a Blood Group Trisaccharide. *J. Org. Chem.* , **2004,** 69, 3391-3399.

19. Mandal, P. K.; Misra, A.K., Concise synthesis of two pentasaccharides corresponding to the alpha-chain oligosaccharides of Neisseria gonorrhoeae and Neisseria meningitides. *Tetrahedron*, **2008**, 64, 8685-8691.

20. Deslongchamps, P. *Stereoelectronic Effects in Organic Chemistry*; Pergamon Press Ltd.: Oxford, 1983; p 83.

21. Lemieux, R.U.; Driguez, H., Chemical synthesis of 2-*O*-(.alpha.-L-fucopyranosyl)-3-*O*-(.alpha.-D-galactopyranosyl)-D-galactose. Terminal structure of the blood-group B antigenic determinant, *J. Am. Chem. Soc.*, **1975**, 97, 4069–4075.

22. Barton, D. H. R.; McCombie, S. W., A New Method for the Deoxygenation of Secondary Alcohols, *J. Chem. Soc. Perkin Trans. 1,***1975**, 137, 1574-1585.

23. Mulard, L.A.; Kovác, P.; Glaudemans, C. P. J., Synthesis of methyl *O*-α-L-rhamnopyranosyl-(1→ 2)-α-D-galactopyranosides specifically deoxygenated at position 3, 4, or 6 of the galactose residue, *Carbohydr. Res.*, **1994**, 251, 213-232.

24. Nicolaou, K. C.; Bockovich, N. J.; Carcanague, D. R., Total Synthesis of Sulfated Le^x and Le^a-type Oligosaccharide Selectin Ligands, *J. Am. Chem. Soc.*, **1993**, 8843.

25. Bleriot, Y.; Untersteller, E.; Fritz, B.; Sinay, P., Total Synthesis of Calditol: Structural Clarification of this Typical Component of Archaea Order *Sulfolobales. Chemistry: A European Journal,* **2002**, 8, 240-246.

26. Becker, D.; Galili, N., Synthesis and utilization of saccharide intermediates, *Carbohydr. Res.,***1993**, 129-141.

27. Garegg, P. J.; Samuelsson, B., Novel reagent system for converting a hydroxy-group into an iodo-group in carbohydrates with inversion of configuration. Part 2, *J. Chem. Soc. Perkin Trans. 1*, **1980**, 2866-2870.

28. Arya, P.; Barkley, A.; Randell, K. D., Automated, High-throughput Synthesis of Artificial Glycopeptides: Small-molecule Probes for Chemical Glycobiology., *J. Comb. Chem.*, **2002**, 4 (3), 193–198

29. Hall, L.; Miller, D. C;, Fluorinated Sulphonic Esters of Sugars: Their Synthesis and Reactions with Pyridine. *Carbohydr. Res*., **1976**, 46, 299-305.

30. Barrette, E. P.; Goodman, L., Convenient and stereospecific synthesis of deoxy sugars. Reductive displacement of trifluoromethylsulfonates., *J. Org. Chem.*, **1984**, 49, 176-178.

31. Parke, S.A.; Birch, G. G,; Dijk, R., Some Taste Molecules and their Solution Properties, *Chem. Senses*, **1999**, 24, 271- 279.

32. Capicciotti, C.; Ben, R., N., unpublished results, 2010.

33. Cocinero, E. J.; Stanca-Kaposta, E. C.; Scanlan, E. M.; Gamblin, D. P.; Davis, B. G.; Simons, J. P., Conformational Choice and Selectivity in Singly and Multiply Hydrated Monosaccharides in the Gas Phase, *Chem. Eur. J.*, **2008**, 14, 8947 – 8955.

34. Tam, R.Y.; Rowley, C. N.; Petrov, I.; Zhang,T.; Afagh, N. A.; Woo T. K.; Ben, R. N., Solution Conformation of *C*-Linked Antifreeze Glycoprotein Analogues and Modulation of Ice Recrystallization, *J. Am. Chem. Soc.*, **2009**, 131, 15745-15753.

35. Ferreira, S. S., M. Sc. Dissertation, University of Ottawa, **2009**.

36. Brase, S.; Gil, C.; Knepper, K.; Zimmermann, V., Organic Azides: An Exploding Diversity of a Unique Class of Compounds, *Angew. Chem. Int. Ed.* **2005**, 44, 5188 – 5240.

37. Yang, J.; Fu, X.; Qiang, J.; Shen, J.; Biggins, J. B.; Jiang, J.; Zhao, J.; Schmidt, J. J.; Wang, P. G.; Thorson, J. S., Studies on the Substrate Specificity of *Escherichia coli* Galactokinase, *Org. Lett.*, **2003**, 5, 2223-2226

38. Schmidt, O. Th. *Methods Carbohydr. Chem,* **1963**, 2, 318.

39. Binkley, R. W., Inversion of Configuration in 2,6-Dideoxy Sugars. Triflate Displacement by Benzoate and Nitrite Anions, *J. Org. Chem*. **1991**, 56, 3892-3896.

40. Gassman, P. G.; Schenk, W. N., A General Procedure for the Base-Promoted Hydrolysis of Hindered Esters at Ambient Temperatures, *J. Org. Chem.*, **1976**, 42, 918-920.

41. Roslund, M. U.; Aitio, O.; Warna, J.; Maaheimo, H.; Murzin,D. Y.; Leino, R., Acyl Group Migration and Cleavage in Selectively Protected β-D-Galactopyranosides as Studied by NMR Spectroscopy and Kinetic Calculations, *J. Am. Chem. Soc.,***2008**, 130, 8769-8772.

42. Blom, P.; Ruttens, B.; Van Hoof, S.; Hubrecht, I.; Van der Eycken, J., A Convergent Ring-Closing Metathesis Approach to Carbohydrate-Based Macrolides with Potential Antibiotic Activity. *J. Org. Chem.***2005**, 70, 10109-10112.

43. Corey, E. J., and Venkateswarlu, A., Protection of hydroxyl groups as tertbutyldimethylsilyl derivatives *J. Am. Chem. Soc.*, **1972**, 94, 6190-6191.

44. Campbell, W., M. Sc. Dissertation, University of Ottawa, **2009**.

45. Trant, J. T.; Biggs, R.; Ben, R. N., unpublished results, **2009**

46. Ibatullin, F. M.; Selivanov, S. I., Reaction of 1,2-trans-Glycosyl Acetates with Phosphorus Pentachloride: New Efficient Approach to 1,2-trans-Glycosyl Chlorides. *Tetrahedron Lett*. **2002**, 52, 9577-9580.

47. Caffarena, E. R.; Grigera, J. R., On the hydrogen bond structure of water at different densities. *Physica A*, **2004**, 342, 34-39.

Chapter 5: Future Directions

5.1 Further assessment of the potential link between cryopreservation ability and IRI activity of simple mono- and disaccharides and DMSO

From the research presented in Chapter 3, several questions must be further addressed. Firstly, the apparent failure of the hydration index to accurately predict the IRI activity of higher concentrations (0.22 M) of disaccharides was unexpected (Section 3.2, p. 62). It was shown that the IRI activity of this concentration of disaccharides was significantly more potent than 0.22 M of monosaccharides. In order to address this issue, testing the IRI activities of monosaccharides at a two-fold increase in concentration will match the carbohydrate concentrations (per molar basis) found in 0.22 M disaccharide solutions. This will demonstrate whether concentration or the carbohydrate structure is important for IRI activity at higher concentrations.

From the IRI activity analyses of solution mixtures of carbohydrates and 5 % DMSO, it was proposed that poor solubility[1] was accounting for loss of IRI activity in high concentrations of carbohydrate (Graph 3.2, p. 66). Performing turbidity measurements and conducting a full IRI activity scan of DMSO concentrations combined with varying concentrations of these sugars is required to determine whether reduced solubility of these sugars in DMSO is affecting their IRI activity.

From the cytotoxicity data collected, it was apparent that high concentrations of disaccharides (0.5 M) were highly toxic to WRL 68 cells (Graph 3.3, p. 69). It was proposed that osmotic shock was a plausible explanation.[2] It would be interesting to obtain the toxicity profile of other non-ionic, non-permeable solutes at similar concentrations for comparison. If osmotic shock is the cause of cell death, the toxicity profiles are expected to be similar.

Given that the specific structure of D-galactose appears to be conferring potent IRI activity and cryopreservation ability relative to other structural isomers (i.e. D-glucose, D-

mannose, D-talose), it would be interesting to probe the effect of other structural derivatives of galactopyranose such as furanoses (ie D-fructose), acyclic carbohydrates/hexitols (ie D-mannitol and D-galactitol), [3,4] and various anomeric substituents on their IRI activity and cryopreservation ability.

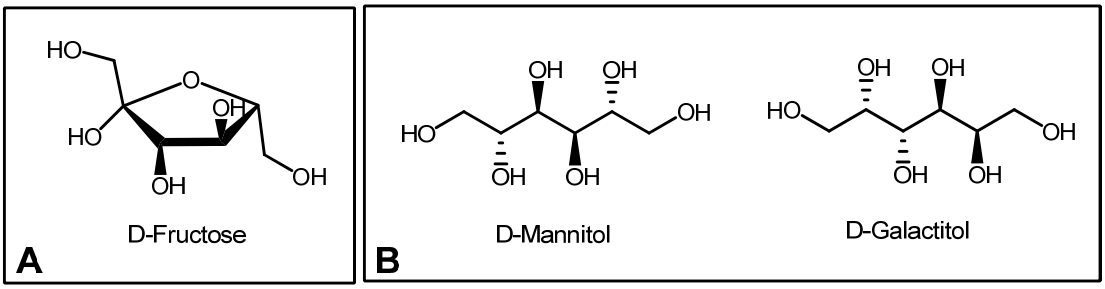

Figure 5.1 Examples of (A) furanose carbohydrates and (B) hexitols

The increased cryopreservation ability of galactose may also be due to its possible internalization via ASGPr found in the cell membranes of hepatic (i.e. WRL-68) cells.[5] This would enable the inhibition of intracellular ice recrystallization, which is proposed to be lethal to cells.[6,7] As some non-hepatic cells such as kidney (HEK 293) cells lack the galactose transport carriers (ASGPr), it was hypothesized that these latter cells will show a decrease in cell viability upon freezing due to the inability of galactose to internalize to inhibit intracellular ice recrystallization. Recent results by Leclere and Tam have supported this notion, as a decrease in viability was observed in HEK 293 cells (Graph 3.8, p. 77).[8] Another method to determine the effect of internalization of galactose on cryopreservation would be to inhibit the function of ASGPrs and compare the post-thaw viability of these cells to that of native hepatic and non-hepatic cells.

Finally, although our study was the first to demonstrate that IRI activity is directly proportional to cryopreservation ability (Section 3.6, p. 72), a larger, more complete, screen of

carbohydrates, carbohydrate derivatives and cell types is required in order to better validate this hypothesis.

5.2 Further structure-function studies and assessment of IRI activity of galactose derivatives

From the conclusions drawn in Chapter 4, it is evident that more synthetic targets must be produced and tested to further investigate the link between the structure and IRI activity of galactose.

Since a full assessment of the effect of each individual hydroxyl group of the galactopyranose ring on IRI activity was undertaken, it is crucial that the syntheses of 3-deoxy-D-galactose and 3-deoxy-α-*C*-allyl-D-galactose be completed as well as those of 3- and 4- azides and amines (Sections 4.2.2, p. 86, 4.2.5, p. 93, and 4.3, p. 102). Surprisingly, 3-deoxy-β-thiophenyl-D-galactose (**68**) exhibited potent IRI activity comparable to galactose despite its lack of a hydroxyl group at position C3 (Graph 4.3, p. 99). To determine if this increased IRI activity is due to the anomeric β-thiophenyl substituent, the synthesis and ice recrystallization inhibition ability of 2-, 4-, and 6-deoxy-β-thiogalactose regioisomers must be achieved and compare their activities to 3-deoxy-β-thiogalactose and β-thiogalactose.

Also, as literature precedence indicates that there may be a link between intramolecular hydrogen bond strength and IRI activity of carbohydrates,[9,10] it would be interesting to determine the IRI activities of galactose regioisomers that have alkyl chain spacers between the hydroxyl group and the pyranose ring (Figure 5.2). Increasing the distance between the hydroxyl group and the pyranose ring may alter its hydrogen bond interaction with adjacent hydroxyl groups and

would further disrupt the intramolecular hydrogen bonding network in the ring.[11-13] If the intramolecular bond is weakened, it is proposed that IRI activity will increase.

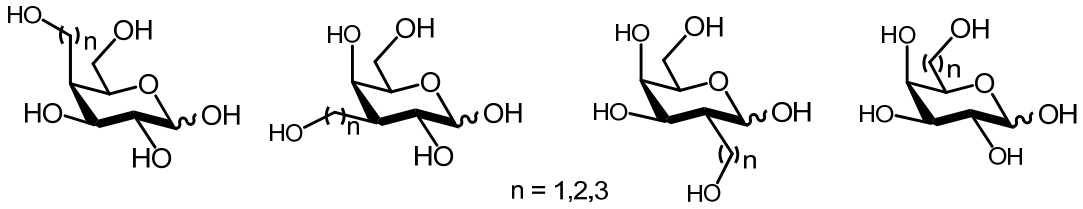

Figure 5.2 Structures of galactopyranosyl derivatives with alkyl chain extensions between each hydroxyl group and the pyranose ring.

With regards to the synthesis of thioalkyl galactosides (Section 4.4, p. 110), it will be important to complete the α-thioalkyl galactose series and compare them to α– and β- *O*-alkyl and *C*-alkyl variations (Figure 5.3). This will allow better insight into the effect of stereochemistry, anomeric atom size and electronegativity on IRI activity.

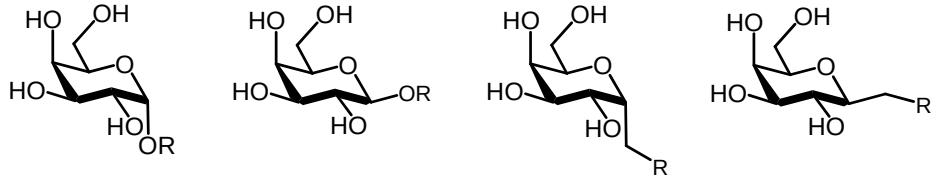

Figure 5.3 Structures of α- and β- *O*-alkyl and *C*-alkyl galactose derivatives

Finally, it would be of interest to determine if increasing the hydrophilicity of the anomeric position of galactose will enhance hydration and thus IRI activity. Therefore, the activity testing on synthesized galactopyranosyl derivatives that include addition of polyalcohol chains such as the hexitols (Figure 5.1) at the anomeric position should be achieved.

References

1. (a) Liu,Q.; Janssen, M. H. A.; van Rantwij, F.; Sheldon, R. A., Room-temperature ionic liquids that dissolve carbohydrates in high concentrations, *Green Chemistry,* **2005**, 7, 39-42.(b) Balakin, K.V.; Savchuk, N.P.; Tetko, I.V., In silico approaches to prediction of aqueous and DMSO solubility of drug-like compounds: Trends, problems and solutions. *Current Medicinal Chemistry,* **2006**, 13, 223-241.

2. Meryman, H.T., Osmotic stress as a mechanism of freezing injury, *Cryobiology*, **1971**, 8, 489-500.

3. Well, H. J.; Wells, W. W., Galactose toxicity and myoinositol metabolism in the developing rat brain, *Biochem.* **1967**, 6, 1168-1173.

4. Nissenson, A. R.; Weston, R. E; Kleeman, C. R., Mannitol, *West J. Med.*, **1979**, 131, 277-284.

5. (a) Ashwell, G.; Harford, J., Carbohydrate-Specific Receptors of the Liver *Ann. Rev. Biochem.* **1982**, 51, 531-554. (b) Ashwell, G..; Morell, A. G., The role of surface carbohydrates in the hepatic recognition and transport of circulating glycoproteins. In: A Meister, Editor, *Advances in Enzymology* Vol. 41, John Wiley & Sons, New York (**1974**), pp. 99–128.

6. Fowler, A.; Toner, M., Cryo-Injury and Biopreservation. *Ann. NY Acad. Sci.* **2006**, 1066, 119-135.

7. Mazur, P., Principles of cryobiology. In: Life in The Frozen State. Fuller BJ, Lane N, Benson EE, eds. **2004**, Boca Raton, FL: CRC Press. p. 3–65.

8. Leclere, M.; Tam, R. Y.; Ben, R. N., (unpublished results), **2010**.

9. Cocinero, E. J.; Stanca-Kaposta, E. C.; Scanlan, E. M.; Gamblin, D. P.; Davis, B. G.; Simons, J. P., Conformational Choice and Selectivity in Singly and Multiply Hydrated Monosaccharides in the Gas Phase, *Chem. Eur. J.*, **2008**, 14, 8947 – 8955.

10. Tam, R.Y.; Rowley, C. N.; Petrov, I.; Zhang,T.; Afagh, N. A.; Woo T. K.; Ben, R. N., Solution Conformation of *C*-Linked Antifreeze Glycoprotein Analogues and Modulation of Ice Recrystallization, *J. Am. Chem. Soc.*, **2009**, 131, 15745-15753.

11. Lopez de la Paz, M.; Ellis, G.; Perez, M.; Perkins, J.; Jimenez-Barbero, J. ; Vincent, C., Carbohydrate Hydrogen-Bonding Cooperativity- Intramolecular Hydrogen Bonds and Their Cooperative Effect on Intermolecular Processes-Binding to a Hydrogen-Bond Acceptor Molecule. *Eur. J. Org. Chem.* **2002**, 2002, 840-855.

12. Baruch, E.; Belostotskii, A. M.; Mastai, Y., Relationship between the antifreeze activities and the chemical structure of polyols. *J. Mol. Struct.* **2008**, 874, 170-177.

13. Dashnau, J.; Sharp, K. A.; Vanderkooi, J. M., Carbohydrate Intramolecular Hydrogen Bonding Cooperativity and Its Effect on Water Structure, *J. Phys. Chem. B.* **2005**, 109, 24152–24159.

Chapter 6: Experimental

6.1 General Procedures

6.1.1 IRI Assay

Analysis of IRI activity was performed using the "splat cooling" technique which is previously described by Tam et al.[1] which consists of dropping a 10 µL sample of analyte dissolved in phosphate buffered saline (PBS) from a height of 3 m onto a polished aluminium block held at -78°C. The resulting ice wafer (1cm wide and 20 µm thick) is transferred to a glass cover slip and further transferred to a Pelletier unit which maintains the temperature at -6.4°C. After 30 min annealing, three images were taken of the ice wafer with a digital camera (Nikon CoolPix 5000) fitted to a microscope. For each sample, three ice wafers were prepared from the same sample and three pictures were taken for each drop. Analysis of the size of twelve crystals contained in each ice wafer was performed using domain recognition software (DRS).[2] This program ensures that the ice crystals are chosen at random and calculates the area of the ice crystal using the following polygon equation (eq 1),

$$A = \frac{1}{2}\sum_{i=0}^{N-1}(x_i y_{i+1} - x_{i+1} y_i)$$

where N is the number of vertices, and Σ_{x0}, Σ_{y0} to Σ_{xN-1}, Σ_{yN-1} are the vertices circumventing the polygon in a clockwise direction. The mean grain (or ice crystal) size (MGS) of each sample was compared to the MGS of the control PBS solution for that same day of testing. All data were plotted and analyzed using Microsoft Excel. Error bars for IRI activity were calculated by dividing the standard error of the mean (SEM) for each sample by the average mean grain size (MGS) for the PBS negative control on the same day of testing. An analysis of variance (ANOVA) confirmed that the error between samples was considerably larger than the error within samples.

6.1.2 Cell Culture

Human embryonic liver cells (WRL-68)(ATCC, CL-48) were cultured in Eagle's minimum essential media (MEM) (Sigma, M4655) supplemented with 10% fetal bovine serum (FBS) (Fisher, 361015856, supplier number SH30397-3C) and 1% penicillin-streptomycin (Sigma, P4333) in 75 cm^2 flasks (Fisher, 10-126-37). Cells were incubated in a 37 °C incubator supplied with 5% CO_2. All cells were removed from the plates using a trypsin-EDTA solution (Sigma, T4174) for use in experiments. Passages 90 to 100 of WRL-68 cells were used in the cytoxicity and cryopreservation studies. No evidence of overgrowth or morphological changes indicating apoptosis was observed.[3]

6.1.3 Cytotoxicity Testing

The MTT assay was performed as previously described.[4] Cells were plated in 96-well plates and treated with 40 µL of Minimum Essential Medium (MEM) supplemented with 22, 200, or 500 mM of the analyte (carbohydrates shown in Figure 2.1) with or without 5% DMSO (Sigma,

D8418) and incubated at 37 °C for 18 h. Cells incubated with MEM without any carbohydrate were used as a negative control, and cells supplemented with 2.5% or 5% DMSO in the absence of carbohydrate were used as positive controls. Following addition of 4 µL MTT (Sigma, M5655) solution (5 mg/mL) in Hank's balanced salt solution (HBSS, Sigma, H8264), plates were then incubated at 37 °C with 5% CO_2 for 3 h. 100 µL of MTT solubilization solution [10% Triton X-100 (Aldrich, X100) plus 0.1 N HCl in isopropanol] was added to each well, and each well was aspirated 5 times. Plates were kept covered in the dark for 18 h and the absorbance of each well was then read at a wavelength of 570 nm with a multiwell plate reader (AD 340C Absorbance Detector, Beckman Coulter, Inc.). Viability was reported as a percentage of the control. All experiments were repeated at least two times in 16 consecutive wells for each condition.[3] Errors bars for cell viability was reported as the standard error of the mean (SEM) for each sample.

6.1.4 Cryopreservation and Thawing

Human embryonic liver cells were cultured and trypsinized as described above. Cells were diluted with MEM and counted using a hemacytometer (VWR, 15170-172). Aliquots containing $1x10^7$ cells were added to 15 mL centrifuge tubes and cells were pelleted by centrifugation for 10 min at 2000 rpm. The supernatant was removed and the cells were re-suspended in 1.5 mL custodial-HTK (Histidine-Tryptophan-Ketoglutarate) solution (Methapharm, Inc.) supplemented with carbohydrate (Figure 2.1) to a concentration of 22, 200 or 500 mM with or without 5% DMSO (Sigma, D8418). HTK supplemented with 2.5% or 5% DMSO served as the positive controls. Cell suspensions were transferred to 2 mL cryogenic vials (VWR, CA16001-102) and placed in a "Mr. Frosty" freezing container (Nalgene, 5100-0001, Sigma, C1562). The container was placed in an ultra-cold freezer (-80 °C) for 24 h. According to the manufacturer, "Mr. Frosty" provides a sample cooling rate of approximately 1 °C/min. Samples were then stored in the vapor phase of liquid nitrogen (-196 °C) for 7 days. Following storage, samples were rapidly thawed in a 37 °C water bath with gentle agitation. Thawed samples were transferred to 15 mL centrifuge tubes (Diamed, STK3217P) and slowly diluted to 3 mL by dropwise addition of Eagle's MEM (Sigma, M4655) cell culture medium. After 3 min samples were further diluted to 9 mL. Cells were pelleted by centrifugation for 10 min at 2000 rpm. The supernatant was decanted and the pellet re-suspended in 5 mL MEM. Centrifuge tubes were stored in a 37 °C water bath for approximately 30 min during transport to the flow cytometer.[3]

6.1.5 Cryopreservation Ability Testing

After cryopreservation and thawing as described above, the cell count was determined using a hemacytometer and an aliquot containing $1x10^6$ cells was transferred to a 15 mL centrifuge tube (Diamed, STK3217P) and diluted to 1 mL with MEM (Sigma, M4655) containing 10% FBS (Fisher, 361015856). Cells were pelleted by centrifugation for 10 min at 2000 rpm and 4 °C. The supernatant was removed and the pellet was resuspended in 1 mL Annexin-V binding buffer (BD Pharmigen, San Diego, Annexin V-PE Apoptosis Detection Kit I, 559763) and 100 µL of the sample was transferred to a flow cytometry tube. Subsequently, 5 µL 7-Aminoactinomycin D (7AAD) (BD Pharmingen, Annexin V-PE Apoptosis Detection Kit I) and 4 µL Annexin V-PE (PE) (BD Pharmingen, Annexin V-PE Apoptosis Detection Kit I) were added and samples were incubated for 20 min in the dark. Following incubation, samples were diluted to 500 µL with 1x

Annexin-V binding buffer. Flow cytometry analysis on 10,000 cells was carried out on a BD LSR flow cytometer using Cell quest software (Becton Dickinson). Annexin V-PE was measured with a 575 nm optical filter (FL-2) while 7AAD was measured with a 629 nm optical filter (FL-3). Complete viability was denoted as Annexin V and 7AAD negative cells. Compensation was set from single stain experiments with 7AAD and Annexin-V. Aliquots from non-cryopreserved samples labeled with equivalent fluorochromes were used to set the control gate excluding 99% 7AAD positive cells. Time between thawing and analysis by flow cytometry was 2 h. All samples were tested at least in duplicate.[3] Errors bars for cell viability was reported as the standard error of the mean (SEM) for each sample.

6.1.6 General Procedures for Chemical Synthesis of Galactopyranoside Derivatives

All anhydrous reactions were performed in flame-dried or oven-dried glassware under a positive pressure of dry argon or nitrogen. Air or moisture-sensitive reagents and anhydrous solvents were transferred with oven-dried syringes or cannulae. All flash chromatography was performed with E. Merck silica gel 60 (230-400 mesh). All solution phase reactions were monitored using analytical thin layer chromatography (TLC) with 0.2mm pre-coated silica gel aluminum plates 60 F254 (E. Merck). Components were visualized by illumination with a short-wavelength (254 nm) ultra-violet light and/or staining (ceric ammonium molybdate, potassium permanganate, phosphomolybdate, orcinol or ninhydrin stain solution). All solvents used for anhydrous reactions were distilled. Tetrahydrofuran (THF) and diethyl ether were distilled from sodium/benzophenone under nitrogen. Dichloromethane, acetonitrile, triethylamine, benzene and diisopropylethylamine (DIPEA) were distilled from calcium hydride under nitrogen. *N*,*N*-dimethylformamide (DMF) was stored over activated molecular sieves 4Å under argon.

^{1}H (300, 400 or 500 MHz) and ^{13}C NMR (75, 101 or 126 MHz) spectra were recorded at ambient temperature on a Bruker Avance (300, 400, 500), or Varian Inova 500 spectrometer, unless otherwise stated. Deuterated chloroform ($CDCl_3$), methanol (CD_3OD), or water (D_2O) were used as NMR solvents. Splitting patterns are designated as follows: s, singlet; d, doublet; t, triplet; q, quartet; m, multiplet and br, broad. Low resolution mass spectrometry was performed on a Micromass Quatro-LC Electrospray spectrometer with a pump rate of 20 μL/min using electrospray ionization (ESI) Analytical and preparatory scale RP-HPLC were carried out with C-18 columns on a Varian Dynomax HPLC system equipped with a Waters Delta 600E HPLC system equipped with a variable wavelength detector.

6.2 Synthesis of Galactopyranoside Derivatives

6.2.1 2,3,4,6-Tetra-*O*-acetyl-α-D-galactopyranosyl bromide (58)[5]

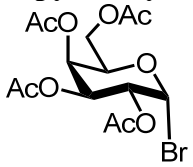

To commercially available D-galactose pentaacetate (2 g, 5.123 mmol), 13 mL of HBr in AcOH (33% solution) was added at room temperature. The reaction was stirred for 1 h and then diluted with CH_2Cl_2. The solution was transferred to a separatory funnel containing ice and the organic layer was washed with ice water until neutral pH. The organic extract was dried over $MgSO_4$,

filtered and co-evaporated with toluene to afford product (Rf = 0.46, 1.97 g, 94% yield). The crude product was crystallized from diethyl ether to form a white solid. ^{1}H NMR (400 MHz, $CDCl_3$) δ 6.70 (1H, d, J = 4.0 Hz), 5.52 (1H, dd, J = 3.3, 1.3 Hz), 5.40 (1H, dd, J = 10.6, 3.3 Hz), 5.05 (1H,dd, J = 10.7, 4.0 Hz), 4.46-4.42 (1H, m), 4.17-4.04 (2H, m), 2.15 (3H, s), 2.11 (3H, s), 2.07 (3H, s), 2.02 (3H, s)

All characterization was in accordance with the literature.[5]

6.2.2 2,3,4,6-Tetra-*O*-acetyl-1-deoxy-D-galactopyranoside (59)[6]

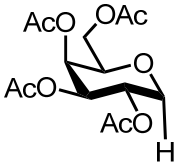

To a solution of compound **58** (0.3086 g, 0.75 mmol) in THF: EtOAc (10mL:1mL), was added 10% w/w Pd/C and triethylamine (0.136 mL, 0.97 mmol) at room temperature. The reaction was purged several times with H_2 under closed atmosphere and left under H_2 atmosphere for 24 h. The solution was transferred onto celite and rinsed several times with EtOAc then dried over $MgSO_4$, filtered and concentrated to afford a yellow oil which was purified by flash chromatography (2:1 hexanes: EtOAc) to afford the product as a clear oil (Rf = 0. 40, 0.19 g, 79 % yield). ^{1}H NMR (400 MHz, $CDCl_3$) δ 5.42 (1H, dd, *J* = 3.4, 1.0 Hz), 5.20 (1H, ddd, *J* = 10.3, 10.3, 5.6 Hz), 5.02 (1H, dd, *J* = 10.2, 3.4 Hz), 4.17 (1H, dd, *J* = 11.2, 5.5 Hz), 4.07 (2H, d, *J* = 6.4 Hz), 3.80 (1H, ddd, *J* = 6.5, 6.5, 1.1 Hz), 3.27 (1H, dd, *J* = 10.5, 11.1 Hz), 2.13 (3H, s), 2.04 (3H, s), 1.99 (3H, s), 2.03 (3H, s); ^{13}C NMR (101 MHz, $CDCl_3$) δ 170.5, 170.2, 170.2, 170.0, 74.9, 71.5, 67.8, 67.1, 66.4, 62.0, 20.8, 20.7, 20.7, 20.6; MS (ESI, CH_3CN): Calcd for $C_{14}H_{20}O_9$ $[(M+Na)^+]$: 355.1. Found 355.1

6.2.3 1-Deoxy-D-galactopyranoside (26)[7]

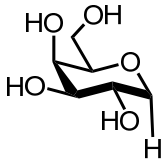

To compound 59 (0.19 g, 0.57 mmol) was added NaOMe/MeOH (1M) and the solution was sonicated for 1 h. Amberlite IR resin (H+ form, pH = 4) was washed several times with HPLC grade MeOH and added to the reaction mixture which was stirred until the pH was between 5 and 6. The solution was filtered and concentrated. Following recrystallization using EtOH and Et_2O and freeze-drying, a white product was obtained (0.08 g, 83 %).^{1}H NMR (400 MHz, H_2O) δ 3.99 (1H, dd, *J* = 11.1, 5.6 Hz), 3.94 (1H, d, *J* = 2.9 Hz), 3.82 (1H, ddd, *J* = 10.3, 10.2, 5.6 Hz), 3.70 (2H, dd, *J* = 6.1, 3.4 Hz), 3.56 (2H, dd, *J* = 9.8, 3.4 Hz), 3.19 (1H, dd, *J* = 10.8, 10.8 Hz); ^{13}C NMR (101 MHz, H_2O) δ 79.4, 74.0, 69.1, 69.1, 66.6, 61.4; MS (ESI, H_2O): Calcd for $C_6H_{12}O_5$ $[(M+K)^+]$: 203.1, $[(2M+H)^+]$: 329.1. Found 203.1, 329.2

6.2.4 1-Thiophenyl- β-D-galactopyranoside (61)[10]

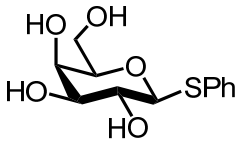

To a stirred solution of 1,2,3,4,6-penta-O-acetyl-β-D-galactopyranose (11.37 g, 29.13 mmol) in 20mL of anhydrous dichloromethane with activated 4Å molecular sieves, benzenethiol (3.87 mL, 37.86 mmol) was added and the solution was cooled to 0°C. Boron trifluoride diethyl etherate (10.97 mL, 87.38 mmol) was added dropwise and the solution was stirred at room temperature for 24 h. The solution was diluted and filtered through celite, extracted three times with dichloromethane, washed twice with brine, dried over $MgSO_4$, filtered and concentrated. The resulting oil was purified by gradient flash chromatography (4:1 hexanes: EtOAc → 1:1 hexanes: EtOAc), dissolved in a solution of NaOMe/MeOH (1M), sonicated for one hour, and stirred in pre-rinsed Amberlite IR resin (H+ form, pH = 4) until pH 5 or 6. The product was recrystallized from hexanes and ether, concentrated to yield white crystals (5.13 g, 82 %).[1]H NMR (400 MHz, MeOD): δ 7.55- 7.53 (2H, m), 7.31- 7.20 (3H, m), 4.58 (1H, d, *J* = 9.7 Hz,), 3.89 (1H, dd, *J* = 3.2, 0.7 Hz), 3.78- 3.68 (2H, m), 3.62- 3.54 (2H, m), 3.49 (1H, dd, *J* = 9.2, 3.3 Hz)

All characterization was in accordance with the literature.[10]

6.2.5 3,4-*O*-Isopropyl-1-thiophenyl-β-D-galactopyranoside (62)[11]

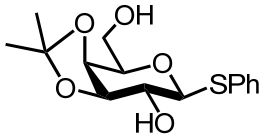

To a solution of compound **61** (2.00 g, 7.36 mmol) in 2,2-dimethoxypropane (9.05 mL, 73.59 mmol) at room temperature was added anhydrous CH_3CN (10 mL) and catalytic amount of p-toluenesulfonic acid monohydrate (0.01 g, 0.05mmol). The reaction mixture was stirred for 15 min and then placed under 300 mbar vacuum for 1 h. Excess triethylamine (3 mL, 21.52 mmol) was added to the mixture which was concentrated and purified by flash chromatography (1:1:0.1 hexanes: EtOAc: triethylamine). The corresponding fractions were collected and concentrated to afford clear oil (Rf = 0.38, 1.23 g, 54 %). ^{1}H NMR (400 MHz, $CDCl_3$) δ 7.54-7.51 (2H, m), 7.33-7.28 (3H, m), 4.47 (1H, d, *J* = 10.2 Hz), 4.18 (1H, dd, *J* = 5.5, 2.2 Hz), 3.81 (1H, dd, *J* = 11.6, 3.9 Hz), 3.56 (1H, dd, *J* = 10.2, 6.9 Hz), 4.11 (1H, dd, *J* = 6.8, 5.6 Hz), 3.98 (1H, dd, *J* = 11.6, 7.2 Hz), 3.87 (1H, ddd, *J* = 7.2, 3.9, 2.2 Hz), 4.47 (1H, d, *J* = 2.2 Hz) 1.41 (3H, s), 1.33 (3H, s)

All characterization was in accordance with the literature.[11]

6.2.6 2,6-Di-*O*-benzyl-3,4-*O*-isopropyl-1-thiophenyl-β-D-galactopyranoside (63)[11]

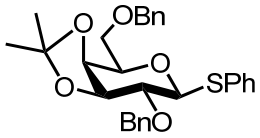

To a solution of sodium hydride (0.52 g, in 60 % oil dispersion, 13.15 mmol) and tetrabutylammonium iodide (0.08 g, 0.22 mmol) in DMF at 0°C was added a solution of compound **62** (0.68 g, 2.19 mmol) in DMF dropwise and the mixture was stirred for 15 min. Benzyl bromide (1.55 mL, 13.15 mmol) was introduced and the solution was stirred for 24 h at room temperature. The reaction mixture was quenched with methanol, diluted with EtOAc, extracted with CH_2Cl_2, washed with water and then dried over $MgSO_4$, filtered and concentrated. The crude oil was purified by flash chromatography (5:1 hexanes: EtOAc) and the corresponding fractions were collected and concentrated to afford clear oil (Rf = 0.45, 0.73 g, 68 %). ^{1}H NMR (400 MHz, $CDCl_3$) δ 7.58–7.55 (2H, m), 7.45–7.22 (13H, m), 4.82 (1H, d, *J* = 11.3 Hz), 4.70-4.68 (1H, m), 4.67 (1H, d, *J*= 10.0 Hz, H-1), 4.60 (1H, d, *J* = 11.9 Hz), 4.53 (1H, d, *J* = 11.8 Hz), 4.27 (1H, dd, *J* = 5.9, 5.9 Hz), 4.22 (1H, dd, *J* = 5.7, 2.0 Hz), 3.95 (1H, ddd, *J* = 6.2, 6.0, 2.0 Hz), 3.84–3.77 (2H, m), 3.53 (1H, dd, *J* = 9.5, 6.1 Hz), 1.42 (3H, s), 1.37 (3H, s)

All characterization was in accordance with the literature.[11]

6.2.7 2,6-Di-*O*-benzyl-1-thiophenyl-β-D-galactopyranoside (64)[11]

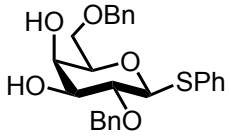

To compound **63** (0.45 g, 0.91 mmol) was added a freshly prepared aqueous solution of trifluoroacetic acid (5 mL, 8:2 TFA: H_2O). The reaction mixture was monitored and upon disappearance of the starting material, triethylamine was added until the pH was neutral. The reaction mixture was extracted several times with CH_2Cl_2, dried over $MgSO_4$, filtered, concentrated and purified by flash chromatography (3:2 EtOAc: hexanes) affording a white solid (Rf = 0.6, 0.17 g, 41 %). ^{1}H NMR (300 MHz, CDCl3) δ 7.60–7.57 (2H, m), 7.39–7.25 (13H, m), 4.95 (1H, d, *J* = 11.0 Hz), 4.69 (1H, d, *J* = 11.0 Hz), 4.57-454 (2H, m), 4.64 (1H, d, *J* = 9.2 Hz), 4.06 (1H, dd, *J* = 3.1, 3.1 Hz), 3.83-3.75 (2H, m), 3.67–3.58 (3H, m), 2.68 (1H, d, *J* = 3.4 Hz, OH3), 2.42 (1H, d, *J* = 5.3 Hz, OH4)

All characterization was in accordance with the literature.[11]

6.2.8 4-*O*-Acetyl-2,6-di-*O*-benzyl-1-thiophenyl-β-D-galactopyranoside (65)[11]

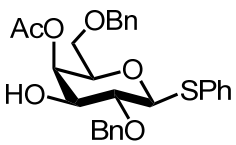

To a solution of compound **64** (0.17 g, 0.38 mmol) in anhydrous benzene (20 mL), was added triethylorthoacetate (1.38 mL, 7.54 mmol) and p-toluenesulfonic acid monohydrate (0.01 g, 0.05 mmol) and the reaction was stirred and monitored until the disappearance of starting material. The reaction was neutralized with addition of triethylamine (0.21 mL, 1.51 mmol) and concentrated down under reduced pressure. To the residue was added 60 % acidic acid in water which was stirred for 20 min, until disappearance of the intermediate. The reaction was then diluted with EtOAc, washed twice with saturated $NaHCO_3$, twice with water and once with brine. The organic layer was dried over $MgSO_4$, filtered, concentrated and purified by flash chromatography (9:1 hexanes: EtOAc) to afford a white crystalline product (Rf = 0.36, 0.17 g, 94 %). ^{1}H NMR (400 MHz, CDCl3) δ 7.60–7.57 (2H, m), 7.40–7.25 (13H, m), 5.41 (1H, dd, *J* = 3.4, 0.6 Hz), 4.95 (1H, d, *J* = 10.8 Hz), 4.70 (1H, d, *J* = 6.2 Hz, H-1), 4.67 (1H, d, *J* = 7.1 Hz), 4.56 (1H, d, *J* = 11.4 Hz), 4.45 (1H, d, *J* = 11.4 Hz), 3.86 (1H, ddd, *J* = 9.0, 3.3, 3.3 Hz), 3.80 (1H, dd, *J* = 6.2, 6.2 Hz), 3.63–3.50 (3H, m), 2.08 (3H, s)

All characterization was in accordance with the literature.[11]

6.2.9 3-Deoxy-4-*O*-acetyl-2,6-di-*O*-benzyl-1-thiophenyl-β-D-galactopyranoside (67)[11]

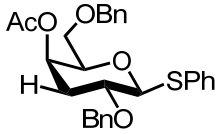

To a solution of compound **65** (0.08 g, 0.16 mmol) in anhydrous CH_2Cl_2 (5 mL), was added phenylchlorothionoformate (0.07 mL, 0.48 mmol) at 0°C. Slow addition of DMAP (0.19g, 1.59 mmol) in small portions was followed by warming and stirring for 24 h at room temperature. The reaction mixture was diluted with CH_2Cl_2, washed with saturated $NaHCO_3$, once with brine and phosphate buffer solution (pH= 7.4), then was dried over $MgSO_4$, filtered and concentrated. The residue was placed under vacuum for 24 h and flushed with argon before anhydrous toluene (5 mL) and tributyltin hydride (0.42 mL, 1.59 mmol) were added and the reaction was heated with stirring to 80°C at which point AIBN (0.01 g, 0.06 mmol) was added and the reaction was refluxed for another 2 h. The reaction was cooled, concentrated and purified by flash chromatography (6:1 hexanes: EtOAc) to afford a white solid (Rf = 0.57, 0.03 g, 43 %). 1H NMR (400 MHz, CDCl3) δ 7.60–7.57 (2H, m), 7.35–7.24 (13H, m), 5.13 (1H, dd, *J* = 3.2, 3.2 Hz), 4.76 (1H, d, *J* = 9.6 Hz,, H-1), 4.68 (1H, d, *J* = 11.3 Hz), 4.57 (1H, d, *J* = 11.3 Hz), 4.54 (1H, d, *J* = 11.8 Hz), 4.41 (1H, d, *J* = 11.8 Hz), 3.80 (1H, ddd, *J* = 6.4, 6.4, 1.4 Hz), 3.65–3.52 (3H, m), 2.45 (1H, ddd, *J* = 14.2, 4.8, 3.4 Hz, H3'), 1.98 (3H, s), 1.72 (1H, ddd, *J* = 14.2, 11.2, 3.0 Hz, H3")

All characterization was in accordance with the literature.[11]

6.2.10 2,6-*O*-Acetyl-3,4-*O*-isopropyl -1-thiophenyl-β-D-galactopyranoside (69)[11,12]

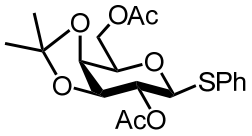

A mixture of compound **62** (0.73 g, 2.33 mmol), acetic anhydride (1.54 mL, 16.4 mmol) and pyridine (1.32 mL, 16.4mmol) was stirred at 0°C under inert argon for 30 min followed by addition of DMAP (0.03 g, 0.23 mmol). The reaction mixture was warmed to room temperature and sonicated for 1 h then washed several times with $CuSO_4$, washed twice with water and once with brine, dried over $MgSO_4$, filtered, concentrated and purified by flash chromatography (4:1 petroleum ether: EtOAc) to afford a colorless oil (Rf = 0.67, 0.58, 63 %). ^{1}H NMR (300 MHz, $CDCl_3$) δ 7.52- 7.49 (2H, m), 7.31- 7.26 (3H, m), 5.08- 5.02 (1H, m), 4.61 (1H, d, *J* = 10.0 Hz), 4.40- 4.32 (2H, m), 4.22- 4.19 (2H, m), 3.99 (1H, ddd, *J* = 6.8, 5.2, 1.5 Hz), 2.13, (3H, s), 2.08 (3H, s), 1.52 (3H, s), 1.33 (3H, s); ^{13}C NMR (101 MHz, $CDCl_3$) δ 170.8, 169.6, 133.5, 132.0, 128.8, 127.8, 111.0, 85.7, 74.2, 73.5, 71.3, 63.6, 27.6, 26.3, 21.0, 20.8; MS (ESI, CH_3CN): Calcd for $C_{19}H_{24}SO_7$ [$(M+Na)^+$]: 419.1. Found 419.2

6.2.11 2,6-*O*-Acetyl -1-thiophenyl-β-D-galactopyranoside (70)[11,12]

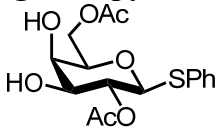

To compound **69** (0.58 g, 1.47 mmol) was added a freshly prepared aqueous solution of trifluoroacetic acid (5 mL, 8:2 TFA: H_2O). The reaction mixture was monitored and upon disappearance of the starting material, triethylamine was added until the pH was neutral. The reaction mixture was extracted several times with CH_2Cl_2, dried over $MgSO_4$, filtered, concentrated and purified by flash chromatography (2:1 EtOAc: hexanes) affording a white solid (Rf = 0.37, 0.43 g, 82 %). ^{1}H NMR (300 MHz, $CDCl_3$) δ 7.50- 7.46 (2H, m), 7.30- 7.26 (3H, s), 4.97 (1H, dd, *J* = 9.3, 9.3 Hz), 4.61 (1H, d, *J* = 10.0 Hz), 4.39 (1H, dd, *J* = 11.6, 6.0 Hz), 4.28 (1H, dd, *J* = 11.6, 6.8 Hz), 3.91 (1H, d, *J* = 2.8 Hz), 3.72- 3.65 (2H, m), 2.15 (3H, s), 2.07 (3H, s); ^{13}C NMR (101 MHz, $CDCl_3$) δ 171.2, 171.1, 132.5, 132.4, 128.9, 128.0, 85.9, 75.7, 73.4, 71.2, 68.7, 62.6, 21.0, 20.8; MS (ESI, CH_3CN): Calcd for $C_{16}H_{20}SO_7$ [$(M+NH_4)^+$]: 374.1, [$(M+Na)^+$]: 379.0, [$(M+K)^+$]: 395.0. Found 374.1, 379.0, 395.0

6.2.12 2,4,6-*O*-Acetyl -1-thiophenyl-β-D-galactopyranoside (71)[11]

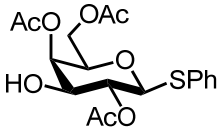

To a solution of compound **70** (0.43 g, 1.21 mmol) in anhydrous CH_3CN (20 mL), was added triethylorthoacetate (4.42 mL, 24.13 mmol) and p-toluenesulfonic acid monohydrate (0.01 g, 0.05 mmol) and the reaction was stirred and monitored until the disappearance of starting material. The reaction was neutralized with addition of triethylamine (0.67 mL, 4.83 mmol) and concentrated down under reduced pressure. To the residue was added 60 % acidic acid in water which was stirred for 20 min, until disappearance of the intermediate. The reaction was then

diluted with EtOAc, washed twice with saturated $NaHCO_3$, twice with water and once with brine. The organic layer was dried over $MgSO_4$, filtered, concentrated and purified by flash chromatography (1:1 hexanes: EtOAc) to afford a white crystalline product (Rf = 0.78, 0.40 g, 83 %). ^{1}H NMR (400 MHz, $CDCl_3$) δ 7.50- 7.48 (3H, m), 7.30- 7.27 (3H, m), 5.33 (1H, dd, *J* = 3.6, 0.9 Hz), 4.99 (1H, t, *J* = 9.8, 9.8 Hz), 4.66 (1H, d, *J* = 10.0 Hz), 4.18- 4.09 (2H, m), 3.87- 3.83 (2H, m), 2.34 (1H, d, *J* = 6.4 Hz, OH3), 2.15 (3H, s), 2.13 (3H, s), 2.03 (3H, s); ^{13}C NMR (101 MHz, $CDCl_3$) δ 171.0, 170.9, 170.5, 132.6, 132.5, 128.9, 128.1, 86.1, 74.8, 72.5, 70.8, 69.9, 62.2, 29.7, 21.0, 20.8, 20.7; MS (ESI, CH_3CN): Calcd for $C_{18}H_{22}SO_8$ $[(M+NH_4)^+]$: 416.1, $[(M+Na)^+]$: 421.1. Found 416.2, 421.1; IR (film): 1174.57, 1224.71, 1369.37, 1743.53

6.2.13 3-Deoxy-2,4,6-*O*-acetyl -1-thiophenyl-β-D-galactopyranoside (72)[11]

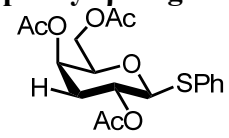

To a solution of compound **71** (0.13 g, 0.32 mmol) in anhydrous CH_2Cl_2 (5 mL), was added phenylchlorothionoformate (0.132 mL, 0.95 mmol) at 0°C. Slow addition of DMAP (0.388g, 3.18 mmol) in small portions was followed by warming and stirring for 24 h at room temperature. The reaction mixture was diluted with CH_2Cl_2, washed with saturated $NaHCO_3$, once with brine and phosphate buffer solution (pH= 7.4), then was dried over $MgSO_4$, filtered and concentrated. The residue was placed under vacuum for 24 h and flushed with argon before anhydrous toluene (5 mL) and tributyltin hydride (0.843 mL, 3.18 mmol) were added and the reaction was heated with stirring to 80°C at which point AIBN (0.01 g, 0.06 mmol) was added and the reaction was refluxed for another 2 h. The reaction was cooled, concentrated and purified by flash chromatography (5:1 petroleum ether: EtOAc) to afford a white solid (Rf = 0.60, 0.11 g, 92 %). ^{1}H NMR (400 MHz, $CDCl_3$) δ 7.53- 7.50 (2H, m), 7.32- 7.27 (3H, m), 5.12- 5.10 (1H, m), 5.06- 4.99 (1H, m), 4.74 (1H, d, *J* = 10.0 Hz), 4.19- 4.11 (1H, m), 3.88 (1H, ddd, *J* = 7.1, 5.75, 1.37 Hz), 2.43 (1H, ddd, *J* = 14.1, 5.1, 3.2 Hz), 2.10 (3H, s), 2.09 (3H, s), 2.04 (3H, s), 1.78 (1H, ddd, *J* = 14.2, 11.3, 3.1 Hz); ^{13}C NMR (101 MHz, $CDCl_3$) δ 170.6, 170.3, 169.6, 133.2, 132.1, 128.8, 127.8, 88.0, 76.5, 67.1, 65.7, 62.6, 34.4, 21.1, 21.0, 20.8; MS (ESI, CH_3CN): Calcd for $C_{18}H_{22}SO_7$ $[(M+NH_4)^+]$: 400.1, $[(M+Na)^+]$: 405.1, $[(M+K)^+]$: 421.1. Found 400.2, 405.1, 421.1; IR (film): 1220.86, 1371.29, 1735.81

6.2.14 3-Deoxy-1-thiophenyl-β-D-galactopyranoside (68)[7]

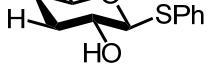

A solution of NaOMe/MeOH (1M) was added to compound **72** (0.08 g, 0.21 mmol) was sonicated for one hour, and stirred in HPLC grade MeOH pre-rinsed Amberlite IR resin (H^+ form, pH = 4) until pH 5 or 6. The product was subjected to reverse phase HPLC (isocratic run, 9:1, ddH_2O: CH_3CN), concentrated and freeze-dried to yield the desired product as a white powder (0.026 g, 49 %). ^{1}H NMR (400 MHz, MeOD) δ 7.56- 7.53 (2H, m), 7.30- 7.20 (3H, m), 4.60 (1H, d, *J* = 9.70 Hz), 3.95 (1H, br s), 3.82 (1H, ddd, *J* = 11.1, 9.9, 5.00 Hz), 3.74- 3.65 (2H, m), 3.55 (1H, ddd, *J* = 6.6, 5.1, 1.2 Hz), 2.28 (1H, ddd, *J* = 13.5, 4.9, 3.2 Hz), 1.71- 1.64 (1H,

m); ^{13}C NMR (101 MHz, MeOD) δ 134.9, 130.6, 128.5, 126.5, 91.5, 80.9, 65.8, 64.1, 61.6, 40.0; MS (ESI, H_2O): Calcd for $C_{12}H_{16}SO_4$ [$(M+NH_4)^+$]: 274.1, [$(M+Na)^+$]: 279.1, [$(M+K)^+$]: 295.0. Found 274.4, 279.0, 295.0

6.2.15 1,2,3,6-Tetra-*O*-pivaloyl-β-D-galactopyranoside (75)[8]

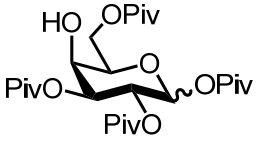

To a solution of pyridine (22.50 mL, 278.19 mmol) and trimethylacetylchloride (22.50 mL, 182.68 mmol) in CH_2Cl_2 at 0°C was added D-galactose (5.33 g, 29.61 mmol) in five portions and the reaction was stirred for 12 h. The reaction mixture was diluted in EtOAc, washed several times with a saturated $CuSO_4$ solution until the organic layer was a pale green, then washed twice with water and once with brine. The organic layer was dried over $MgSO_4$, filtered and evaporated and the crude product was separated and purified by flash chromatography (9:1 hexanes: EtOAc) affording the major product as a white powder (Rf = 0.77, 6.25 g, 41 %, 9:1,β: α). ^{1}H NMR (400 MHz, $CDCl_3$) δ 5.66 (1H, d, *J* = 8.4 Hz), 5.46 (1H, dd, *J* = 10.2, 8.4 Hz), 5.01 (1H, dd, *J* = 10.2, 3.3 Hz), 4.34 (1H, dd, *J* = 11.5, 6.3 Hz), 4.28 (1H, dd, *J* = 11.4, 6.6 Hz), 4.03 (1H, d, *J* = 2.8 Hz), 3.89 (1H, dd, *J* = 6.4, 0.9 Hz), 1.20 (1H, s), 1.19 (9H, s), 1.18 (9H, s), 1.13 (9H, s); ^{13}C NMR (101 MHz, $CDCl_3$) δ 178.4, 177.4, 176.6, 176.5, 92.3, 73.0, 67.6, 66.9, 61.7, 38.9, 38.8, 38.8, 27.1, 27.1, 26.9; MS (ESI, CH_3CN): Calcd for $C_{26}H_{44}O_{10}$ [$(M+NH_4)^+$]: 534.3, [$(M+K)^+$]: 555.3. Found 534.3, 555.2; IR (film): 1141.78, 1278.72, 1735.81

6.2.16 1,2,3,6-Tetra-*O*-pivaloyl-4-iodo-β-D-galactopyranoside (76)[9]

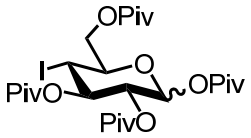

To a solution of compound **75** (1.33 g, 2.60 mmol) in toluene at 0°C was slowly added imidazole (0.877 g, 9.70 mmol) and triphenylphosphine (2.03 g, 7.7 mmol). Iodine (1.963 g, 7.70 mmol) was added in portions over 15 min and the reaction mixture was warmed to room temperature, heated to 90°C and stirred for 19 h. The reaction mixture was cooled, diluted in toluene, washed several times with a saturated $Na_2S_2O_3$ solution until the organic layer was colorless, then washed twice with water and once with brine. The organic layer was dried over $MgSO_4$, filtered and evaporated and the crude product was purified by flash chromatography (8:2 hexanes: EtOAc) affording a white powder (0.80, 1.42 g, 88 %, 9.1:0.9, β: α). ^{1}H NMR (400 MHz, $CDCl_3$) δ 5.69 (1H, d, *J* = 8.40 Hz), 5.41 (1H, dd, *J* = 10.4, 9.5 Hz), 5.06 (1H, dd, *J* = 9.2, 8.5 Hz), 4.55 (1H, dd, *J* = 12.2, 1.9 Hz), 4.40 (1H, dd, *J* = 12.2, 5.0 Hz), 4.02 (1H, ddd, *J* = 10.8, 5.1, 2.0 Hz), 3.94 (1H, dd, *J* = 10.7, 10.7 Hz), 1.20 (9H, s), 1.20 (9H, s), 1.14 (9H, s), 1.10 (9H, s); ^{13}C NMR (126 MHz, $CDCl_3$) δ 176.4, 176.3, 176.1, 91.9, 77.2, 75.4, 74.7, 70.7, 64.5, 38.9, 38.9, 38.7, 38.7, 27.3, 27.1, 27.1, 26.8; MS (ESI, CH_3CN): Calcd for $C_{26}H_{43}IO_9$ [$(M+Na)^+$]: 649.2. Found 649.1; IR (film): 1139.85, 1278.72, 1481.23, 1720.39, 1737.74

6.2.17 1,2,3,6-Tetra-*O*-pivaloyl-4-deoxy-β-D-galactopyranoside (77)[6]

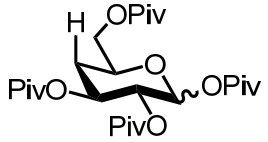

To a solution of compound **76** (0.42 g, 0.67 mmol) in MeOH: EtOAc (5:1) at room temperature was added 10% w/w Pd/C and triethylamine (85.5 μL, 0.61 mmol). The reaction mixture was purged several times with H_2 under closed atmosphere and left under H_2 atmosphere for 48 h. The solution was transferred onto celite and rinsed several times with EtOAc then dried over $MgSO_4$, filtered and concentrated to afford a yellowish white solid which was purified by flash chromatography (9:1 petroleum ether: EtOAc) to afford the product as a white solid (Rf = 0.60, 0.25 g, 75 % yield, 9.7:0.3, β: α). ^{1}H NMR (400 MHz, $CDCl_3$) δ 5.63 (1H, d, *J* = 7.99 Hz), 5.12-5.02 (2H, m), 4.18 (1H, dd, *J* = 11.6, 6.3 Hz), 4.08 (1H, dd, *J* = 11.6, 4.4 Hz), 3.93- 3.86 (1H, m), 2.14 (1H, ddd, *J* = 12.6, 5.0, 2.0 Hz), 1.60- 1.51 (1H, m), 1.19 (9H, s), 1.17 (9H, s), 1.15 (9H, s), 1.13 (9H, s); ^{13}C NMR (101 MHz, $CDCl_3$) δ 178.1, 177.6, 176.6, 176.5, 92.2, 70.6, 70.4, 70.3, 64.8, 38.8, 38.8, 38.7, 32.4, 27.1, 27.1, 27.0, 26.9; MS (ESI, CH_3CN): Calcd for $C_{26}H_{44}O_9$ [$(M+NH_4)^+$]: 518.3, [$(M+Na)^+$]: 523.3, [$(M+K)^+$]: 539.3. Found 518.3, 523.2, 539.2; IR (film): 1145.64, 1737.74

6.2.18 4-Deoxy-D-galactopyranoside (28)[7]

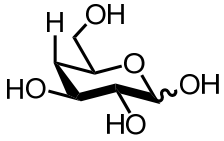

To compound **77** (0.25 g, 0.45 mmol) was added NaOMe/MeOH (1M) and the solution was sonicated for 3 h and left to stir for 72 h at room temperature. Amberlite IR resin (H+ form, pH = 4) was washed several times with HPLC grade MeOH and added to the reaction mixture which was stirred until the pH was between 5 and 6. The solution was filtered and concentrated. Following recrystallization using EtOH and Et_2O and freeze-drying, a white product was obtained (0.08 g, 97 %, 2:1, β: α). ^{1}H NMR (500 MHz, H_2O) δ 4.43 (1H, d, *J* = 7.9 Hz, α), 5.12

(1H, d, *J* = 3.7 Hz, β), 3.96 – 3.92 (1H, m), 3.81 (1H, ddd, *J* = 11.5, 9.8, 5.2 Hz), 3.66-3.39 (4H, m), 3.31 (1H, dd, *J* = 9.7, 3.8 Hz), 3.13-2.96 (1H, m), 1.90-1.77 (2H, m), 1.34-1.24 (2H, m); ^{13}C NMR (126 MHz, H_2O) δ 96,1 (C1β), 92.7 (C1α), 76.0, 73.2, 72.5, 70.4, 68.4, 66.9, 63.7, 63.6, 34.2; MS (ESI, H_2O): Calcd for $C_6H_{12}O_5$ [(2M+)]: 328.2, [(2M+Na)$^+$]: 351.1. Found 328.2., 351.2

6.2.19 2-Deoxy-3,4,6-*O*-Tri-acetyl-1-*C*-allyl-α-D-galactopyranoside (79)[13]

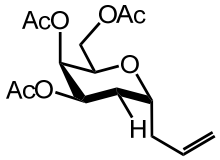

To a solution of commercially available 2-deoxy-D-galactose (0.22 g, 1.36 mmol) was added acetic anhydride (0.9 mL, 9.56 mmol) and pyridine (0.77 mL, 9.56 mmol) at 0°C under inert argon and was stirred for 30 min followed by addition of DMAP (0.02 g, 0.14 mmol). The reaction mixture was warmed to room temperature and sonicated for 1 h then washed several times with $CuSO_4$, washed twice with water and once with brine, dried over $MgSO_4$, filtered and concentrated. The residue was dissolved in anhydrous CH_3CN, cooled to 0°C and allyltrimethylsilane (0.56 mL, 3.49 mmol) and boron trifluoride diethyl etherate (0.83 mL, 1.13 mmol) were added dropwise to the reaction mixture which was stirred for 24 h. The solvent was evaporated and the residue was dissolved in CH_2Cl_2, washed once with water, saturated $NaHCO_3$, dried over $MgSO_4$, filtered, concentrated and purified by flash chromatography (3:2 hexanes: EtOAc) to afford a colorless oil (Rf = 0.67, 0.29 g, 79 %). ^{1}H NMR (400 MHz, $CDCl_3$) δ 5.80- 5.70 (1H, m), 5.23- 5.19 (2H, m), 5.12- 5.06 (2H, m), 4.31 (1H, dd, *J* = 11.2, 7.5 Hz), 4.15- 4.03 (3H, m), 2.50- 2.42 (1H, m), 2.30- 2.20 (1H, m), 2.08 (3H, s), 2.04 (3H, s), 2.02 (3H, s), 1.69- 1.63 (1H, m); ^{13}C NMR (101 MHz, $CDCl_3$) δ 171.3, 170.7, 170.1, 133.9, 117.6, 69.6, 69.4, 67.2, 66.7, 61.8, 36.6, 30.0, 21.0, 20.8, 20.8; MS (ESI, CH_3CN): Calcd for $C_{15}H_{22}O_7$ [(M+NH_4)$^+$]: 332.2, [(M+Na)$^+$]: 337.1, [(M+K)$^+$]: 353.1. Found 322.1, 337.1, 353.1

6.2.20 2-Deoxy-1-*C*-allyl-α-D-galactopyranoside (30)[7]

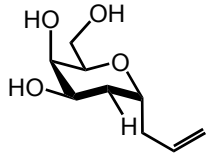

To compound **79** (0.29 g, 0.92 mmol) was added NaOMe/MeOH (1M) and the solution was sonicated for 1 h at room temperature. Amberlite IR resin (H+ form, pH = 4) was washed several times with HPLC grade MeOH and added to the reaction mixture which was stirred until the pH was between 5 and 6. The solution was filtered and concentrated. Following recrystallization using EtOH and Et_2O and freeze-drying, a white product was obtained (0.12 g, 70 %). ^{1}H NMR (500 MHz, H_2O suppression) δ 5.87- 5.77 (1H, m), 5.15 (1H, ddd, *J* = 17.1, 3.4, 1.4 Hz), 5.10 (1H, d, *J* = 10.2 Hz), 4.14-4.08 (1H, m), 4.03 (1H, ddd, *J* = 11.6, 4.6, 3.0 Hz), 3.81- 3.64 (4H, m), 2.6- 2.5 (1H, m), 2.32- 2.24 (1H, m), 1.93 (1H, ddd, *J* = 13.1, 11.6, 5.9 Hz), 1.69 (1H, dd, *J* = 13.4, 4.7 Hz); ^{13}C NMR (126 MHz, H_2O) δ 135.0, 117.1, 72.0, 71.8, 67.7, 65.2, 61.2, 34.7, 29.8; MS (ESI, H_2O): Calcd for $C_9H_{16}O_4$ [(M+Na)$^+$]: 211.1. Found 211.1

6.2.21 4-Deoxy-2,3,4-*O*-Tri-pivaloyl-1-*C*-allyl-α-D-galactopyranoside (80)[13]

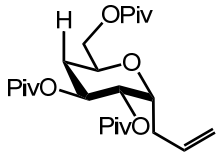

To a solution of compound **77** (0.41 g, 0.82 mmol) in anhydrous CH_3CN, at 0°C was added allyltrimethylsilane (0.39 mL, 2.45 mmol) and boron trifluoride diethyl etherate (0.58 mL, 4,67 mmol) dropwise and the reaction mixture was stirred for 24 h. The solvent was evaporated and the residue was dissolved in CH_2Cl_2, washed once with water, saturated $NaHCO_3$, dried over $MgSO_4$, filtered, concentrated and purified by flash chromatography (9:1 hexanes: EtOAc) to afford colorless oil (Rf = 0.65, 0.29 g, 80 %). ^{1}H NMR (400 MHz, $CDCl_3$) δ 5.80- 5.70 (1H, m), 5.12- 5.08 (3H, m), 4.94 (1H, dd, *J* = 8.2, 4.8 Hz), 4.27 (1H, dd, *J* = 11.5, 7.5 Hz), 4.18 (1H, ddd, *J* = 10.7, 4.45, 4.45 Hz), 4.03- 3.98 (1H, m), 3.94 (1H, dd, *J* = 11.47, 3.60 Hz) 2.49- 2.41 (1H, m), 2.21- 2.09 (2H, m), 1.50- 1.42 (1H, m), 1.14 (9H, s), 1.13 (9H, s), 1.12 (9H, s); ^{13}C NMR (126 MHz, CDCl3) δ 178.3, 177.5, 177.2, 133.7, 117.4, 71.2, 70.1, 67.3, 66.9, 65.1, 38.8, 38.7, 38.7, 31.5, 30.8, 29.7, 27.2, 27.1, 27.1; MS (ESI, CH_3CN): Calcd for $C_{24}H_{40}O_7$ $[(M+NH_4)^+]$: 458.3, $[(M+Na)^+]$: 463.3, $[(M+K)^+]$: 479.2. Found 458.3, 463.2, 479.2

6.2.22 4-Deoxy-1-*C*-allyl-α-D-galactopyranoside (32)[7]

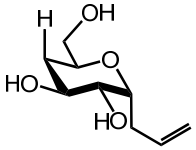

To compound **80** (0.35 g, 0.79 mmol) was added NaOMe/MeOH (1M) and the solution was sonicated for 1 h at room temperature. Amberlite IR resin (H+ form, pH = 4) was washed several times with HPLC grade MeOH and added to the reaction mixture which was stirred until the pH was between 5 and 6. The solution was filtered and concentrated. Following recrystallization using minimum EtOH and Et_2O and freeze-drying, a white product was obtained (0.133 g, 92 %). ^{1}H NMR (400 MHz, H_2O) δ 5.88-5.78 (1H, m), 5.18 (1H, dd, *J* = 17.2, 1.3 Hz), 5.12 (1H, d, *J* = 10.2 Hz), 4.11- 4.05 (1H, m), 3.95- 3.85 (2H, m), 3.62 (1H, dd, *J* = 9.2, 5.6 Hz), 3.57 (1H, d, *J* = 4.9 Hz), 2.48 (1H, ddd, *J* = 14.9, 11.2, 8.0 Hz), 2.37 (1H, ddd, *J* = 15.0, 5.9, 4.3 Hz), 2.00 (1H, ddd, *J* = 12.9, 5.0, 2.7 Hz), 1.38 (1H, ddd, *J* = 12.8, 10.9, 10.9 Hz); ^{13}C NMR (126 MHz, H_2O) δ 134.9, 117.3, 75.0, 72.6, 69.2, 67.2, 63.7, 33.9, 29.5; MS (ESI, H_2O): Calcd for $C_9H_{16}O_4$ $[(M+Na)^+]$: 211.1. Found 211.1.

6.2.23 6-Deoxy-2,3,4-*O*-Tri-acetyl-1-*C*-allyl-α-D-galactopyranoside (82)[13]

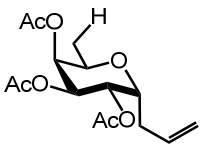

To a solution of commercially available D-fucose (0.49 g, 3.02 mmol) was added acetic anhydride (1.99 mL, 21.1 mmol) and pyridine (1.71 mL, 21.1 mmol) at 0°C under inert argon and was stirred for 30 min followed by addition of DMAP (0.04 g, 0.30 mmol). The reaction mixture was warmed to room temperature and sonicated for 1 h then washed several times with

$CuSO_4$, washed twice with water and once with brine, dried over $MgSO_4$, filtered and concentrated. The residue was dissolved in anhydrous CH_3CN, cooled to 0°C and allyltrimethylsilane (0.76 mL, 4.79 mmol) and boron trifluoride diethyl etherate (1.14 mL, 9.09 mmol) were added dropwise to the reaction mixture which was stirred for 24 h. The solvent was evaporated and the residue was dissolved in CH_2Cl_2, washed with water, saturated $NaHCO_3$, dried over $MgSO_4$, filtered, concentrated and purified by flash chromatography (3:2 hexanes: EtOAc) to afford colorless oil (Rf = 0.79, 0.25 g, 53 %). ^{1}H NMR (400 MHz, $CDCl_3$) δ 5.80- 5.70 (1H, m), 5.29 (1H, dd, *J* = 10.0, 5.6 Hz), 5.25 (1H, dd, *J* = 3.4, 1.9 Hz), 5.20 (1H, dd, *J* = 10.0, 3.4 Hz), 5.13- 5.06 (2H, m), 4.26 (1H, ddd, *J* = 10.4, 5.08, 5.08 Hz), 3.95 (1H, dq, *J* = 6.4, 1.7 Hz), 2.53- 2.45 (1H, m), 2.30- 2.23 (1H, m), 2.13 (3H, s), 2.03 (3H, s), 1.99 (3H, s), 1.12 (3H, d, *J* = 6.45 Hz); ^{13}C NMR (101 MHz, $CDCl_3$) δ 170.6, 170.2, 170.0, 133.8, 117.4, 72.0, 70.7, 68.5, 68.2, 65.6, 30.6, 20.8, 20.7, 20.7, 15.9; MS (ESI, CH_3CN): Calcd for $C_{15}H_{22}O_7$ $[(M+NH_4)^+]$: 332.2, $[(M+Na^+]$: 337.1, $[(M+K)^+]$: 353.1. Found 332.1, 337.1, 353.1

6.2.24 6-Deoxy-1-*C*-allyl-α-D-galactopyranoside (33)[7]

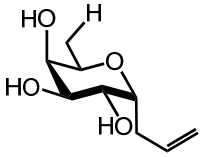

To compound **82** (0.25 g, 0.79 mmol) was added NaOMe/MeOH (1M) and the solution was sonicated for 1 h at room temperature. Amberlite IR resin (H+ form, pH = 4) was washed several times with HPLC grade MeOH and added to the reaction mixture which was stirred until the pH was between 5 and 6. The solution was filtered and concentrated. Following recrystallization using EtOH and Et_2O and freeze-drying, a white product was obtained (0.09 g, 60 %). ^{1}H NMR (400 MHz, H_2O) δ 5.87- 5.77 (1H, m), 5.19 (1H, d, *J* = 17.1 Hz), 5.14 (1H, d, *J* = 10.1 Hz), 4.06 (1H, ddd, *J* = 11.7, 6.0, 3.7 Hz), 3.98- 3.93 (2H, m), 3.83- 3.77 (2H, m), 2.52 (1H, ddd, *J* = 15.2, 11.6, 8.4 Hz), 2.39- 2.33 (1H, m), 1.16 (3H, d, *J* = 6.5 Hz); ^{13}C NMR (101 MHz, H_2O) δ 135.1, 117.4, 75.2, 71.8, 69.8, 67.9, 66.9, 28.7, 15.5; MS (ESI, H_2O): Calcd for $C_9H_{16}O_4$ $[(M+Na)^+]$: 211.1. Found 211.1.

6.2.25 1-*C*-Allyl-α-D-galactopyranoside (25)[13,14]

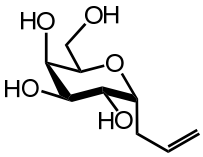

To a solution of commercially available β-D-galactose pentaacetate (6.0 g, 15.37 mmol) in anhydrous CH_3CN (50 mL) at 0°C, was added allyltrimethylsilane (7.50 mL, 46.99 mmol) and boron trifluoride diethyl etherate (11 mL, 87.58 mmol) dropwise before the reaction mixture was stirred for 24 h. The solvent was evaporated and the residue was dissolved in CH_2Cl_2, washed with water, saturated $NaHCO_3$, dried over $MgSO_4$, filtered, concentrated and purified by flash chromatography (3:1 hexanes: EtOAc) to afford a colorless oil (9:1,α:β mixture). The mixture was dissolved in a solution of NaOMe/MeOH (1M) and the reaction was sonicated for 1 h. Pre-rinsed Amberlite IR resin (H+ form, pH = 4) was added to the reaction mixture until a pH of 5 or 6 was attained. The resin was filtered off and the α-anomer was selectively recrystallized using

MeOH and Et_2O to afford a white crystalline product (2.16 g, 69 %). 1H NMR (400 MHz, MeOD) δ 5.90-5.83 (1H, dddd, J = 7.0, 7.0, 10.2, 17.1 Hz), 5.10 (1H, dd, J = 1.9, 17.2 Hz), 5.04-4.99 (1H, m), 4.01-3.93 (1H, m), 3.94-3.91 (1H, m), 3.88 (1H, dd, J = 5.3, 8.8 Hz), 3.76-3.61 (4H, m), 2.49-2.31 (2H, m)

All characterization was in accordance with the literature.[13,14]

6.2.26 3,4-*O*-Isopropyl-1-*C*-allyl-α-D-galactopyranoside (83)[14,16]

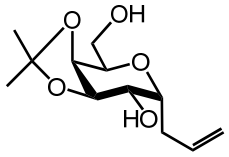

To a solution of compound **25** (0.600 g, 2.94 mmol) in 2,2-dimethoxypropane (0.31 mL, 3.23 mmol) at room temperature was added anhydrous CH_3CN (10 mL) and catalytic amount of p-toluenesulfonic acid monohydrate (0.01 g, 0.05mmol). The reaction mixture was stirred for 15 min and then placed under 300 mbar vacuum for 1 h. Excess triethylamine (3 mL, 21.52 mmol) was added to the mixture which was concentrated and purified by flash chromatography (1:1:0.1 hexanes: EtOAc: triethylamine). The corresponding fractions were collected and concentrated to afford white solid (Rf = 0.35, 0.58 g, 81%). ^{1}H NMR (400 MHz, CDCl3) δ 5.89- 5.79 (1H, m), 5.16 (1H, ddd, *J* = 17.1, 3.2, 1.5 Hz), 5.10 (1H, d, *J* = 10.2 Hz), 4.31 (1H, dd, *J* = 7.2, 1.9 Hz), 4.27 (1H, dd, *J* = 7.3, 3.2 Hz), 4.07- 4.02 (2H, m), 3.86- 3.79 (2H, m), 3.71 (1H, ddd, *J* = 11.5, 9.3, 4.5 Hz), 2.41- 2.36 (2H, m), 1.47 (3H, s), 1.32 (3H, s)

All characterization was in accordance with the literature.[14]

6.2.27 2,6-O-Acetyl-3,4-O-isopropyl-1-C-allyl-α-D-galactopyranoside (84)

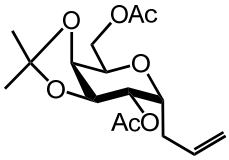

A mixture of compound **83** (0.49 g, 2.00 mmol), acetic anhydride (1.33 mL, 14.0 mmol) and pyridine (1.14 mL, 14.0mmol) was stirred at 0°C under inert argon for 30 min followed by addition of DMAP (0.03 g, 0.23 mmol). The reaction mixture was warmed to room temperature and sonicated for 1 h then washed several times with $CuSO_4$, washed twice with water and once with brine, dried over $MgSO_4$, filtered, concentrated and purified by flash chromatography (petroleum ether: EtOAc: triethylamine, 2:1:0.1) to afford a colorless oil (0.56, 0.55 g, 84 %). ^{1}H NMR (400 MHz, $CDCl_3$) δ 5.79- 5.69 (1H, m), 5.08- 4.99 (3H, m), 4.26- 4.22 (4H, m), 4.15 (1H, ddd, *J* = 7.8, 6.8, 3.0 Hz), 4.06 (1H, dd, *J* = 6.2, 6.2 Hz), 2.36- 2.99 (1H, m), 2.20- 2.15 (1H, m), 2.10 (3H, s), 2.07 (3H, s), 1.47 (3H, s), 1.30 (3H, s); ^{13}C NMR (101 MHz, $CDCl_3$) δ 170.9, 169.8, 133.5, 117.6, 110.2, 72.2, 72.1, 69.7, 69.6, 67.8, 64.3, 35.0, 26.6, 24.6, 21.0, 20.9; MS (ESI, CH_3CN): Calcd for $C_{16}H_{24}O_7$ [$(M+H)^+$]: 329.2, [$(M+Na)^+$]: 352.1, [$(M+K)^+$]: 367.1. Found 329.1, 351.1, 367.1

6.2.28 1,2,3,4-*O*-Isopropyl-α-D-galactopyranoside (89)[15]

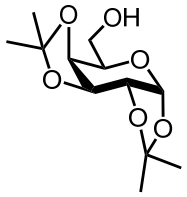

To a solution of D-galactose (2.00 g, 11.10 mmol) in acetone (50 mL) was added anhydrous copper sulfate (4.00g, 25.07 mmol) and sulfuric acid (0.25 mL, 4.69 mmol) and the reaction mixture was stirred at room temperature for 72 h. A saturated solution of $NaHCO_3$ was added to neutralize the reaction and acetone was removed under reduced pressure. The resulting aqueous layer was extracted several times with CH_2Cl_2, then the combined organic layers were washed once with brine, dried over $MgSO_4$, filtered, concentrated and purified by flash chromatography (1:1:0.1 petroleum ether: EtOAc: triethylamine) to afford a colorless oil (Rf = 0.59, 3.42 g, 66 %). ^{1}H NMR (400 MHz, $CDCl_3$) δ 5.56 (1H, d, *J* = 5.0 Hz), 4.60 (1H, dd, *J* = 7.9, 2.4 Hz), 4.33 (1H, dd, *J* = 5.0, 2.4 Hz), 4.26 (1H, dd, *J* = 7.9, 1.2 Hz), 3.88- 3.82 (2H, m), 3.75- 3.72 (1H, m), 1.52 (3H, s), 1.44 (3H, s), 1.32 (6H, s)

All characterization was in accordance with the literature.[15]

6.2.29 6-Deoxy-6-azido-1,2,3,4- *O*-isopropyl-α-D-galactopyranoside (90)[15]

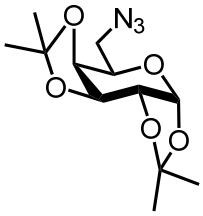

To a solution of compound **89** (0.27 g, 0.88 mmol) in anhydrous pyridine (5 mL, 61.80 mmol) was added p-toluenesulfonyl chloride (0.17 g, 0.88 mmol) at 0°C. The reaction was warmed to room temperature and stirred for 24 h. Upon completion of the reaction, water was added (10 mL) and the mixture was poured over ice water and stirred for 1 h to re-crystallize the product. The crystals were collected and dissolved in toluene and azeotroped several times followed by re-crystallization using EtOH to afford white crystalline product (0.30 g, 70%). The intermediate was dried under vaccum for 24 h, flushed under argon for 15 min and dissolved in dimethylformamide (20 mL). To the solution was added sodium azide (Rf = 0.74, 0.16 g, 2.48 mmol) and the reaction mixture was refluxed at 130°C, under argon, for 17 h. The reaction was quenched with water, concentrated under reduced pressure, dissolved in a minimum of CH_2Cl_2 and purified by flash chromatography (9:1:0.1 hexanes: EtOAc: triethylamine) to afford a clear oil (0.22 g, 96 %). ^{1}H NMR (400 MHz, CDCl3) δ 5.53 (1H, d, *J* = 5.0 Hz), 4.61 (1H, dd, *J* = 7.9, 2.5 Hz), 4.32 (1H, dd, *J* = 5.0, 2.5 Hz), 4.18 (1H, dd, *J* = 7.9, 1.9 Hz), 3.91- 3.87 (1H, m), 3.49 (1H, dd, *J* = 12.7, 7.8 Hz), 3.34 (1H, dd, *J* = 12.7, 5.4 H), 1.52 (3H, s), 1.43 (3H, s), 1.32 (6H, s); IR (film): 2100.34

All characterization was in accordance with the literature.[15]

6.2.30 6-Deoxy-6-azido-D-galactopyranoside (38)[15]

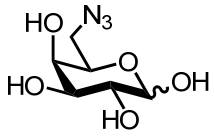

To compound **90** (0.22 g, 0.77 mmol) was added an aqueous solution of trifluoroacetic acid (5 mL, 8:2 TFA: H_2O) and the solution was monitored using TLC (EtOAc: MeOH: H_2O: CH_3CN, 4:1:1:1). Once completed, the reaction was neutralized using triethylamine, concentrated under reduced pressure, azeotroped using toluene, re-crystallized using EtOH and further freeze-drying yielded a white powder (0.16 g, 65 %, 2:1 α: β). ^{1}H NMR (400 MHz, H_2O) δ 5.22 (1H, d, *J* = 3.7 Hz), 4.56 (1H, d, *J* = 7.9 Hz), 4.15 (1H, dd, *J* = 8.4, 4.4 Hz), 3.91 (1H, d, *J* = 2.8 Hz), 3.85- 3.73 (3H, m), 3.61- 3.37 (5H, m)

All characterization was in accordance with the literature.[15]

6.2.31 4-Deoxy-4-azido-1,2,3,6-Tetra-*O*-pivaloyl-β-D-glucopyranoside (91)[15]

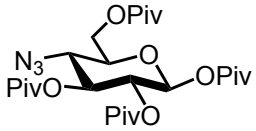

To a solution of compound **75** (0.49 g, 0.95 mmol) in anhydrous CH_2Cl_2 (20 mL) was added anhydrous pyridine (2 mL, 24.73 mmol) and anhydrous trifluoromethane sulfonyl anhydride (0.18 mL, 1.05 mmol) at -10°C. The reaction was warmed to room temperature and stirred for 30 min. The reaction mixture was dissolved in EtOAc, washed twice with 10 % HCl, then once with water, saturated $NaHCO_3$ and brine, followed by drying over $MgSO_4$, filtering, concentrating, drying under reduced pressure for 3 h and flushing with argon for 30 min. To this intermediate was added anhydrous dimethylformamide (10 mL) and sodium azide (0.25 g, 3.82 mmol) and the reaction mixture was stirred at room temperature for 24 h. The reaction was further diluted with EtOAc and washed several times with water then once with brine, dried over $MgSO_4$, filtered, concentrated and purified by flash chromatography (9:1 hexanes: EtOAc) to afford white solid (Rf = 0.67, 0.45 g, 96 %). ^{1}H NMR (400 MHz, $CDCl_3$) δ 5.65 (1H, d, *J* = 8.3 Hz), 5.25 (1H, dd, *J* = 9.3, 9.3 Hz), 5.13 (1H, dd, *J* = 9.5, 8.4 Hz), 4.40 (1H. dd, *J* = 12.2, 2.1 Hz), 4.29 (1H, dd, *J* = 12.3, 4.3 Hz), 3.66- 3.56 (2H, m), 1.23 (9H, s), 1.21 (9H, s), 1.16 (9H, s), 1.12 (9H, s); ^{13}C NMR (101 MHz, CDCl3) δ 177.8, 176.9, 176.5, 176.3, 91.7, 73.0, 72.8, 70.0, 62,.4, 61.2, 38.9, 38.8, 38.8, 38.7, 27.1, 27.1, 27.0, 26.8; MS (ESI, CH_3CN): Calcd for $C_{26}H_{43}N_3O_9$ [$(M+NH_4)^+$]: 559.3, [$(M+K)^+$]: 580.3. Found 559.5, 580.4; IR (film): 2113.84

6.2.32 1,2,3,6-Tetra-*O*-pivaloyl-β-D-glucopyranoside (94)[15,16]

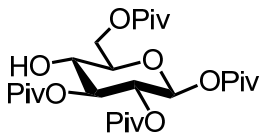

To a solution of compound **75** (0.14 g, 0.26 mmol) in anhydrous CH_2Cl_2 (20 mL) was added anhydrous pyridine (0.5 mL, 6.18 mmol) and anhydrous trifluoromethane sulfonyl anhydride (0.05 mL, 0.29 mmol) at -10°C. The reaction was warmed to room temperature and stirred for 30

min. The reaction mixture was then dissolved in EtOAc, washed twice with 10 % HCl, then once with water, saturated $NaHCO_3$ and brine, followed by drying over $MgSO_4$, filtering, concentrating, drying under reduced pressure for 3 h and flushing with argon for 30 min. To this intermediate was added anhydrous dimethylformamide (20 mL) and sodium nitrite (0.07 g, 1.05 mmol) and the reaction mixture was stirred at room temperature for 24 h. The reaction was further diluted with EtOAc and washed several times with water then once with brine, dried over $MgSO_4$, filtered, concentrated and purified by flash chromatography (9:1 hexanes: EtOAc) to afford white solid (Rf = 0.26, 0.08 g, 59 %). ^{1}H NMR (400 MHz, $CDCl_3$) δ 5.67 (1H, d, *J* = 7.87 Hz), 5.17- 5.08 (2H, m), 4.46 (1H, dd, *J* = 12.2, 4.7 Hz), 4.31 (1H, dd, *J* = 12.2, 2.5 Hz), 3.66 (1H, ddd, *J* = 9.8, 4.6, 2.5 Hz), 3.53 (1H, ddd, *J* = 9.6, 9.2, 4.8 Hz), 2.99 (1H, d, *J* = 4.8 Hz), 1.22 (9H, s), 1.18 (9H, s), 1.17 (9H, s), 1.12 (9H, s); ^{13}C NMR (101 MHz, CDCl3) δ 179.1, 178.9, 176.5, 91.9, 75.2, 75.0, 69.6, 69.5, 62.4, 39.0, 38.9, 38.7, 38.7, 27.1, 27.1, 27.1, 26.8; MS (ESI, CH_3CN): Calcd for $C_{26}H_{44}O_{10}$ [$(M+NH_4)^+$]: 534.3, [$(M+Na)^+$]: 539.3. Found 534.6, 539.5.

6.2.33 4-Deoxy-4-azido-1,2,3,6-Tetra-*O*-pivaloyl-β-D-galactopyranoside (95)[16]

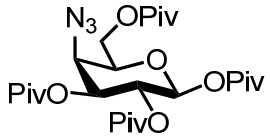

To a solution of compound **94** (0.20 g, 0.39 mmol) in anhydrous CH_2Cl_2 (20 mL) was added anhydrous pyridine (0.06 mL, 0.78 mmol) and anhydrous trifluoromethane sulfonyl anhydride (0.06 mL, 0.39 mmol) at -10°C. The reaction was warmed to room temperature and stirred for 30 min. The reaction mixture was dissolved in EtOAc, washed twice with 10 % HCl, then once with water, saturated $NaHCO_3$ and brine, followed by drying over $MgSO_4$, filtering, concentrating, drying under reduced pressure for 3 h and flushing with argon for 30 min. To the intermediate was added anhydrous dimethylformamide (10 mL) and sodium azide (0.10 g, 1.56 mmol) and the reaction mixture was stirred at room temperature for 24 h. The reaction was diluted with EtOAc and washed several times with water then once with brine, dried over $MgSO_4$, filtered, concentrated and purified by flash chromatography (9:1 hexanes: EtOAc) to afford white powder (Rf = 0.41, 0.13 g, 63 %). ^{1}H NMR (400 MHz, $CDCl_3$) δ 5.62 (1H, d, *J* = 8.3 Hz), 5.43 (1H, dd, *J* = 10.2, 8.2 Hz), 5.18 (1H, dd, *J* = 10.1, 3.8 Hz), 4.32 (1H, dd, *J* = 11.2, 6.4 Hz), 4.17 (1H, dd, *J* = 11.3, 6.8 Hz), 4.01 (1H, dd, *J* = 3.8, 1.2 Hz), 3.97 (1H, ddd, *J* = 6.8, 6.7, 1.4 Hz,), 1.22 (9H, s), 1.20 (9H, s), 1.17 (9H, s), 1.12 (9H, s); ^{13}C NMR (101 MHz, CDCl3) δ 177.8, 177.5, 176.5, 176.3, 92.1, 72.7, 71.5, 67.6, 62.0, 60.5, 39.2, 38.8, 38.7, 27.1, 26.8; MS (ESI, CH_3CN): Calcd for $C_{26}H_{43}N_3O_9$ [$(M+NH_4)^+$]: 559.3, [$(M+Na)^+$]: 564.3, [$(M+K)^+$]: 580.3. Found 559.2, 564.2, 580.2; IR (film): 2108.05

6.2.34 Propyl-1-thio-β-D-galactopyranoside (48)[10]

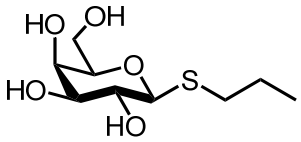

To a stirred solution of 1,2,3,4,6-penta-*O*-acetyl-β-D-galactopyranose (0.21 g, 0.51 mmol) in 20 mL of anhydrous dichloromethane with activated 4Å molecular sieves, propanethiol (0.07 mL, 0.77 mmol) was added and the solution was cooled to 0°C. Boron trifluoride diethyl etherate (0.34 mL, 2.69 mmol) was added dropwise and the solution was stirred at room

temperature for 24 h. The solution was diluted and filtered through celite, extracted three times with dichlormethane, washed twice with brine, dried over $MgSO_4$ and concentrated under reduced pressure. The resulting yellow oil was purified by gradient flash chromatography (4:1 hexanes: EtOAc → 1:1 hexanes: EtOAc), dissolved in a solution of NaOMe/MeOH (1M), sonicated for 1 h, and stirred in Amberlite IR resin (H+ form, pH = 4) for 5 min. The product was recrystallized from hexanes and ether, concentrated and freeze-dried to yield white crystals (0.05 g, 42 %). ^{1}H NMR (400 MHz, D_2O): δ 4.45 (1H, d, *J* = 9.7 Hz), 3.96 (1H, d, *J* = 3.1 Hz), 3.77-3.67 (2H, m), 3.63 (1H, dd, *J* = 3.5. 9.4 Hz), 3.54 (1H, dd, *J* = 9.7 Hz), 2.79- 2.65 (2H, m), 1.69- 1.59 (3H, m), 0.96 (3H, t, *J* = 7.4 Hz); ^{13}C NMR (101 MHz, D_2O): δ 85.9, 78.8, 73.9, 69.6, 68.8, 61.0, 32.0, 22.8, 12.6; MS (ESI): Calcd for $C_9H_{18}O_5S$ [$(M+Na)^+$]: 261.3. Found 261.1

6.2.35 Butyl-1-thio-β-D-galactopyranoside (49)[10]

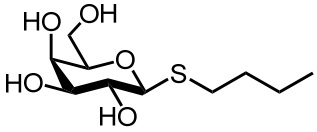

To a stirred solution of 1,2,3,4,6-penta-*O*-acetyl-β-D-galactopyranose (0.10 g, 0.26 mmol) in 10 mL of anhydrous dichloromethane with activated 4Å molecular sieves, butanethiol (0.04 mL, 0.38 mmol) was added and the solution was cooled to 0°C. Boron trifluoride diethyl etherate (0.16 g, 1.28 mmol) was added dropwise and the solution was stirred at room temperature for 24 h. The solution was diluted and filtered through celite, extracted three times with dichlormethane, washed twice with brine, dried over $MgSO_4$ and concentrated under reduced pressure. The resulting yellow-brown oil was purified by gradient flash chromatography (4:1 hexanes: EtOAc → 1:1 hexanes: EtOAc), dissolved in a solution of NaOMe/MeOH (1M), sonicated for 1 h, and stirred in Amberlite IR resin (H+ form, pH = 4) for 5 min. The product was recrystallized from hexanes and ether, concentrated and freeze-dried to yield white crystals (0.046 g, 71 %). ^{1}H NMR (400 MHz, MeOD): δ 4.28 (1H, d, *J* = 9.4 Hz), 3.86 (1H, d, *J* = 2.6 Hz), 3.75- 3.65 (2H, m), 3.6- 3.5 (2H, m), 3.43 (1H, dd, *J* = 3.2, 9.1 Hz), 2.79- 2.65 (2H, m), 1.65- 1.56 (2H, m), 1.47- 1.40 (2H, m), 0.92 (3H, t, *J* = 7.1 Hz); ^{13}C NMR (101 MHz, MeOD): δ 87.7, 80.6, 76.3, 71.5, 70.5, 62.6, 33.2, 30.6, 23.0, 14.0; MS (ESI): Calcd for $C_{10}H_{20}O_5S$ [$(M+Na)^+$]: 275.3, [$(2M+Na)^+$]: 527.6. Found 275.2, 527.4

6.2.36 Hexyl-1-thio-β-D-galactopyranoside (50)[10]

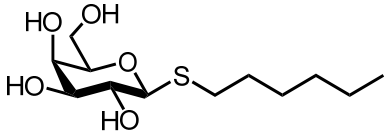

To a stirred solution of 1,2,3,4,6-penta-*O*-acetyl-β-D-galactopyranose (0.51 g, 1.28 mmol) in 10 mL of anhydrous dichloromethane with activated 4Å molecular sieves, hexanethiol (0.27 mL, 1.92 mmol) was added and the solution was cooled to 0°C. Boron trifluoride diethyl etherate (0.82 mL, 6.53 mmol) was added dropwise and the solution was stirred at room temperature for 24 h. The solution was diluted and filtered through celite, extracted three times with dichlormethane, washed twice with brine, dried over $MgSO_4$ and concentrated under reduced pressure. The resulting yellow oil was purified by gradient flash chromatography (4:1 hexanes: EtOAc → 1:1 hexanes: EtOAc), dissolved in a solution of NaOMe/MeOH (1M),

sonicated for 1 h, and stirred in Amberlite IR resin (H+ form, pH = 4) for 5 min. The product was recrystallized from hexanes and ethanol, concentrated and freeze-dried to yield white crystals (0.044 g, 12 %). ^{1}H NMR (400 MHz, MeOD): δ 4.28 (1H, d, *J* = 9.5 Hz), 3.9 (1H, d, *J* = 2.49 Hz), 3.75- 3.65 (2H, m), 3.55- 3.49 (2H, m), 3.44 (1H, dd, *J* = 3.4, 8.6 Hz), 2.78- 2.64 (2H, m), 1.64- 1.59 (2H, m), 1.43- 1.37 (2H, m), 1.33- 1.28 (4H, m), 0.90 (3H, t, *J* = 7.0 Hz); ^{13}C NMR (101 MHz, MeOD): δ 87.8, 80.6, 76.3, 71.5, 70.5, 62.6, 32.6, 31.1, 30.9, 29.7, 23.7, 14.4; MS (ESI): Calcd for $C_{12}H_{24}O_5S$ [$(M+Na)^+$]: 303.4. Found 303.3

6.2.37 Octyl-1-thio-β-D-galactopyranoside (51)[10]

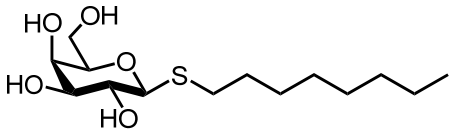

To a stirred solution of 1,2,3,4,6-penta-*O*-acetyl-β-D-galactopyranose (0.51 g, 1.28 mmol) in 10 mL of anhydrous dichloromethane with activated 4Å molecular sieves, octanethiol (0.34 mL, 1.92 mmol) was added and the solution was cooled to 0°C. Boron trifluoride diethyl etherate (0.82 mL, 6.53 mmol) was added dropwise and the solution was stirred at room temperature for 24 h. The solution was diluted and filtered through celite, extracted three times with dichlormethane, washed twice with brine, dried over $MgSO_4$ and concentrated under reduced pressure. The resulting yellow oil was purified by gradient flash chromatography (4:1 hexanes:EtOAc → 1:1 hexanes: EtOAc), dissolved in a solution of NaOMe/MeOH (1M), sonicated for 1 h, and stirred in Amberlite IR resin (H+ form, pH = 4) for 5 min. The product was recrystallized from hexanes and ethanol, concentrated and freeze-dried to yield white crystals (0.11 g, 27 %). ^{1}H NMR (400 MHz, MeOD): δ 4.28 (1H, d, *J* = 9.4 Hz), 3.87 (1H, d, *J* = 3.4 Hz), 3.75- 3.65 (2H, m), 3.55- 3.49 (2H, m), 3.44 (1H, dd, *J* = 3.4, 10.1 Hz), 2.78- 2.64 (2H, m), 1.64- 1.59 (2H, m), 1.42- 1.37 (2H, m), 1.29 (8H, br s), 0.89 (3H, t, *J* = 6.8 Hz); ^{13}C NMR (101 MHz, MeOD): δ 87.8, 80.6, 76.3, 71.5, 70.5, 62.6, 33.1, 31.2, 30.9, 30.4, 30.4, 30.1, 23.8, 14.5; MS (ESI): Calcd for $C_{14}H_{28}O_5S$ [$(M+Na)^+$]: 331.4. Found 331.3

References

1. Tam, R. Y.; Ferreira, S. S.; Czechura, P.; Chaytor, J. L.; Ben, R. N., Hydration Index A Better Parameter for Explaining Small Molecule Hydration in Inhibition of Ice Recrystallization. *J. Am. Chem. Soc.* **2008**, 130, 17494-17501

2. Jackman, J.; Noestheden, M.; Moffat, D.; Pezacki, J. P.; Findlay, S.; Ben, R. N., Assessing antifreeze activity of AFGP 8 using domain recognition software. *Biochem. Biophys. Res. Commun.***2007**, 354, 340-344.

3. Chaytor, J. L.; Tokarew, J. M.; Wu, L. K.; Guolla, L.; von Moos, E.; C. Scott Findlay, C. S. ; David S. Allan, D. S.; Ben, R. N., Inhibiting Ice Recrystallization and Optimization of Cell Viability after Cryopreservation, *Glycobiology*, **2010**, submitted manuscript.

4. Inada, T.; Modak, P. R. Growth control of ice crystals by poly(vinyl alcohol) and antifreeze protein in ice slurries. *Chem. Eng. Sci*. **2006**, 61, 3149-3158.

5. Malkar, N. B.; Lauer-Fields J. L.; Fields, G. B, Convenient synthesis of glycosylated hydroxylysine derivatives for use in solid-phase peptide synthesis, *Tetrahedron Letters*, **2000**, 1137–1140.

6. Zhang, Z; Magnusson, G., Synthesis of double-chain bis-sulfone neoglycolipids of the 2’-, 3’-, and 6’-deoxyglobotrioses, *J. Org. Chem.*, **1995**, 7304-7315.

7. Zemplen, G.; Kunz, A., *Chem. Ber.*, **1923**, 1705.

8. Becker, D.; Galili, N., Synthesis and utilization of saccharide intermediates, *Carbohydr. Res.,***1993**, 129-141.

9. Garegg, P. J.; Samuelsson, B., Novel reagent system for converting a hydroxy-group into an iodo-group in carbohydrates with inversion of configuration. Part 2, *J. Chem. Soc. Perkin Trans. 1*, **1980**, 2866-2870. Garegg, P. J.; Samuelsson, B., Novel reagent system for converting a hydroxy-group into an iodo-group in carbohydrates with inversion of configuration. Part 2, *J. Chem. Soc. Perkin Trans. 1*, **1980**, 2866-2870.

10. Ohlsson, J.; Magnusson, G., Galabiosyl donors; efficient synthesis from 1,2,3,4,6-penta-*O*-acetyl-β-D-galactopyranose. *Carbohydr. Res.*, **2000**, 329, 49-55.

11. Janczuk, A. J.; Zhang, W.; Andreana, P. R.; Warrick, J.; Wang P. G, The synthesis of deoxy-α-Gal epitope derivatives for the evaluation of an anti-α-Gal antibody binding, *Carbohydr. Res.,* **2002,** *337,* 1247-1259.

12. Nicolaou, K. C.; Bockovich, N. J.; Carcanague, D. R., Total Synthesis of Sulfated Le^x and Le^a-type Oligosaccharide Selectin Ligands, *J. Am. Chem. Soc.*, **1993**, 8843.

13. Arya, P.; Barkley, A.; Randell, K. D., Automated, High-throughput Synthesis of Artificial Glycopeptides: Small-molecule Probes for Chemical Glycobiology., *J. Comb. Chem.*, **2002**, *4* (3), pp 193–198.

14. Czechura, P.; Tam, R.Y.; Dimitrijevic, E; Murphy, A.V; Ben, R. N., The Importance of Hydration for Inhibiting Ice Recrystallization with *C*-Linked Antifreeze Glycoproteins, *J. Am. Chem. Soc.*, **2008,** 130 (10) 2928-2929.

15. Yang, J.; Fu, X.; Qiang, J.; Shen, J.; Biggins, J. B.; Jiang, J.; Zhao, J.; Schmidt, J. J.; Wang, P. G.; Thorson, J. S., Studies on the Substrate Specificity of *Escherichia coli* Galactokinase, *Org. Lett.*, **2003**, 5, 2223-2226.

16. Binkley, R. W., Inversion of Configuration in 2,6-Dideoxy Sugars. Triflate Displacement by Benzoate and Nitrite Anions, *J. Org. Chem*. **1991**, 56, 3892-3896.

APPENDIX

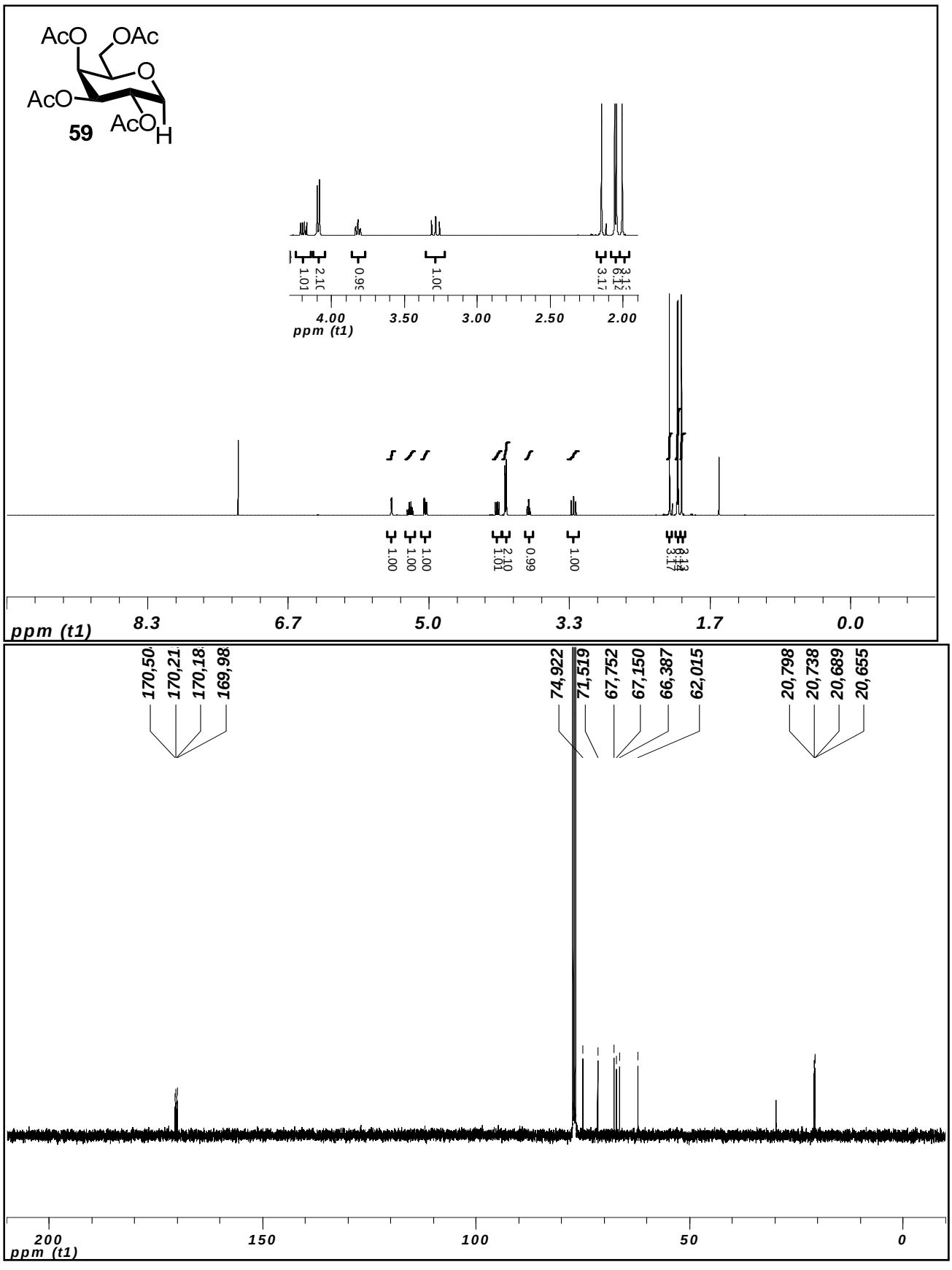
AcO
OAc
O
AcO
AcO
H
59
4.00
3.50
3.00
2.50
2.00
ppm (t1)
8.3
6.7
5.0
3.3
1.7
0.0
ppm (t1)
170,50
170,21
170,18
169,98
74,922
71,519
67,752
67,150
66,387
62,015
20,798
20,738
20,689
20,655
200
150
100
50
0
ppm (t1)

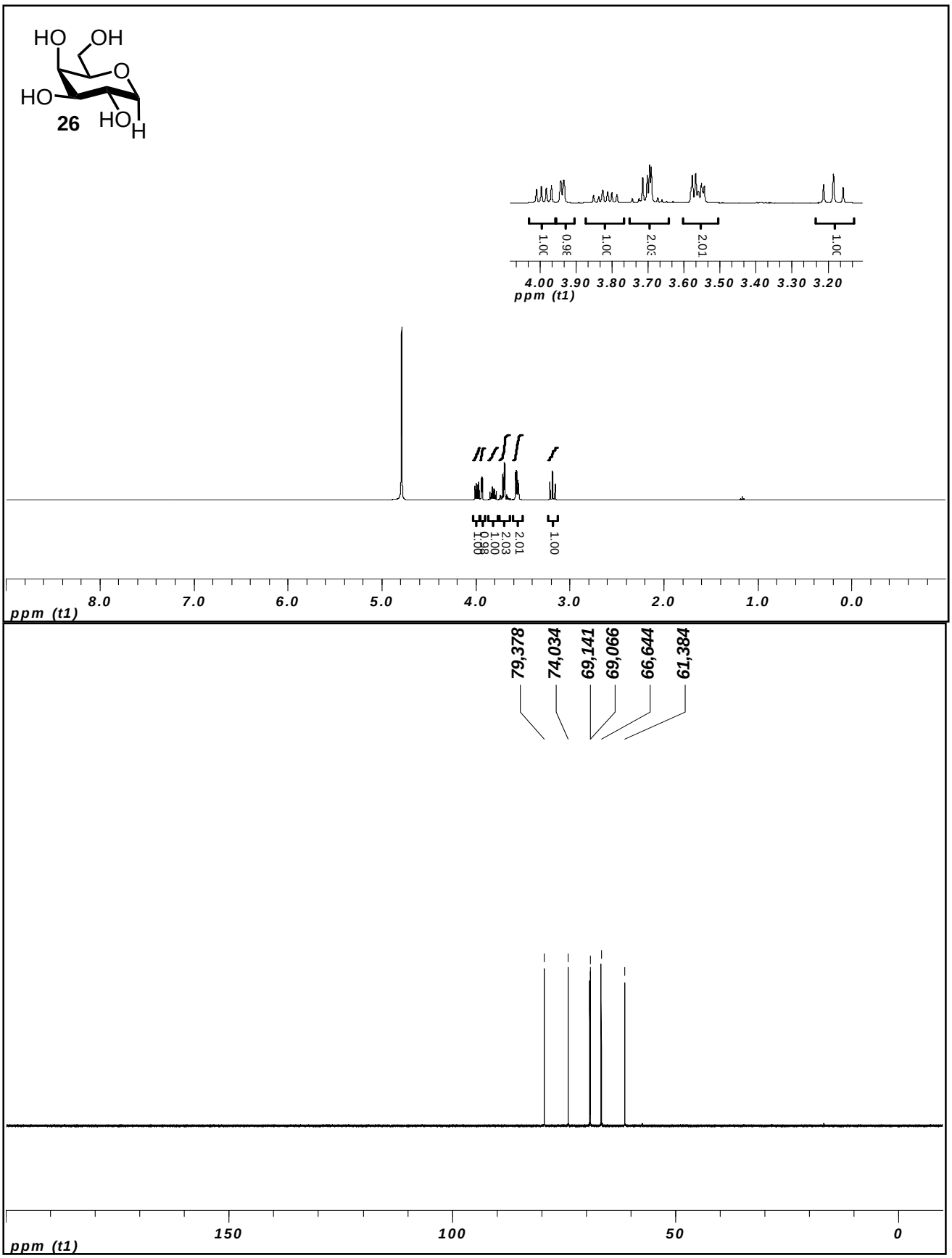
HO
OH
O
HO
HO
H
26
1.00
0.93
1.00
2.03
2.01
1.00
4.00 3.90 3.80 3.70 3.60 3.50 3.40 3.30 3.20
ppm (t1)
1.00
0.98
1.00
2.03
2.01
1.00
8.0 7.0 6.0 5.0 4.0 3.0 2.0 1.0 0.0
ppm (t1)
79,378
74,034
69,141
69,066
66,644
61,384
150 100 50 0
ppm (t1)

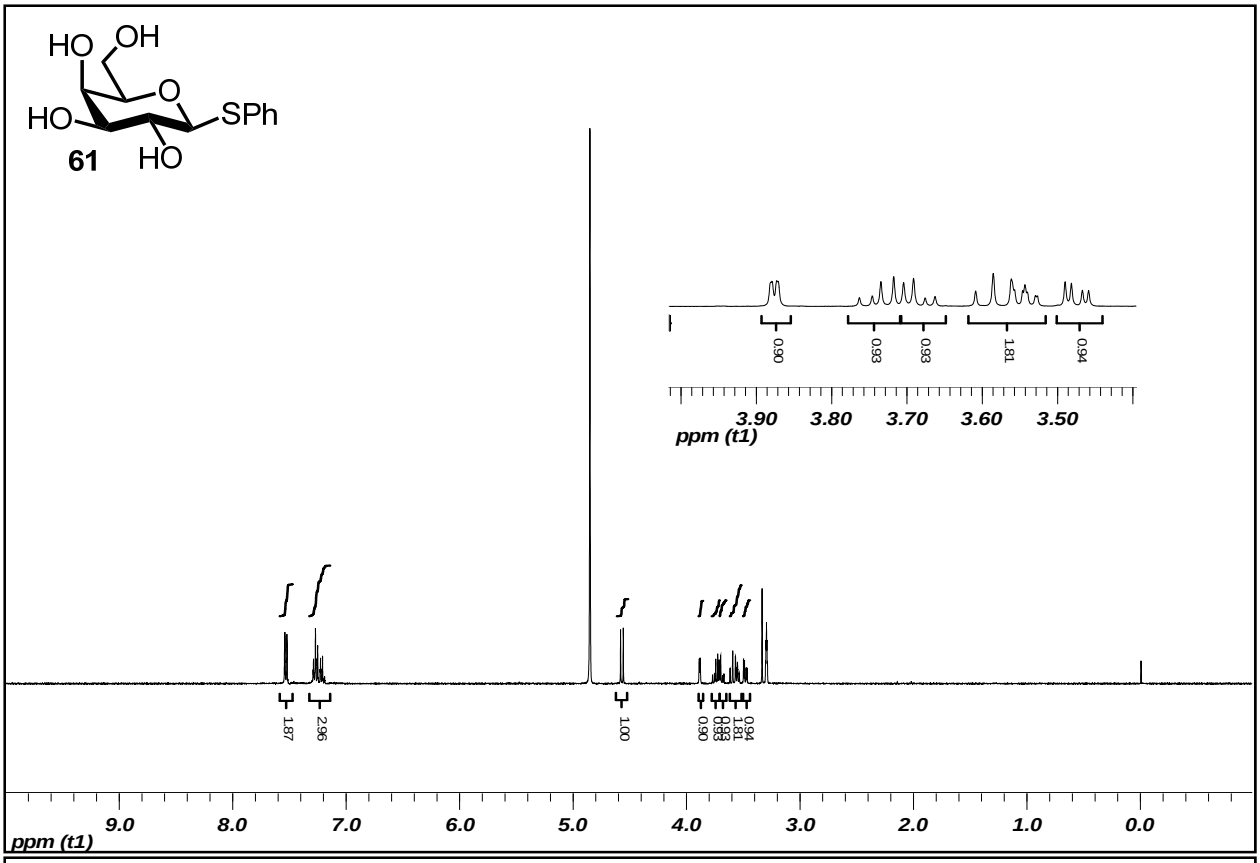
HO
OH
O
HO
SPh
HO
61
0.90
0.93
0.93
1.81
0.94
3.90
3.80
3.70
3.60
3.50
ppm (t1)
1.87
2.96
1.00
0.90
0.93
0.93
1.81
0.94
9.0
8.0
7.0
6.0
5.0
4.0
3.0
2.0
1.0
0.0
ppm (t1)

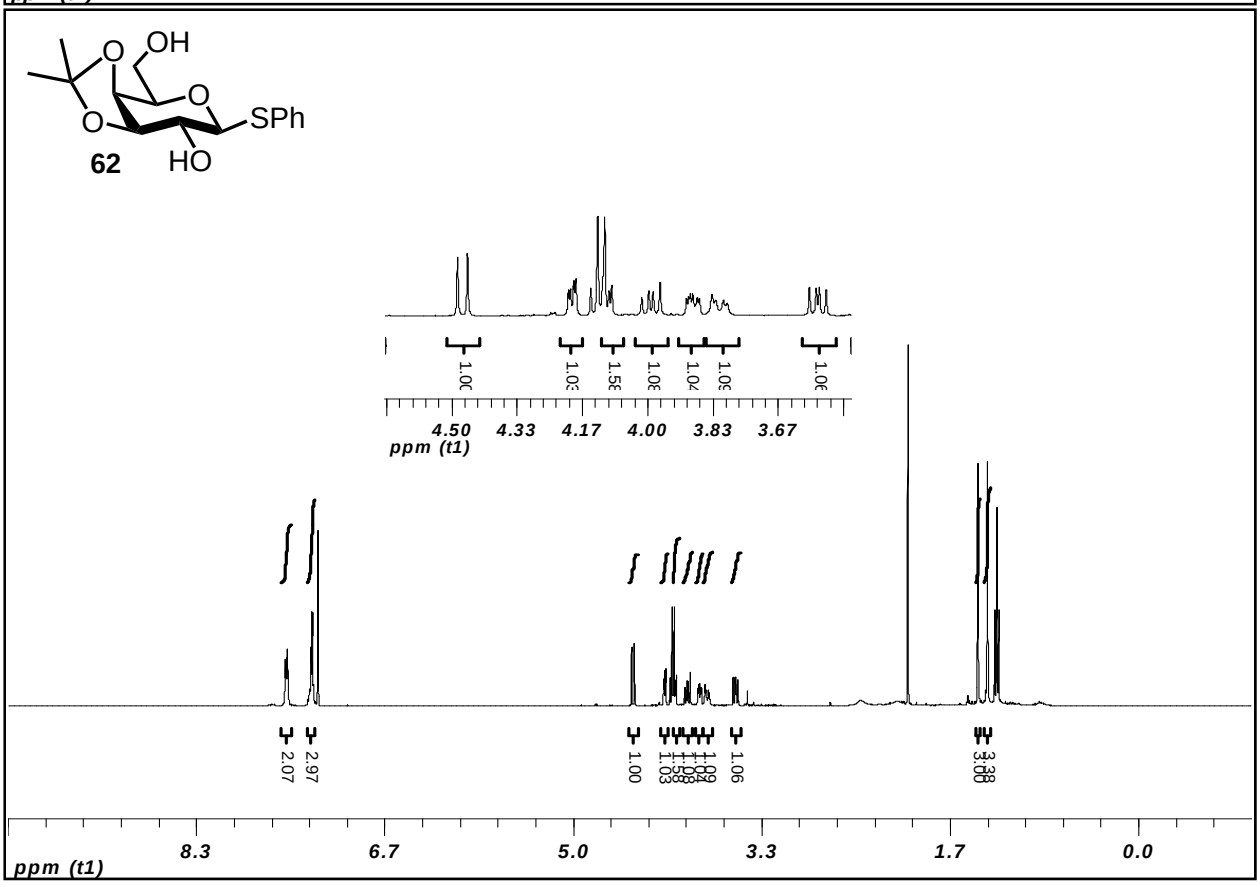
O
OH
O
O
SPh
HO
62
1.0
1.0
1.5
1.0
1.0
1.0
1.0
4.50
4.33
4.17
4.00
3.83
3.67
ppm (t1)
2.07
2.97
1.00
1.06
3.38
8.3
6.7
5.0
3.3
1.7
0.0
ppm (t1)

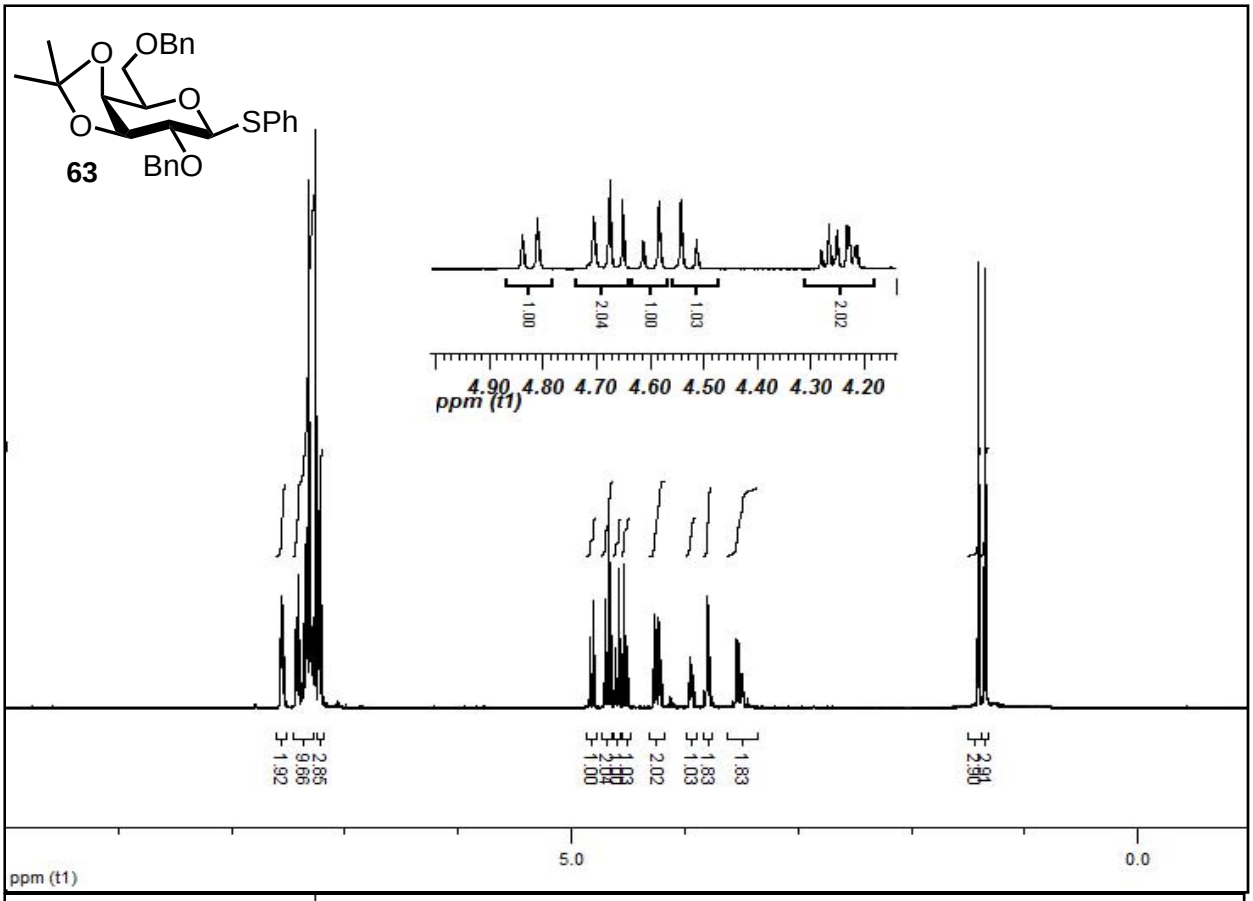
OBn
O
O
O
SPh
BnO
63
1.00
2.04
1.00
1.03
2.02
4.90 4.80 4.70 4.60 4.50 4.40 4.30 4.20
ppm (t1)
1.92
9.66
2.85
1.00
2.02
1.83
1.03
1.83
2.90
2.91
5.0
0.0
ppm (t1)

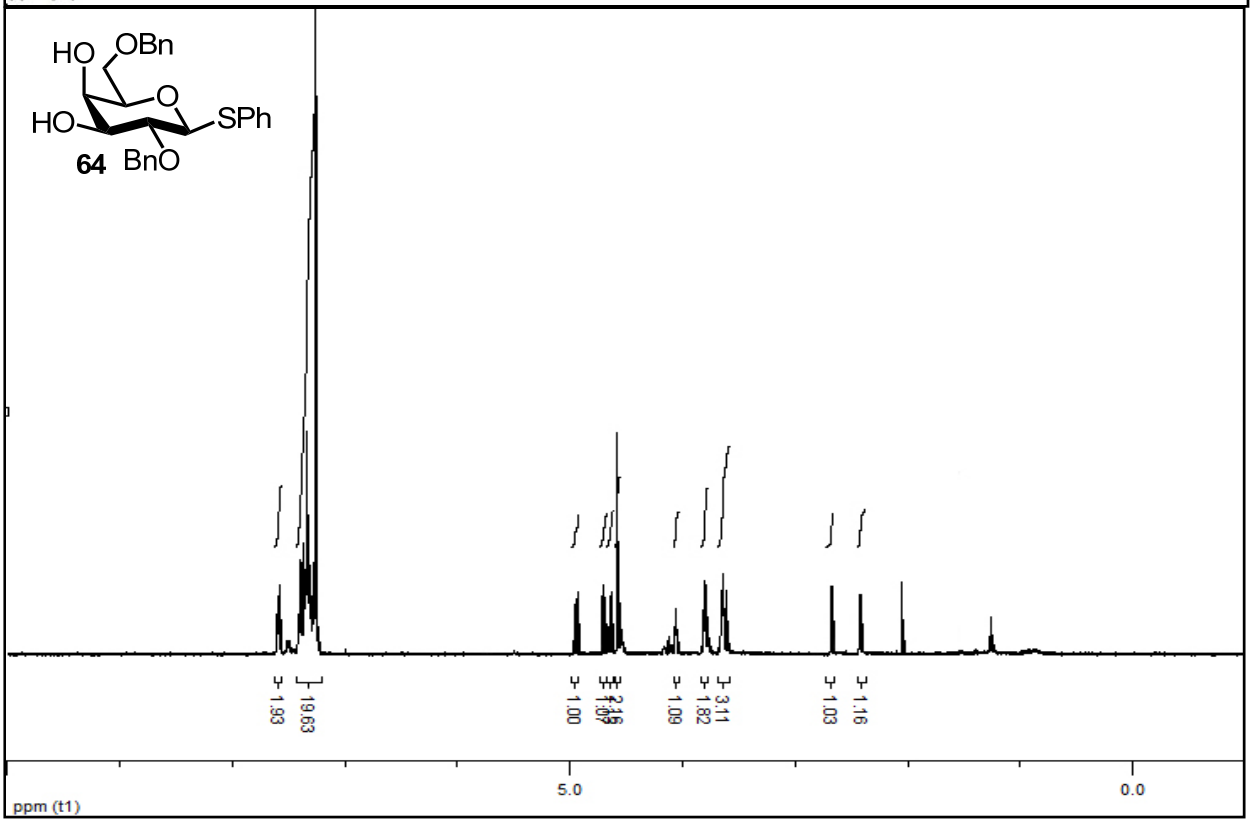
HO
OBn
O
HO
SPh
64
BnO
1.93
19.63
1.00
1.09
1.82
3.11
1.03
1.16
5.0
0.0
ppm (t1)

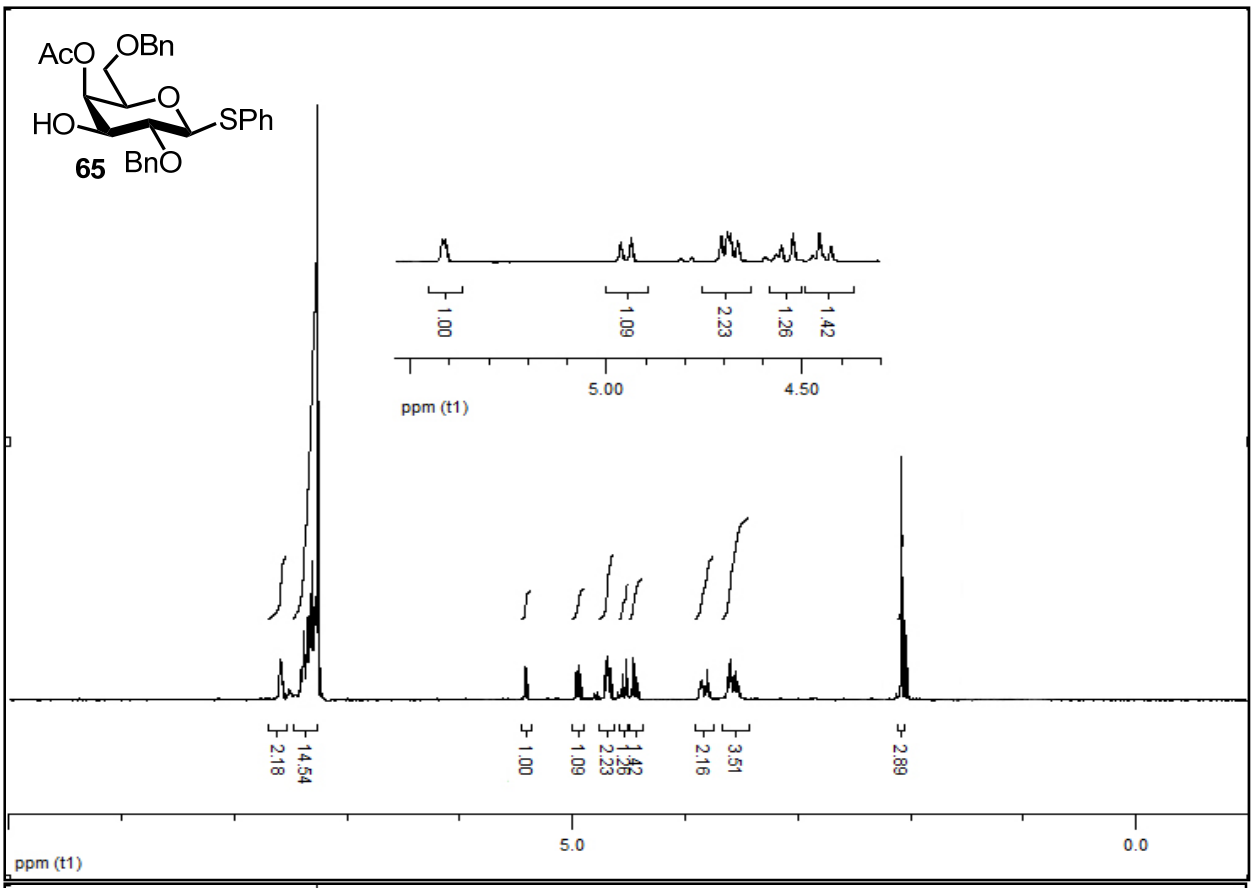
AcO
OBn
O
HO
SPh
65
BnO
1.00
1.09
2.23
1.26
1.42
5.00
4.50
ppm (t1)
2.18
14.54
1.00
1.09
2.16
3.51
2.89
5.0
0.0
ppm (t1)

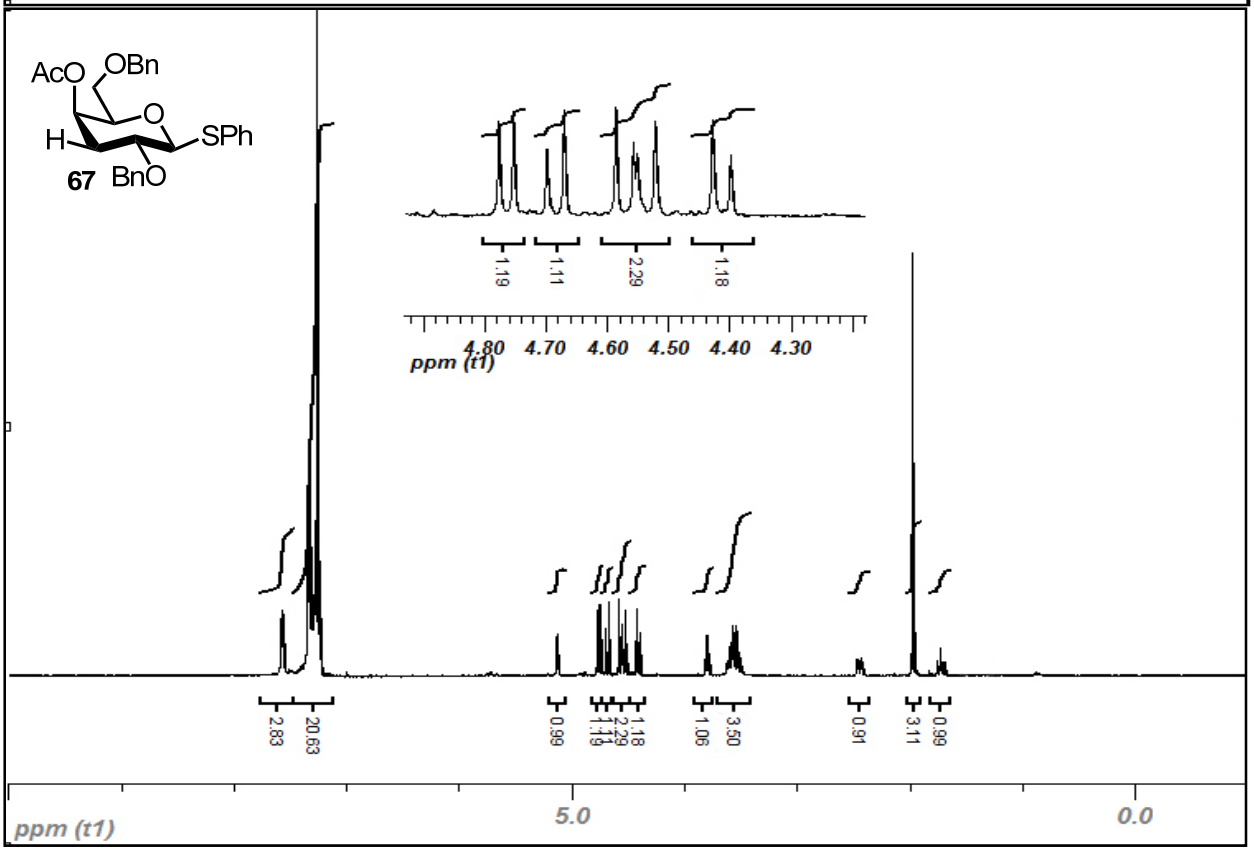
AcO
OBn
O
H
SPh
67
BnO
1.19
1.11
2.29
1.18
4.80
4.70
4.60
4.50
4.40
4.30
ppm (t1)
2.83
20.63
0.99
1.18
1.06
3.50
0.91
3.11
0.99
5.0
0.0
ppm (t1)

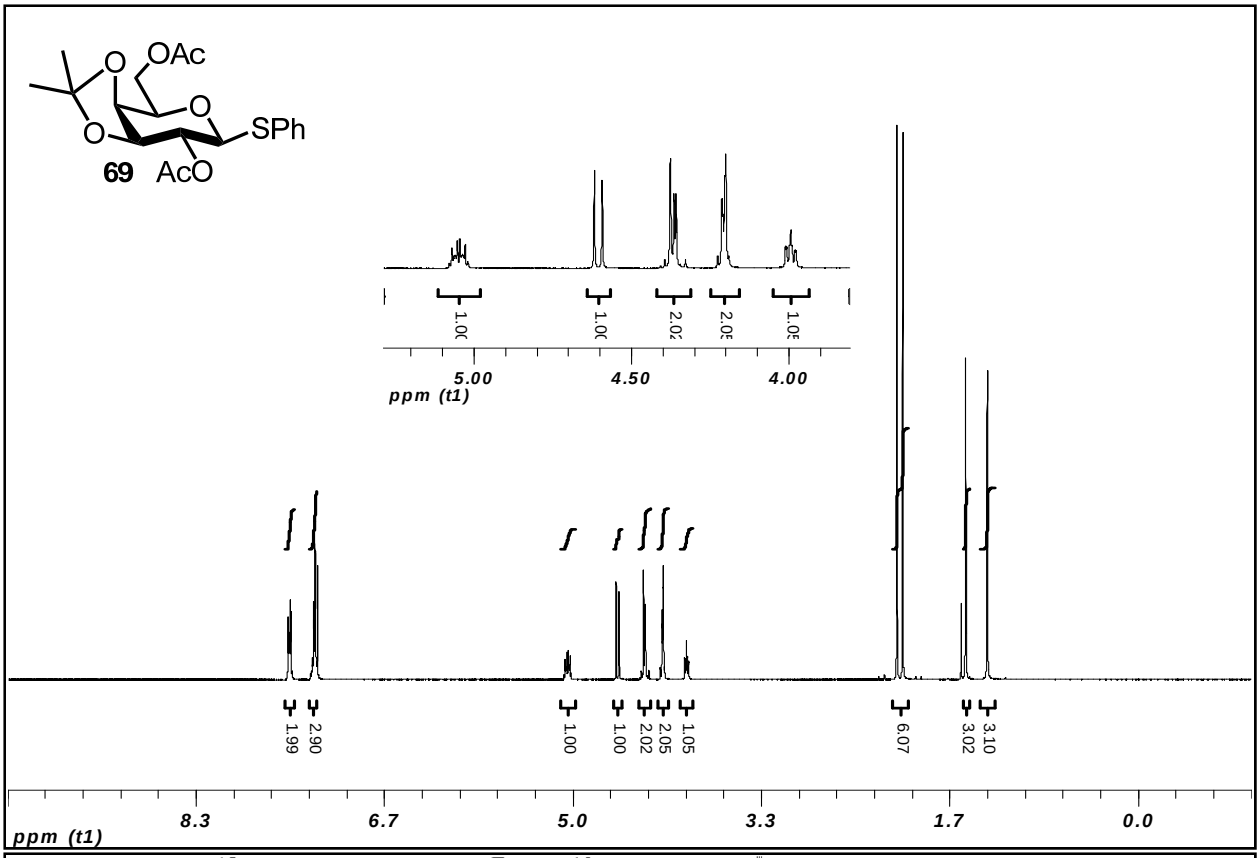
OAc
O
O
O
SPh
69 AcO
1.00
1.00
2.02
2.05
1.05
5.00
4.50
4.00
ppm (t1)
1.99
2.90
1.00
1.00
2.02
2.05
1.05
6.07
3.02
3.10
8.3
6.7
5.0
3.3
1.7
0.0
ppm (t1)

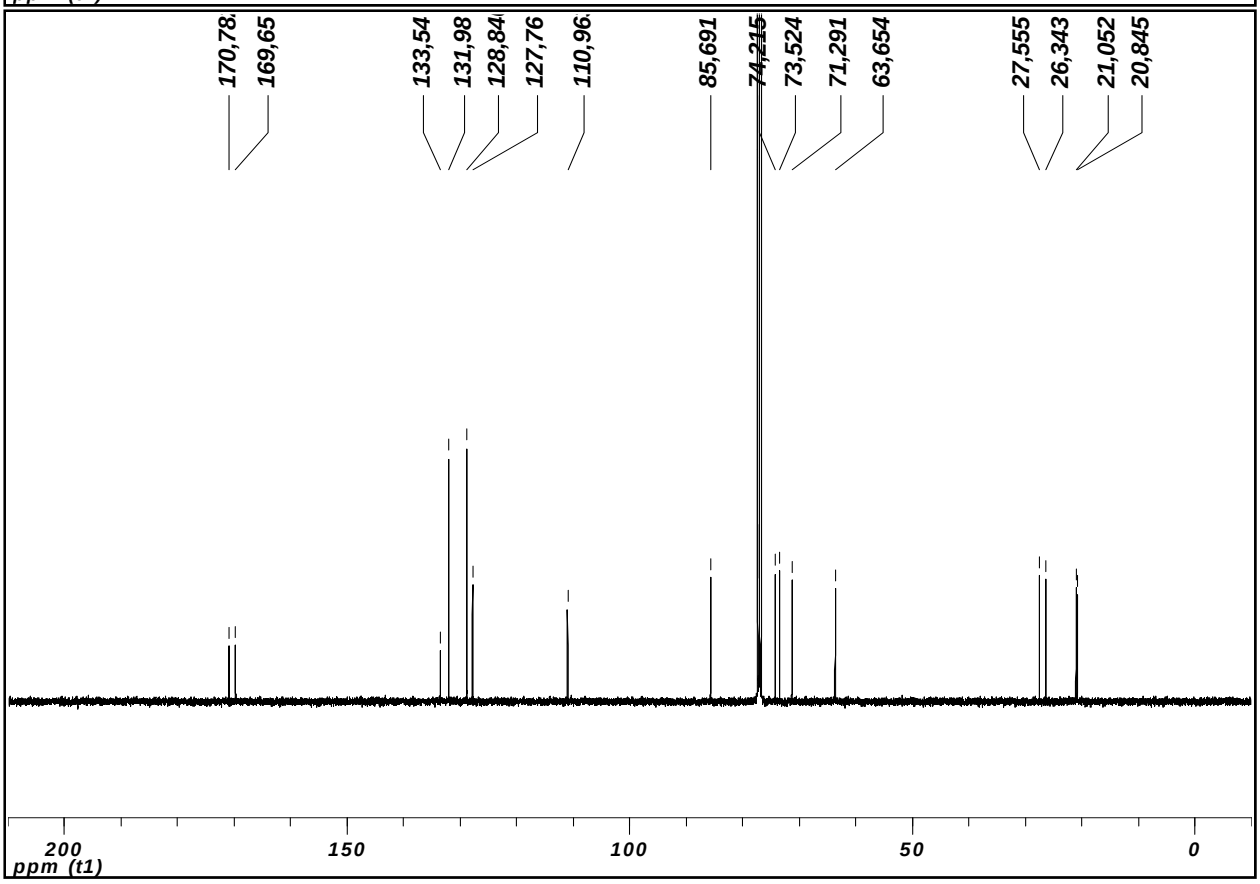
170,78
169,65
133,54
131,98
128,84
127,76
110,96
85,691
74,215
73,524
71,291
63,654
27,555
26,343
21,052
20,845
200
150
100
50
0
ppm (t1)

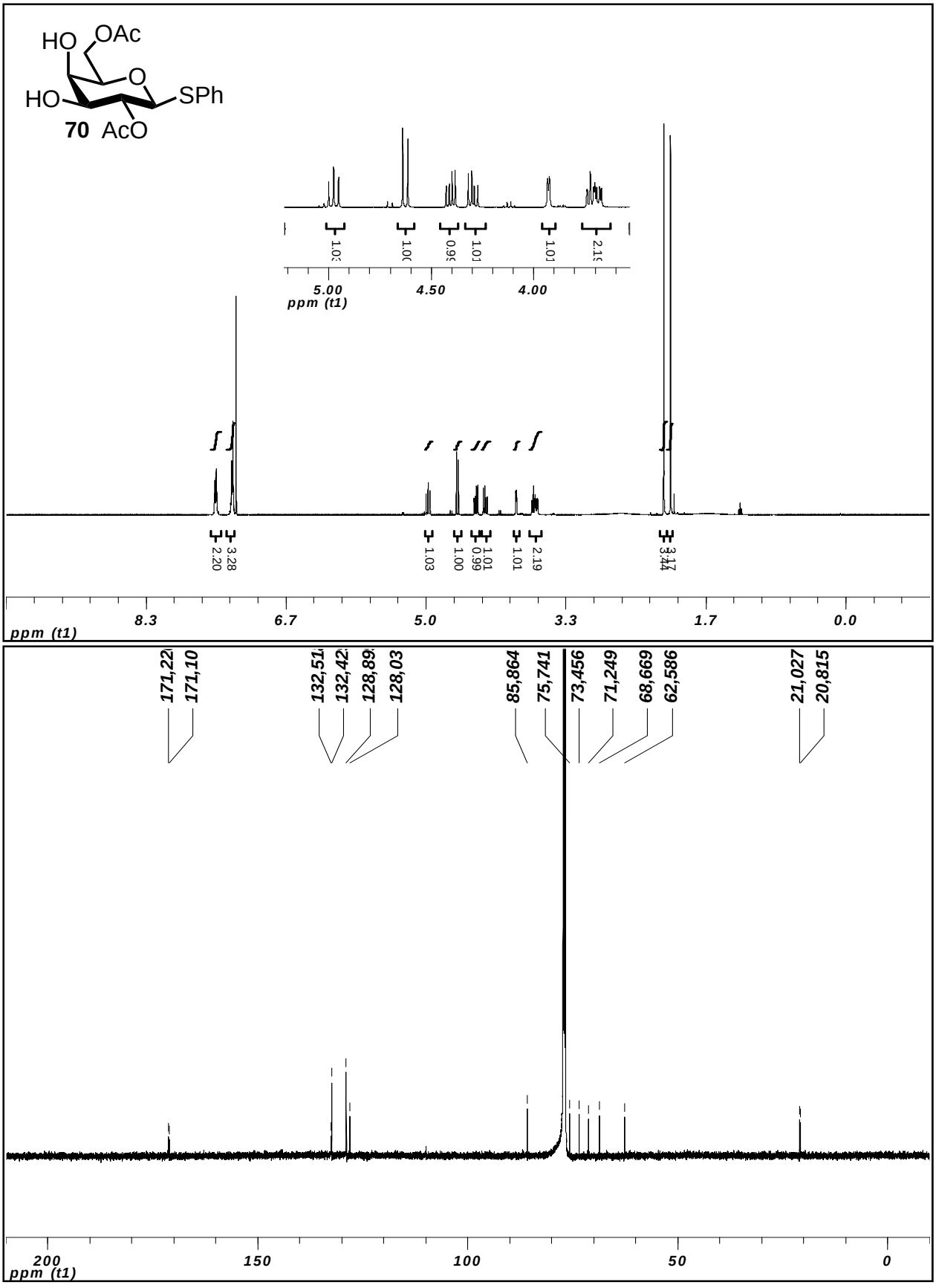
HO
OAc
O
HO
SPh
70 AcO
5.00
4.50
4.00
ppm (t1)
2.20
3.28
1.03
1.00
0.99
1.01
1.01
2.19
3.17
3.44
8.3
6.7
5.0
3.3
1.7
0.0
ppm (t1)
171,22
171,10
132,51
132,42
128,89
128,03
85,864
75,741
73,456
71,249
68,669
62,586
21,027
20,815
200
150
100
50
0
ppm (t1)

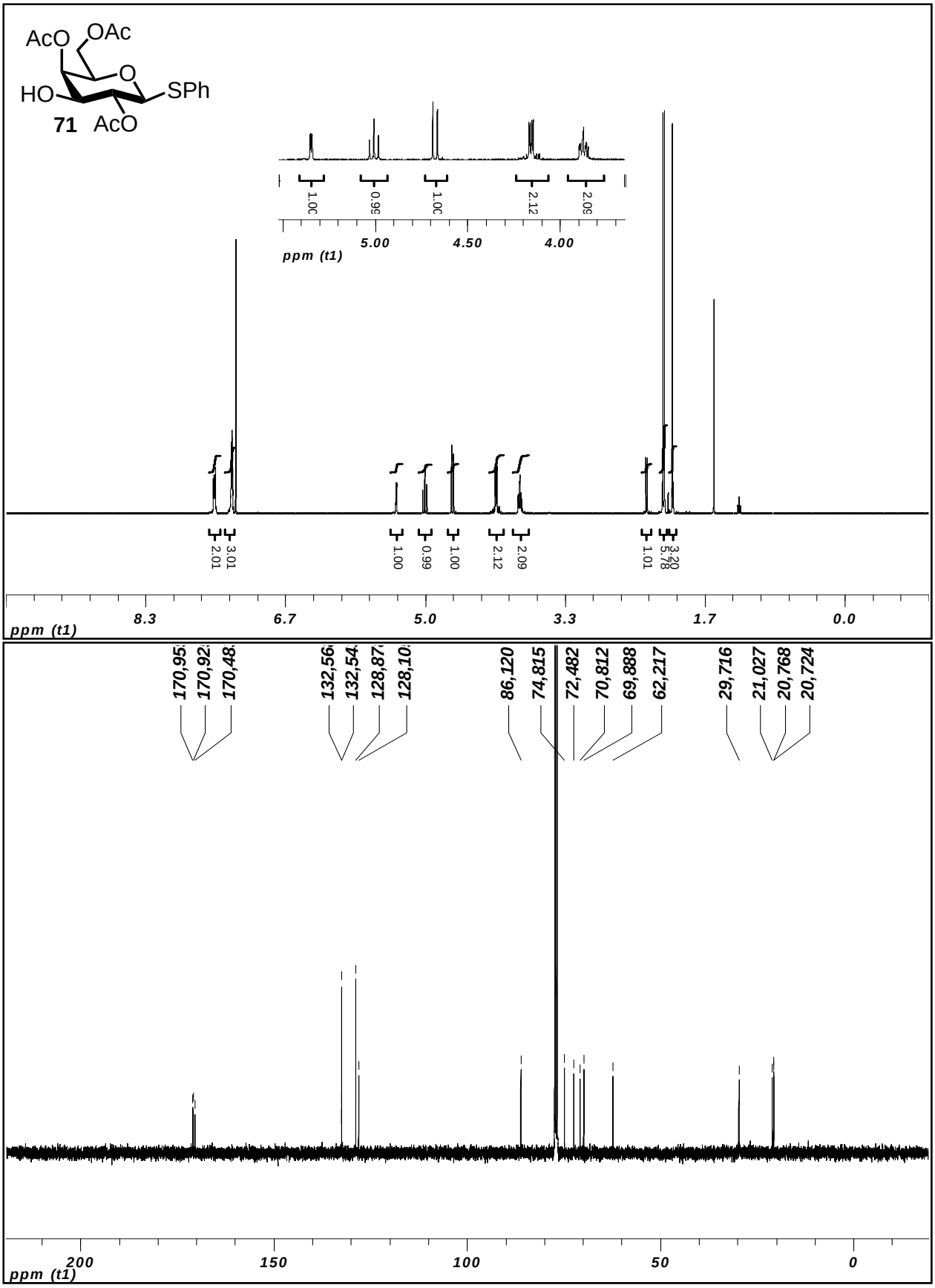
AcO
OAc
O
HO
SPh
71
AcO
1.00
0.99
1.00
2.12
2.09
5.00
4.50
4.00
ppm (t1)
2.01
3.01
1.00
0.99
1.00
2.12
2.09
1.01
3.20
5.78
8.3
6.7
5.0
3.3
1.7
0.0
ppm (t1)
170,95
170,92
170,48
132,56
132,54
128,87
128,10
86,120
74,815
72,482
70,812
69,888
62,217
29,716
21,027
20,768
20,724
200
150
100
50
0
ppm (t1)

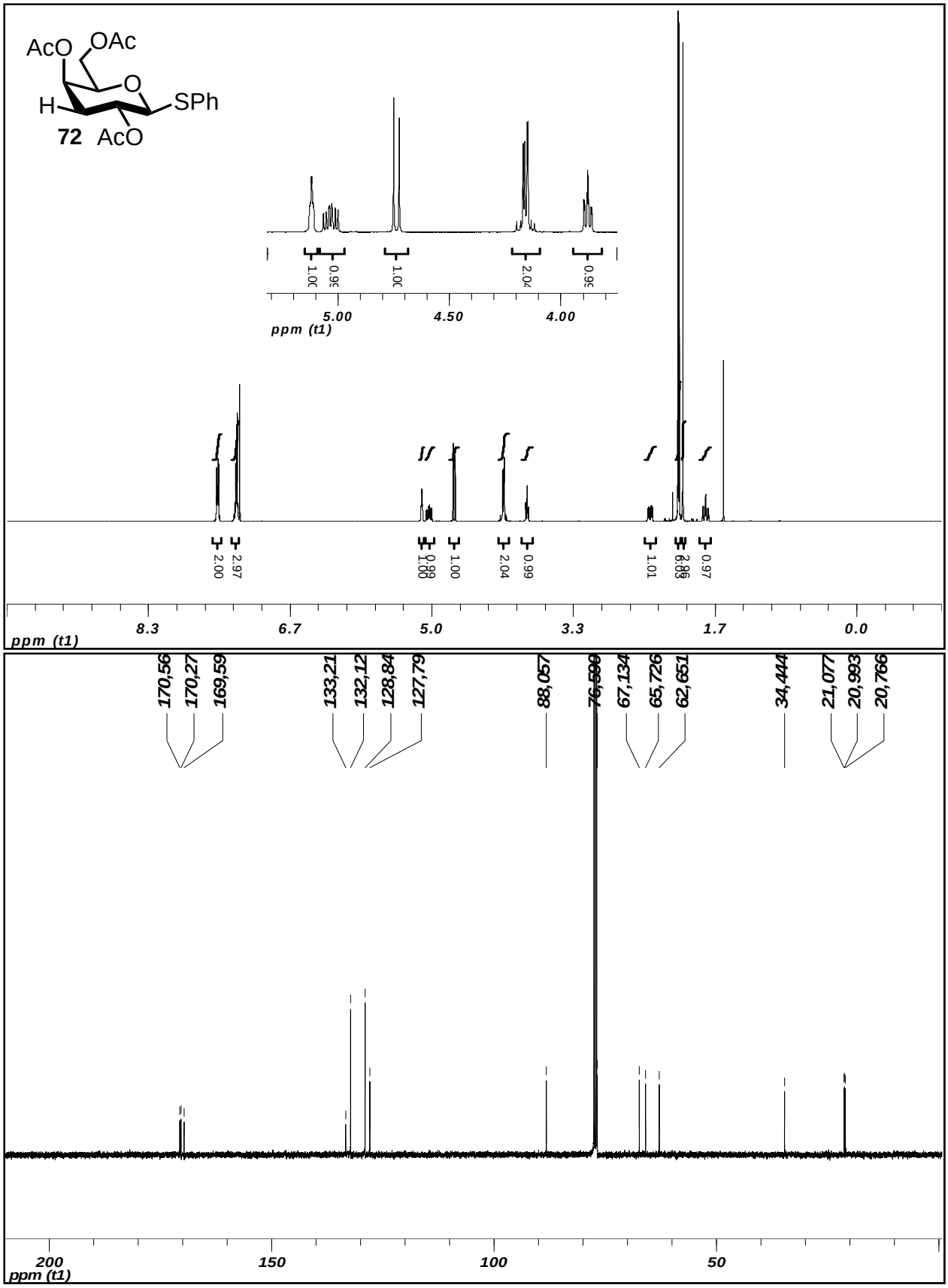
AcO
OAc
O
H
SPh
72 AcO
1.00
0.96
1.00
2.04
0.96
5.00
4.50
4.00
ppm (t1)
2.00
2.97
0.89
1.00
1.00
2.04
0.99
1.01
8.03
0.97
8.3
6.7
5.0
3.3
1.7
0.0
ppm (t1)
170,56
170,27
169,59
133,21
132,12
128,84
127,79
88,057
76,590
67,134
65,726
62,651
34,444
21,077
20,993
20,766
200
150
100
50
ppm (t1)

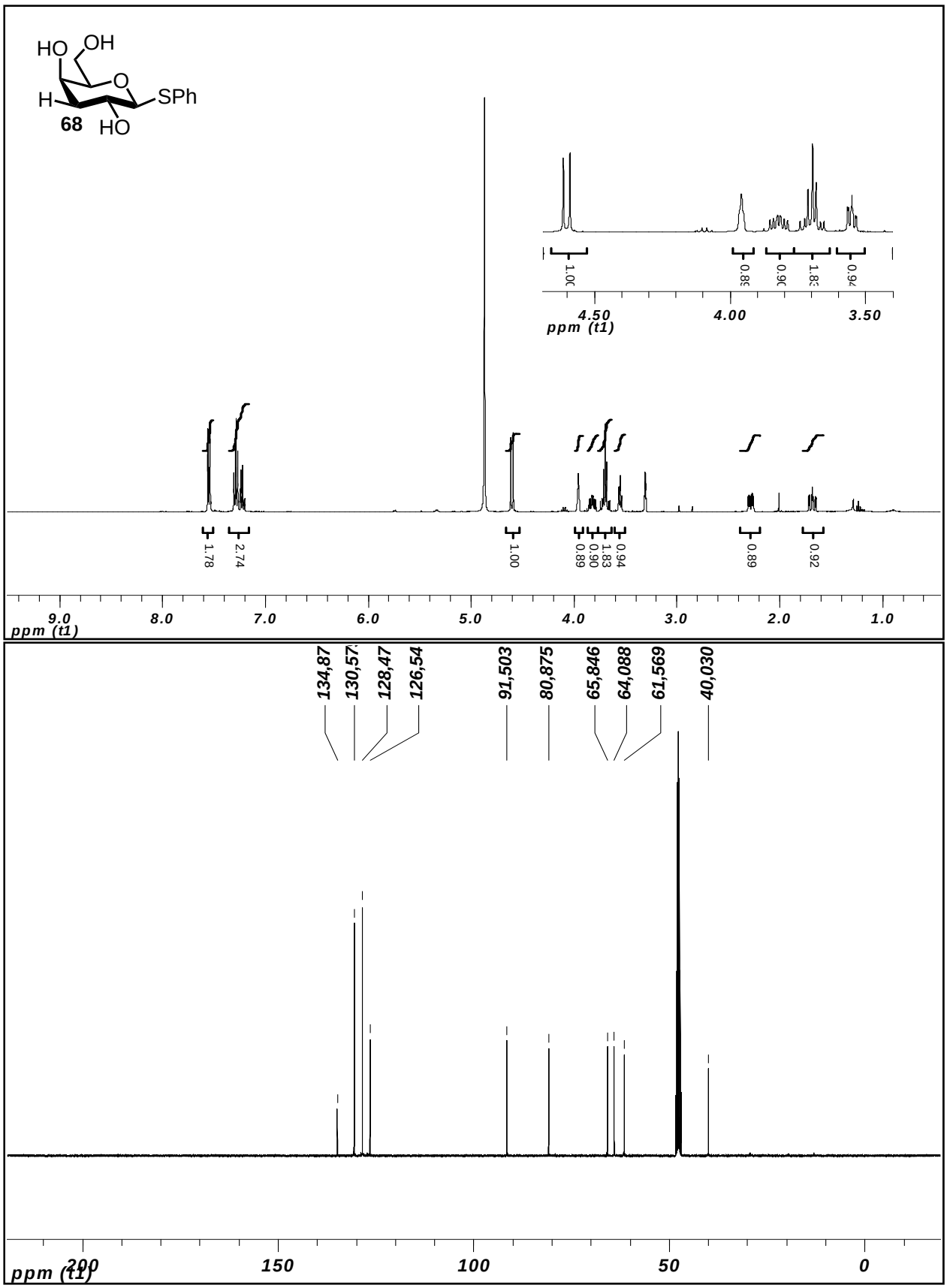
HO
OH
O
H
SPh
68
HO
1.78
2.74
1.00
0.89
0.90
1.83
0.94
0.89
0.92
9.0
8.0
7.0
6.0
5.0
4.0
3.0
2.0
1.0
ppm (t1)
4.50
4.00
3.50
ppm (t1)
134,87
130,57
128,47
126,54
91,503
80,875
65,846
64,088
61,569
40,030
200
150
100
50
0
ppm (t1)

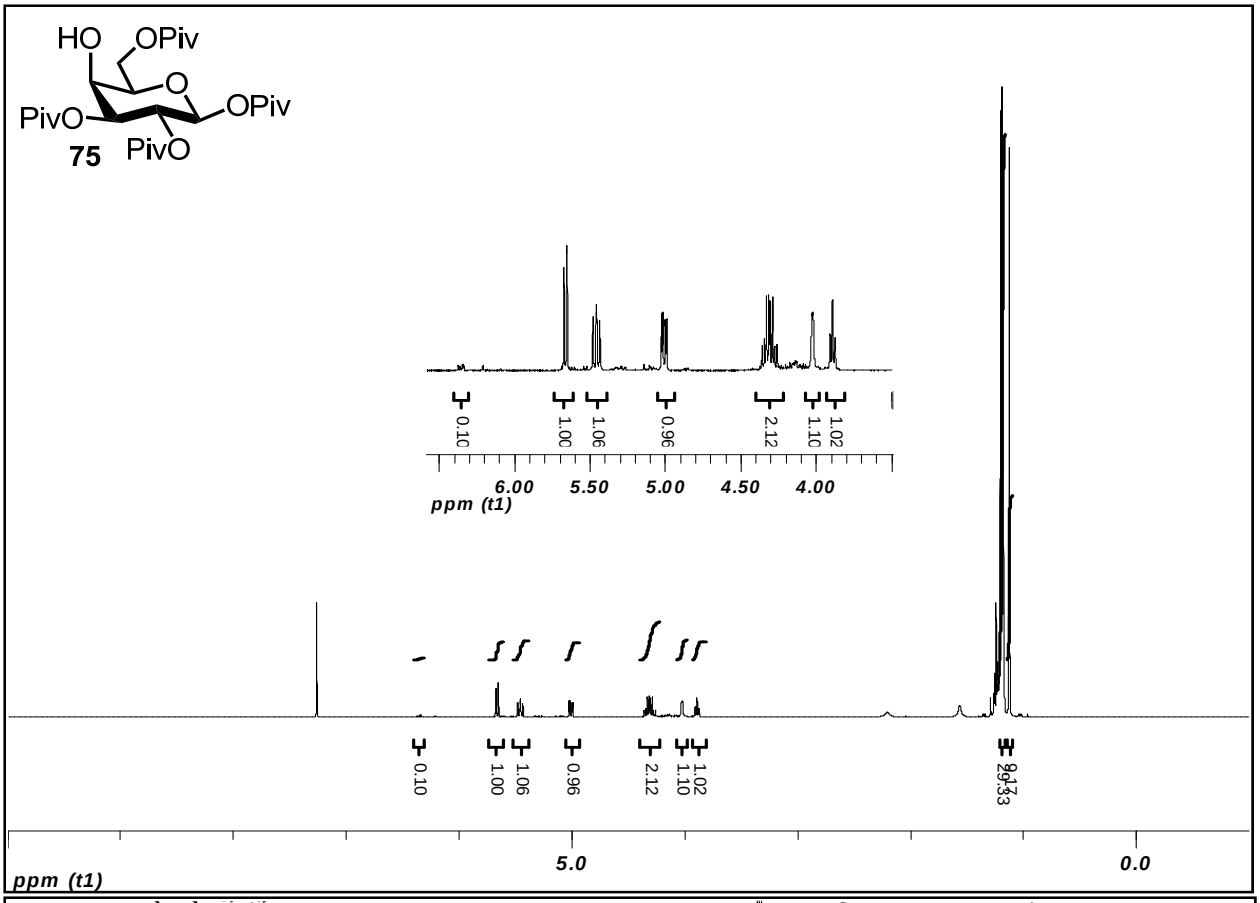
HO
OPiv
O
PivO
OPiv
PivO
75
0.10
1.00
1.06
0.96
2.12
1.10
1.02
6.00
5.50
5.00
4.50
4.00
ppm (t1)
0.10
1.00
1.06
0.96
2.12
1.10
1.02
9.17
29.33
5.0
0.0
ppm (t1)

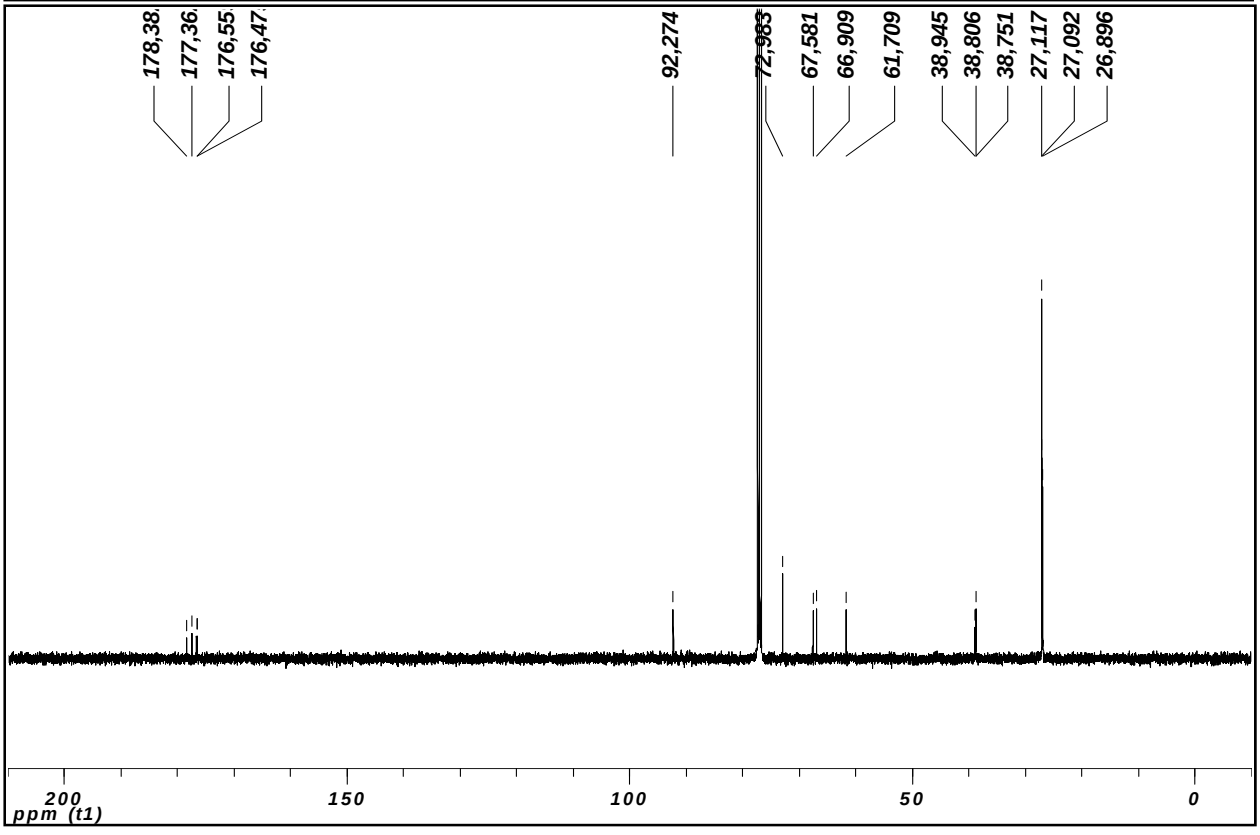
178,38
177,36
176,55
176,47
92,274
72,983
67,581
66,909
61,709
38,945
38,806
38,751
27,117
27,092
26,896
200
150
100
50
0
ppm (t1)

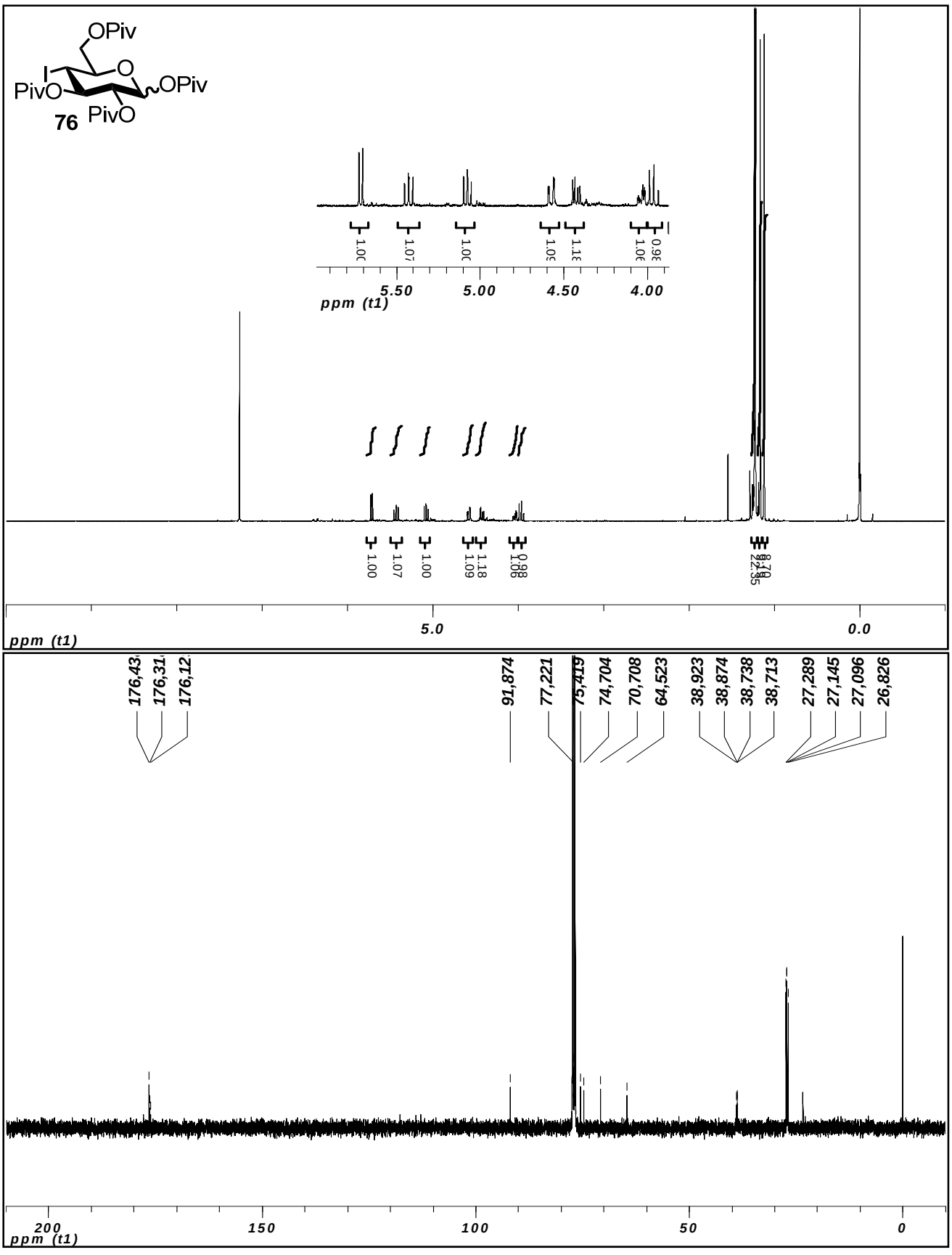
OPiv
PivO
O
OPiv
PivO
76
1.00
1.07
1.00
1.18
1.09
0.88
0.88
22.35
8.70
ppm (t1)
5.0
0.0
176,43
176,31
176,12
91,874
77,221
75,419
74,704
70,708
64,523
38,923
38,874
38,738
38,713
27,289
27,145
27,096
26,826
200
150
100
50
0
ppm (t1)

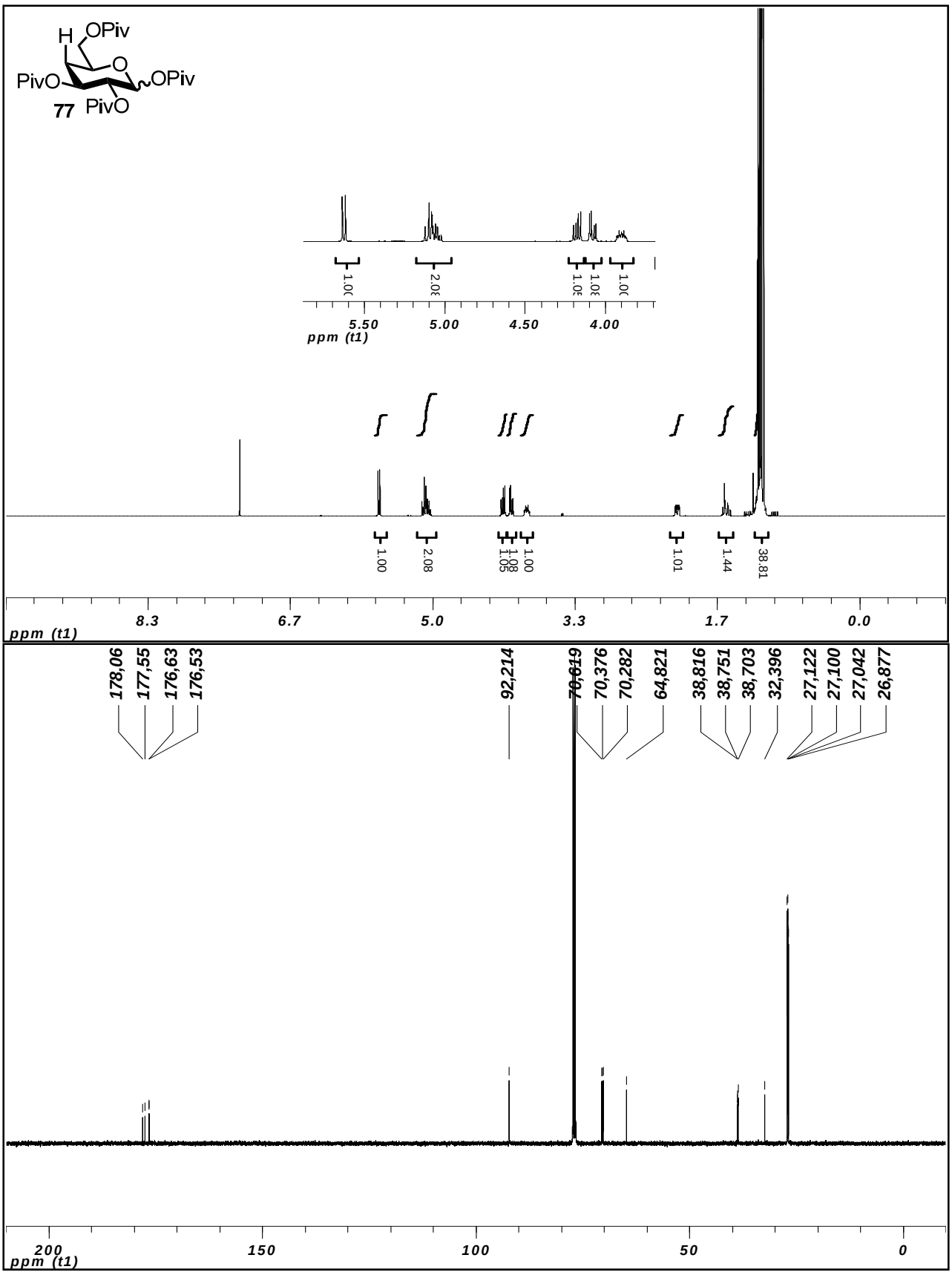
H
OPiv
O
PivO
OPiv
77
PivO
1.00
2.08
1.00
1.08
1.05
1.00
1.01
1.44
38.81
8.3
6.7
5.0
3.3
1.7
0.0
ppm (t1)
178,06
177,55
176,63
176,53
92,214
70,619
70,376
70,282
64,821
38,816
38,751
38,703
32,396
27,122
27,100
27,042
26,877
200
150
100
50
0
ppm (t1)

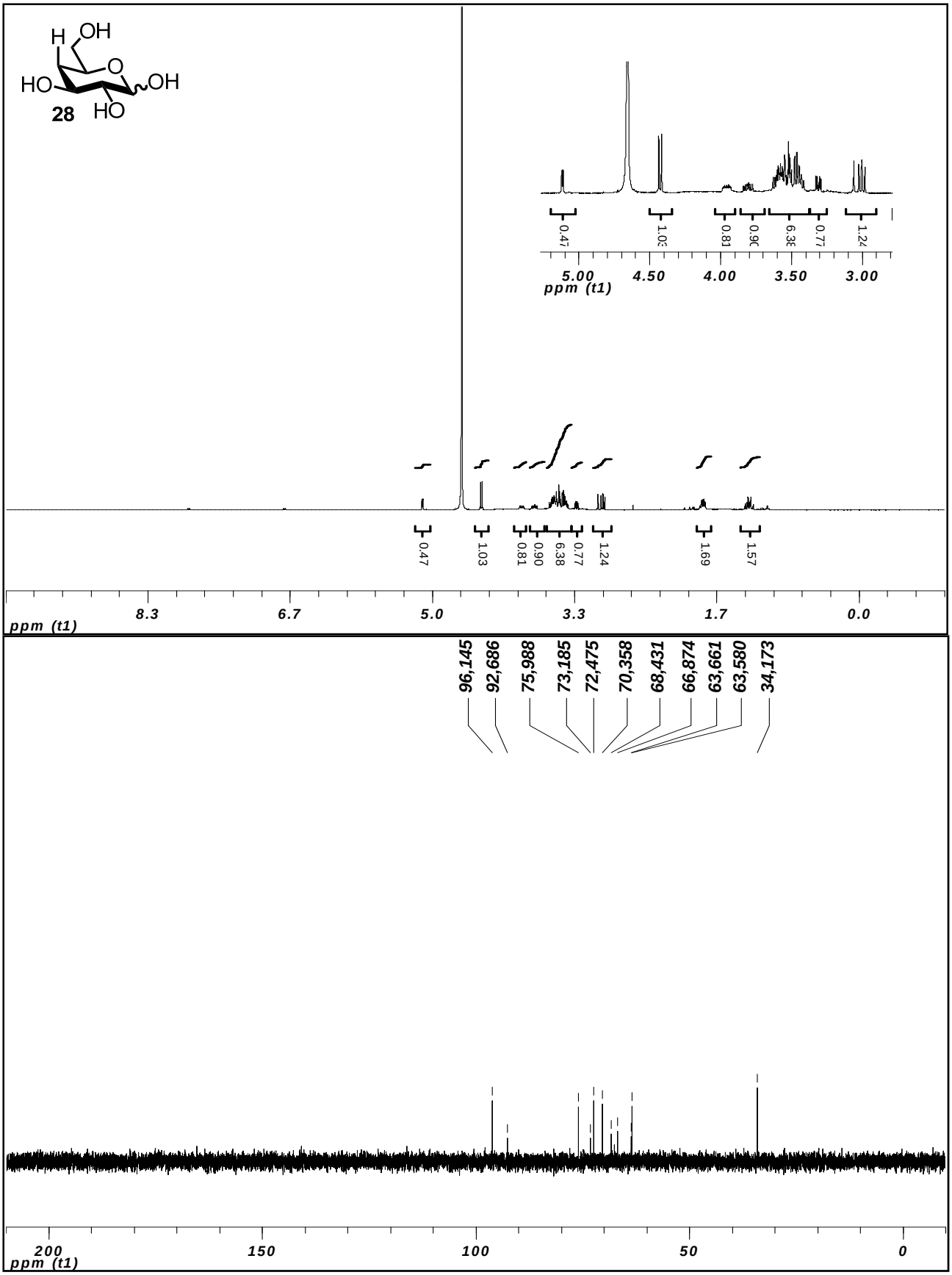
H
OH
O
HO
OH
HO
28
0.47
1.03
0.81
0.90
6.38
0.77
1.24
1.69
1.57
8.3
6.7
5.0
3.3
1.7
0.0
ppm (t1)
96,145
92,686
75,988
73,185
72,475
70,358
68,431
66,874
63,661
63,580
34,173
200
150
100
50
0
ppm (t1)

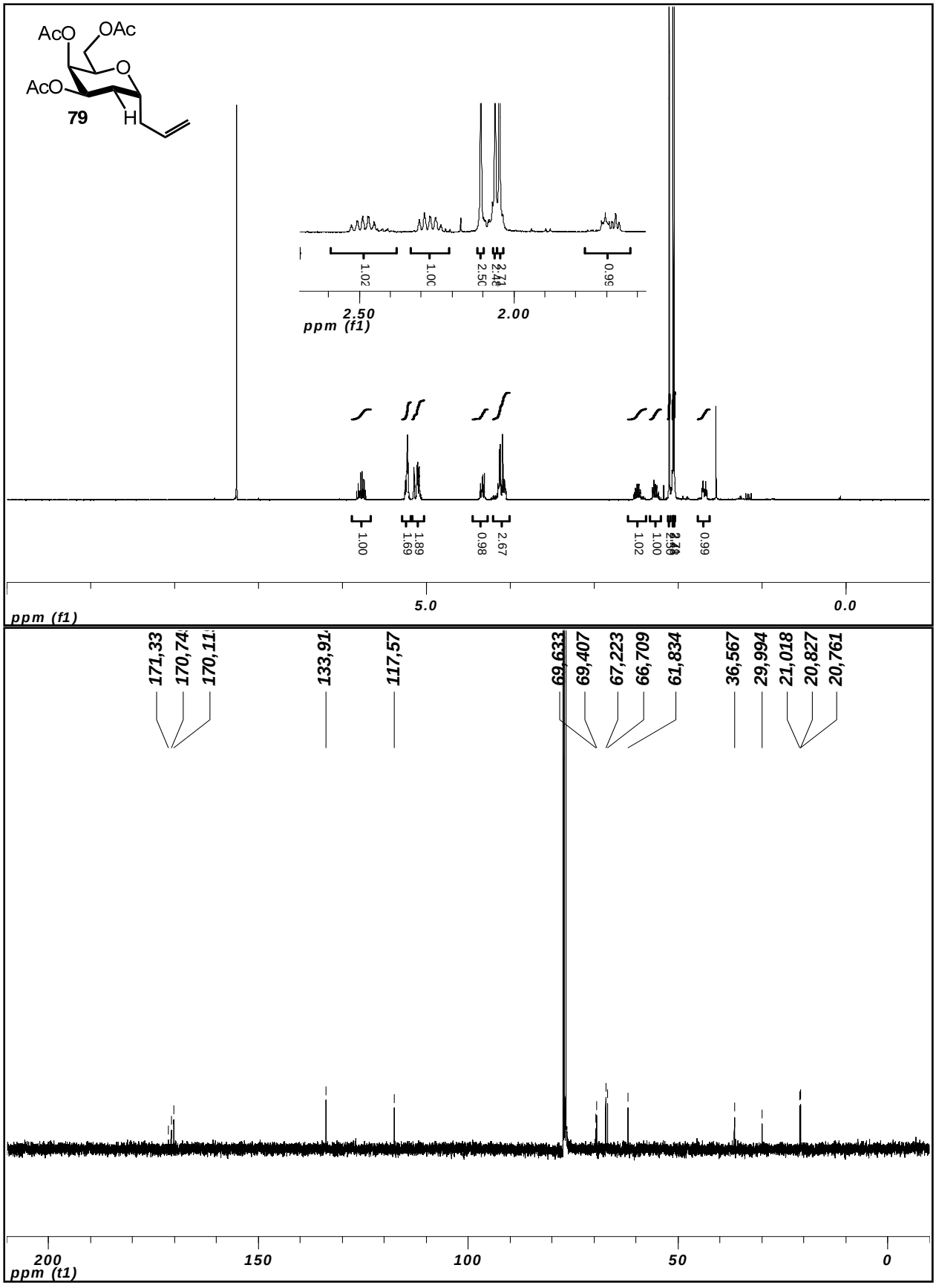
AcO
OAc
O
AcO
79
H
1.02
1.00
2.50
2.71
0.95
2.50
2.00
ppm (f1)
1.00
1.89
0.98
2.67
1.02
1.00
0.99
5.0
0.0
ppm (f1)
171,33
170,74
170,11
133,91
117,57
69,633
69,407
67,223
66,709
61,834
36,567
29,994
21,018
20,827
20,761
200
150
100
50
0
ppm (t1)

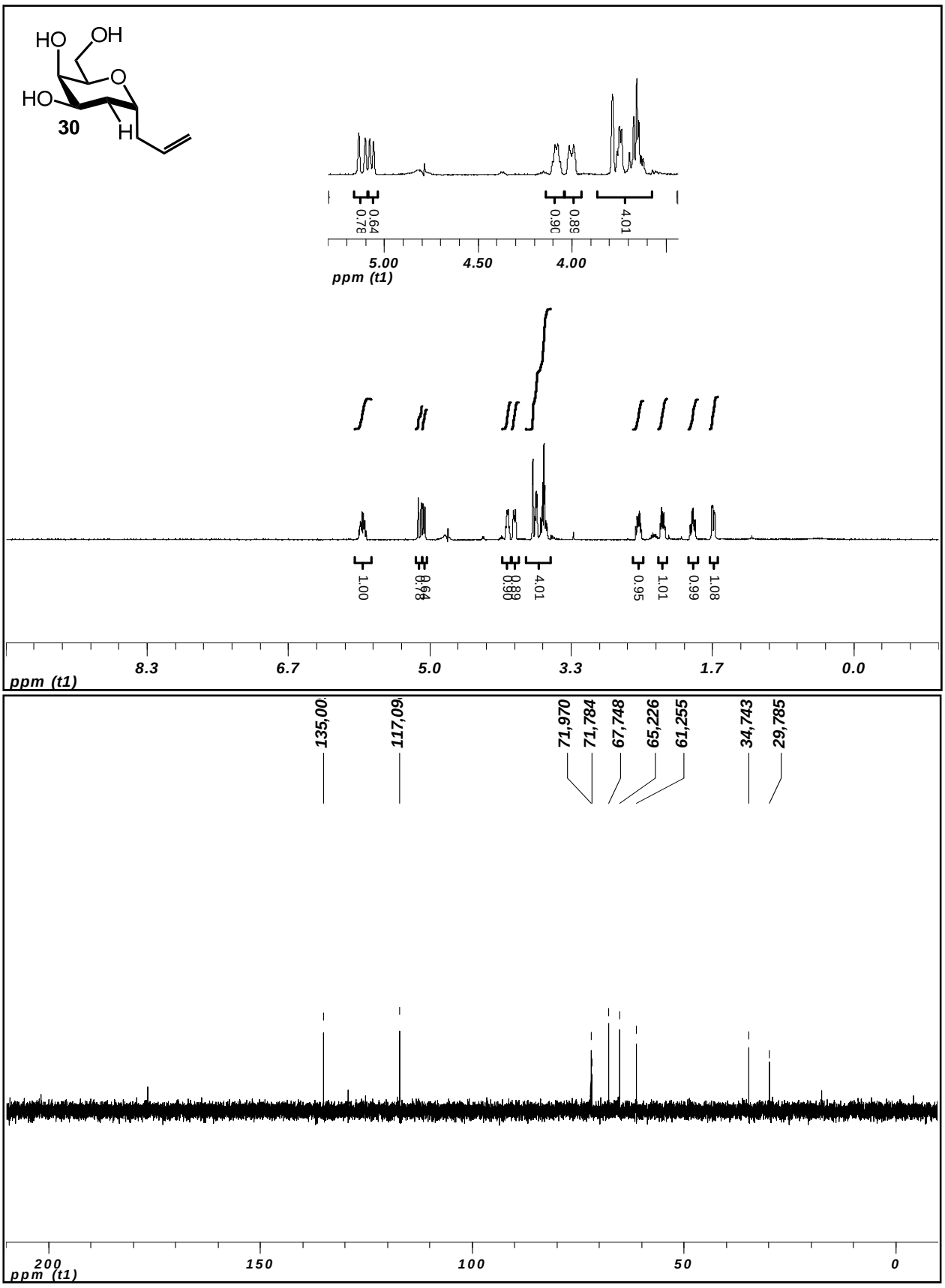
HO
OH
O
HO
30
H
0.64
0.78
0.89
0.90
4.01
5.00
4.50
4.00
ppm (t1)
1.00
0.64
0.88
0.90
4.01
0.95
1.01
0.99
1.08
8.3
6.7
5.0
3.3
1.7
0.0
ppm (t1)
135,00
117,09
71,970
71,784
67,748
65,226
61,255
34,743
29,785
200
150
100
50
0
ppm (t1)

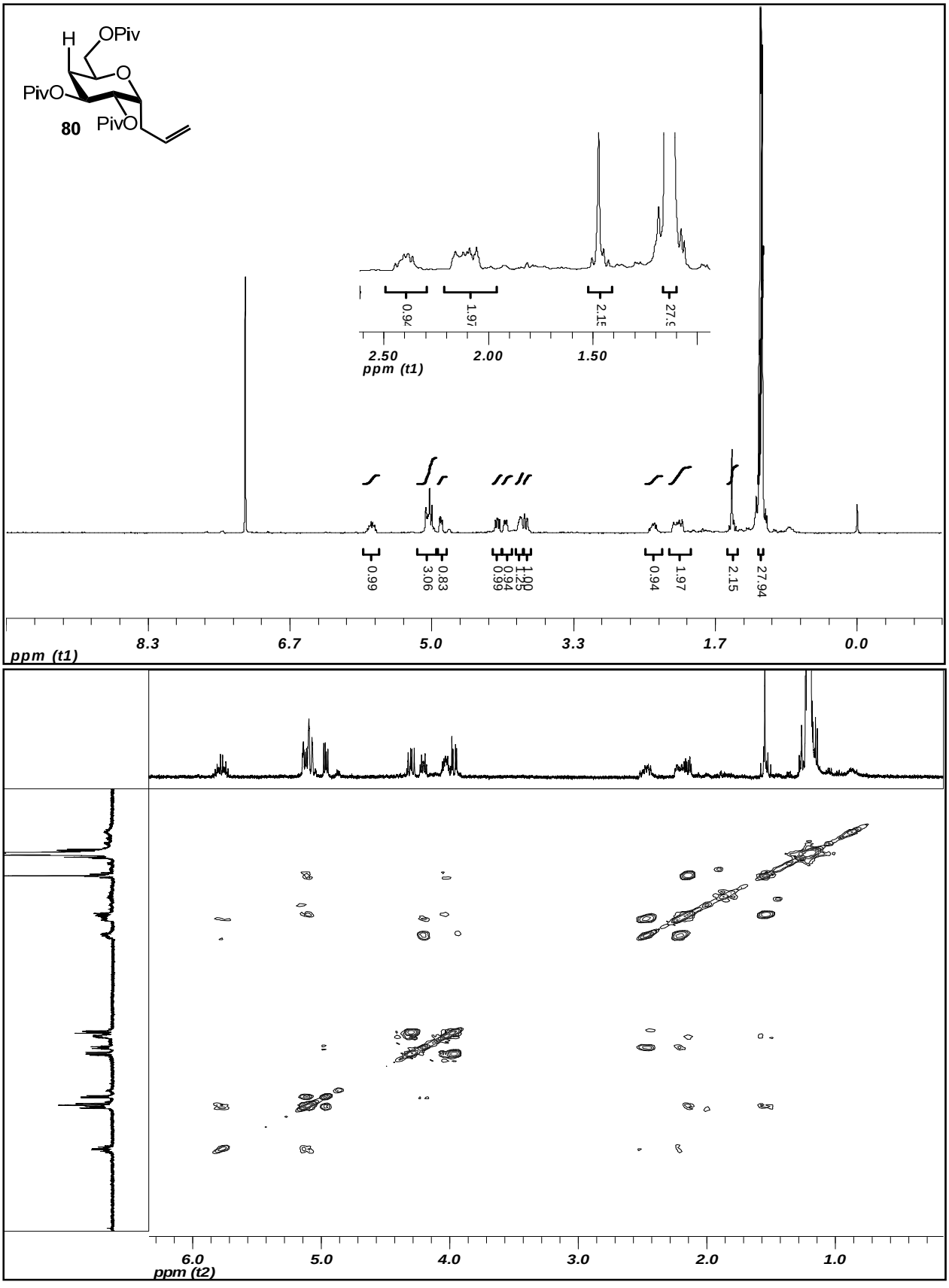
H
OPiv
O
PivO
PivO
80
0.99
3.06
0.83
0.94
0.99
0.94
1.97
2.15
27.94
8.3
6.7
5.0
3.3
1.7
0.0
ppm (t1)
2.50
2.00
1.50
ppm (t1)
6.0
5.0
4.0
3.0
2.0
1.0
ppm (t2)

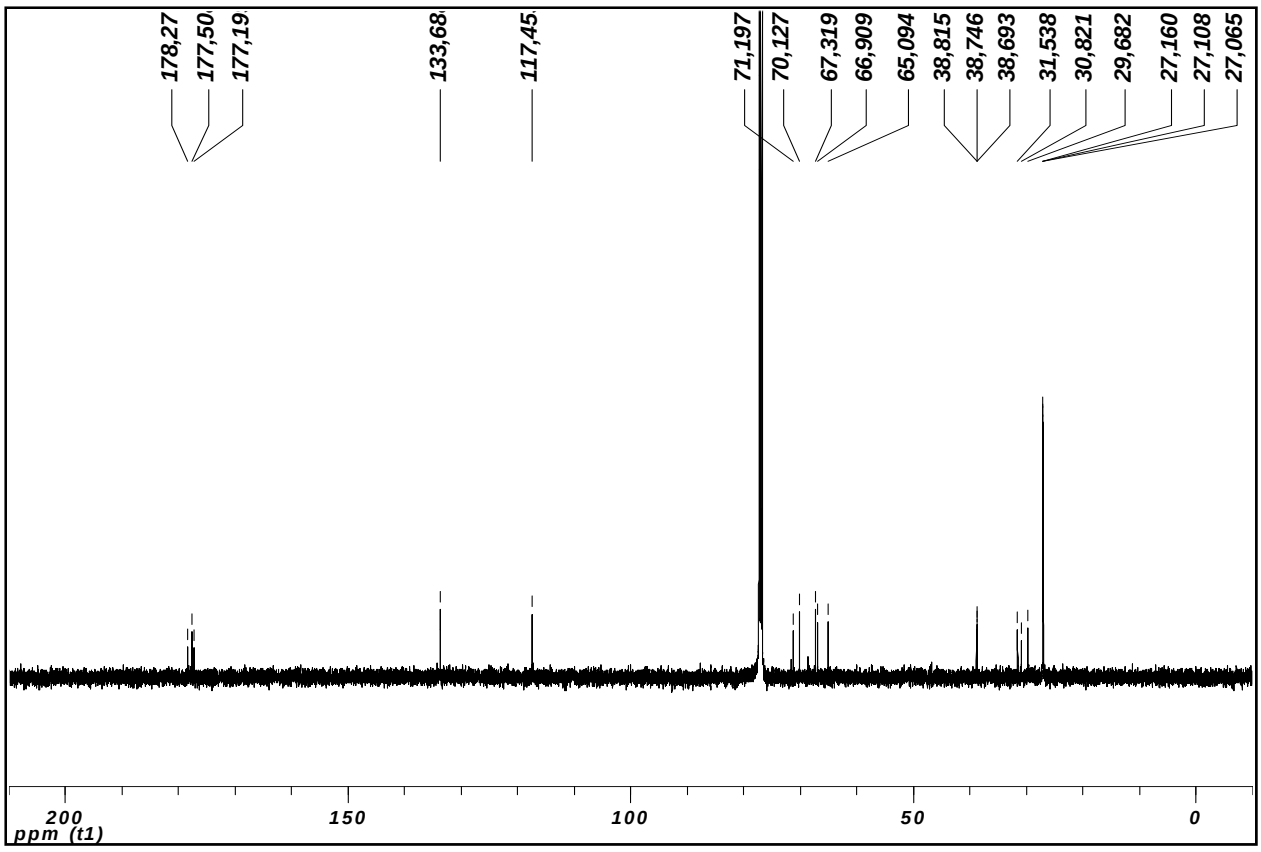
178,27
177,50
177,19
133,68
117,45
71,197
70,127
67,319
66,909
65,094
38,815
38,746
38,693
31,538
30,821
29,682
27,160
27,108
27,065
200
150
100
50
0
ppm (t1)

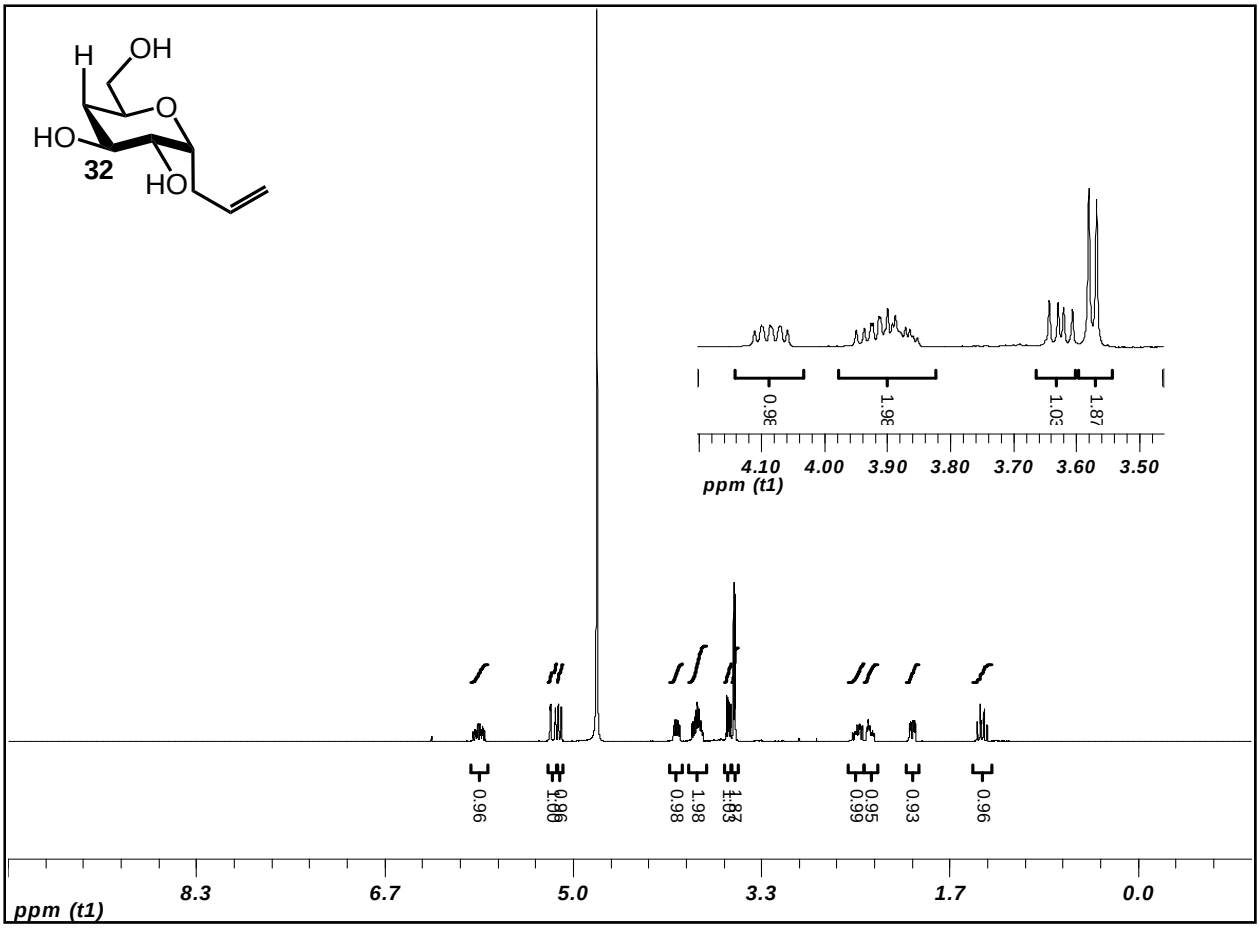
H
OH
O
HO
32
HO
0.96
1.96
1.03
1.87
4.10
4.00
3.90
3.80
3.70
3.60
3.50
ppm (t1)
0.96
1.00
0.98
1.98
1.87
0.99
0.95
0.93
0.96
8.3
6.7
5.0
3.3
1.7
0.0
ppm (t1)

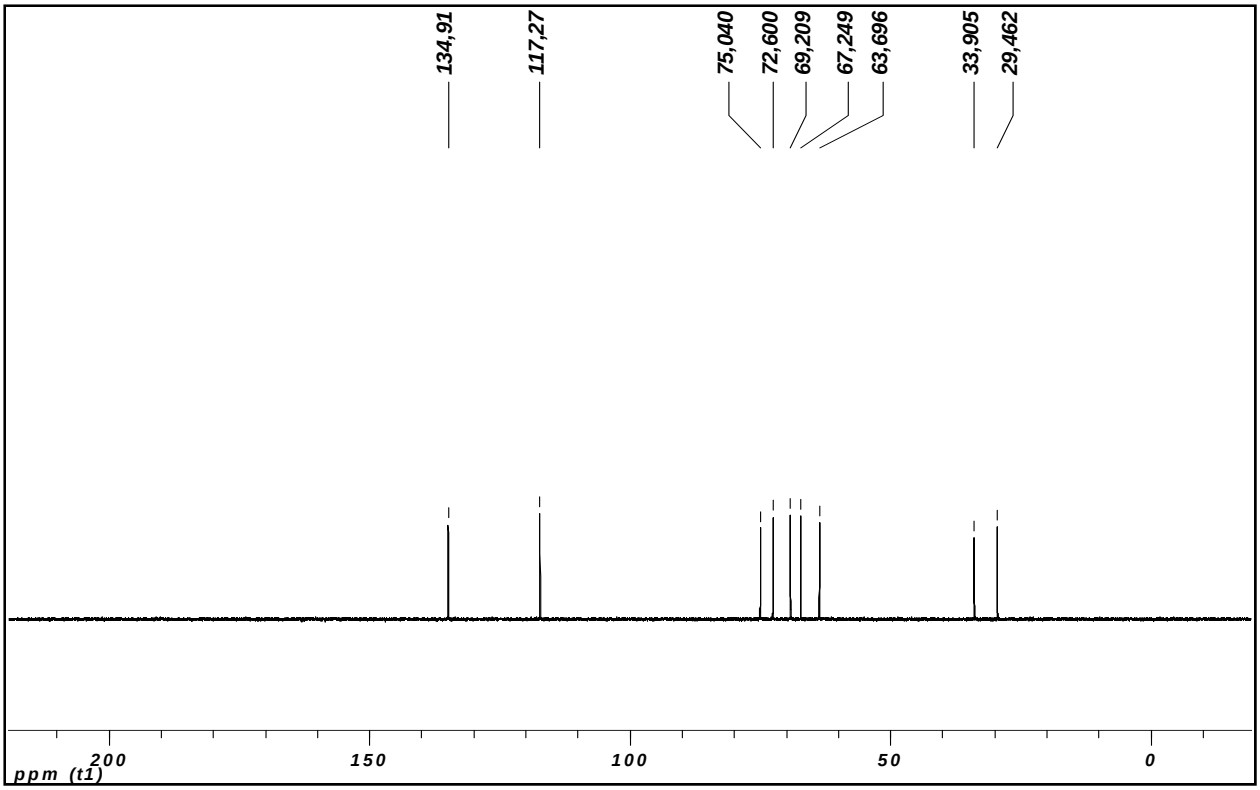
134,91
117,27
75,040
72,600
69,209
67,249
63,696
33,905
29,462
200
150
100
50
0
ppm (t1)

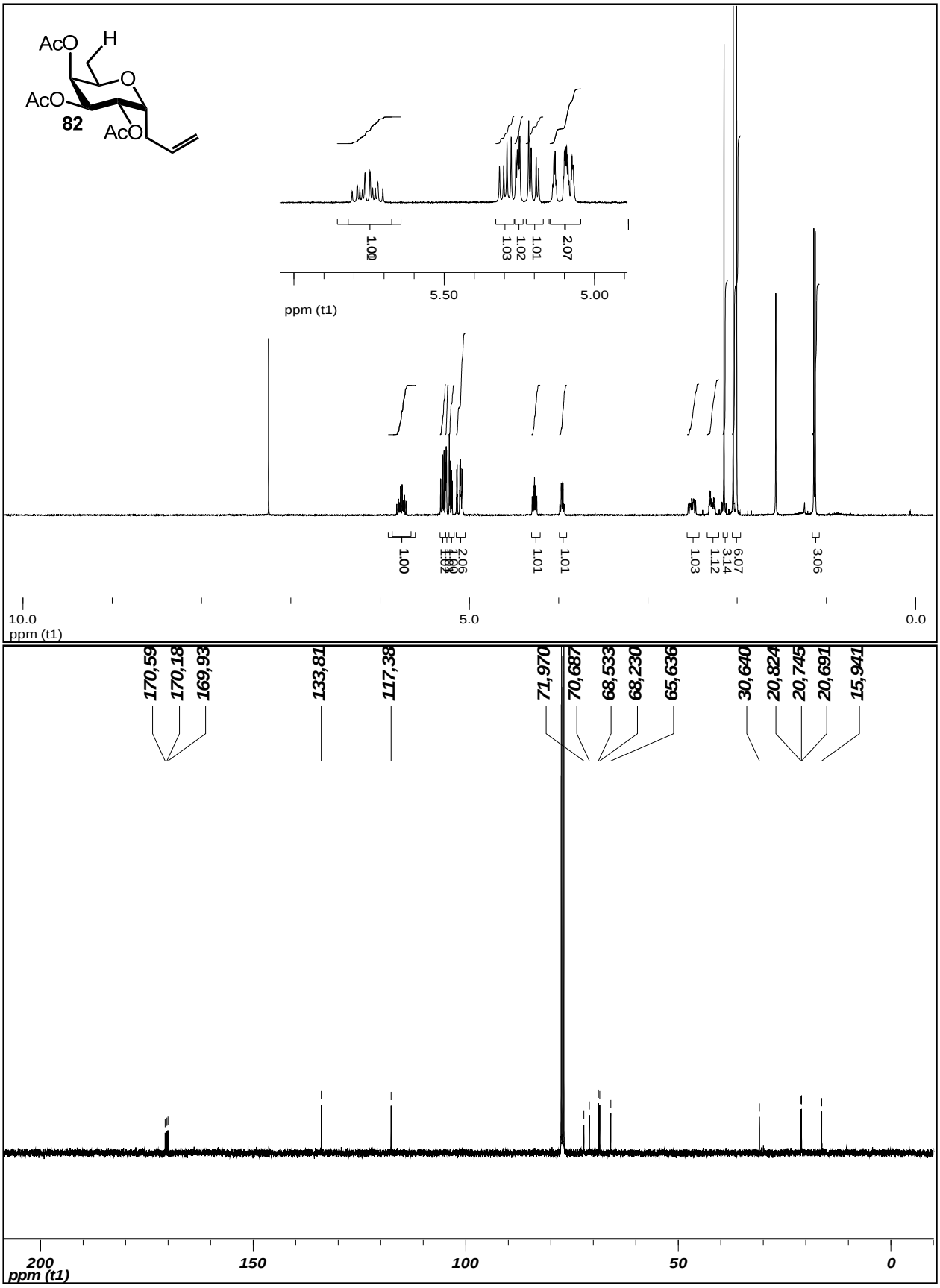
AcO
H
O
AcO
82
AcO
1.00
1.03
1.02
1.01
2.07
5.50
5.00
ppm (t1)
1.00
2.06
1.01
1.01
1.03
1.12
3.14
6.07
3.06
10.0
5.0
0.0
ppm (t1)
170,59
170,18
169,93
133,81
117,38
71,970
70,687
68,533
68,230
65,636
30,640
20,824
20,745
20,691
15,941
200
150
100
50
0
ppm (t1)

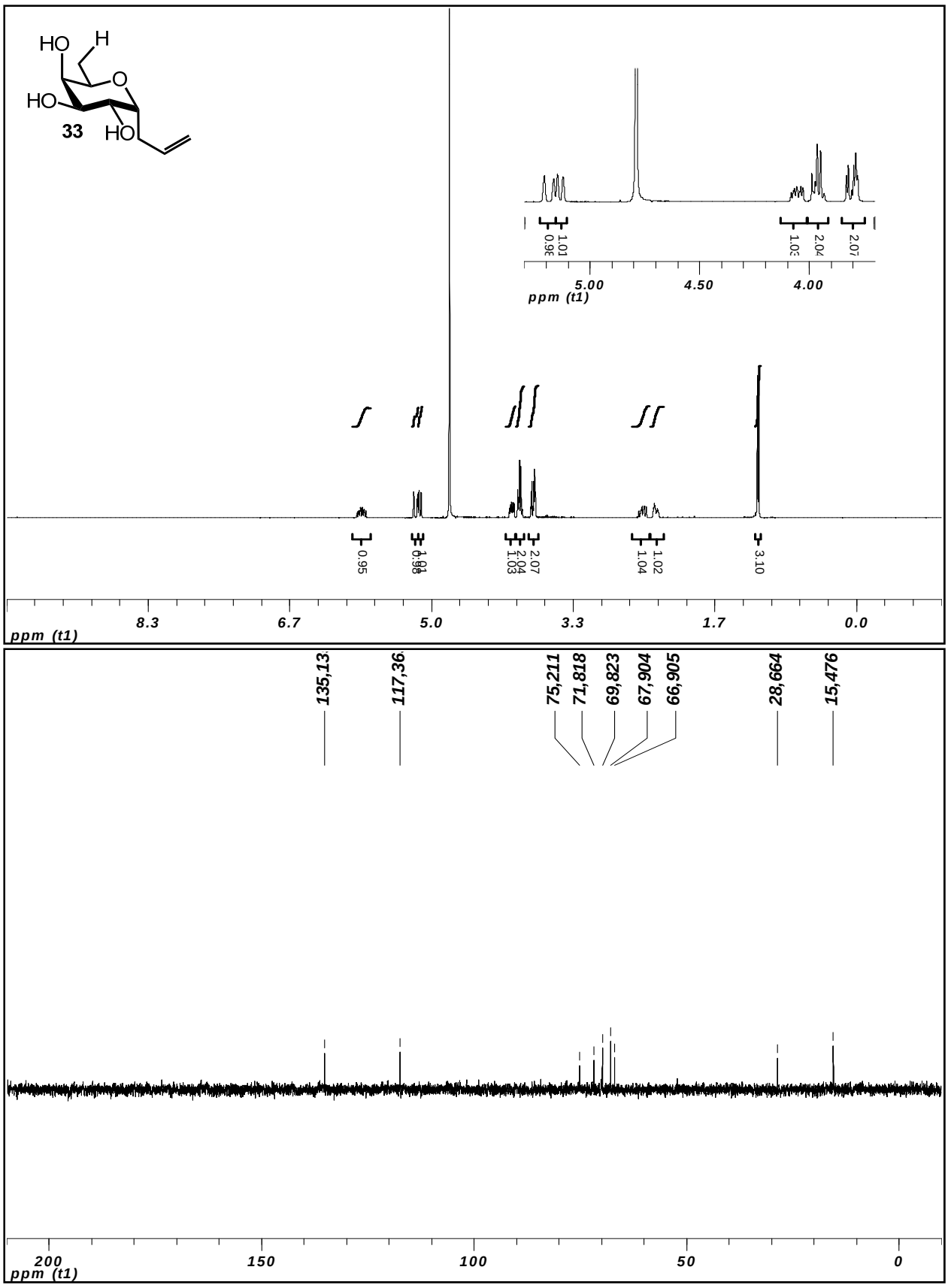
HO
H
O
HO
33
HO
0.95
0.98
2.04
1.03
2.07
1.04
1.02
3.10
8.3
6.7
5.0
3.3
1.7
0.0
ppm (t1)
0.93
1.01
1.03
2.04
2.07
5.00
4.50
4.00
ppm (t1)
135,13
117,36
75,211
71,818
69,823
67,904
66,905
28,664
15,476
200
150
100
50
0
ppm (t1)

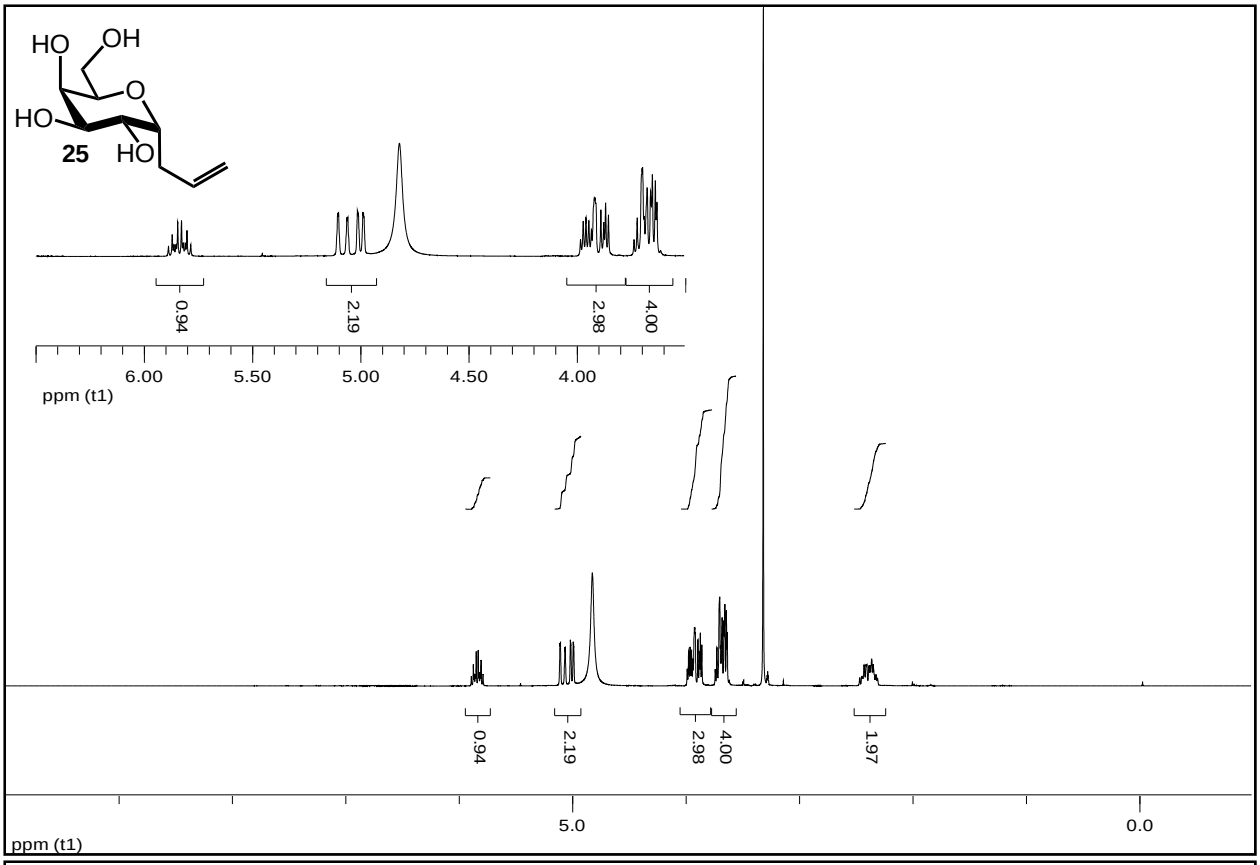
HO
OH
O
HO
HO
25
0.94
2.19
2.98
4.00
6.00
5.50
5.00
4.50
4.00
ppm (t1)
0.94
2.19
2.98
4.00
1.97
5.0
0.0
ppm (t1)

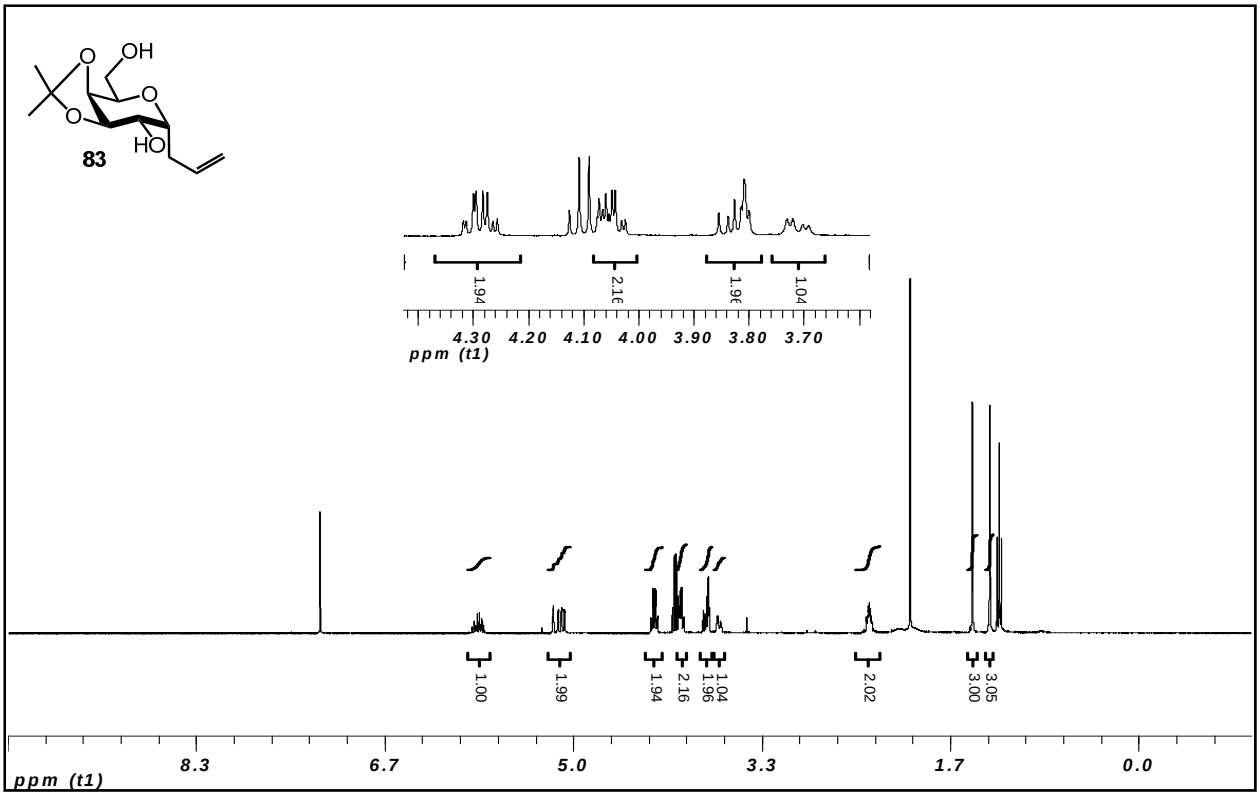
O
OH
O
O
HO
83
1.94
2.16
1.96
1.04
4.30
4.20
4.10
4.00
3.90
3.80
3.70
ppm (t1)
1.00
1.99
1.94
2.16
1.96
1.04
2.02
3.00
3.05
8.3
6.7
5.0
3.3
1.7
0.0
ppm (t1)

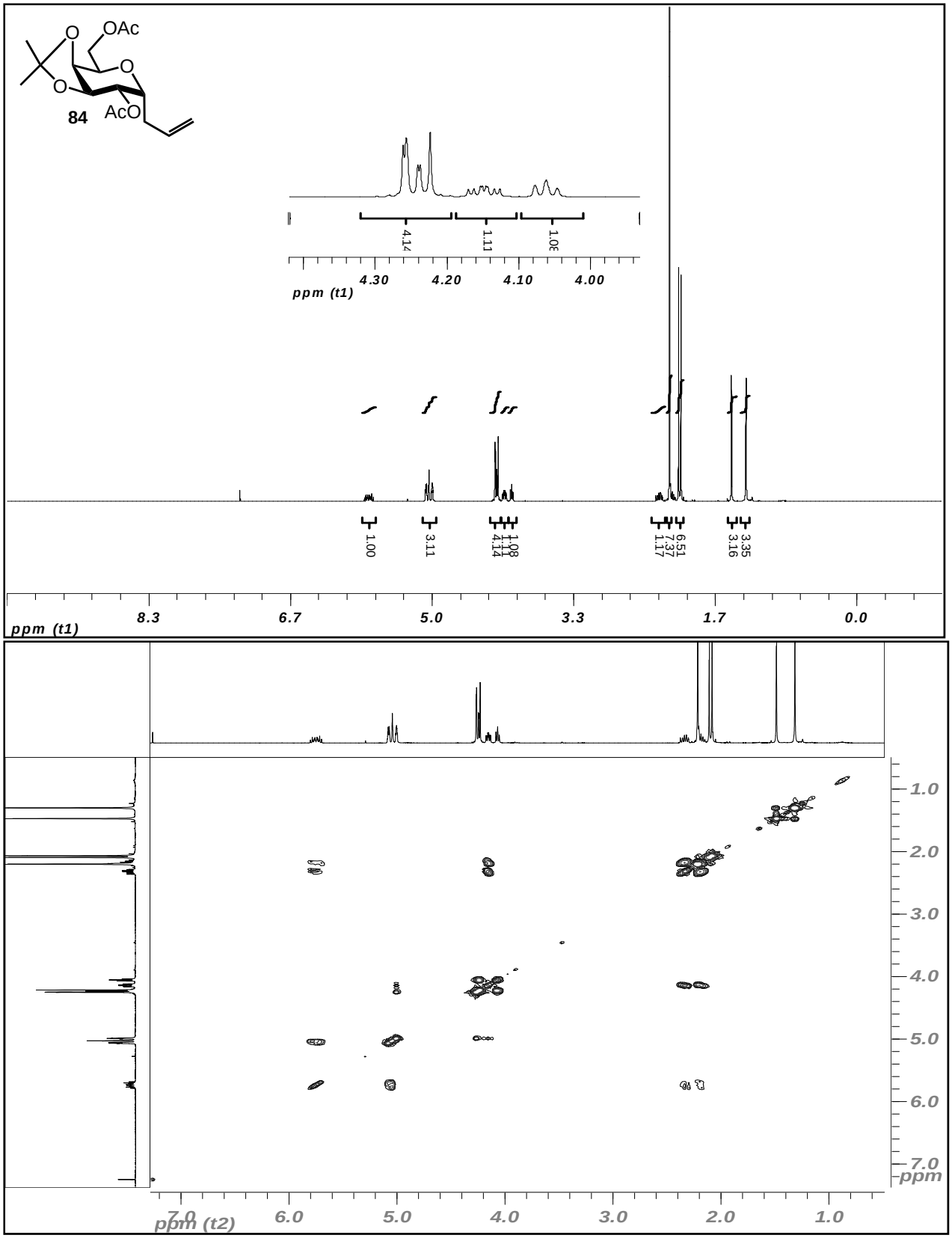
OAc
O
O
O
AcO
84
4.14
1.11
1.08
4.30
4.20
4.10
4.00
ppm (t1)
1.00
3.11
1.08
1.11
4.14
6.51
7.37
1.17
3.35
3.16
8.3
6.7
5.0
3.3
1.7
0.0
ppm (t1)
1.0
2.0
3.0
4.0
5.0
6.0
7.0
ppm
7.0
6.0
5.0
4.0
3.0
2.0
1.0
ppm (t2)

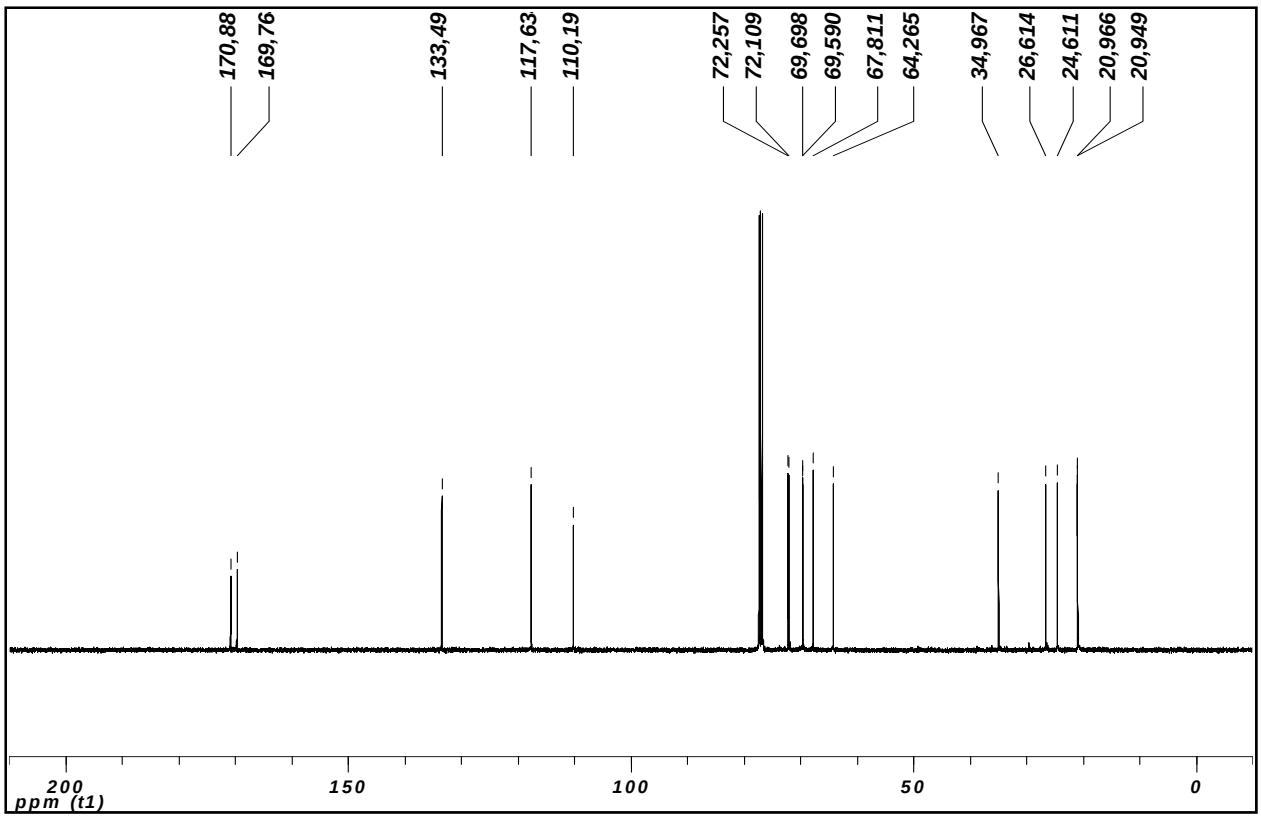
170,88
169,76
133,49
117,63
110,19
72,257
72,109
69,698
69,590
67,811
64,265
34,967
26,614
24,611
20,966
20,949
200
150
100
50
0
ppm (t1)

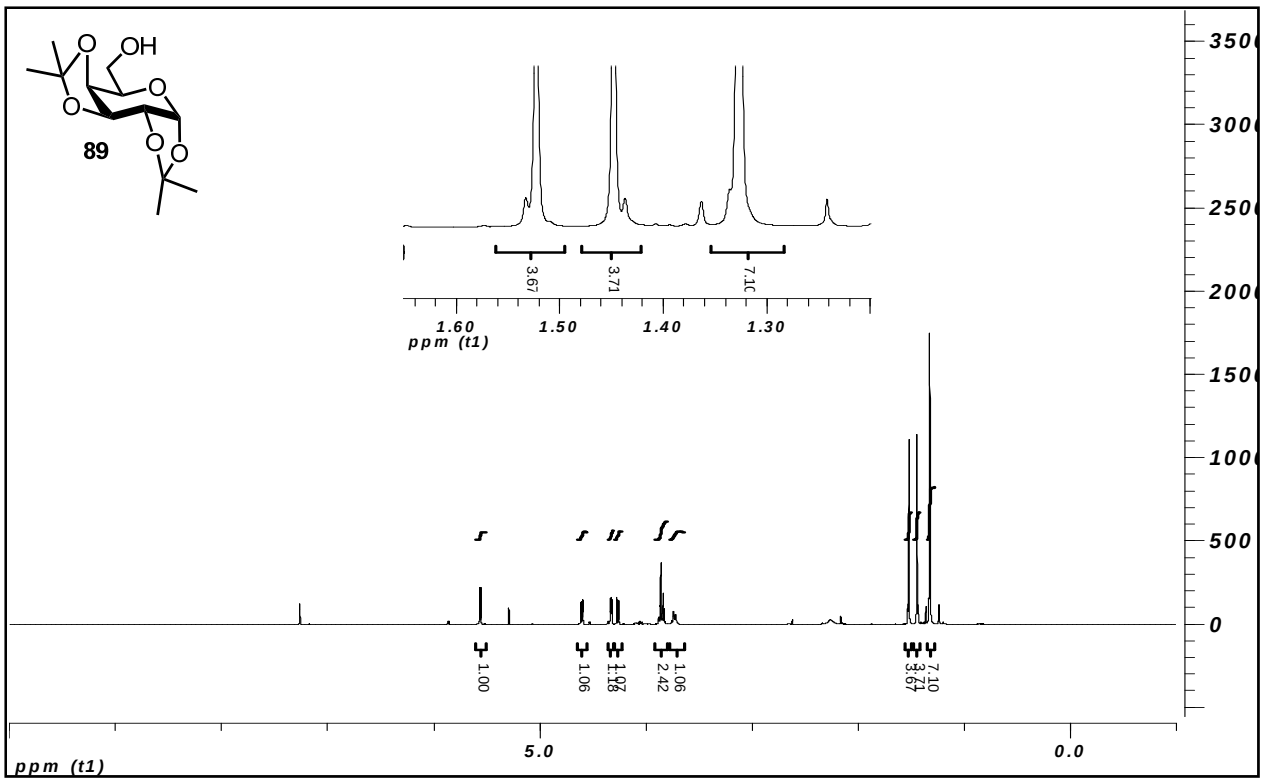
89
OH
O
O
O
O
O
3.67
3.71
7.10
1.60
1.50
1.40
1.30
ppm (t1)
1.00
1.06
1.07
1.08
2.42
1.06
7.10
3.71
3.67
5.0
0.0
ppm (t1)

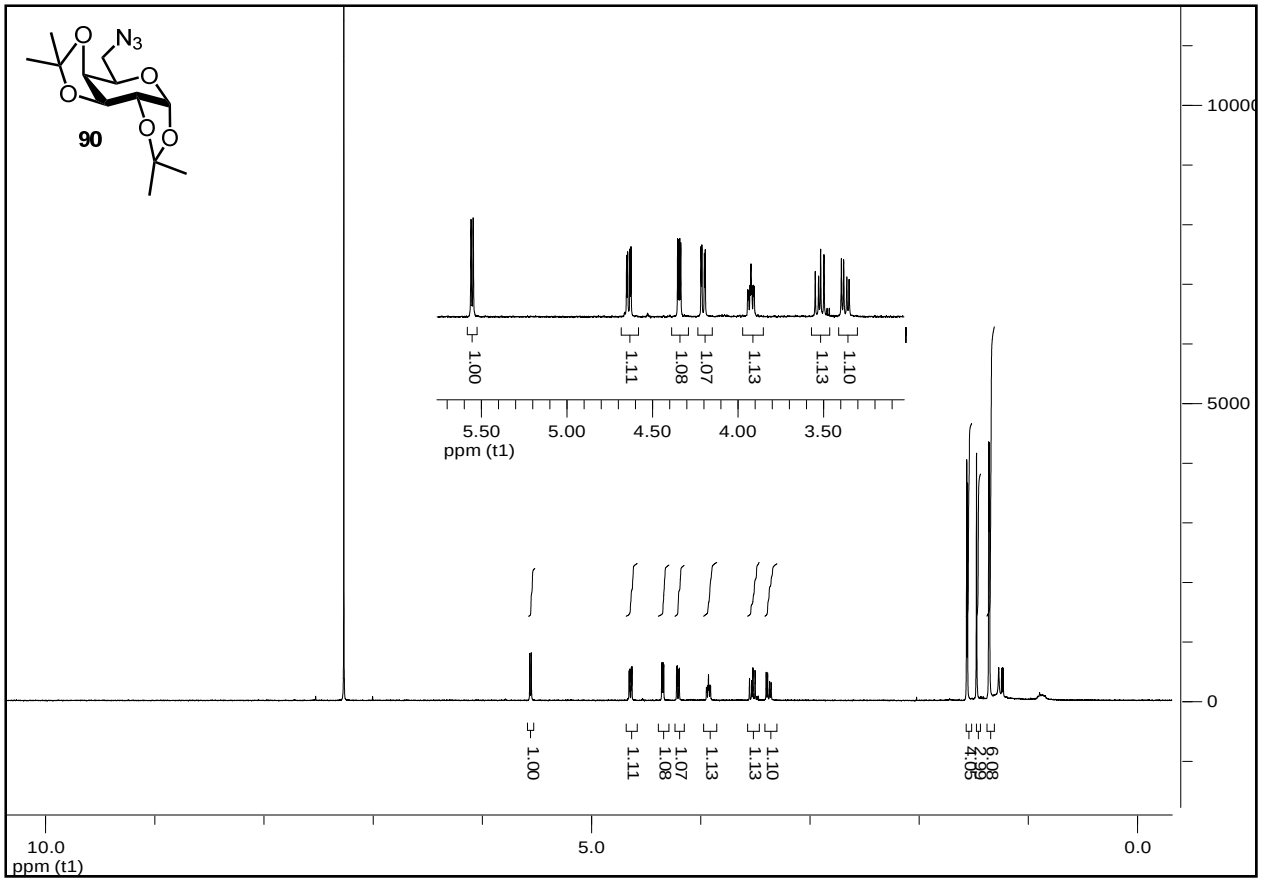
90
N3
O
O
O
O
O
1.00
1.11
1.08
1.07
1.13
1.13
1.10
5.50
5.00
4.50
4.00
3.50
ppm (t1)
10000
5000
0
1.00
1.11
1.08
1.07
1.13
1.10
1.13
6.08
4.05
10.0
5.0
0.0
ppm (t1)

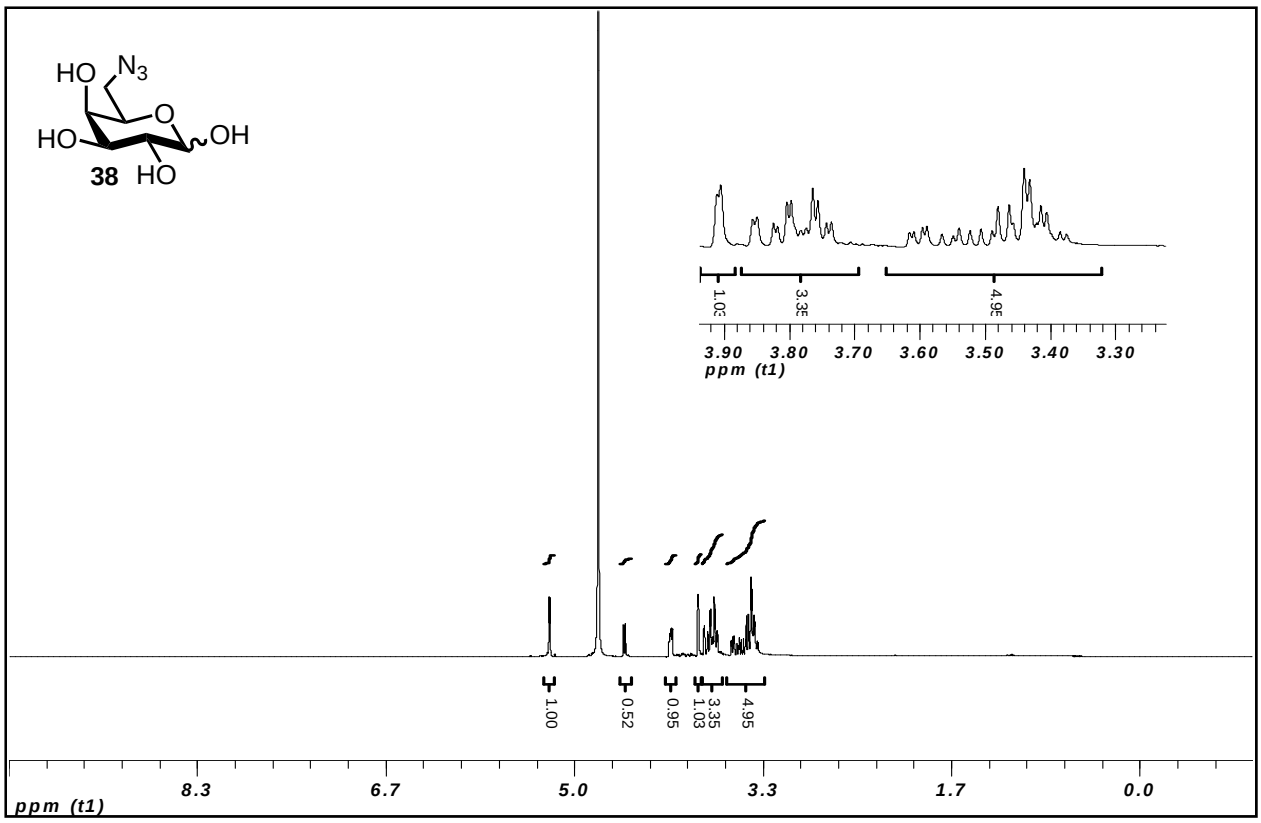
HO
N3
O
HO
OH
38
HO
3.90
3.80
3.70
3.60
3.50
3.40
3.30
ppm (t1)
1.00
0.52
0.95
1.03
3.35
4.95
8.3
6.7
5.0
3.3
1.7
0.0
ppm (t1)

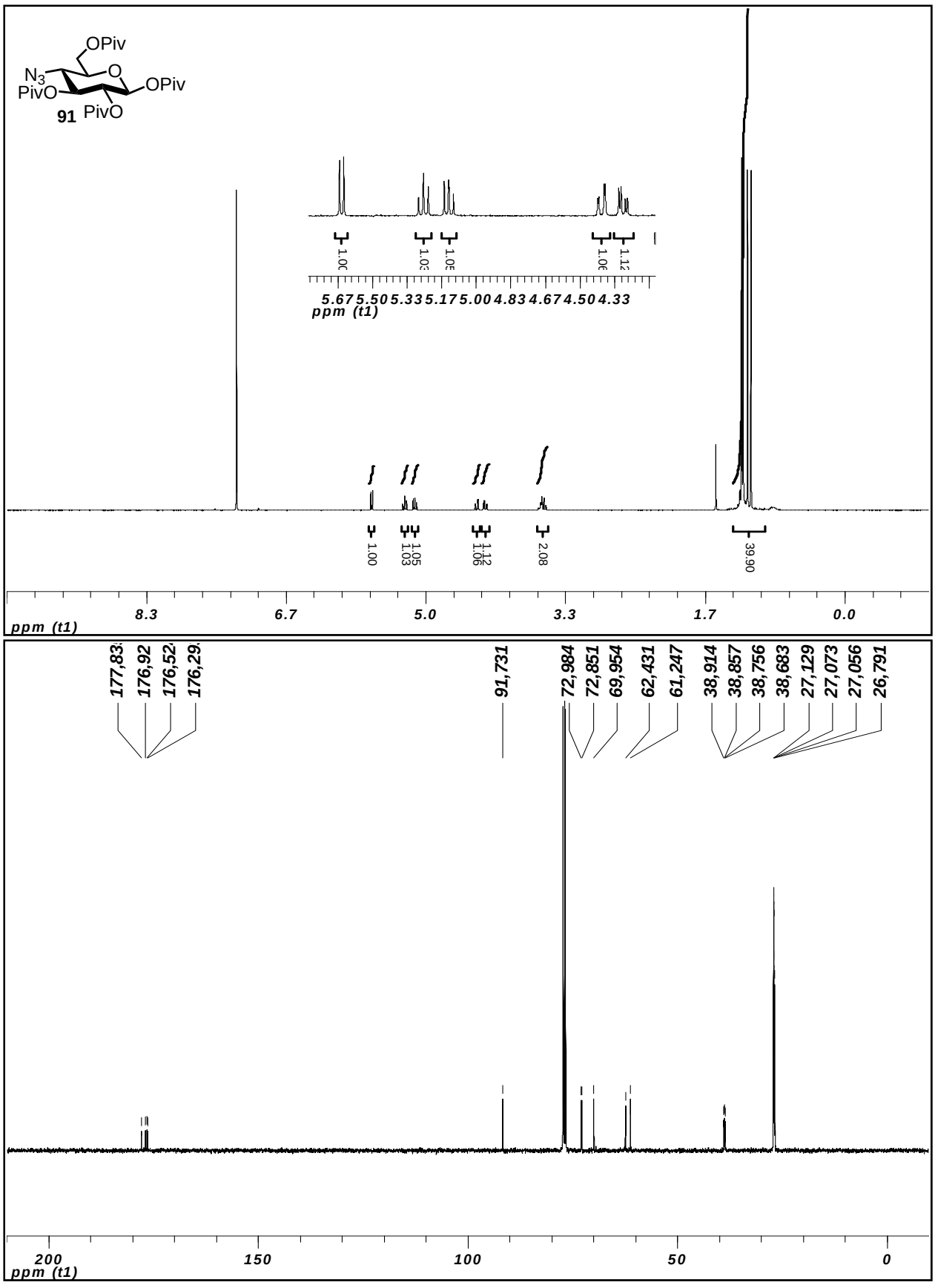
OPiv
N3
PivO
O
OPiv
PivO
91
PivO
5.67 5.50 5.33 5.17 5.00 4.83 4.67 4.50 4.33
ppm (t1)
1.00
1.03
1.05
1.06
1.12
2.08
39.90
8.3 6.7 5.0 3.3 1.7 0.0
ppm (t1)
177,83
176,92
176,52
176,29
91,731
72,984
72,851
69,954
62,431
61,247
38,914
38,857
38,756
38,683
27,129
27,073
27,056
26,791
200 150 100 50 0
ppm (t1)

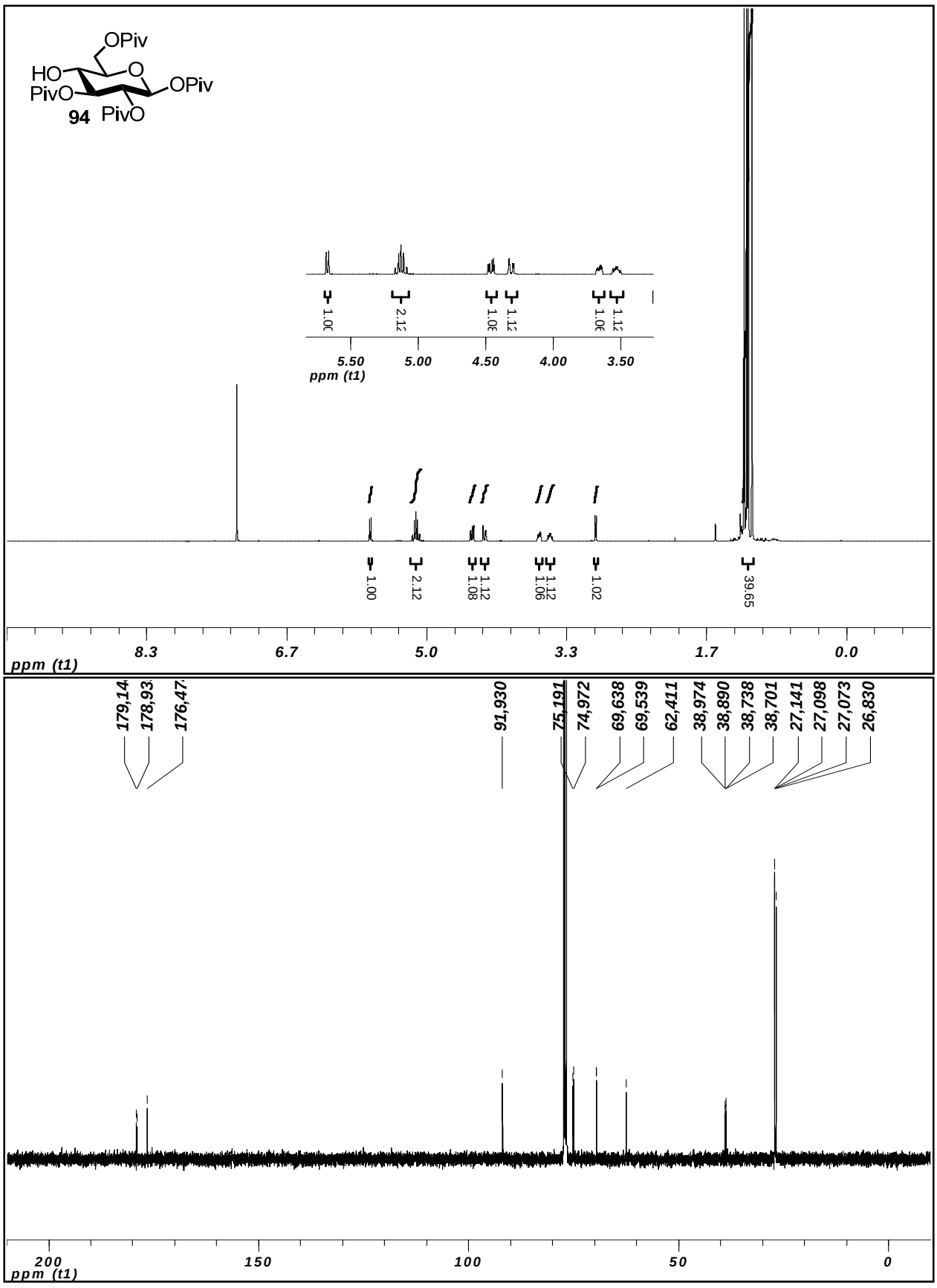
OPiv
HO
O
OPiv
PivO
PivO
94
1.00
2.12
1.08
1.12
1.06
1.12
1.02
39.65
8.3
6.7
5.0
3.3
1.7
0.0
ppm (t1)
179,14
178,93
176,47
91,930
75,191
74,972
69,638
69,539
62,411
38,974
38,890
38,738
38,701
27,141
27,098
27,073
26,830
200
150
100
50
0
ppm (t1)

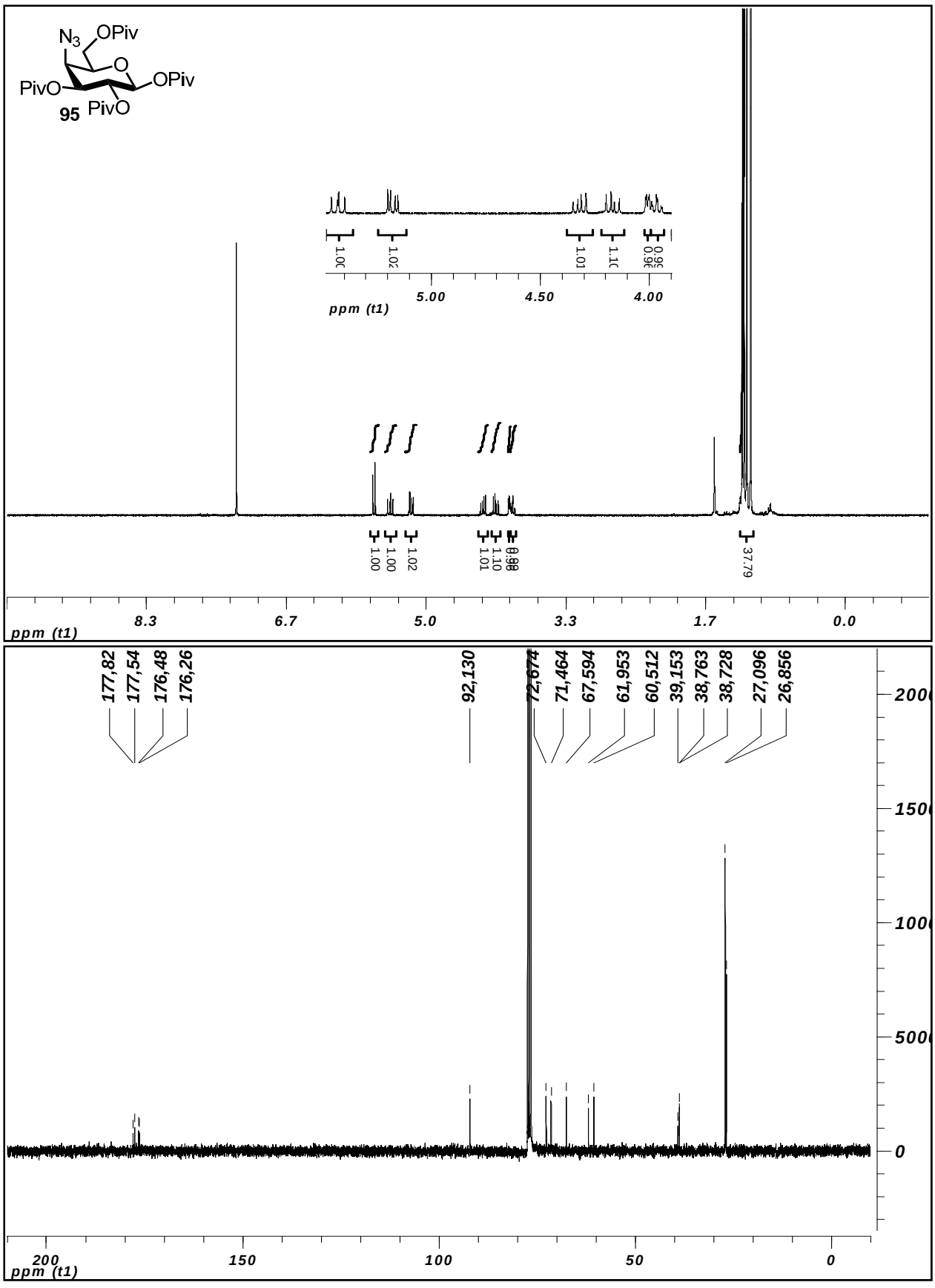
N3
OPiv
O
OPiv
PivO
PivO
95
ppm (t1)
8.3
6.7
5.0
3.3
1.7
0.0
177,82
177,54
176,48
176,26
92,130
72,674
71,464
67,594
61,953
60,512
39,153
38,763
38,728
27,096
26,856
200
150
100
50
0

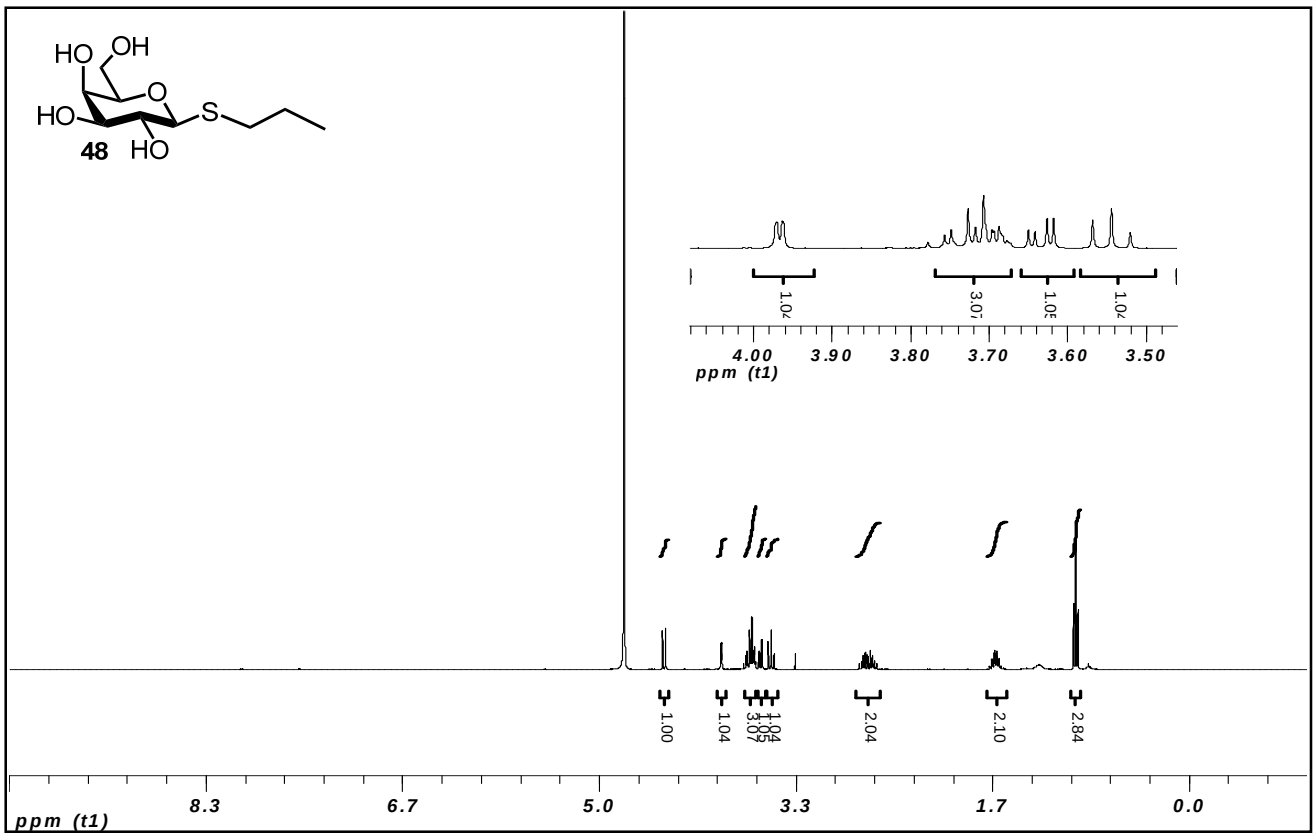
HO
OH
O
HO
S
48
HO
4.00
3.90
3.80
3.70
3.60
3.50
ppm (t1)
1.00
1.04
3.07
2.04
2.10
2.84
8.3
6.7
5.0
3.3
1.7
0.0
ppm (t1)

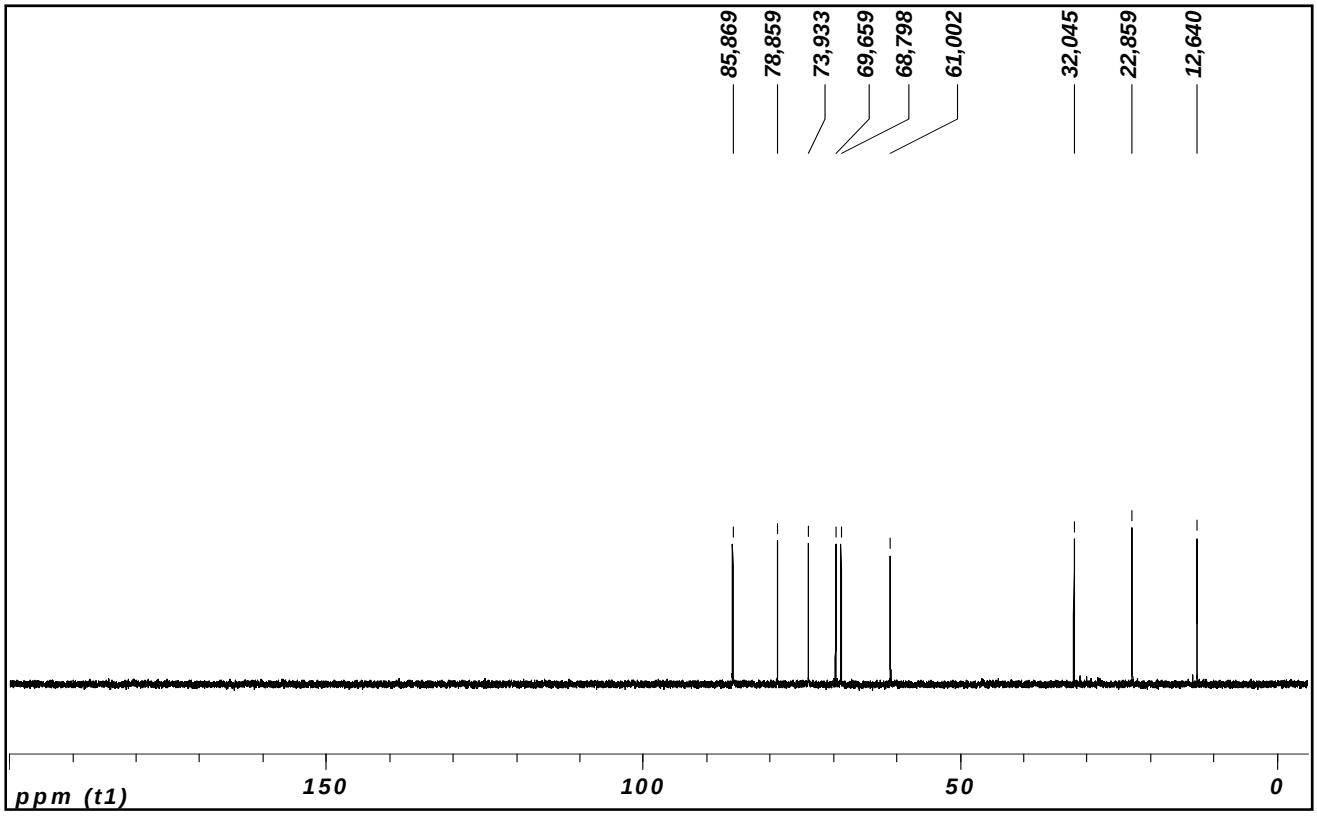
85,869
78,859
73,933
69,659
68,798
61,002
32,045
22,859
12,640
150
100
50
0
ppm (t1)

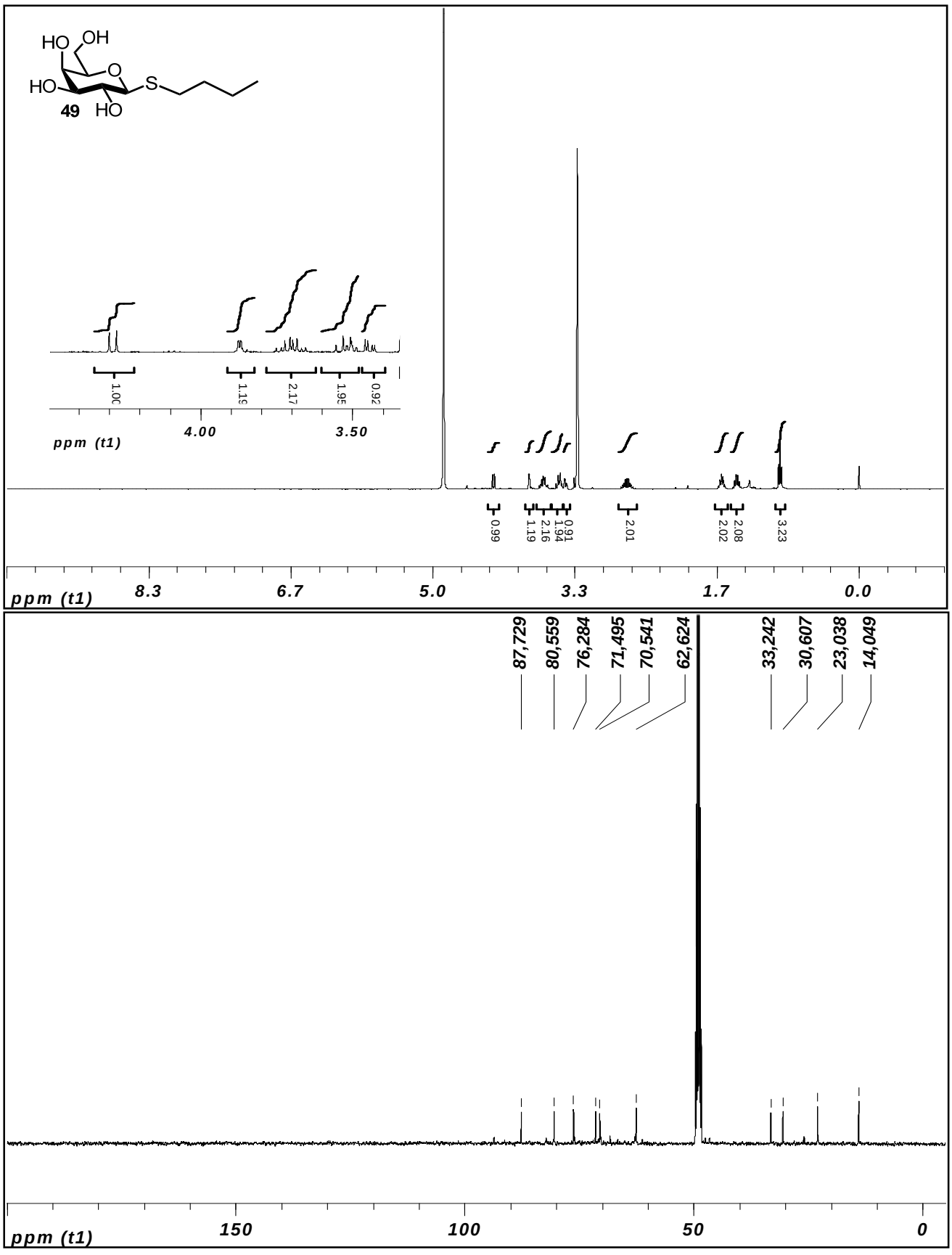
HO
OH
O
HO
S
49
HO
1.00
1.19
2.17
1.95
0.92
4.00
3.50
ppm (t1)
0.99
1.19
2.16
1.94
0.91
2.01
2.02
2.08
3.23
8.3
6.7
5.0
3.3
1.7
0.0
ppm (t1)
87,729
80,559
76,284
71,495
70,541
62,624
33,242
30,607
23,038
14,049
150
100
50
0
ppm (t1)

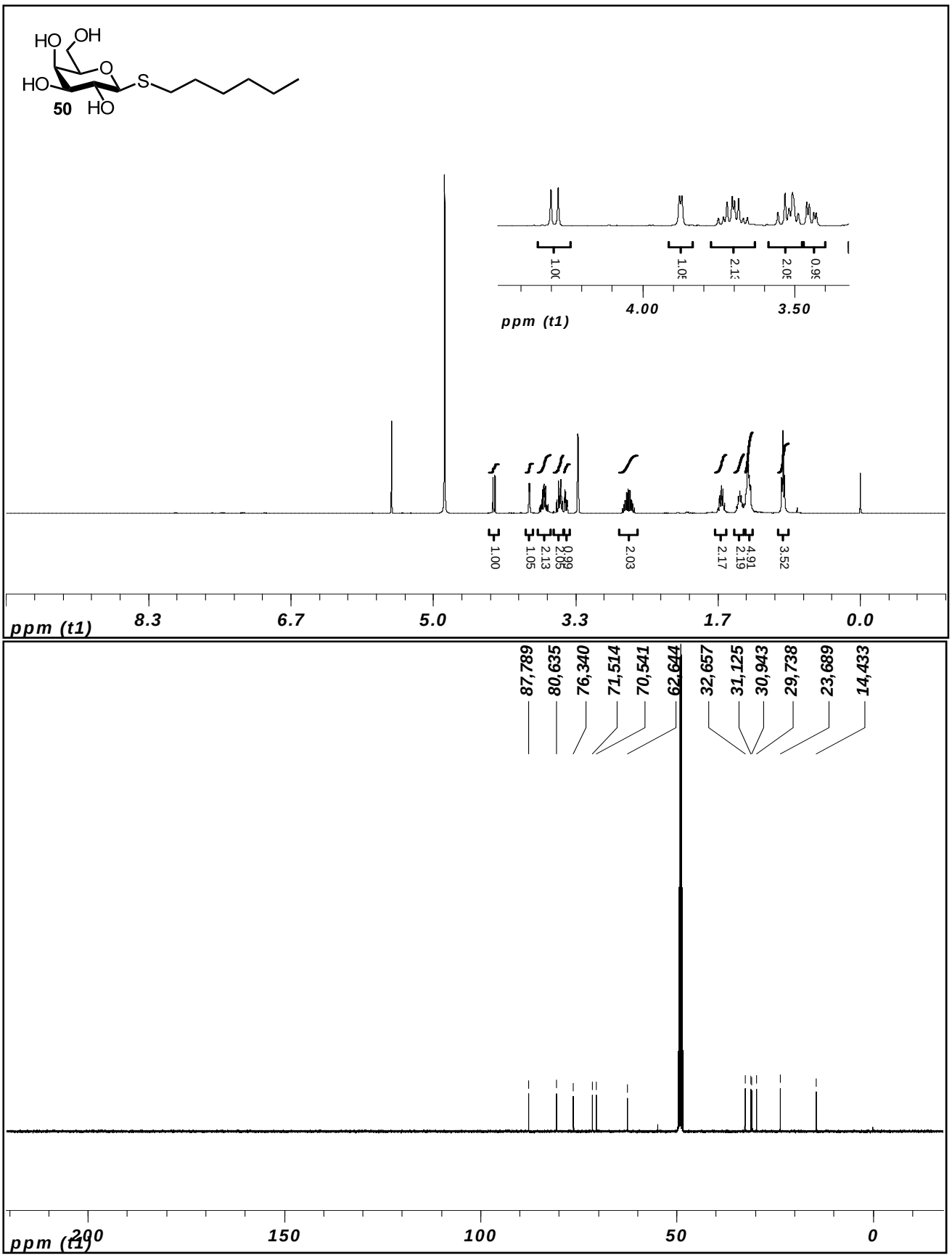
HO
OH
O
HO
S
50
HO
4.00
3.50
ppm (t1)
1.00
1.05
2.13
2.05
2.03
2.17
2.19
4.91
3.52
8.3
6.7
5.0
3.3
1.7
0.0
87,789
80,635
76,340
71,514
70,541
62,644
32,657
31,125
30,943
29,738
23,689
14,433
200
150
100
50
0

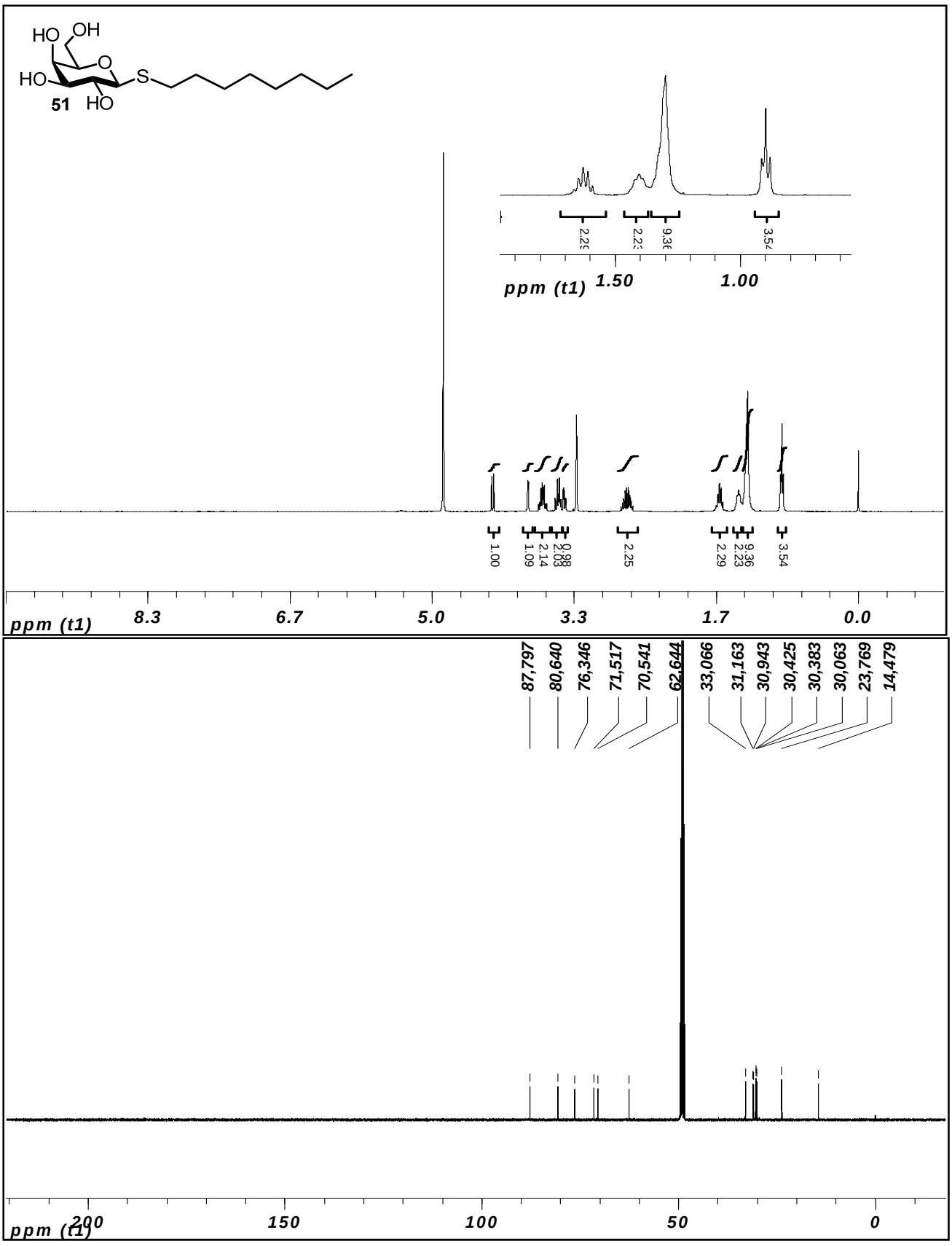
HO
OH
O
HO
S
HO
51
ppm (t1)
1.50
1.00
1.00
1.09
2.14
2.25
2.29
9.36
3.54
8.3
6.7
5.0
3.3
1.7
0.0
87,797
80,640
76,346
71,517
70,541
62,644
33,066
31,163
30,943
30,425
30,383
30,063
23,769
14,479
200
150
100
50
0